Review of Biomechanical impact Response and injury in the Automotive Environment

Technical Report Documentation Page

1. Report No.	2. Government Accession No.	3. Recipient's Catalog No.

4. Title and Subtitle	5. Report Date / 6. Performing Organization Code / 8. Performing Organization Report No.
REVIEW OF BIOMECHANICAL IMPACT RESPONSE AND INJURY IN THE AUTOMOTIVE ENVIRONMENT	5. Report Date: March 1985 6. Performing Organization Code:
7. Author(s): John W. Melvin and Kathleen Weber, Editors	8. Performing Organization Report No.: UMTRI-85-3
9. Performing Organization Name and Address: The University of Michigan Transportation Research Institute 2901 Baxter Road Ann Arbor, Michigan 48109	10. Work Unit No. (TRAIS) 11. Contract or Grant No.: DTNH22-83-C-07005
12. Sponsoring Agency Name and Address: U.S. Department of Transportation National Highway Traffic Safety Administration Washington, DC 20590	13. Type of Report and Period Covered: 6/83 - 3/85 TASK B FINAL REPORT 14. Sponsoring Agency Code

15. Supplementary Notes

NHTSA Contract Technical Manager:
Mark P. Haffner, Office of Crashworthiness Research

16. Abstract

This literature review incorporates published research available through the end of 1984. It is divided by body region and includes the following chapters: Head, Spine, Thorax, Abdomen, Pelvis, and Lower Extremities. Each chapter addresses the anatomy, clinical injury experience, and results of laboratory impact studies for each region. The experimental studies include information on biomechanical response to impact as well as injury mechanisms, tolerance, and criteria.

17. Key Words	18. Distribution Statement
Human Impact Tolerance Biomechanical Response Literature Review	This document is available to the public through the National Technical Information Service, Springfield, VA 22161

19. Security Classif. (of this report)	20. Security Classif. (of this page)	21. No. of Pages	22. Price
None	None	201	

Form DOT F 1700.7 (8-72) Reproduction of completed page authorized

ACKNOWLEDGMENTS

The completion of this major review involved significant efforts of several people in addition to the chapter authors. First, we would like to acknowledge the indispensable UMTRI Library, under the direction of Ann C. Grimm, whose extensive literature on each body region was retrieved with the able assistance of Marlene Dyer. We also greatly appreciate the consultation of Jule Brinn, Roger P. Daniel, and Harold J. Mertz, whose knowledge and experience in this field were frequently drawn upon for clarification and background information.

PREFACE

This literature review incorporates published research available through the end of 1984. It is divided by body region and includes the following chapters: Head, Spine, Thorax, Abdomen, Pelvis, and Lower Extremities. Each chapter addresses the anatomy, clinical injury experience, and results of laboratory impact studies for the various regions. The experimental studies include information on biomechanical response to impact as well as injury mechanisms, tolerance, and criteria.

The introduction to each chapter refers to the results of an analysis of National Accident Sampling System (NASS) data for 1980 and 1981 that places the cost of injuries to a particular body region in perspective relative to the cost to society for all moderate-to-fatal injuries to automobile occupants. Details of this procedure are described by Carsten and O'Day (1984)[1] and are briefly indicated here. The NASS files were first augmented to incorporate an impairment factor that goes beyond the Abbreviated Injury Scale (AIS). This factor takes into account the consequences of injury as determined by two panels of physicians as well as a percentage impairment based on American Medical Association guidelines. Then a factor was generated from an economic cost model to account for expected lifetime earnings had the person not been injured. The impairment factors for the actual NASS injuries were multiplied by the expected earnings factors for individual injured persons to create an Injury Priority Rating (IPR). For this report, the IPRs were aggregated for each body region and are expressed in terms of a percentage of the total IPR. This percentage indicates the relative contribution of injuries in each body region to the total societal cost of all automobile occupant injuries.

---

[1]Carsten, O.; and O'Day, J. (1984) *Injury priority analysis.* AATD Task A report. Report no. UMTRI-84-24. University of Michigan Transportation Research Institute, Ann Arbor.

CONTENTS

CHAPTER 1

HEAD

P. Prasad
Ford Motor Company
Dearborn, Michigan

J.W. Melvin and D.F. Huelke
The University of Michigan
Ann Arbor, Michigan

A.I. King and G.W. Nyquist
Wayne State University
Detroit, Michigan

The head is considered the most critical part of the body to protect from injury because of the irreversible nature of injury to the brain. In the Injury Priority Analysis, head injury constitutes nearly 45% of the total IPR. Facial injury, however, accounts for an additional 10.5%. The costly facial injuries are primarily lacerations to younger occupants. While these injuries are not likely to be life-threatening, the impairment to the individual from facial nerve damage and/or facial disfigurement as well as the need for reconstructive surgery make such injuries relatively costly to society. The face will therefore receive special attention within this review on the head.

ANATOMY OF THE HEAD

The various features of the head's anatomy, illustrated in Figure 1-1, are described in order from the outer surface to the internal structures. Facial anatomy is included at the end of this section.

Scalp. The scalp is 5 to 7 mm (0.20 to 0.28 in) in thickness and consists not only of the hair-bearing skin but also of layered soft tissues between the skin and the skull. When a traction force is applied to the scalp, its outer three layers (the hair-and-skin layer, a subcutaneous connective tissue layer, and a muscle and fascial layer) move together as one. Next there is a loose connective tissue layer plus the fibrous membrane that covers bone (periosteum). The thickness, firmness, and mobility of the outer three layers of scalp as well as the rounded contour of the cranium function as protective features.

Skull. The bony framework of the head is the most complex structure of the skeleton, because the skull is neatly molded around and fitted to the brain, eyes, ears, nose, and teeth. The thickness of the skull varies between 4 and 7 mm (0.16 and 0.28 in) to snugly accommodate these components and to provide reinforcement of the brain case (the calvarium), so that the skull forms a strong box around them. The skull is composed of eight bones that form the brain case, fourteen bones that form the face, as well as the teeth. Excluding the face, the cranial vault is formed by the ethmoid, sphenoid, frontal, two temporal, two parietal, and occipital bones. The inner surface of the cranial vault is concave and relatively smooth. The base of the brain case is a thick irregular plate of bone

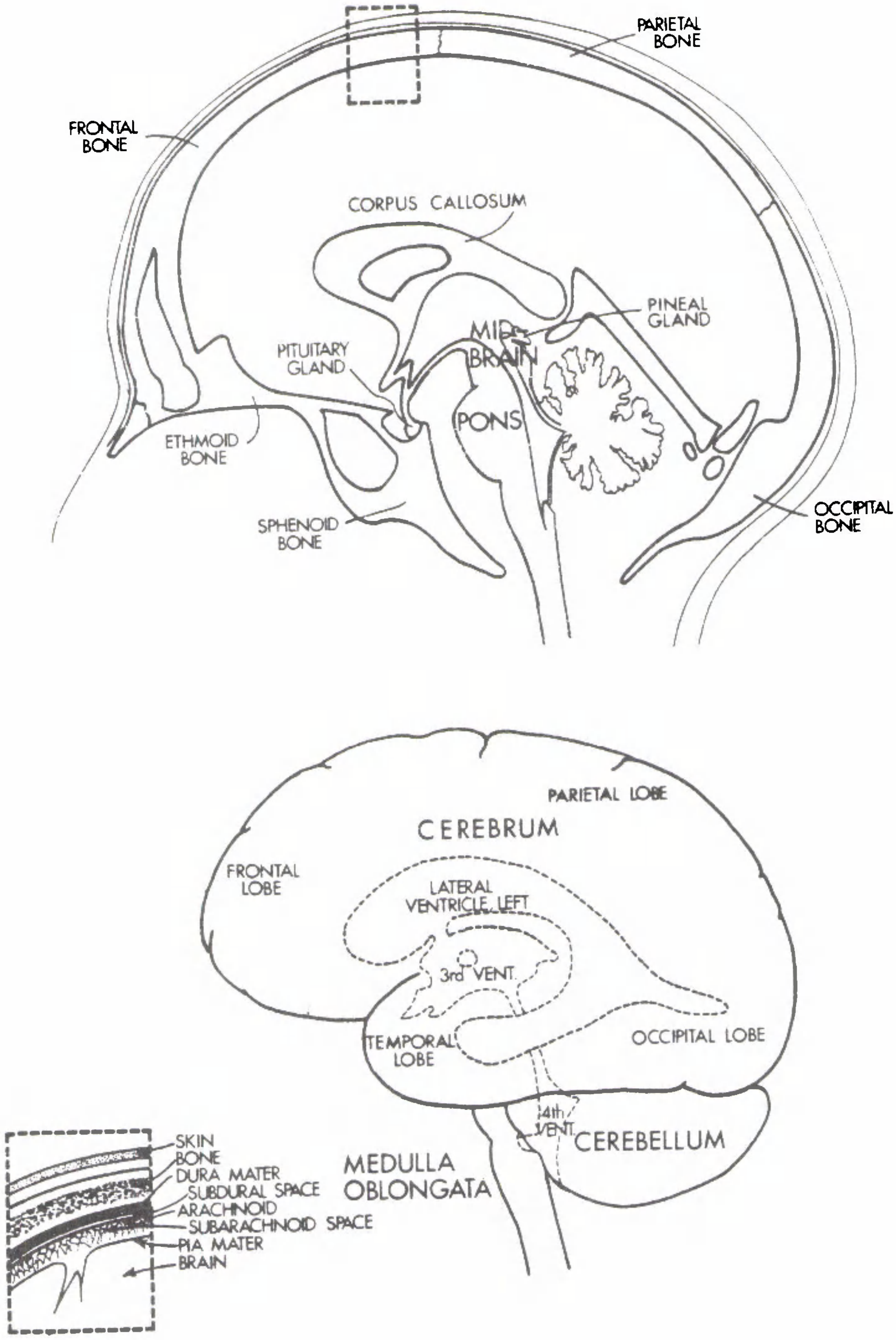

FIGURE 1-1. Anatomy of the head.

containing depressions and ridges plus small holes for arteries, veins, and nerves, as well as the large hole (the foramen magnum) that is the transition area between the spinal cord and the brain.

Meninges. Three membranes known as the meninges protect and support the brain and spinal cord. One function of the meninges is to separate the brain and spinal cord from the surrounding bones. The meninges consist primarily of connective tissue, and they also form part of the walls of blood vessels and the sheaths of nerves as they emerge from the skull.

The meninges are known individually as the dura mater, the arachnoid, and the pia mater. The dura mater is a tough, fibrous membrane that surrounds the spinal cord and, in the skull, is divided into two layers. The outer cranial layer of dura mater, or periosteal layer, lines the inner bony surface of the calvarium, while the inner layer, or meningeal layer, covers the brain. In the brain case, the two layers of dura mater are fused except where they separate and form sub-structures such as the venous sinuses, which drain blood from the brain; the falx cerebri, a fold of the inner layer of dura mater that projects into the longitudinal fissure between the right and left cerebral hemispheres; and the tentorium cerebelli, a fold of the inner layer of dura mater forming a shelf on which the posterior cerebral hemispheres are supported.

The arachnoid layer is a delicate spider-web-like membrane that is separated from the dura mater by the narrow subdural space. Within this space, a thin film of watery fluid, known as cerebrospinal fluid, encloses and bathes the brain. In the sagittal sinus and transverse sinuses, the arachnoid mater forms structures called arachnoid granulations, which reabsorb cerebrospinal fluid into the blood. The arachnoid mater extends down the spinal canal to the level of the second sacral vertebra, where it surrounds the terminal filament of the spinal cord.

The pia mater is a thin membrane of fine connective tissue invested with numerous small blood vessels. It is separated from the arachnoid by the subarachnoid space, which is filled with cerebrospinal fluid. The pia mater covers the surface of the brain, dipping well into its fissures. The pia mater that covers the spinal cord is thicker than the cranial pia mater. The former becomes the terminal filament of the spinal cord at the second lumbar level.

Cerebrospinal Fluid. The subarachnoid space and the ventricles of the brain (see below) are filled with a colorless fluid (cerebrospinal fluid or CSF), which provides some nutrients for the brain and cushions the brain from mechanical shock. For normal movement, a shrinkage or expansion of the brain is quickly balanced by an increase or decrease of CSF. The specific gravity of cerebrospinal fluid is about 1.008 in the adult, which is approximately that of blood plasma. About 140 ml of CSF constantly circulates and surrounds the brain on all sides, so that it serves as a buffer and helps to support the brain's weight. Since the subarachnoid space of the brain is directly continuous with that of the spinal cord, the spinal cord is suspended in a tube of CSF.

Central Nervous System. Macroscopically, the central nervous system (CNS) is the brain and the spinal cord. Microscopically, the CNS is largely a network of neurons and supportive tissue functionally arranged into areas that are gray or white in color. Named for this color distinction, gray matter is composed primarily of nerve cell bodies concentrated in locations on the surface of the brain and also deep within the brain; white matter is composed of myelinated nerve cell processes that largely form tracts to connect parts of the central nervous system to each other. There is a difference in density between gray matter and white matter.

The Brain. The brain can be divided structurally and functionally into five parts: cerebrum, cerebellum, midbrain, pons, and medulla oblongata. In addition, it has four ventricles (CSF cisterns with exits), three membranes (meninges), two glands (pituitary and pineal), twelve pairs of cranial nerves, and the cranial arteries and veins. The brain snugly fills the cranial cavity. The average length of the brain is about 165 mm (6.5 in), and its greatest transverse diameter is about 140 mm (5.5 in). Because of size differences, its average weight is 1.36 kg (3.0 lb) for the male and a little less for the female. The specific gravity of the brain averages 1.036, and it is gelatinous in consistency. The brain constitutes 98 percent of the weight of the central nervous system. The adult brain represents about 2 percent of the weight of the body. Looking down on the brain from above, the cerebrum consists of two cerebral hemispheres that conceal the rest of the brain. Behind and below the cerebral hemispheres lie the two cerebellar hemispheres. Beneath the cerebrum and cerebellum are the smaller midbrain, pons, and medulla oblongata.

Cerebrum. The cerebrum makes up seven–eighths of the brain and is divided into right and left cerebral hemispheres. These are incompletely separated by a deep midline cleft called the longitudinal cerebral fissure. The falx cerebri process projects downward from the top of the skull into this fissure. Beneath the longitudinal cerebral fissure, the two cerebral hemispheres are connected by a mass of white matter called the corpus callosum. Within each cerebral hemisphere is a cistern for cerebrospinal fluid called the lateral ventricle. Each cerebral hemisphere has a surface layer of gray matter called the cerebral cortex. The cerebral cortex is arranged into a number of folds, which are separated by fissures. These fissures further separate the cerebral hemispheres into lobes, so that each hemisphere is divided into four lobes, each lobe being named by its association to the nearest cranial bone. Thus, the four lobes are the frontal, parietal, temporal, and occipital lobes.

The interior of each cerebral hemisphere is composed of white matter or nerve fibers. These are arranged in tracts and serve to connect one part of a cerebral hemisphere with another, to connect the cerebral hemispheres to each other, and to connect the cerebral hemispheres to the other parts of the central nervous system. In addition, within these interior areas of white matter are a number of areas of gray matter.

Midbrain. The midbrain connects to the cerebral hemispheres above and to the pons below. Anteriorly the midbrain is composed of two stalks that are mainly fibers passing to and from the cerebral hemispheres above. Within the midbrain is a narrow canal that connects to the third ventricle above and the fourth ventricle below.

Pons. The pons lies below the midbrain, in front of the cerebellum, and above the medulla oblongata. It is composed of white matter nerve fibers connecting the cerebellar hemispheres. Lying deep within its white matter are areas of gray matter that are nuclei for some of the cranial nerves.

Medulla Oblongata. The medulla oblongata appears continuous with the pons above and the spinal cord below. In the lower part of the medulla oblongata, motor fibers cross from one side to the other so that fibers from the right cerebral cortex pass to the left side of the body. Some sensory fibers passing upward toward the cerebral cortex also cross from one side to the other in the medulla oblongata. The medulla oblongata also contains areas of gray matter within its white matter. These are nuclei for cranial nerves and relay stations for sensory fibers passing upward from the spinal cord.

Cerebellum. The cerebellum lies behind the pons and the medulla oblongata. Its two hemispheres are joined at the midline by a narrow strip-like structure called the vermis. The outer cortex of the cerebellar hemispheres is gray matter; the inner cortex is white matter. The outer surface of the cerebellum forms into narrow folds separated by deep fissures. Nerve fibers enter the cerebellum in three pairs of stalks that connect the cerebellar hemispheres to the midbrain, pons, and medulla oblongata.

Spinal Cord. The spinal cord comprises two percent by weight of the central nervous system and averages 45 cm (17.7 in) in length. Thirty-one pairs of nerves originate at the spinal cord. The spinal cord is protected by the bony spinal column, the membranes meninges, and pressurized CSF. The spinal dura mater forms a one-layer loose protective covering for the spinal cord and corresponds to the inner layer of cranial dura mater. The space between the bones of the spinal column and the dura mater, or extradural space, is filled with fat and a venous network.

Facial Anatomy. The face is defined as that area from the forehead to the lower jaw and includes fourteen bones. These bones are basically fused together through complete sutures, with the exception of the mandible that has free and movable joints. The face is covered by relatively thin skin with muscles within it that allow for movement about the nasal, orbital, and mouth openings. These "muscles of facial expression" are so named because they show expressiveness and emotions. Deep within the skin are the blood vessels to the facial structures, as well as the facial nerve that supplies the facial muscles. Immediately in front of the ear is the parotid gland and its horizontally placed parotid duct that opens into the mouth.

The fourteen facial bones are irregular in shape, frequently hollow, and some are extremely thin. The thinnest bones of the body are the lacrimal bones forming the front portion of the medial walls of the orbits. Immediately behind is the ethymoid bone, forming the major portion of the medial wall of the orbit. It resembles a hardened sponge with many small air cells within and is very fragile.

The mandible is a "U"-shaped bone that has two movable attachments to the base of the skull, immediately in front of the ear openings, called the temporomandibular joints. Attaching to the base of the skull, this is the only bone of the body that has a "double attachment" to basically the same structure.

HEAD INJURY FROM CLINICAL EXPERIENCE

Incidence. A recent study of the incidence of brain injury among the residents of San Diego, California, by Kraus et al. (1984) has identified 3,358 cases representing a rate of 180 brain injuries per 100,000 population. The incidence among males is 2.2 times higher than among females. The rates were highest among the 15 to 24 year olds. Forty-eight percent of all cases were from transport-related causes, followed by falls (21%), and assaults (12%). Over 11% of the sample were dead-on-arrival, and 16% were classified as having moderate or severe brain damage on admission to a hospital. Close to 7% of all cases discharged alive from an acute-care hospital had significant neurologic sequelae. Eight-two percent of all hospitalized cases had mild brain injuries, as defined by a Glasgow Coma Scale of 13 to 15.[2] The authors of the above study have further estimated an incidence of 410,000 new cases of brain injuries in the 1980 U.S. population.

---

[2]For Glasgow Coma Scale, see Tabaddor 1982. A fully alert and oriented patient would have a score of 15, while a mute, flaccid patient with no eye opening to any stimuli would receive a score of 3.

Types of Brain Injuries. Clinically brain injuries can be classified in two broad categories: diffuse injuries and focal injuries. The diffuse injuries consist of brain swelling, concussion, and diffuse white matter shearing injuries (DWSI). The focal injuries consist of epidural hematomas (EDH), subdural hematomas (SDH), intra-cerebral hematomas (ICH), and contusions (coup and contra-coup). Recent studies by Gennarelli (1981, 1984), Tarrière (1981), and Chapon et al. (1983) have attempted to describe the incidence and sequelae of the above brain injuries. The results of these studies vary somewhat, however, mainly due to the criterion of selection of the patients in the studies. For example, the patients in the Chapon et al. study were all critically injured (AIS 5) with immediate unconsciousness without a lucid interval after accidents involving automobiles (occupants and pedestrian) and two-wheelers. Only 7% of their sample contained injuries from falls and sports. Gennarelli's study contained 48% patients whose injuries were due to falls and assaults while the other 52% were from automobile accidents (occupants and pedestrians). The mean AIS in Gennarelli's data was 3.5. This difference in the population considered may explain the different results in the two series, since Gennarelli's study shows a marked difference in the type of brain injuries sustained by automobile accident victims as compared to assault and fall victims. In this study, it was found that three out of four automobile/pedestrian brain injuries were of the diffuse type, and one out of four were of the focal type. The assault and fall victims had one out of four diffuse injuries and three out of four focal injuries.

Gennarelli's study points out that acute subdural hematoma and diffuse shearing lesions were the two most important causes of death. These two lesions together accounted for more head injury deaths than all other lesions combined. The injuries most often associated with a good or moderate recovery were cerebral concussion and cortical contusion.

Diffuse Injuries. Diffuse brain injuries form a spectrum of injuries ranging from mild concussion to diffuse white matter shearing injuries. In the mildest forms, there is mainly physiological disruption of brain function and, at the most severe end, physiological and anatomical disruptions of the brain occur.

Mild concussion does not involve loss of consciousness. Confusion, disorientation, and a brief duration of post-traumatic and retrograde amnesia may be present. This is the most common form of diffuse brain injury, completely reversible, and due to its mildness may not be brought to medical attention. According to Scott (1981), minor concussions form approximately 10% of all AIS 1-3 injuries involving the brain, skull, and spinal column.

The classical cerebral concussion involves immediate loss of consciousness following injury. Clinically, the loss of consciousness should be less than 24 hours and is reversible. Post-traumatic and retrograde amnesia is present, and the duration of amnesia is a good indicator of the severity of concussion. Thirty-six percent of these cases involve no lesions of the brain. The remainder may be associated with cortical contusions (10%), vault fracture (10%), basilar fracture (7%), depressed fracture (3%), and multiple lesions (36%) (Gennarelli 1982). Hence, the clinical outcome of patients with this type of symptom depends on the associated brain injuries. In general, 95% of the patients have good recovery at the end of one month. Close to 2% of the patients might have severe deficit, and 2% might have moderate deficit (Gennarelli 1982).

The injury considered to be the transition between pure physiological dysfunction of the brain to anatomical disruption of the brain generally involves immediate loss of consciousness lasting for over 24 hours. This injury is also called diffuse brain injury. It involves occasional decerebrate posturing, amnesia lasting for days, mild to moderate memory deficit, and mild motor deficits. At the end of one month, only 21% of these cases have good recovery. Fifty percent of the cases end up with moderate to severe deficits, 21% of the cases have vegetative survival, and 7% are fatal (Gennarelli 1982). The incidence of diffuse injury among severely injured patients is 13% (Gennarelli 1982) to 22% (Chapon et al. 1983).

Diffuse white matter shearing injury (DWSI), also known as diffuse axonal injury (DAI), is the most severe form of diffuse injury. It is associated with severe mechanical disruption of many axons in the cerebral hemispheres. Axonal disruptions extend below the midbrain and into the brain stem to a variable degree (Gennarelli 1982). These are differentiated from the less severe diffuse injuries by the presence and persistence of abnormal brain stem signs. Microscopic examination of the brain disclose axonal tearing throughout the white matter of both cerebral hemispheres. It also involves degeneration of long white matter tracts extending into the brain stem. High resolution CT scans may show small hemorrhages of the corpus collosum, superior cerebellar penduncle, or periventricular region. These hemorrhages are quite small and may often be missed on CT scans.

DWSI (DAI) involves immediate loss of consciousness lasting for days to weeks. Decerebrate posturing, with severe memory and motor deficits, are present. Post-traumatic amnesia may last for weeks. At the end of one month, 55% of the patients are likely to have died, 36% might have vegetative survival, and 9% would have severe deficit (Gennarelli 1982). Approximately 4% of the severely injured patients in Gennarelli's study (1984) had DWSI compared to 20% in the Chapon et al. study (1983).

Brain swelling, or an increase in intravascular blood within the brain, may be superimposed on diffuse brain injuries, adding to the effects of the primary injury by increased intracranial pressure (Gennarelli 1982). Penn and Clasen (1982) report from 4% to 16% of all head-injured patients and 28% of pediatric head-injured patients have brain swelling. Tarrière (1981) has reported the incidence of edema in 21% of CT-scanned head-injured subjects. It should be noted that in general brain swelling and edema are not the same but are often used interchangeably in the literature. Cerebral edema is a special situation in which the brain substance is expanded because of an increase in tissue fluid (Penn and Clasen 1982). The course of treatment for the two may be different. According to Penn and Clasen (1982), the mortality rate due to brain swelling among adults is 33% to 50% and 6% in children.

Focal Injuries. Acute subdural hematoma (ASDH) is caused by three sources: direct lacerations of cortical veins and arteries by penetrating wounds, large contusion bleeding into the subdural space, and tearing of veins that bridge the subdural space as they travel from the brain's surface to the various dural sinuses. The last mechanism is the most common in the production of ASDH (Gennarelli and Thibault 1982). This paper reports a high incidence (30%) of ASDH among severely head-injured patients, with a 60% mortality rate. From various earlier studies, Cooper (1982b) reports the incidence rates of ASDH to be between 5% and 13% of all severe head injuries. According to Cooper, *acute* subdural hematomas generally coexist with severe injury to the cerebral parenchyma, leading to poorer outcome when compared to *chronic* subdural and extradural hematomas that generally do not coexist with injuries to the cerebral parenchyma. The mortality rate in most studies is greater than 35% and greater than 50% in some.

Extradural hematoma (EDH) is an infrequently occurring sequel to head trauma (0.2% to 6%). It occurs as a result of trauma to the skull and the underlying meningeal vessels and not due to brain injury (Cooper 1982b). Usually skull fracture is found, but EDH may occur in the absence of fracture. From 50% to 68% of the patients have no significant intracranial pathology (Cooper 1982b). The remainder of the patients may have subdural hematoma and cerebral contusions associated with the EDH. These associated lesions influence the outcome of the EDH. The mortality rate from various studies ranges from 15% to 43%. This rate is greatly influenced by age, presence of intradural lesions, the time from injury to the appearance of symptoms, level of consciousness, and neurological deficit (Cooper 1982b).

Cerebral contusion is the most frequently found lesion following head injury. It consists of heterogeneous areas of necrosis, pulping, infarction, hemorrhage, and edema. Some studies have shown the occurrence of contusions in 89% of the brains examined post-mortem (Cooper 1982b). CT-scan studies have shown incidence rates from 21% to 40%. A recent CT-scan study by Tarrière (1981) shows an incidence of 31% for contusions alone and 55% associated with other lesions. In contrast, Gennarelli's study (1982) shows an incidence of contusions in only 13% of the patients studied.

Contusions generally occur at the site of impact (coup contusions) and at remote sites from the impact (contrecoup contusions). The contrecoup lesions are more significant than the coup lesions (Cooper 1982b). They occur predominantly at the frontal and temporal poles, which are impacted against the irregular bony floor of the frontal and middle fossae. Contusions of the corpus collosum and basal ganglia have also been reported (Cooper 1982b). Contusions are most often multiple and are frequently associated with other lesions (cerebral hemorrhage, SDH, and EDH). Contusions are frequently associated with skull fracture (60% to 80%). In some cases they appear to be more severe when a fracture is present than when it is absent (Cooper 1982b). Mortality from contusions is reported to range from 25% to 60% (Cooper 1982b). Adults over 50 years of age fare worse than children. Patients in coma have a generally poor outcome.

Intracerebral hematomas (ICH) are well defined homogeneous collections of blood within the cerebral parenchyma and can be distinguished from hemorrhagic contusions (mixture of blood and contused and edematous cerebral parenchyma) by CT scans. They are most commonly caused by sudden acceleration/deceleration of the head. Other causes are penetrating wounds and blows to the head producing depressed fractures below which ICH develop. Hemorrhages begin superficially and extend deeply into the white matter. In one-third of the cases they extend as far as the lateral ventricle. Some cases of the hematomas extending into the corpus collosum and the brain stem have been reported (Cooper 1982b).

According to Cooper, the incidence of ICH has been underestimated in the past. With the advent of the CT scan, better estimates are now available. Recent studies show the incidence to be between 4% and 23%. Gennarelli (1982) shows an incidence rate of 4%. Chapon et al. (1983) show an incidence rate of 8% in severely injured patients.

Depending on the study, the mortality for traumatic ICH has been as high as 72% and as low as 6%. The outcome is affected considerably by the presence or absence of consciousness of the patient (Cooper 1982b).

Skull Fractures. Clinically the presence or absence of linear skull fracture does not have much significance on the course of brain injury, although the subject is still controversial. This controversy continues because some studies show that, when dangerous complications develop after an initial mild injury, they are associated with skull fracture (Jennett 1976). According to Cooper (1982c), failure to detect fractures would have little effect on the management of the patient. Cooper further cites a study where half the patients with extradural hematomas had skull fracture and half did not. Another study showed the occurrence of subdural hematomas in twice the number of patients without skull fracture than with skull fractures.

Gennarelli (1980) found the incidence of fracture to be similar across all severities of brain injuries (AIS 1-6) in 434 patients. There was a slight tendency of increasing severity of fracture as the severity of brain injuries increased. However, this tendency was not statistically significant. Similar conclusions were drawn by Chapon et al. (1983). Cooper (1982c) states that there is no consistent correlation between simple linear skull fractures and neural injury. Comminuted skull fractures result from severe impacts and are likely to be associated with neural injury. Cooper further states that clinically depressed fractures are significant where bone fragments are depressed to a depth greater than the thickness of the skull.

The incidence of depressed skull fracture is 20 per 1,000,000 persons per year, with an associated mortality rate of 11% related more to the central nervous system (CNS) injury than the depression itself. From 5% to 7% have coexisting intracranial hematoma and 12% have involvement of an underlying venous sinus (Cooper 1982c).

Clinically, basal skull fractures are significant because the dura may be torn adjacent to the fracture site, placing the CNS in contact with the contaminated or potentially contaminated paranasal sinuses. The patient will be predisposed to meningitis (Landesman and Cooper 1982).

The incidence of basal fracture is estimated to be between 3.5% and 24%. Part of the reason for such variation in estimates is that it is hard to see basal fractures during clinical examination. Further, they are difficult to visualize radiographically.

HEAD IMPACT RESPONSE[3]

The impact response of the head will be described in terms of its acceleration responses to prescribed impact conditions and/or the interaction forces that occur between the head and the contact surface for the prescribed impacts. Both of these impact response parameters are dependent on the head's mass, its mass distribution, the dynamic force–deformation characteristics of the skull and the soft flesh covering the skull, and on the location and direction of the impact force. Determination of the head's acceleration response is particularly important since most head injury criteria are based on measured head accelerations.

Inertial Properties. There are several sources of data on the inertial properties of the human head. Mertz (1967) measured the inertial properties of two decapitated cadaver heads. Walker et al. (1973) presented anthropometric and inertial data on the heads of 20 male cadaver heads. Reynolds et al. (1975) evaluated 6 male cadavers and Beir et al. (1980) evaluated the heads of 19 male cadavers. McConville et al. (1980) measured the anthropometry of 31 live male subjects and developed regression equations to estimate inertial properties from anthropometric measurements. Robbins (1983) used these regression methods to estimate the mean inertial properties of a mid-sized male based on measurements from a sample of 25 male subjects.

---

[3]Portions of this section are taken from the draft text of SAE J1460 (1985) developed by the SAE Human Mechanical Response Task Force (HMRTF), whose members include authors of this chapter.

Hubbard and McLeod (1974) analyzed the head mass data of Hodgson and Thomas (1971) and Hodgson et al. (1972) for 11 cadaver heads whose dimensions were consistent with those of the 50th percentile male head and found an average value of 4.54 kg (9.98 lb). They also analyzed the work of Walker et al. (1973) and included sixteen of the twenty heads in that study as being close to average male dimensions. The mean head mass for the sixteen embalmed cadavers was 4.49 kg (9.88 lb). The mean body weight for the sixteen cadavers was 67.1 kg (147.7 lb).

Reynolds et al. (1975) measured the inertial properties of six cadavers with an average body mass of 65.2 kg (143.4 lb). The average measured head mass was 3.98 kg (8.76 lb). The SAE Human Mechanical Response Task Force has analyzed this data and adjusted both the average head mass and the average head mass moments of inertia to account for the low body mass of the six cadavers. Using the U.S. 50th percentile male nude body mass of 76.9 kg (169.2 lb) from the 1971-1974 Health and Nutrition Examination Survey (Abraham et al. 1979), they scaled the average head mass up to 4.69 kg (10.32 lb).

Beier et al. (1980) measured the inertial properties of 19 unembalmed male cadavers with an average body mass of 74.7 kg (164.3 lb) and an average head mass of 4.32 kg (9.50 lb). The studies of McConville et al. (1980) and Robbins (1983) both used live male subjects and estimated head volumes from anthropometric measurements. McConville et al. found that their technique overestimated the volume by about 5%. They found an estimated head volume of 4369 cm^3 (266.5 in^3), which would give a corrected volume of 4150 cm^3 (253.2 in^3). Robbins (1983) determined an adjusted head volume of 4137 cm^3 (252.3 in^3). The average specific gravity of the head as found from the results of three studies (Walker et al. 1973, Dempster 1955, and Clauser et al. 1969) is 1.097 (range 1.07-1.11). Using this density of 1.097 g/cm^3 yields an average head mass of 4.55 kg (10.01 lb) for the McConville et al. study and 4.54 kg (9.98 lb) for the Robbins study.

The results of the above studies, summarized in Table 1-1, support the mean head mass of the average male as 4.55 kg (10.01 lb).

The mass moments of inertia measured in the above studies are summarized in Table 1-2. The values from the Robbins (1983) analysis, when adjusted by a head specific gravity of 1.097, are very close to the mean values for each of the three mass moments of inertia as determined in the Walker et al. (1973), Beier et al. (1980), McConville et al. (1980), and Robbins (1983) studies.

Cranial Impact Response. Two sets of data are available from Wayne State University researchers Hodgson and Thomas (1973, 1975) who performed a series of embalmed human cadaver drop tests during which the head impacted a flat, rigid surface mounted on a force transducer. While some of these tests involved the use of decapitated heads, others involved complete cadavers that were strapped to a lightweight pallet that was supported by a pivot point at the feet. The pallet was released at various angles from the horizontal and allowed to drop freely under the influence of gravity, causing the head to impact the rigid surface. An equivalent free-fall drop height was computed from the

TABLE 1-1

AVERAGE MALE HEAD MASS

Reference	Number of Subjects	Avg. Body Mass (kg)	Avg. Head Mass (kg)
Walker et al. 1973	16	67.1	4.49
Hubbard and McLeod 1974	11		4.54
Reynolds et al. 1975	6	65.2	3.98
Adjusted per HMRTF	6	76.9	4.69
Beier et al. 1980	19	74.7	4.32
McConville et al. 1980	31	77.5	4.55*
Robbins 1983	25	76.7	4.54**

*Based on an adjusted head volume of 95% of the reported head volume (4396 cm^3) and a head specific gravity of 1.097.

**Based on an estimated head volume of 4137 cm^3 and a head specific gravity of 1.097.

TABLE 1-2

AVERAGE MASS MOMENTS OF INERTIA* OF THE MALE HEAD
($kg \cdot m^2 \times 10^{-3}$)

Reference	I_{xx}	I_{yy}	I_{zz}
Walker et al. 1973		23.3	
Reynolds et al. 1975	17.4	16.4	20.3
Adjusted per HMRTF	22.6	21.3	26.3
Beier et al. 1980 (16 male subjects only)	20.7	22.6	14.9
McConville et al. 1980	20.4	23.2	15.1
Adjusted by sp. gr. of 1.097	22.4	25.5	16.6
Robbins 1983	20.0	22.2	14.5
Adjusted by sp. gr. of 1.097	22.0	24.3	15.9

*The mass moments of inertia given are about the x, y, or z anatomical axes through the CG of the head.

head velocities[4] measured just prior to impact. The cadaver responses were evaluated for three impact locations: frontal, lateral, and rear (i.e., frontal, parietal, and occipital). While separate response definitions for each of the three individual impact directions are of interest for a comprehensive definition of head response, the paucity of data and their scatter preclude such detail. Qualitatively, the available data did not indicate any dramatic dependence of response on impact location. A pragmatic decision was made that a response definition based on the pooled data is preferable to no definition at all. The results of these tests are summarized in Figures 1-2 and 1-3, which illustrate the responses in terms of peak force[5] and peak acceleration as a function of head drop height.

Due to scatter[6] in the data and the quantity of data points, it is not practical to plot each individual test result. Furthermore, attempts to fit meaningful regression curves proved to be futile. Instead, the results have been reduced to four response regions, A through D in Figures 1-2 and 1-3. Regions A and B provide "windows" of peak force versus drop height, whereas Regions C and D are peak acceleration versus drop height windows. Regions A and C are based on tests where skull fracture did not occur. There were fifty such tests on seven cadavers, with equivalent drop heights ranging from 76 to 188 mm (3 to 7.4 in). The windows represent mean values plus and minus one-half standard deviation, both for drop height and for force and acceleration. Regions B and D are based on tests where fracture did occur. There were fifteen such tests on fifteen cadavers, with equivalent drop heights ranging from 330 to 1060 mm (13 to 41.7 in). The window in each of these cases represents the linear regression line plus and minus approximately one-half standard deviation of force or acceleration.

A second source of head impact response information is availble from unpublished human cadaver studies performed at the University of Michigan Transportation Research Institute (UMTRI). The tests were conducted with unembalmed human cadavers, which were seated before a pneumatic impactor. Frontal impacts were conducted with the axis of the impactor in the midsagittal plane and the head tipped forward, so that the forehead plane was normal to the impactor axis, and the axis passed through the approximate head center-of-gravity. For side impacts, a similar positioning of the head was used with the plane of the side of the head normal to the impactor axis, which passed through the head just above the external auditory meatus. Only one impact per test subject was performed. The impactor had a rigid flat circular surface and a mass of 10 kg (22 lb). Impact force was measured by an inertia-compensated piezoelectric load cell. The results of four lateral impacts and one frontal impact are listed in Table 1-3. There were no fractures produced in these impacts. One additional impact test, using similar techniques but with brain vascular system pressurization and 3-D accelerometry, was reported by Stalnaker et al. (1977). This nonfracture rigid frontal impact (76A144) is also included in Table 1-3.

---

[4]Velocities reported in Hodgson and Thomas (1973, 1975) for pallet drop tests were determined to be erroneous. In cooperation with the SAE Human Biomechanics and Simulation Subcommittee, Hodgson made additional velocity measurements using a Hybrid III dummy. This information was found to be consistent with analytical predictions and was used to adjust the originally-reported values. Equivalent free-fall drop heights were then computed from these velocities.

[5]In consultation with Hodgson, the peak forces in Hodgson and Thomas (1973) have been adjusted upward by 19% to account for an original data reduction procedure thought to have been erroneous.

[6]The spread in the data reflects the effects of (1) different head sizes and masses of the cadaver subjects, and (2) the changes in skin characteristics that occur when the same site on a cadaver's head is impacted more than once.

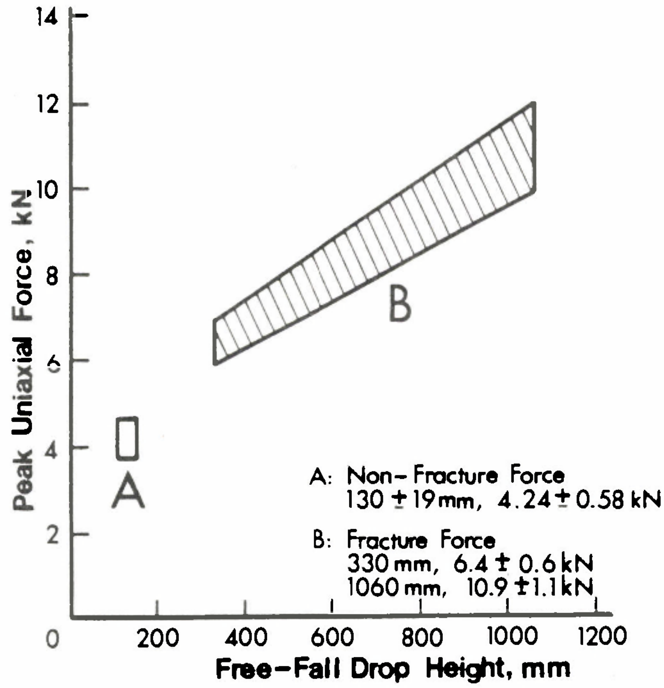

FIGURE 1-2. Impact response of the head (WSU embalmed cadaver data): Peak force versus drop height.

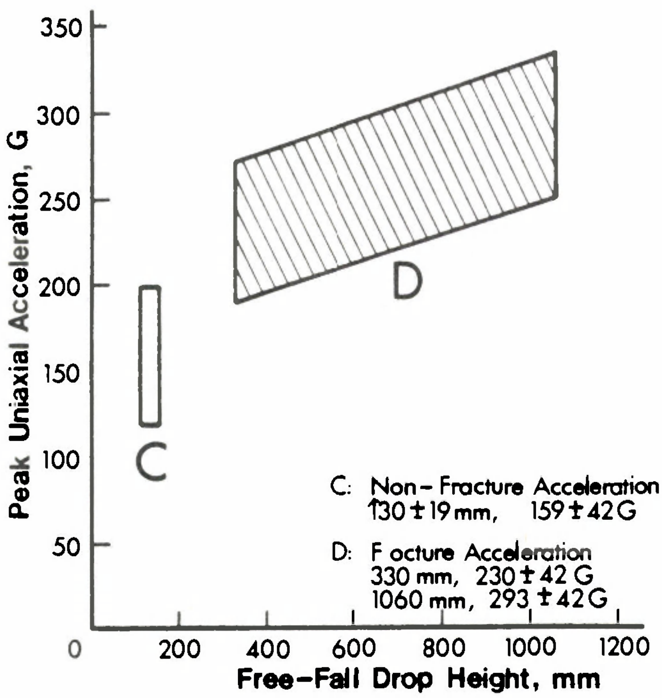

FIGURE 1-3. Impact response of the head (WSU embalmed cadaver data): Peak acceleration versus drop height.

TABLE 1-3

UMTRI RIGID NON-FRACTURE HEAD IMPACT TEST SUMMARY

Test No.	Sex	Age (yrs)	Height (cm)	Weight (kg)	Impactor Velocity (m/s)	Equiv Drop Test Vel (m/s)	Impact Point	Peak Force (kN)	Duration (ms)
C-2	M	66	160	36	5.7	4.7	Left	13.79	4.8
C-3	M	50	173	80	5.9	4.9	Left	17.79	3.8
C-4	M	78	175	72	7.4	6.1	Left	18.02	4.2
C-5	M	84	168	42	5.8	4.8	Left	13.35	6.0
C-6	M	72	173	58	6.0	5.0	Front	14.23	6.4
76A144	M	45	168	75	6.6	5.5	Front	14.60	3.8

The head impact force response plot developed by the SAE Human Mechanical Response Task Force (Figure 1-2) has been replotted in Figure 1-4 using impact velocity instead of drop height. The conversion was based on the relationship of velocity being equal to the square root of twice the product of the drop height and the acceleration of gravity. The UMTRI test data from Table 1-3 have also been plotted here using a calculated equivalent drop test velocity, V_{drop}, given by

$$V_{drop} = \sqrt{m_I/(m_I + m_H)} \cdot V_I$$

where:
V_I = impactor velocity
m_I = impactor mass (22 lb)
m_H = head mass (assumed at 10 lb average)

In each of the biomechanical studies summarized above, force data and sometimes acceleration data are presented. Specification of performance in terms of force has the practical advantage that anthropomorphic dummy heads can be tested without the necessity of instrumentation mounted on the head. A disadvantage, however, stems from the fact that dummy heads are normally instrumented with accelerometers located at the center of gravity, these accelerometers being used to assess the severity of a blow from the standpoint of injury. Therefore fidelity of head acceleration response is important. Unfortunately, all cadaver head accelerations have been monitored by affixing accelerometers to the head externally. Thus, cadaver and dummy accelerations may not be directly comparable. The acceleration data of Hodgson and Thomas presented in this review involve laterally-placed accelerometers for frontal and occipital impacts and occipitally-placed accelerometers for lateral impacts. If dummy and cadaver heads were of equal structural stiffness and if in these tests there was negligible angular acceleration of the head upon impact, a comparison of dummy and cadaver data would be meaningful. It is believed that, for the foreseeable future, metal dummy headforms will be used, and the significant differences in stiffness between such metal headforms and the human skull will continue to be a problem in head injury research. For future studies, it is recommended that angular acceleration be measured in all tests, since it is needed to compute the acceleration at the center of gravity, particularly in cadaver experiments.

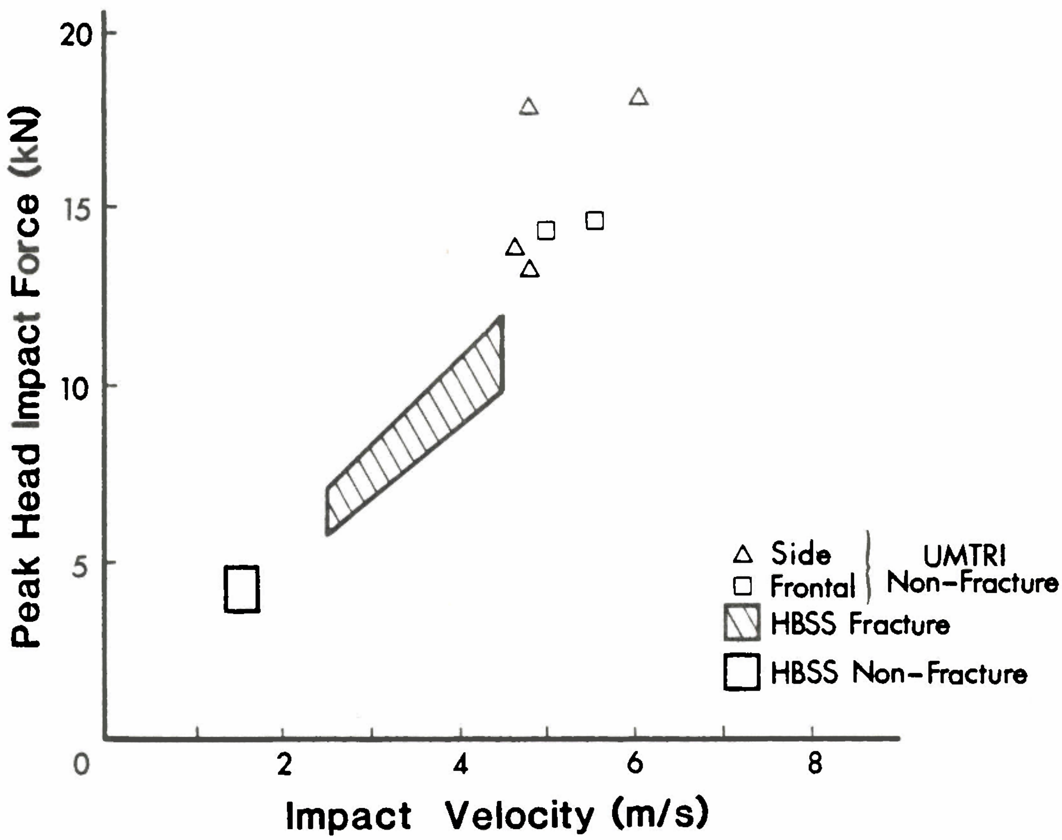

FIGURE 1-4. Impact force response of the head
(WSU embalmed and UMTRI fresh cadaver data).

Facial Impact Response. The influence of facial structures on head impact response has received little attention. The primary concern in head injury research has been to prevent serious brain injury. Injury to the face, while presenting the problem of possible disfigurement, has not been considered as serious in nature as that of brain injury. In addition to producing injury to the facial structures through damage to the soft and hard tissues of the face, these same failure mechanisms can have an effect on the loading that the brain will receive.

The mechanical response of the face depends upon the properties of the overlying soft tissues and the fourteen facial bones. While biomechanical studies have been conducted for the zygoma (cheek bone), the mandible (lower jaw bone), and the maxilla (upper jaw bone), the primary thrust was to attempt to establish tolerable force values. As such, the majority of the experiments were not structured to provide impact response directly in terms of force-displacement response. Two exceptions follow.

A series of sub-fracture experiments on a single, instrumented, embalmed cadaver were conducted by Hodgson et al. (1966). Static loads were applied to the zygoma or to the zygomatic arch, and the resulting deflections were recorded for both loading sites with loads up to 100 lb (445 N) for the arch and 200 lb (890 N) for the zygoma. The resulting spring rates were found to be 9900 lb/in (1734 N/mm) for the zygomatic arch and 28,200 lb/in (4939 N/mm) for the zygoma. Generally similar force-strain relationships were found for both the static and dynamic loads.

Tarrière et al. (1981) conducted drop tests of unembalmed cadaver faces with and without a rigid mask against a flat rigid plate. The mask served to distribute the impact load across the entire face and allowed the researchers to estimate the total energy absorption of the face during impact. For a drop height of 2.5 m (8.2 ft) in one test without the mask, a peak head acceleration of 165 G was measured. With the mask at a drop height of 3.5 m (11.5 ft), the peak acceleration was reduced to 135 G, but the peak forces were essentially the same (8.8 vs. 8.7 kN or 1980 vs 1960 lb). These response characteristics are considerably lower than those of the skull. Thus impact to the face produces significantly lower head acceleration and force than a similar impact to the skull.

HEAD INJURY MECHANISMS, TOLERANCE, AND CRITERIA

Head injuries can be classified under four major groups: scalp damage, skull fractures, extracerebral bleeding or hematoma, and brain damage. Scalp damage may consist of bruising, abrasion, or laceration of the skin. Skull fractures can further be classified as depressed, linear, indented (occurring mainly in children), and crushed (static). Extracerebral bleeding may consist of clots in the epidural space or subdural clots in the arachnoid space. Brain damage may be further classified as concussion, contusion, intercerebral hematoma, and laceration, with laceration being the most serious form of injury since it involves tearing of neural tissue (Goldsmith 1972, Ommaya 1984). Concussive brain injury has been divided into six grades by Ommaya. Grades I and II involve mental confusion and amnesia without coma. The outcome of such concussive injuries are normal except for Post-Concussive Syndrome (dizziness, headache, fatigue, irritability, anxiety, and lack of concentration, Boll 1982), and occasional vascular complications. Grades III to VI concussive injuries involve increasing durations of coma, with death occurring within twenty-four hours at Grade VI. Grades III to VI also involve increasing intensity and distribution of diffuse axonal injuries (DAI) and/or intracranial bleeding (Ommaya 1984).

Skull fractures and the force levels required to cause the fracture have been studied by many researchers. A compilation of static and dynamic fracture forces against flat and curved, rigid and padded surfaces from various sources has been made in the SAE J885-84, *Human Tolerance to Impact Conditions as Related to Motor Vehicle Design.*

In contrast to skull injuries, which are mainly due to direct head impact, brain damage can be produced either by impact to the head or by acceleration of the head without contact. Three relatively independent mechanisms have been suggested by various researchers as causing brain damage. Translational and angular acceleration of the skull are two mechanisms that cause relative motion of the brain with respect to the skull. The third mechanism consists of stretching of the cervical cord due to motion of the head relative to the cervical spine. This third mechanism also may involve stretch of the spinal cord resulting in brain stem damage.

The historical development of the above three injury mechanisms has been described by Goldsmith (1972). The majority of the research in this area has been in the production of reversible concussion in animals, linear fractures in human cadaver heads, and scaling of animal and cadaver data to determine the threshold of reversible concussion in man. There are many reasons for studying reversible concussion. It is by far the most prevalent form of brain trauma and is the first functional impairment of the brain as head impact severity increases. Concussion accompanies 80% of all linear skull fractures, rendering cadaver data (where skull fracture can easily be observed) useful for establishing tolerance under these conditions. However, the majority of real-world concussions occurs in the absence of skull fracture. An important consideration in the study of concussion was that it could be reproduced in animal experiments, whereas other forms of brain injuries could not. Only recently have acute subdural hematoma due to ruptured bridging veins and diffuse axonal injuries been consistently produced experimentally in laboratory primates (Gennarelli and Thibault 1982; Gennarelli et al. 1982).

Effects of Contact Impact and/or Acceleration on the Brain. Papers by Gurdjian et al. (1968) and Hodgson et al. (1969) have summarized the state of understanding at that time of brain injury mechanisms from head impacts. Specifically, the papers mentioned (1) direct brain contusion from skull deformation at the point of impact; (2) indirect contusion produced by negative pressure on the opposite side of the impact; (3) brain deformation as it responds to pressure gradients, causing shear stresses at the craniospinal junction; (4) brain contusion from movements of the brain against rough and irregular interior skull surfaces; and (5) subdural hematoma from movement of the brain relative to its dural envelope, resulting in tears of connecting blood vessels.

Also reported in the first two references were results of experiments, conducted by Gurdjian et al. (1965) on dogs, to which blows were delivered to fixed and free heads. A particularly interesting result of these experiments was that cellular damage in the upper cervical spinal cord occurred as frequently with the head fixed as with the head free to move. The authors concluded that the cellular damage occurred principally by the shear stresses at the craniospinal junction as a result of pressure gradients in the brain. The results also showed that head/neck movements at the craniospinal junction are not necessary for cellular damage to occur in that area.

Holbourn (1943) and Gurdjian et al. (1955) also recognized that movement of the brain relative to the skull, resulting in brain injuries, can be caused by head rotation. Based on the incompressible nature of the brain tissue, Holbourn hypothesized that translational acceleration of the skull would be harmless to the brain, but rotational acceleration could develop the tensile and shear strains required to produce the diffuse effects needed for concussive brain injuries. According to this hypothesis, the outcome of a certain level of head rotational acceleration to the brain would be the same whether such acceleration is produced through direct impact to the head or by an indirect loading, such as the purely inertial loading of the head during "whiplash." Ommaya et al. (1966) found that abrupt rotation with impact could affect sensory responses. They also found that a cervical collar reduced the rotational acceleration of monkey heads and raised the concussion threshold for occipital impacts. However, Holbourn's hypothesis could not be proved, because the angular accelerations required to produce concussion in monkeys by direct impact to the head were approximately half of those required to produce concussion by pure inertial loadings. This also indicated the important role of the "contact phenomenon" to the skull (Ommaya 1984), which caused skull deformation. Hirsch and Ommaya (1970) reported that rotational motion appeared to be more critical to the production of brain injury than translational motion. The authors further stated that "no convincing evidence has to this date been presented which relates brain injury and concussion to translational motion of the head for short-duration force inputs, whether through whiplash or direct impact."

Further investigations into the relative role of translational and angular accelerations in causing brain injuries were reported by Gennarelli et al. (1972). An apparatus called the HAD-II was used, which was capable of producing non-deforming pure translational and pure angular accelerations. Twelve adult squirrel monkeys were subjected to pure translation and thirteen were subjected to pure angular accelerations. The impacts were arranged to produce approximately the same levels of A-P accelerations in the two sets of animals. None of the translated group of animals were concussed as opposed to all the animals in the rotated group. The translated group had an average of 2.2 visible brain lesions as opposed to 7.2 brain lesions in the rotated group. The shear stresses produced under the rotational conditions appeared to be widely distributed and did not indicate a primary concentration at the brain stem. The absence of significant vascular or cellular abnormalities in the brain stem in the presence of cerebral concussion indicated that the pathology of cerebral concussion was far more complex than its simplistic attribution to "brain stem damage."

Unterharnscheidt (1971) also studied the differences between brain injuries produced by translational and angular accelerations. The injury mechanism from pure translational motion appears to be pressure gradients, while the injury mechanism from pure rotational acceleration appears to be shear stress as the skull rotates relative to the brain.

Along the same line of investigation, Hodgson and Thomas (1979) conducted several tests on a monkey brain hemisection. Pure translation and pure rotation were imparted to the brain hemisection, and motion of the various parts of the brain was studied photographically. The observed displacements throughout the brain were small, but the displacements in the cortex due to translational accelerations were approximately 20% of those observed in the case of rotation. Significant shear strains or rotational distributions in the brain stem were observed in both the translational and the rotational impacts. However, the shear strains due to translational accelerations were 0.1 radian as opposed to 0.22 radian for the head rotation case. Qualitatively, these results agree with mathematical modeling exercises conducted by Ward and Chan (1980).

Mucciardi et al. (1977) demonstrated an interesting approach to predicting brain injury by analyzing head motion. Data from head impacts to monkeys performed by UMTRI were used. Measured translational and rotational acceleration and velocity waveforms were treated by a nonlinear Adaptive Learning Network (ALN) program developed to produce empirically derived predictive models of head injury. The injury criterion was a special computed overall AIS. Time derivatives were used to create "jerk" waveforms to be used in addition to the measured waveforms. From thirty-four available kinematic parameters, the ALN model successfully predicted the observed integer AIS (using seven parameters), the unconsciousness AIS (using six parameters), and the time of unconsciousness (using seven parameters). The authors concluded that the overall AIS was a function of the total momentum transferred from the impact and the rate of momentum transfer. Their results suggested that rotational motion might be a prominent factor in causing unconsciousness, but that the overall AIS was primarily dependent upon translational motion.

Ono et al. (1980) found no correlation between the occurrence of concussion in monkeys and rotational acceleration. The occurrence of concussion was highly correlated with the translational acceleration parameters. However, the duration of concussion in monkeys subjected to pure angular acceleration of the head was an average of three times longer than those subjected to head impacts having linear and rotational components.

In summary, based on all animal experiments performed to date, both rotational and translational accelerations of the head can produce cerebral concussion and other brain injuries. If localized skull deformation is eliminated by the use of yielding surfaces or helmets, cerebral concussion is produced at higher acceleration levels than if the contact phenomenon were present.

The Cavitation Hypothesis of Brain Injury. The cavitation hypothesis of brain injury, which involves bubble formation and collapse, was advanced by Gross (1958a,b). It was postulated that contrecoup cavitation is a result of pressure gradients generated in the brain due to an impact to the head. Coup cavitation would occur as a result of skull elastic snap-back subsequent to the initial skull indentation during impact. Resonance cavitation would be caused by negative pressures produced by radial oscillations of the skull or by other wave phenomena. Depending on the location of the cavitation, a variety of brain functions could be disrupted. Unterharnscheidt (1970) attributed the generation of lesions in the central brain to increases in cranial volume under certain conditions of deformation of the skull undergoing impact. The volume increase would lead to cavitation, since it occurs faster than any possible inflow of fluid, particularly in the ventricular region. The possibility of cavitation bubbles actually occurring in the brain tissue has been questioned by Hodgson (1970) and Kenner (1971).

Further investigations of this cavitation phenomenon were carried out by Lubock and Goldsmith (1980) using a physical model of a head/neck system. It was concluded that cavitation damage in the brain from a blow to the skull is possible in the fluid components but is highly unlikely in the neural tissue. Kallieris et al. (1980) have reported the results of short duration impacts to head models and cadaver heads. These impacts were approximately 50 microseconds in duration and of low enough energy level that appreciable movements between the skull and brain did not occur. Since the pulse duration was close to half that required for a disturbance to travel across the head (100 microseconds), the resulting effects to the brain were attributed to wave propagation and cavitation. Histological examination of the cadaver brains showed hemorrhages of the arachnoid membrane, blood vessel lacerations with hemorrhages, and lacerations of the arachnoid and pial membranes, of the cortex, and of the cerebrum white matter fibers.

Flexion-Extension at the Head/Neck Junction. A number of experiments were conducted by Friede (1960, 1961a,b) on cats. It was shown that all the typical symptoms of experimental concussion could be produced by stretching the cervical region of the cats without any impact or imparted motion to the skull. Histogical examination of the central nervous system revealed neuronal lesions in the nuclei of the brain stem. Other alterations in the brain stem and the cervical cord have been discussed by Unterharnscheidt (1983). Whether such concussion can be classified as cerebral concussion has been questioned by Thomas (1970) and Unterharnscheidt (1983). Thomas believed that loss of medullary functions in anesthetized animals can produce the "classic symptoms" of concussion. However, loss of consciousness may not be guaranteed in the anesthetized animals, and no good evidence connecting cervical stretch and loss of consciousness existed. Unterharnscheidt's objections were based on the fact that, in Friede's experiments, concussion was not morphologically traceless. Using Unterharnscheidt's criterion for concussion, even rotational acceleration does not produce the symptoms of "true" cerebral concussion. However, whether or not the symptoms observed by Friede could be classified as "true" cerebral concussion, damages in the brain stem area classify them as brain injuries. This is why they are included in this review.

The role of neck stretch in producing concussion in Navy pilots involved in aircraft ditching was suspected by Ewing (1963) and Ewing and Unterharnscheidt (1976). Further investigation of this phenomenon was carried out at the Naval Biodynamics Laboratory with twenty-eight Rhesus monkeys subjected to increasing levels of $-G_x$ impact acceleration. The torsos of the monkeys were completely restrained, but the head and neck were unrestrained. Details of the experimental protocol are described by Thomas and Jessop (1983). The injuries to the animals are described by Unterharnscheidt (1983). Sled accelerations in the 100-G range resulted in fatal head and neck injuries. Avulsions of the basilar portion of the occipital bone and the atlanto-occipital articulation were noted in many of the severe injury cases. Transection of the cervical cord at the C-1 level as well as hemorrhages in the spino-medullary areas and in the cerebellum were also observed. In some instances, subdural hemorrhages over both cerebral hemispheres due to ruptured bridging veins were observed and were attributed to the rotational acceleration.

The injuries to the spino-medullary area were attributed to the following three injury mechanisms, either occurring simultaneously or consecutively: (1) localized crushing of the ventral aspect of the spinal cord in the area of the lower medulla and C-1, caused by excessive movement of the tip of the odontoid process (dens) of the axis (C-2); (2) excessive stretch of the upper spinal cord and medulla oblongata to which the cord merges; and (3) a shearing action between the rim of the foramen magnum and the arches of the atlas as the neck is both stretched and rotated relative to the head.

Spinal cord injury by the odontoid process as a possible mechanism for concussion of helmeted pilots undergoing a combination of $+G_z$ and $-G_x$ accelerations during crashes has been advanced by King et al. (1978).

Static neck stretch tests on a 12.2-kg (26.8-lb) eight-year-old baboon performed by Lenox et al. (1982) have shown interruption of Somatosensory Averaged Evoked Responses at 595 N (134 lb) axial force. This interruption was hypothesized as being due to blockage of neural transmission at the spino-medullary junction. Death followed at 1040 N (234 lb), and neck structural failure took place at 1170 N (263 lb). These results are in agreement with those of Sances et al. (1981).

Head Impact Tolerance. The development of three approaches to establishing tolerable limits to frontal head impact resulting in translational acceleration are discussed below. These are the Wayne State Tolerance Curve, the Gadd Severity Index, and the Head Injury Criterion.

Wayne State Tolerance Curve. The Wayne State Tolerance Curve (WSTC), first suggested by Lissner et al. (1960), is the foundation upon which most currently accepted indexes of head injury tolerance are based. As originally presented, the "curve" included six points that represented the relationship between acceleration level and impulse duration (in the range of 1 to 6 ms) found to produce linear skull fracture in embalmed cadaver heads. Simply put, short pulses of high acceleration will cause injury, while lower acceleration levels require longer duration to do harm. The curve was later extended to pulse durations above 5 ms with comparative animal and cadaver impact data and with human volunteer acceleration test data. The details of the history of the WSTC are described in SAE J885-84 and will not be repeated here.

The reader should be aware, however, of the physical nature of the experiments of Lissner et al. that produced the first data points to be used in the WSTC. Embalmed human cadavers were used as opposed to fresh cadavers or severed heads. Instrumentation consisted of pressure transducers in the right temporal and left posterior regions of the skull and an accelerometer on the center rear of the skull. The impact was on the forehead. The membranes surrounding lobes of the brain were mechanically punctured and torn to allow all parts of the cranial cavity to communicate. The impacts were accomplished by dropping the cadavers onto automotive instrument panels, damped steel plates, steel anvils, and padded steel anvils.

The important points for the present discussion are that (1) pressure gradients in the region of the foramen magnum were understood to be the primary brain stem injury mechanism; (2) the original WSTC reported peak accelerations and peak pressures for translational impact with hard, flat surfaces in the anterior-posterior direction; (3) the authors cautioned that much data was needed to validate the curve; but (4) it was the first graphical representation of critical injury threshold based on impact conditions. The authors also provided insight into the goal for energy absorbing materials or structures:

> Any padding arrangement or reduction in stiffness of the [instrument] panel, or both, which increases the time duration of impact in an equal or diminished ratio to the decrease in acceleration or pressure produced, will be an improvement with regard to prevention of injury.

The relative decreases and increases necessary are described by a curved line, such as the WSTC.

Soon thereafter, Gadd (1961) suggested plotting the injury threshold curve on logarithmic scales to achieve a straight line fit. The extent to which the slope of this line was steeper than -1 would indicate a greater dependence of injury on the intensity of loading, as opposed to dependence on time of loading. He also suggested that multiple impulses could be analyzed for injury potential by integrating the acceleration over the entire impulse profile, using the power weighting factor, derived above from the slope, on the acceleration portion of the profile. This fundamental engineering advice for those thinking of establishing an index of injury tolerance was later to be developed into the Gadd Severity Index, discussed later in this chapter.

Before this index was finalized, however, changes were made in the WSTC. To make the triangular peak acceleration levels compatible with irregular wave forms and with the trapezoidal waves of human volunteer tests summarized by Eiband (1959), the ordinate of the curve was changed to "effective" or average acceleration. A plot in this form appears in Patrick et al. (1965a). The asymptote of the curve, or the low-level acceleration threshold for very long time durations, was given as 42 G. The authors stated, however, that humans are known to have withstood considerably higher accelerations in cases where there was no impact. They suggested a threshold of from 60 G to 80 G, and they themselves used 80 G as the upper safe limit on effective acceleration for impacts with a padded surface. It must be remembered, however, that for nonrectangular wave forms, peak accelerations can be higher than 80 G. The authors cited permissible peaks of 110 G for sinusoidal pulses and 160 G for triangular pulses as well as the avoidance of high acceleration peaks lasting longer than 1 ms.

The Wayne State Tolerance Curve has been criticized over the years on various grounds: few data points, questionable instrumentation, poor documentation regarding scaling of animal data, etc. More fundamental objections include the fact that it is based on translational acceleration responses of the skull and that it is not a continuous criterion, i.e., increasing severities of brain injury cannot be predicted from this curve. Support for the curve, however, can be found in reports of experimental results. Slobodnik (1980) simulated helmet damage of twelve helmet wearers involved in accidents, and Haley et al. (1983) reported a comparison of the head acceleration responses of these simulations with the WSTC. The data appear to reinforce the validity of the WSTC.

Further reinforcement of the WSTC comes from the experiments of Ono et al. (1980) using primates and cadaver skulls. The authors demonstrated that cerebral concussion in monkeys can be produced by impacts producing pure translational acceleration of the skull. Utilizing scaling techniques proposed first by Stalnaker et al. (1971, 1973), a tolerance curve for the threshold of cerebral concussion to humans was developed and called the Japan Head Tolerance Curve (JHTC). The JHTC and WSTC have been compared by Ono et al. (1980), Backaitis (1981), and Newman (1982). The difference between the two curves in the 1-ms to 10-ms time duration range is negligible. Minor differences between the two curves exist in the longer duration pulses. The data of Ono et al. show that the threshold for skull fracture is slightly higher than that for cerebral concussion.

Gadd Severity Index (SI). In Gadd (1966), the author brought to maturity the ideas presented in 1961. Although a log-log plot of the WSTC resulted in a somewhat curved line, Gadd felt his straight-line approximation was "sufficient at this time" because of the scatter of the data. The slope of his line was −2.5. and thus 2.5 became his power weighting factor. Using the Severity Index (SI) formula $\int a^{2.5}dt$, Gadd showed that a triangular pulse having the same area as a square pulse would have an injury potential 1.61 times as great. Near the end of his paper, Gadd returned to the question of his straight line approximation and suggested that, as more data became available, a curve could be constructed. He credited J.P. Danforth with the suggestion that the weighting exponent need not be constant but could vary as a function of acceleration. It was suggested that if the SI exceeded 1000, a danger to life was indicated. Further justification and rebuttal to the criticisms voiced by Newman (1975, 1980) regarding the SI were presented by Gadd (1981).

An early test of the validity of the SI concept was conducted by Hodgson et al. (1970). Frontal head impacts to nine cadavers and occipital impacts to twenty-nine stumptail monkeys were used. The SI for threshold levels of skull fracture varied from 540 to 1760 with an average value of 870. It was postulated that, although threshold linear fractures are associated with concussion, such fractures do not necessarily pose a threat to life. As a result, the average value of SI is expected to be below 1000. It was also found that the SI delineated monkey concussions better than the peak head accelerations.

Head Injury Criterion. The Fifteenth Stapp Car Crash Conference, held in the fall of 1971, included special sessions on head injury and became a forum for the discussion of head injury mechanisms, tolerance thresholds, and test criteria. Translation versus rotation was again discussed. Unterharnscheidt (1971), Gennarelli et al. (1971), and Gadd (1971) suggested that, based on rocket sled experiments, the SI 1000 limit was much too conservative for non-contact, whole-body accelerations; and Fan (1971) introduced the Revised Brain Model (RBM). Versace (1971) presented a mathematical critique of the SI and suggested an alternative method for calculating the index number, in which the effective acceleration, defined as $1/t \int a^n dt$, was raised to the 2.5 power and multiplied by the time duration. Versace argued the approach was still inadequate because of two factors: (1) biomechanical data were insufficient to accurately arrive at an appropriate exponent, and (2) the index represented only an intermediate stage in the injury chain of events. A measure of the actual response of the brain to head impact would be more relevant.

Versace's formula was immediately popular in regulatory circles, however, because it was able to handle the seemingly high tolerance levels in cases of long duration, low-level acceleration, and in cases of two or more high peak accelerations associated with two or more impacts. In March 1972, a proposal was made by NHTSA to replace the SI in FMVSS 208 with the following expression:

$$\left[\frac{1}{t_2-t_1}\int_{t_1}^{t_2} a\cdot dt\right]^{2.5} \quad (t_2-t_1) < 1000$$

where a is the resultant acceleration and t_1 and t_2 are any two points in time during the crash. This proposal was said to be based on research information that "head acceleration exposure is not always additive relative to head injury." Although not formally labeled at that time, the new index soon became known as the Head Injury Criterion (HIC).

In the month prior to the HIC proposal, NHTSA issued a rule that extended the current injury criteria for automatic restraint systems (the SI) to manual lap/shoulder belts. Vehicle manufacturers commented that, as long as the head does not contact anything, belt systems allow the head to flop loosely forward, creating a high SI value while not contributing significantly to injury. When the HIC was adopted as a rule in June 1972, NHTSA restricted the definition of t_2 and t_1 to be "any two points in time after the head contacts a part of the vehicle other than the belt system." The issue was not yet resolved, however, and in October a further restriction was made to discount the effects of glancing blows. The regulation then specified "any two points in time during any interval in which the head is in continuous contact with a part of the vehicle other than the belt system."

In subsequent regulatory notices, it was required to calculate the HIC for the entire impact duration, whether head contact took place or not. The use of HIC in non-head-contact situations has been questioned by Lesterlin et al. (1982) on grounds that it deviates from the data base from which HIC was derived, and that, in the non-contact phase, head acceleration is generated from neck reaction forces and moments. Additionally, field accident data show little evidence of brain injuries in the absence of head contact.

For a few years after its inception, no physical interpretation of the HIC was available. At best it seemed to identify a period in the impact pulse during which danger to the brain was at its maximum. During the Head and Neck Injury Criteria Workshop in March 1981, Backaitis (1981) and Eppinger (1981), in separate presentations, attempted to place the HIC formulation on a theoretical basis. According to both, the HIC could be interpreted as a measure of the rate of change of specific kinetic energy imparted to the head, analogous to the peak power criterion developed by DiLorenzo (1976). During the same workshop, Goldsmith (1981) voiced his disapproval of such concepts.

In an attempt to determine the validity of the HIC threshold of 1000, Got et al. (1978) calculated the HIC for forty-two free-fall impacts to the heads of human cadavers. Some were helmeted, some were not. Using their own method of measuring accelerations to calculate the resultant, the authors found that tolerance to head impact without fracture was much greater than the HIC would allow. They suggested that a HIC of 1500 was the appropriate regulatory limit for both frontal and lateral impacts.

The data generated by the above authors, by Nahum and Smith (1976), and by Nahum et al. (1977) formed a baseline data set to be examined by the U.S. representatives to Working Group 6 of ISO/TC22/SC12 (1983). Since the technique for detecting brain injury in the cadaver heads in the above studies depended on the detection of India ink extravasated in the brain tissues, it was assumed that any such extravasation represented a threat-to-life at the AIS-4 level, since it indicated arterial ruptures. It was also assumed that it was highly unlikely that any test specimen was subjected to the level of stimulus that was required to *just* produce a prescribed injury severity level. The only thing that could be deduced from a test result was whether or not the stimulus was greater or less than the level required to produce a prescribed injury severity level. The amount that the stimulus exceeded or was below the threshold stimulus for the specimen was unknown. Hence there was a need to statistically analyze the data. Such a technique does exist and has been described by Mertz and Weber (1982).

A statistical analysis of the data, using this technique, showed that 16% of the adult population would be expected to experience a life-threatening brain injury at a HIC level of 1000, while 56% would experience such injuries at a level of 1500. A position paper was presented to the ISO/TC22/SC12/WG6 in June 1983 (ISO, WG6 1983). Further investigation of this data base also showed the lack of any data in which the HIC durations exceeded 13.5 ms. As a result it was suggested that no experimental basis for using HIC for HIC durations greater than 15 ms existed. Further, the U.S. delegation did not endorse the use of HIC in non-contact situations.

The statistical analysis method of Mertz and Weber has stimulated more studies into the area of analysis of tolerance data. By the end of 1984, many other methods of statistical analysis will be evaluated.

Tolerance Criteria Based on Mathematical Models. The preceding sections have discussed the evolution of the currently used Head Injury Criterion. Controversies surrounding its use obviously exist (Newman 1975, 1980). Over the years, various other injury indicators based on the use of translational acceleration data have been advanced. The majority of these were simple spring-mass-damper mathematical models whose responses approximated the Wayne State Tolerance Curve. Examples of these are the J Tolerance Index (JTI) of Slattenschek (described in English in Slattenschek and Tauffkirchen 1970), the Effective Displacement Index (EDI) of Brinn and Staffeld (1970), and the Revised Brain Model (RBM) of Fan (1971).

An independent formulation (not based on the WSTC) using driving point impedance test results on cadaver and monkey skulls was advanced by Stalnaker and McElhaney (1970). This formulation consisted of two masses linked by a spring and a damper. Response of the model was compared with animal injuries, and an injury index called the Maximum Strain Criterion (MSC) was developed. The MSC curve indicated a tolerance threshold significantly lower than did the WSTC. It also showed that injury tolerance was dependent on the impact wave form. The MSC for human lateral head impact was also presented for the first time and was shown to be 50% lower than for longitudinal impact. Some of the differences between the MSC curve and the WSTC probably can be accounted for by the differences in input acceleration and masses to the model (Fan 1971) and to cadaver and dummy heads, as discussed later.

Further refinements of the MSC were presented by McElhaney et al. (1973) at the Symposium on Human Impact Response in October 1972. The injury prediction capability of the MSC was compared with other indexes, i.e., SI, HIC, JTI, EDI, and RBM.

The MSC was revised to represent the Mean (rather than maximum) Strain Criterion, where "mean strain" was defined as "the displacement of one side of the head relative to the other, divided by the distance across the cranium." Basing a tolerance curve on average rather than peak acceleration levels was more consistent with other criteria. The mean tolerable strain for human heads was calculated to be 0.0061. Comparing the MSC to other indexes for several simulated crashes, the JTI, EDI, and RBM predictions were similar to the MSC, but the SI and HIC were much more conservative. In the final section of the paper, the authors summarized data from human cadaver impact tests, undertaken to establish force- and acceleration-time histories of the human head, so that dummy head impact responses could be specified.

An advantage of the MSC over other criteria is that it allows a continuous type of criterion. This can occur because the outputs of the model were associated with various levels of injuries. Due primarily to this feature of the MSC and to the fact that it obtained its physical parameters directly from experimental efforts, the MSC has been recommended by Ommaya (1984) for evaluation of contact and translational components of head impact. The MSC has also been recommended for evaluation of industrial safety helmet performance by Cook (1980).

Because the MSC model consists of a 0.6-lb (0.27-kg) "forehead mass" and a 10-lb (4.55-kg) "head mass" and the input acceleration is to the forehead mass, it is not clear as to how the model can be used in automotive type testing, in which the acceleration at the center of gravity of the dummy head is measured. This would equally be true in cadaver testing, in which accelerations are measured on the back of the skull.

Finite Element Models for Impact Tolerance. In the mid-1970s, new modeling efforts were launched using finite element analysis methods. Finite element models differ from traditional "infinitesimal models" primarily in the manner in which continuity is expressed. Generally, the former are more adaptable to digital computation techniques and more readily accept various forms of calculation tolerances. The ability of this type of approach to handle irregular shapes and nonhomogeneous materials made it particularly suitable for modeling the mechanical structures and responses of the head. These efforts were hampered, however, by the lack of a complete set of data describing the properties of the various materials of the head.

Chan (1974), following a discussion of shell models and a careful review of the continuum mechanics research on impact loading of head-like forms, presented a finite element model that predicted both shear strain and reduced pressure effects. The model was three-dimensional and had a symmetric axis of revolution. A more complex model, but still of idealized shape, was later developed by Khalil and Hubbard (1977).

Two models reflecting the actual geometry of the head were developed under NHTSA sponsorship. These were reported by Shugar (1975) and Ward and Thompson (1975). The Shugar model concentrated on the mechanics of skull deformation and fracture, treating the brain as a homogenous, nearly incompressible material. The Ward model, on the other hand, assumed the skull to act as a rigid shell and only addressed the complex effects of impact and abrupt acceleration on the brain itself. For practical and economic reasons, these two approaches could not be integrated because each had several hundred degrees of freedom. Since the Ward model was more appropriate than the Shugar model for the longer-duration impacts experienced in crash environments having energy absorbing materials and structures, its further development was supported by NHTSA. The current status of the brain model originally developed by Ward and Thompson is described by Ward (1982, 1983).

An attempt to validate the model against a variety of data from many sources is described in Ward (1983). Model responses in simulations of injury-producing tests with animals, repressurized cadaver specimens, and simulations of helmet impacts producing concussion have led the author to select intracranial pressure as a measure of brain response magnitude. The author has concluded that when peak pressure in the brain is above 34 psi (235 kPa), serious injuries are likely to occur. Between 25 and 34 psi moderate injuries would be expected, and below 25 psi (173 kPa) the injuries should be no more than minor. Brain pressure tolerance (BPT) curves for a variety of head acceleration profiles have been developed. The BPT has been compared with other injury criteria like the WSTC, HIC, JHTC, and MSC. The WSTC, HIC, and JHTC permit much higher accelerations for short impacts (<5 ms) than the BPT curves. The MSC is similar to the BPT in this range. The BPT in the 5- to 10-ms duration range is best approximated by the HIC and the JHTC. The head accelerations permitted by the WSTC and MSC are lower than the accelerations permitted by the brain pressure tolerance curves in the range of 5 to 10 ms.

The marked differences between the BPT and the WSTC are surprising because part of the WSTC was developed based on pressures applied directly to the unopened dura of dogs, as reported by Hodgson et al. (1970). This paper also refers to a study by Lissner and Gurdjian (1961), in which it was determined that both pressure magnitude and time duration were responsible for concussive effects in the dog, and a pressure-time concussion tolerance curve for this species was obtained. Another study performed by Rinder (1969) on rabbits has been quoted by Goldsmith (1972). This study, too, shows a dependence of peak pressure on pulse duration for the production of concussion. It is not known whether this effect has been taken into account in the BPT curves. Hence, it appears that further verification of the BPT curves is required. Perhaps simulations of windshield impacts may help in this area, since the inertial spike produced in the windshield cracking phase produces nearly triangular pulses of short durations (1 to 5 ms) (Hodgson et al. 1973).

Whether the Ward model will develop into an injury model is not clear at this time. Various shortcomings of this model have been identified by Khalil and Viano (1982) and Goldsmith (1981). The role of skull deformation in producing injury cannot be studied by this model. The variation of Poisson's ratio as the duration of impact changes has been controversial according to the above authors. The integration time step used in the above studies has been questioned by Goldsmith. The time steps used are too long to investigate stress wave propagation effects.

Tolerance Criterion Based on Loads. An analysis of load cell data of helmeted and padded cadaver head impacts conducted by Got et al. (1978) and padded impactor tests conducted by Stalnaker et al. (1977) has been carried out by Haley et al. (1983). Linear regression of the peak load versus AIS (brain) revealed a good correlation between peak force and AIS levels. The results of the analysis showed similarities in the two data sets both in magnitude of the force and slope of the regression line. A similar analysis was carried out with Slobodnik's data (1980) on laboratory humanoid headform reconstructions of helmet damage for aviators involved in crashes. It was found that Slobodnik's data correlated well for the level of zero injury (AIS 0), but the load for AIS-5 injury was approximately 75% higher than that from the cadaver tests. This difference in load levels at AIS-5 injury level was attributed to the difference between the age of cadavers (approximately 64 years) and the age of the aviators (approximately 30 years). Based on the load levels producing AIS-1 level injuries from the three data sets, the authors have suggested 6000 N (1339 lb) as the threshold load for AIS-1 injuries in helmeted impacts. This load corresponds to an acceleration of 136 G for a 4.5-kg (10-lb) head and effective neck mass. Interestingly, an acceleration of 130 G peak with a total pulse duration of 17 ms is considered an injury threshold based on boxing data analyzed by Johnson et al. (1975). Tarrière et al. (1982) found no brain injuries in their series of tests with cadavers if the translational head accelerations were below 100 G except for 3-ms durations in frontal impacts.

It should be noted that the above data correlating loads or head accelerations with brain injury are valid only in impact situations where the external loads are applied directly to the head and local skull fractures are prevented by proper load distribution.

Brain Tolerance to Angular Acceleration. Ommaya et al. (1967) were the first to propose a human tolerance level to concussion due to angular acceleration of the head about left-right axes. The proposed tolerance curve was based on an extensive study of the angular velocities and accelerations required to produce concussion in squirrel monkeys, rhesus monkeys, and chimpanzees. A scaling relationship (i.e., damaging angular acceleration is inversely proportional to the 2/3 power of the brain mass) was utilized to extrapolate the animal data to the adult human. The scaling technique led the authors to conclude that angular accelerations of approximately 1800 rad/s^2 corresponded to a 50% probability of cerebral concussion for pulse durations greater than 20 ms. For pulse durations less than 20 ms, the relationship between angular acceleration and pulse duration should be such that an angular velocity change of 30 rad/s must take place. Ommaya and Hirsch (1971) and Ommaya (1984) have further stated that the animal data from which the human tolerance levels were extrapolated were reliable for the rhesus and sketchy for the chimpanzee. As a result, the extrapolated human data were said to be speculative and require verification from accident reconstructions.

Löwenhielm (1975) has studied the mechanisms causing ruptures of the parasagittal bridging veins using a viscoelastic model of the human brain. Löwenhielm's (1974a,b) earlier studies had indicated that the strain capacity of the bridging veins was dependent on strain rate. This rate sensitivity data, in conjunction with the above mathematical modeling exercises, led Löwenhielm to hypothesize that parasagittal bridging vein ruptures are not likely to occur if the peak angular acceleration of the head does not exceed 4500 rad/s^2 or the change in angular velocity does not exceed 70 rad/s.

Mathematical modeling studies by Advani et al. (1982) have shown that damage thresholds due to brain surface shear strains can be reached around 2000 to 3000 rad/s^2.

From a review of the above experimental and theoretical studies, Ommaya (1984) has proposed tolerance levels for the human head subjected to angular acceleration a in the midsagittal plane. For angular velocity changes less than 30 rad/s, angular accelerations less than 4500 rad/s^2 are considered safe. However, angular accelerations greater than 4500 rad/s^2 correspond to AIS-5 injuries. For angular velocities greater than 30 rad/s, angular accelerations 1700, 3000, 3900, and 4500 rad/s^2 correspond to AIS-2, 3, 4, and 5 levels of brain injuries.

It should be mentioned here that slight variations in the assumed material properties of the brain (e.g., shear modulus and loss tangent) in mathematical models can shift tolerance curves substantially (Liu et al. 1975). As a result, accurately determined material properties of the brain are required before much confidence can be placed on tolerance levels derived from mathematical models.

Skull Fracture and Head Acceleration During Direct Impact. Based on cadaver head drops on rigid, flat plates, Hodgson and Thomas (1971) have shown that frontal bone fracture occurs in the human cadaver at the same level of acceleration predicted by the Wayne State Tolerance Curve. It should be noted, however, that the impact durations were all less than 8 ms. Ono et al. (1980) have also developed a human cadaver skull fracture curve showing the relationship between average head acceleration and pulse duration. This curve is slightly higher than their proposed curve for threshold of concussion. Lesterlin et al. (1982) report that under direct impact to the head, HIC of 1000 is a reasonable estimate of skull fracture tolerance level.

A compilation of eighteen cadaver head impacts against windshields (Hodgson et al. 1973), seventeen cadaver head impacts conducted by Hodgson and Thomas (1973) against flat, rigid, and padded surfaces, and twenty helmeted and unhelmeted cadaver head impacts against flat surfaces, was done by the U.S. representatives to Working Group 6 of ISO/TC22/SC12 (1983). Analysis of the data showed that the lowest HIC corresponding to a skull fracture was 450, and the highest HIC without a skull fracture was 2351. Interestingly, these two data points were associated with the thinnest and the thickest skulls in the data bank. Analysis of the data using the Median Ranking technique proposed by Mertz and Weber (1982) showed that a HIC level of 1400 corresponds to a 50% probability of skull fracture in the cadaver population studied.

Head Impact Tolerance in Lateral and Superior-Inferior Directions. The majority of all head injury research has been confined to impacts directed parallel to the midsagittal plane. The few studies on lateral impact to the head do not agree with one another. Investigations by Gennarelli et al. (1982) seem to show that "the duration of coma, degree of post-traumatic disability, and extent of diffuse axonal injury increased from the sagittally to the obliquely to the laterally accelerated monkeys." The monkeys in the above series were subjected to pure non-deforming skull angular accelerations. Hodgson et al. (1983) found that for similar levels of energy input into monkey heads, the temporoparietal impacts produced the longest duration of unconsciousness when compared with frontal and occipital impacts. Earlier studies of Stalnaker and McElhaney (1970) also showed that, using the MSC, the tolerance levels for lateral impact were 50% lower than for longitudinal impacts. In contrast to the above studies, recent studies of Nakamura et al. (1981) and Kikuchi et al. (1982) show a higher tolerance in lateral impacts when compared to frontal or occipital impacts.

Two studies conducted at the University of Michigan Transportation Research Institute (Culver et al. 1978 and Alem et al. 1982) have investigated head and neck responses to crown (S-I) impacts. In this impact direction, the role of the neck and its initial orientation relative to the impact vector is important. The authors of the latter study do not recommend the use of HIC for predicting injury potential in the S-I direction of head impacts. The sample size of the test specimens utilized was too small for any accurate assessment of injury criterion.

Facial Injury. The discussion of facial injury is divided into soft tissue injury and bone fracture.

Soft Tissue Injury. Soft tissue injuries of the face are usually lacerations of the skin, but deeper penetration can involve the facial nerve and blood vessels, with an injury to the facial nerve being very serious because of the paralysis of the muscles supplied. Penetrating wounds through the parotid gland can involve the major stem of the facial nerve, completely paralyzing all the muscles on that side of the face.

Most of the studies on facial soft tissue injuries have been related to windshield glass, for it has been identified as the automotive component associated with the highest frequency of facial soft tissue injuries (Huelke et al. 1966). The lacerative effects of the windshield on unrestrained dummies and cadavers that were catapulted into car windshields were studied at Wayne State University (Patrick and Daniel 1966; Patrick 1966, 1967).

Even though facial lacerations were significantly reduced by the introduction of the new HPR-laminated windshield in the mid-1960s, research continued. In 1967, for example, the lacerative potential of safety glass was evaluated using simulated tissue (Rieser and Chabal 1967). In subsequent studies, the same authors were able to document injury reduction that could be possible with improved windshield design, but the problem of quantifying the laceration severities still existed (Rieser and Chabal 1969). Pickard et al. (1973) developed a laceration severity index. Others utilized this severity index to assess certain windshield modifications and did note the reduction in laceration severity according to the index (Kay et al. 1973).

Gadd et al. (1970) conducted a test series to characterize the resistance of impact loading of the skin, the soft tissue of the scalp, and other selected areas of the body using unembalmed cadaver materials. Leung et al. (1977), using four living individuals, selected skin specimens from them as well as tissue from unembalmed cadavers. They conducted 372 tests on these specimens, attempting to quantify the lacerative resistance of the skin relative to the shape of the impactor, impact velocity, etc. It was found that lacerative sensitivity was less resistant along the "crease lines" of the skin, and that the resistance of the skin to laceration increases with the age of the subject.

Facial Bone Tolerances. The earliest work on facial bone tolerances was published in 1900 by René Le Fort, a French surgeon who studied the types of fractures produced by blunt impacts to the various portions of the mid-face (Tilson et al. 1972). In a very primitive biomechanical study, he impacted the face in various areas using a mallet, a piece of wood, or table edges to produce fractures. The results reported only descriptions of the types and locations of the fractures produced. From this work came the mid-face fracture classification of Le Fort I, II, and III. These mid-face fractures vary in their extent and the area involved. The Le Fort I fracture is a horizontal fracture across the maxillary alveolar process (the supporting bone of the teeth) which is, in general, a horizontal fracture beneath the nasal opening. A Le Fort II loosens the upper jaw, with the fracture line usually extending up into the nasal opening, so that the upper jaw and palate are relatively free. The Le Fort III fracture disassociates the mid-face from the cranial vault. In general, the fracture line passes through the lateral aspects of the orbit, across the area of the bridge of the nose, and to the opposite side, thereby separating the entire mid-face region from the cranial vault.

Obviously there can be simple fractures of many of the bones of the face such as the nasal bone, the zygomatic bone, or of the mandible. Some of the bones of the face, including the bone of the nasal septum (the vomer), are relatively protected and infrequently fractured.

Mandibular fractures are quite common and can occur in any section of the bone. Frequently, fractures of the areas directly beneath the condyle (the subcondylar region) are common in occurrence because the cross section of the bone is relatively small in that region. Blows to the chin are usually the cause of subcondylar fractures. The etiology of mandibular fractures has been shown to vary among hospitals as to the location in which the hospital is found (Huelke and Hagan 1961; Huelke 1961a; Huelke et al. 1961; Huelke et al. 1962; Huelke 1962; Huelke and Burdi 1964). For example, in large city hospitals, mandibular fractures are usually caused by person to person violence, whereas in other institutions automobile accidents are the leading cause of mandibular fractures (Huelke and Hagan 1961). Experiments by Huelke and Harger (1968) and Huelke and Patrick (1964) have shown that the mandible fails in tension and that, at the site of impact, the mandible often fractures with the potential for energy being dissipated on the opposite side, or both sides, usually in the subcondylar region. Huelke (1961b) dropped a 1-in (2.5-cm) diameter steel rod weighing one pound on dry mandibles and found that 5 ft• lb (6.8 N• m) would cause single or multiple fractures. High-speed cinematography was used to observe the fractures.

The tolerances of facial bones have been studied by several investigators. Swearingen (1965) studied the strength of cadaver facial bones due to direct impact with a circular 1-in (2.5-cm) diameter impactor. He found that fractures could readily be produced to individual facial bones, and that the force required to produce a fracture was basically dependent on the area over which the force was applied. Later Hodgson (1967) studied facial bone fracture tolerances, finding that not only was the loading condition important but that the line of action, the center of the load application, as well as the area of force application were important factors. His study concentrated primarily on zygomatic zone. About the same time, Patrick et al. (1967) was applying static loads to human skulls that were stress-coated, to attempt to determine the stress distribution in the skull and the face and thus identify areas of weakness.

Nahum et al. (1968) performed impacts to cadaver heads, concentrating their work on frontal, temporal, parietal, and zygomatic bones. Because of the irregularity of the surface of the face, they used an impactor approximately 1 in (2.5 cm) in diameter. They found that female bones were less strong than the male counterparts and that the tolerances were independent of impulse duration. Some tolerances, as found by Schneider and Nahum (1972), are presented in Table 1-4.

TABLE 1-4

FACIAL IMPACT TOLERANCE OF CADAVER HEADS
(Schneider and Nahum 1972)

Bone	Force (lb)	Force (kN)
Mandible (A-P)	400	1.78
Mandible (Lateral)	200	0.89
Maxilla	150	0.66
Zygomatic Arch	200	0.89
Frontal	900	4.00
Zygomatic Areas	200	0.89

Tarrière et al. (1981), in their facial impact tests, found that the distributed-load-carrying ability of the face is considerably greater than those found in Table 1-4 for individual bones. The average fracture load was 7.325 kN (1650 lb) for four subjects.

SUMMARY AND CONCLUSIONS

The head is considered the most critical part of the body to protect from injury because of the irreversible nature of injury to the brain. The head and face together contribute 55.5% to the total IPR.

A variety of mechanisms have been postulated for mechanical damage to the brain from impacts to the head. They include: (1) direct brain contusion from skull deformation at the point of contact; (2) indirect brain contusion produced by negative pressure on the side opposite the impact; (3) brain contusion from movements of the brain against rough and irregular interior skull surfaces; (4) brain and spinal cord deformation in response to pressure gradients and motions relative to the skull, resulting in stress in the tissues; and (5) subdural hematoma from movement of the brain relative to its dural envelope, resulting in tears of connecting blood vessels. The latter three mechanisms have also been postulated for mechanical damage resulting from head motions due to indirect impact.

The data presently available for defining the response of the head to impact are limited to rigid impacts and are predominantly based on embalmed cadaver tests. The data are adequate to define general response specifications for rigid impacts to the front and side of the head, in terms of peak contact force over a range of impact velocities from 1 to 8 m/s. The corresponding acceleration response data are limited to an impact velocity range of 1 to 5 m/s.

There is a need for additional studies to define the impact response of the human head using unembalmed cadavers with rigid impact surfaces and current acceleration measurement techniques. A repeatable and reproducible method for producing padded impacts also needs to be developed to allow cadaver studies to be conducted for padded head impact response definition.

The parameters of head motion that have been associated with the production of brain injury are translational acceleration, rotational acceleration, and rotational velocity. Of these, most attention has been given to translational acceleration in terms of developing head injury criteria. For direct impacts to the head, the Wayne State Tolerance Curve and the Japan Head Tolerance Curve, both based on head translational acceleration, are in close agreement. Injury criteria that have evolved from the tolerance curve approach would be expected to provide accurate assessment of injury potential during direct head impacts.

The Head Injury Criterion (HIC), based on the resultant translational acceleration of the center of gravity of the head, is the most commonly used method of evaluating head-impact data. Statistical analysis of direct head impact cadaver test data has been used to define the relationship between HIC values and the probability of sustaining a particular level of injury, thus providing a continuous ability to interpret HIC values. A HIC level of 1000 was found to produce an expected 16% incidence of life-threatening brain injury to the adult population.

The validity of the HIC for long duration and non-contact head accelerations remains in question. Injury criteria based on head angular acceleration and angular velocity have been proposed for such situations, but they lack the extensive evaluation and review that has been given the HIC for short duration (less than 15 ms) head impacts. Mathematical models of the head hold promise for evolving into injury predictive models given proper development and evaluation. Simple models, such as the Mean Strain Criterion (MSC), which are based on translational acceleration, have the potential for describing the dependence of the injury response on impact waveform and direction of impact. The application of the MSC to dummy head accelerations, however, remains to be developed. More sophisticated finite element models of the brain and skull have been developed, but their complexities and lack of validation have hampered their development into injury predictive models.

The response of facial structures to impact loads has been studied to a limited extent. The fracture and collapse of the facial bones during distributed loading significantly reduces the peak forces and resulting head accelerations in comparison to those produced by similar impact tests to the skull.

The tolerance of the facial bones to direct impact loading has been studied by a number of researchers, and fracture loads for individual bones and the whole face have been determined. The failure characteristics of facial soft tissues due to laceration from sharp edges has been studied, and rating systems for the assessment of the severity of the lacerations have been developed. There is a need, however, to study the mechanisms of lacerations to facial tissue due to blunt impact.

REFERENCES

Abraham, S.; Johnson, C.L.; and Najjar, M.F. (1979) Weight and height of adults 18–74 years of age: United States, 1971–74. *Vital and Health Statistics*, Series 11, No. 211. U.S. Public Health Service, Hyattsville, Md.

Advani, S.; Ommaya, A.K.; and Yang, W.J. (1982) Head injury mechanisms: Characterizations and clinical evaluation. *Human Body Dynamics: Impact, Occupational, and Athletic Aspects*, pp. 1–37. Edited by D.N. Ghista. Clarendon Press, Oxford.

Alem, N.M.; Nusholtz, G.S.; and Melvin, J.W. (1982) *Superior–inferior head impact tolerance levels.* Report no. UMTRI-82-42. University of Michigan Transportation Research Institute, Ann Arbor.

Backaitis, S.H. (1981) The head injury criterion. *Head and Neck Injury Criteria: A Consensus Workshop*, pp. 175–177. Edited by A.K. Ommaya. U.S. Department of Transportation, National Highway Traffic Safety Administration, Washington, D.C.

Beier, G.; Schuller, E.; Schuck, M.; Ewing, C.; Becker, E.; and Thomas, D. (1980) Center of gravity and moments of inertia of human head. *Proc. 5th International Conference on the Biokinetics of Impacts*, pp. 218–228. IRCOBI, Birmingham, England.

Boll, T.J. (1982) Behavioral sequelae of head injury. *Head Injury*, pp. 363–376. Edited by P.R. Cooper. Williams and Wilkins, Baltimore/London.

Brinn, J.; and Staffeld, S.E. (1970) Evaluation of impact test accelerations: A damage index for the head and torso. *Proc. 14th Stapp Car Crash Conference*, pp. 188–220. Society of Automotive Engineers, New York.

Chan, H.S. (1974) Mathematical model for closed head impact. *Proc. 18th Stapp Car Crash Conference*, pp. 557–578. Society of Automotive Engineers, Warrendale, Pa.

Chapon, A.; Verriest, J.P.; Dedoyan, J.; Trauchessec, R.; and Artru, R. (1983) Research on brain vulnerability from real accidents. ISO Document No. ISO/TC22/SC12/GT6/N139.

Clauser, C.E.; McConville, J.T.; and Young, J.W. (1969) *Weight, volume, and center of mass segment of the human body.* AMRL–TR–69–70. Aerospace Medical Research Laboratory, Wright-Patterson AFB, Ohio.

Cook, W.I. (1980) Mathematical models of head injury: A ranking experiment. *Journal of Safety Research*, 12(3):127–137.

Cooper, P.R. (1982a) Epidemiology of head injury. *Head Injury*, pp. 1–14. Edited by P.R. Cooper. Williams and Wilkins, Baltimore/London.

Cooper, P.R. (1982b) Post-traumatic intracranial mass lesions. *Head Injury*, pp. 185–232. Edited by P.R. Cooper. Williams and Wilkins, Baltimore/London.

Cooper, P.R. (1982c) Skull fracture and traumatic cerebrospinal fluid fistulas. *Head Injury*, pp. 65–82. Edited by P.R. Cooper. Williams and Wilkins, Baltimore/London.

Culver, R.; Bender, M.; and Melvin, J. (1978) *Mechanisms, tolerances, and responses obtained under dynamic superior-inferior head impact.* UM–HSRI–78–2. The University of Michigan, Highway Safety Research Institute, Ann Arbor.

Dempster, W.T. (1955) *Space requirements of the seated operator.* WADC–TR–55–159 (AD87802). Wright Air Development Center, Wright–Patterson AFB, Ohio.

DiLorenzo, F. (1976) *Power and bodily injury.* SAE Paper No. 760014. Society of Automotive Engineers, Warrendale, Pa.

Eiband, A.M. (1959) *Human tolerance to rapidly applied accelerations: A summary of the literature.* NASA Memorandum 5–19–59E. NASA Lewis Research Center, Cleveland.

Eppinger, R.H. (1981) Comments during panel discussion of injury criteria. *Head and Neck Injury Criteria: A Consensus Workshop*, p. 204. Edited by A.K. Ommaya. U.S. Department of Transportation, National Highway Traffic Safety Administration, Washington, D.C.

Ewing, C.L. (1963) Design criteria and parameters of life support helmets. *Effective Life Support Helmets: Proceedings of an Invited Symposium.* Biotechnology, Inc., Washington, D.C.

Ewing, C.L.; and Unterharnscheidt F. (1976) Neuropathology and cause of death in U.S. Naval aircraft accidents. *Recent Experience/Advances in Aviation Pathology, AGARD Conference Proc. No. CP–190*, paper no. B16. Advisory Group for Aerospace Research and Development, Neuilly Sur Seine, France.

Fan, W.R.S. (1971) Internal head injury assessment. *Proc. 15th Stapp Car Crash Conference*, pp. 645–665. Society of Automotive Engineers, New York.

Friede, R.L. (1960) Specific cord damage at the atlas level as a pathogenic mechanism in cerebral concussion. *Journal of Neuropathology Experimental Neurology*, 19:266-279.

Friede, R.L. (1961a) *The pathology and mechanics of experimental cerebral concussion.* Wright-Patterson AFB, Ohio.

Friede, R.L. (1961b) Experimental concussion acceleration: Pathology and mechanics. *Archives of Neurology*, 4:449-462.

Gadd, C.W. (1961) Criteria for injury potential. *Impact Acceleration Stress Symposium*, pp. 141-144. National Research Council publication no. 977. National Academy of Sciences, Washington, D.C.

Gadd, C.W. (1966) Use of a weighted impulse criterion for estimating injury hazard. *Proc. 10th Stapp Car Crash Conference*, pp. 164-174. Society of Automotive Engineers, New York.

Gadd, C.W. (1971) Tolerable severity index in whole-head nonmechanical impact. *Proc. 15th Stapp Car Crash Conference*, pp. 809-816. Society of Automotive Engineers, New York.

Gadd, C.W. (1981) Head injury discussion paper. *Head and Neck Injury Criteria: A Consensus Workshop*, pp. 179-184. Edited by A.K. Ommaya. U.S. Department of Transportation, National Highway Traffic Safety Administration, Washington, D.C.

Gadd, C.W.; Nahum, A.M.; Schneider, D.C.; and Madeira, R.G. (1970) Tolerance and properties of superficial soft tissues in situ. *Proc. 14th Stapp Car Crash Conference*, pp. 356-368. Society of Automotive Engineers, New York.

Gennarelli, T.A. (1980) Analysis of head injury severity by AIS-80. *Proc 24th Annual Conference of the American Association of Automotive Medicine*, pp. 147-155. AAAM, Morton Grove, Ill.

Gennarelli, T.A. (1981) Mechanistic approach to head injuries: Clinical and experimental studies of the important types of injury. *Head and Neck Injury Criteria: A Consensus Workshop*, pp. 20-25. Edited by A.K. Ommaya. U.S. Department of Transportation, National Highway Traffic Safety Administration, Washington, D.C.

Gennarelli, T.A. (1982) Cerebral concussion and diffuse brain injuries. *Head Injury*, pp. 83-98. Williams and Wilkins, Baltimore/London.

Gennarelli, T.A. (1984) *Head injury lesion analysis by CT scan: Correlations to neurological variables and to outcome.* Contract DOT-HS-9-02088. University of Pennsylvania Hospital, Philadelphia (in press).

Gennarelli, T.A.; and Thibault, L.E. (1982) Biomechanics of acute subdural hematoma. *Journal of Trauma*, 22:680-686.

Gennarelli, T.A.; Ommaya, A.K.; and Thibault, L.E. (1971) Comparison of translational and rotational head motions in experimental cerebral concussion. *Proc. 15th Stapp Car Crash Conference*, pp. 797-803. Society of Automotive Engineers, New York.

Gennarelli, T.A.; Thibault, L.E.; and Ommaya, A.K. (1972) Pathological responses to rotational and translational accelerations of the head. *Proc. 16th Stapp Car Crash Conference*, pp. 296-308. Society of Automotive Engineers, New York.

Gennarelli, T.A.; Thibault, L.E.; Hume Adams, J.; Graham, D.I.; Thompson, C.J.; and Marcincin, R.P. (1982) Diffuse axonal injury and traumatic coma in the primate. *Annals of Neurology*, 12:564–574.

Goldsmith, W. (1972) Biomechanics of head injury. *Biomechanics: Its Foundations and Objectives*, pp. 585–634. Edited by Y.C. Fung et al. Prentice-Hall, Englewood Cliffs, N.J.

Goldsmith, W. (1981) Some aspects of the physical and mathematical modeling of loading to head/neck systems and implications of current DOT injury criteria. *Head and Neck Injury Criteria: A Consensus Workshop*, pp. 133–148. Edited by A.K. Ommaya. U.S. Department of Transportation, National Highway Traffic Safety Administration, Washington, D.C.

Got, C.; Patel, A.; Fayon, A.; Tarriére, C.; and Walfisch, G. (1978) Results of experimental head impacts on cadavers: The various data obtained and their relations to some measured physical parameters. *Proc. 22nd Stapp Car Crash Conference*. pp. 57–99. Society of Automotive Engineers, Warrendale, Pa.

Gross, A.G. (1985a) A new theory on the dynamics of brain concussion and brain injury. *Journal of Neurosurgery*, 15:548–561.

Gross, A.G. (1985b) Impact thresholds of brain concussion. *Journal of Aviation Medicine*, 29:725–732.

Gurdjian, E.S.; Webster, J.E.; and Lissner, H.R. (1955) Observations of the mechanism of brain concussion, contusion, and laceration. *Surgery, Gynecology, and Obstetrics*, 101:680–690.

Gurdjian, E.S.; Fernando, O.V.; Hodgson, V.R.; Thomas, L.M.; and Chason, J.L. (1965) Cellular changes in the nervous system following compressive and accelerative impacts in the dog. *Trabajos del Instituto Cajal de Investigaciones Biologicas*, Supplemento al tomo LVII, p. 39. Madrid.

Gurdjian, E.S.; Hodgson, V.R.; Thomas, L.M.; and Patrick, L.M. (1968) Significance of relative movements of scalp, skull, and intracranial contents during impact injury of the head. *Journal of Neurosurgery*, 29(1):70–72.

Haley, J.L., Jr.; Shanahan, D.F.; Reading, T.E.; and Knapp, S.C. (1983) Head impact hazards in helicopter operations and their mitigation through improved helmet design. *Impact Injury of the Head and Spine*, pp. 549–577. Edited by C.L. Ewing et al. Charles C. Thomas, Springfield, Ill.

Hess, R.L.; Weber, K.; and Melvin, J.W. (1980) *Review of literature and regulation relating to head impact tolerance and injury criteria*. Report no. UM-HSRI-80-52-1. The University of Michigan, Highway Safety Research Institute, Ann Arbor.

Hirsch, A.E.; and Ommaya, A.K. (1970) Protection from brain injury: The relative significance of translational and rotational motions of the head after impact. *Proc. 14th Stapp Car Crash Conference*, pp. 299–328. Society of Automotive Engineers, New York.

Hodgson, V.R. (1967) Tolerance of the facial bones to impact. *American Journal of Anatomy*, 120:113–122.

Hodgson, V.R. (1970) Physical factors related to experimental concussion. *Impact Injury and Crash Protection*, pp. 275-307. Edited by E.S. Gurdjian et al. Charles C. Thomas, Springfield, Ill.

Hodgson, V.R.; and Thomas, L.M. (1971) Comparison of head acceleration injury indices in cadaver skull fracture. *Proc. 15th Stapp Car Crash Conference*, pp. 190–206. Society of Automotive Engineers, New York.

Hodgson, V.R.; and Thomas, L.M. (1973) *Breaking strength of the human skull versus impact surface curvature.* Wayne State University, Detroit.

Hodgson, V.R.; and Thomas, L.M. (1975) *Head impact response.* Vehicle Research Institute, Society of Automotive Engineers, Warrendale, Pa.

Hodgson, V.R.; and Thomas, L.M. (1979) Acceleration induced shear strains in a monkey brain hemisection. *Proc. 23rd Stapp Car Crash Conference*, pp. 587–612. Society of Automotive Engineers, Warrendale, Pa.

Hodgson, V.R.; Nakamura, C.S.; and Talwalker, R.K. (1966) Response of the facial structure to impact. *Proc. 8th Stapp Car Crash Conference*, pp. 229–250. Wayne State University Press, Detroit.

Hodgson, V.R.; Thomas, L.M.; Gurdjian, E.S.; Fernando, O.V.; Greenberg, S.W.; and Chason, J.L. (1969) Advances in understanding of experimental concussion mechanisms. *Proc. 13th Stapp Car Crash Conference*, pp. 18–37. Society of Automotive Engineers, New York.

Hodgson, V.R.; Thomas, L.M.; and Prasad, P. (1970) Testing of validity and limitations of the severity index. *Proc. 14th Stapp Car Crash Conference*, pp. 169–187. Society of Automotive Engineers, New York.

Hodgson, V.R.; Thomas, L.M.; and Brinn, J. (1973) Concussion levels determined by HPR windshield impacts. *Proc. 17th Stapp Car Crash Conference*, pp. 171–190. Society of Automotive Engineers, New York.

Hodgson, V.R.; Thomas, L.M.; and Khalil, T.B. (1983) The role of impact location in reversible cerebral concussion. *Proc. 27th Stapp Car Crash Conference*, pp. 225–240. Society of Automotive Engineers, Warrendale, Pa.

Holbourn, A.H.S. (1943) Mechanics of head injury. *Lancet*, 2:438–441.

Hubbard, R.P.; and McLeod, D.G. (1974) Definition and development of a crash dummy head. *Proc. 18th Stapp Car Crash Conference*, pp. 599–628. Society of Automotive Engineers, Warrendale, Pa.

Huelke, D.F. (1961a) Mechanisms involved in the production of mandibular fractures: A study with the "stresscoat" technique, part 1—symphyseal impacts. *Journal of Dental Research*, 40:1042–1056.

Huelke, D.F. (1961b) High speed photography of mandibular fractures. *Journal of Biological Photography*, 29:137–144.

Huelke, D.F. (1962) Biomechanical studies on the bones of the face. *Impact Acceleration Stress: A Symposium*, pp. 131–133. National Academy of Sciences, National Research Council, Washington, D.C.

Huelke, D.F.; and Burdi, A.R. (1964) Location of mandibular fractures related to teeth and edentulous regions. *Journal of Oral Surgery*, 22:396–406.

Huelke, D.F.; and Hagan, E.H. (1961) An analysis of 319 case reports of mandibular fractures. *Journal of Oral Surgery, Anesthesia. and Hospital Dental Service*, 19:93-104.

Huelke, D.F.; and Harger, J.H. (1968) The mechanisms of the production of mandibular fractures: An experimental study. *Journal of Oral Surgery*, 26:86–91.

Huelke, D.F.; and Patrick, L.M. (1964) Mechanics in the production of mandibular fractures: Strain gauge measurements of impacts to the chin. *Journal of Dental Research*, 43:437–446.

Huelke, D.F.; Burdi, A.R.; and Eyman, C.E. (1961) Mandibular fractures as related to site of trauma and state of dentition. *Journal of Dental Research*, 40:1262–1274.

Huelke, D.F.: Burdi, A.R.; and Eyman, C.E. (1962) Association between mandibular fractures and site of trauma, dentition and age. *Journal of Oral Surgery, Anesthesia and Hospital Dental Service*, 20:478–481.

Huelke, D.F.; Grabb, W.C.; and Gikas, P.W. (1966) Injuries and deaths from windshield and instrument panel impacts. *Proc. 8th Stapp Car Crash and Field Demonstration Conference*, pp. 167–184. Edited by L.M. Patrick. Wayne State University Press, Detroit.

International Organization for Standardization, Working Group 6, U.S. Delegation. (1983) *Position paper on HIC levels.* ISO Document No. ISO/TC22/SC12/GT6/N146.

Jennett, B. (1976) Some medicolegal aspects of the management of acute head injury. *British Medical Journal*, 1:1383–1385.

Johnson, J.; Shorecki, J.; and Wells, R.P. (1975) Peak accelerations of the head experienced in boxing. *Medical and Biological Engineering*, 13(3):396–404.

Kallieris, D.; Schmidt, G.; and Häusler, E. (1980) Brain injuries under high speed loadings: A study with models and cadaver heads. *Proc. 5th International Conference on the Biokinetics of Impacts*, pp. 229–240. IRCOBI, Bron, France.

Kay, S.E.; Pickard, J.; and Patrick, L.M. (1973) Improved laminated windshield with reduced laceration properties. *Proc. 17th Stapp Car Crash Conference*, pp. 127–169. Society of Automotive Engineers, New York.

Kenner, V.H. (1971) *On the dynamic loading of fluid-filled spherical shells: A model for head injury.* Ph.D. Dissertation. University of California, Berkeley.

Khalil, T.B.; and Hubbard, R.P. (1977) Parametric study of head response by finite element modeling. *Journal of Biomechanics*, 10(2):119–131.

Khalil, T.B.; and Viano, D.C. (1982) Critical issues in finite element modeling of head impact. *Proc. 26th Stapp Car Crash Conference*, pp. 87-102. Society of Automotive Engineers, Warrendale, Pa.

Kikuchi, A.; Ono, K.; and Nakamura, N. (1982) Human head tolerance to lateral impact deduced from experimental head injuries using primates. *Proc. 9th International Technical Conference on Experimental Safety Vehicles*, pp. 251-261. U.S. Department of Transportation, National Highway Traffic Safety Administration, Washington, D.C.

King, H.I.; Nakhla, S.S.; and Mital, N.K. (1978) Simulation of head and neck response to $-G_x$ and $-G_z$ impacts. *Models and Analogues for the Evaluation of Human Biodynamic Response, Performance, and Protection, AGARD Conference Proc. No. CP-253*, paper no. A7. Advisory Group for Aerospace Research and Development, Neuilly Sur Seine, France.

Kraus, J.F.; Black, M.A.; Hessol, N.; Ley, P.; Rokaw, W.; Sullivan, C.; Bowers, S.; Knowlton, S.; and Marshall, L. (1984) The incidence of acute brain injury and serious impairment in a defined population. *American Journal of Epidemiology*, 119(2):186-200.

Landesman, S.; and Cooper, P R. (1982) Infectious complications of head injury. *Head Injury*, pp. 343-362. Edited by P.R. Cooper. Williams and Wilkins, Baltimore/ London.

Lenox, J.B.; Stalnaker, R.L.; White, C.D.: Moore, G.T.; Anderson, O.M.; Schleicher, R.R.; Peel, H.H.; Martin, S.S.; Driscoll, G.D.; Huntington, H.W.; Carey. K.D.; Haffner, M.P.; and Ommaya, A.K. (1982) Development of neck injury tolerance criteria in human surrogates. 1. Static tensile loading in the baboon neck: Preliminary observations. *Proc. 9th International Technical Conference on Experimental Safety Vehicles*, pp. 279-286. U.S. Department of Transportation, National Highway Traffic Safety Administration, Washington, D.C.

Lesterlin, D.; Tarriére, C.; Walfisch, G.; Fayon, A.; Got, C.; Patel, A.; and Hureau, J. (1982) Proper use of HIC under different typical collision environments. *Proc. 9th International Technical Conference on Experimental Safety Vehicles*, pp. 321-336. U.S. Department of Transportation, National Highway Traffic Safety Administration.

Leung, Y.C.; Lopat, E.; Fayon, A.; Banzet, P.; and Tarriére, C. (1977) Lacerative properties of the human skin during impact. *Proc. 3rd International Conference on Impact Trauma*, pp. 399-411. IRCOBI, Bron.

Lissner, H.R.; and Gurdjian, E.S. (1961) *Experimental cerebral concussion.* ASME 60-WA-273. American Society of Mechanical Engineers, New York.

Lissner, H.R.; Lebow, M.; and Evans, F.G. (1960) Experimental studies on the relation between acceleration and intracranial pressure changes in man. *Surgery, Gynecology, and Obstetrics*, 111:329-338.

Liu, Y.K.; Chandran, K.B.; and vonRosenburg, D.V. (1975) Angular acceleration of viscoelastic (Kelvin) material in a rigid spherical shell: A rotation head injury model. *Journal of Biomechanics*, 8:285-292.

Löwenhielm, P. (1974a) Dynamic properties of the parasagittal bridging veins. *Zeitschrift fur Rechtsmedizin*, 74:55-62.

Löwenhielm, P. (1974b) Strain tolerance of the vv. cerebri sup. (bridging veins) calculated from head-on collision tests with cadavers. *Zeitschrift fur Rechtmedizin*, 75:131-144.

Löwenhielm, P. (1975) Mathematical simulation of gliding contusions. *Journal of Biomechanics*, 8:351-356.

Lubock, P.; and Goldsmith, W. (1980) Experimental cavitation studies in a model head-neck system. *Journal of Biomechanics*, 13:1041-1052.

McConville, J.T.; Churchill, T.D.; Kaleps, I.; Clauser, C.E.; and Cuzzi, J. (1980) *Anthropometric relationships of body and body segment moments of inertia.* AMRL-TR-80-119. Aerospace Medical Research Laboratory, Wright-Patterson AFB, Ohio.

McElhaney, J.H.; Stalnaker, R.L.; and Roberts, V.L. (1973) Biomechanical aspects of head injury. *Human Impact Response—Measurement and Simulation, Proceedings of the Symposium on Human Impact Response*, pp. 85-110. Edited by W.F. King and H.J. Mertz. Plenum Press, New York.

Mertz, H.J. (1967) *The kinematics and kinetics of whiplash.* Ph.D. Dissertation. Wayne State University, Detroit.

Mertz, H.J.; and Weber, D.A. (1982) Interpretations of the impact responses of a 3-year-old child dummy relative to child injury potential. *Proc. 9th International Technical Conference on Experimental Safety Vehicles*, pp. 368-376. U.S. Department of Transportation, National Highway Traffic Safety Administration, Washington, D.C.

Mucciardi, A.N.; Sanders, J.D.; and Eppinger, R.H. (1977) Prediction of brain injury measures from head motion parameters. *Proc. 21st Stapp Car Crash Conference*, pp. 369-415. Society of Automotive Engineers, Warrendale, Pa.

Nahum, A.M.; and Smith, R.W. (1976) An experimental model for closed head impact injury. *Proc. 20th Stapp Car Crash Conference*, pp. 783-814. Society of Automotive Engineers, Warrendale, Pa.

Nahum, A.M.; Gatts, J.D.; Gadd, C.W.; and Danforth, J. (1968) Impact tolerance of the skull and face. *Proc. 12th Stapp Car Crash Conference*, pp. 302-316. Society of Automotive Engineers, New York.

Nahum, A.M.; Smith, R.; and Ward, C.C. (1977) Intracranial pressure dynamics during head impact. *Proc. 21st Stapp Car Crash Conference*, pp. 339-366. Society of Automotive Engineers, Warrendale, Pa.

Nakamura, N.; Masuzawa, H.; Sekino, H.; Kono, H.; Kikuchi, A.; and Ono, K. (1981) Which is the more severe impact on the head: Sagittal or lateral? *Head and Neck Injury Criteria: A Consensus Workshop*, pp. 61-68. Edited by A.K. Ommaya. U.S. Department of Transportation, National Highway Traffic Safety Administration, Washington, D.C.

National Center for Health Statistics. (1965) Weight, height and selected body dimensions of adults: United States, 1960–1962. *Vital and Health Statistics*, Series 11, No. 8. U.S. Public Health Service, Washington, D.C.

Newman, J.A. (1975) On the use of head injury criterion (HIC) in protective headgear evaluation. *Proc. 19th Stapp Car Crash Conference*, pp. 615–640. Society of Automotive Engineers, Warrendale, Pa.

Newman, J.A. (1980) Head injury criteria in automotive crash testing. *Proc. 24th Stapp Car Crash Conference*, pp. 703–747. Society of Automotive Engineers, Warrendale, Pa.

Newman, J.A. (1982) Temporal characteristics of translational acceleration in the prediction of helmeted head injury. *Impact Injury Caused by Linear Acceleration: Mechanisms, Prevention and Cost, AGARD Conference Proc. No. CP-322*, pp. 4.1–4.7. Advisory Group for Aerospace Research and Development, Neuilly Sur Seine, France.

Ommaya, A.K. (1984) Biomechanics of head injuries: Experimental aspects. *Biomechanics of Trauma*. Edited by A. Nahum and J.W. Melvin. Appleton-Century-Crofts, East Norwalk, Conn. (in press).

Ommaya, A.K.; and Hirsch, A.E. (1971) Tolerances for cerebral concussion from head impact and whiplash in primates. *Journal of Biomechanics*, 4:13–20.

Ommaya, A.K.; Hirsch, A.E.; and Martinez, J.L. (1966) The role of whiplash in cerebral concussion. *Proc. 10th Stapp Car Crash Conference*, pp. 314–324. Society of Automotive Engineers, New York.

Ommaya, A.K.; Yarnell, P.; Hirsch, A.E.: and Harris, E.H. (1967) Scaling of experimental data on cerebral concussion in sub-human primates to concussion threshold for man. *Proc. 11th Stapp Car Crash Conference*, pp. 47–52. Society of Automotive Engineers, New York.

Ono, K.; Kikuchi, A.; Nakamura, M.; Kobayashi, H.; and Nakamura, N. (1980) Human head tolerance to sagittal impact reliable estimation deduced from experimental head injury using subhuman primates and human cadaver skulls. *Proc. 24th Stapp Car Crash Conference*, pp. 101–160. Society of Automotive Engineers, Warrendale, Pa.

Patrick, L.M. (1966) Cadaver windshield research. *Plastic and Reconstructive Surgery*, 37:314–323.

Patrick, L.M. (1967) Prevention of instrument panel and windshield head injuries. *Proc. of the Prevention of Highway Injury Symposium*, pp. 169–181. Edited by M.L. Selzer, P.W. Gikas, and D.G. Huelke. The University of Michigan, Highway Safety Research Institute, Ann Arbor.

Patrick, L.M.; and Daniel, R.P. (1966) Comparison of standard and experimental windshields. *Proc. 8th Stapp Car Crash and Field Demonstration Conference*, pp. 147–166. Edited by L.M. Patrick. Wayne State University Press, Detroit.

Patrick, L.M.; Lissner, H.R.; and Gurdjian, E.S. (1965a) Survival by design: Head protection. *Proc. 7th Stapp Car Crash Conference*, pp. 483–499. Charles C. Thomas, Springfield, Ill.

Patrick, L.M.; Lange, W.A.; and Hodgson, V.R. (1965b) Facial injuries: Causes and prevention. *Proc. 7th Stapp Car Crash Conference*, pp. 541-568. Edited by D.M. Severy. Charles C. Thomas, Springfield, Ill.

Patrick, L.M.; Lange, W.A.; and Hodgson, V.R. (1967) Facial injuries: Cause and prevention. *Proc. 7th Stapp Car Crash Conference*, pp. 541–568. Charles C. Thomas Publishers, Springfield, Ill.

Penn, R.D.; and Clasen, R.A. (1982) Traumatic brain swelling and edema. *Head Injury*, pp. 233-256. Edited by P.R. Cooper. Williams and Wilkins, Baltimore/London.

Pickard, J.; Brereton, P.A.; and Hewson, A. (1973) An objective method of assessing laceration damage to simulated facial tissue. *Proc. 17th Annual Conference of the American Association of Automotive Medicine*, pp. 148–165. AAAM, Morton Grove, Ill.

Reynolds, H.M.; Clauser, C.E.; McConville, J.; Chandler, R.; and Young, J.W. (1975) *Mass distribution properties of the male cadaver.* SAE paper no. 750424. Society of Automotive Engineers, Warrendale, Pa.

Rieser, R.B.; and Chabal, J. (1967) Safety performance of laminated glass configurations. *Proc. 11th Stapp Car Crash Conference*, pp. 86–105. Society of Automotive Engineers, New York.

Rieser, R.B.; and Chabal, J. (1969) Laboratory studies on laminated safety glass and installations on performance. *Proc. 13th Stapp Car Crash Conference*, pp. 76–116. Society of Automotive Engineers, New York.

Rinder, L. (1969) *Experimental brain concussion by sudden intracranial input of fluid.* Ph.D. Dissertation. University of Göteborg, Sweden.

Robbins, D.H. (1983) *Development of anthropometrically based design specifications for an advanced adult anthropomorphic dummy family. Volume 2: Anthropometric specifications for mid-sized male dummy.* Report no. UMTRI 83-53-2. University of Michigan Transportation Research Institute, Ann Arbor.

Sances, A., Jr.; Mykelburst, J.; Cusick, J.F.; Weber, R.; Houterman, C.; Larson, S.J.; Walsch, P.; Chilbert, M.; Prieto, T.; Zyvoloski, M.; Ewing, C.L.; Thomas, D.; and Saltzburg, B. (1981) Experimental studies of brain and neck injury. *Proc. 25th Stapp Car Crash Conference*, pp. 149–196. Society of Automotive Engineers, Warrendale, Pa.

Schneider, D.C.; and Nahum, A.M. (1972) Impact studies of facial bones and skull. *Proc. 16th Stapp Car Crash Conference*, pp. 186-203. Society of Automotive Engineers, New York.

Scott, W.E. (1981) Epidemiology of head and neck trauma in victims of motor vehicle accidents. *Head and Neck Injury Criteria: A Consensus Workshop*, pp. 3-6. Edited by A.K. Ommaya. U.S. Department of Transportation, National Highway Traffic Safety Administration, Washington, D.C.

Shugar, T.A. (1975) Transient structural response of the linear skull–brain system. *Proc. 19th Stapp Car Crash Conference Proceedings*, pp. 581–614. Society of Automotive Engineers, Warrendale, Pa.

Slattenschek, A.; and Tauffkirchen, W. (1970) Critical evaluation of assessment methods for head impact applied in appraisal of brain injury hazard, in particular in head impact on windshields. *1970 International Automobile Safety Conference Compendium*, pp. 1084–1112. Society of Automotive Engineers, New York.

Slobodnik, B.A. (1980) *SPH-4 helmet damage and head injury correlation.* USAARL 80-7. U.S. Army Aeromedical Research Laboratory, Fort Rucker, Al.

Society of Automotive Engineers, Human Injury Criteria Task Force. (1984) *Human tolerance to impact conditions as related to motor vehicle design.* SAE Handbook Supplement J885-84. Society of Automotive Engineers, Warrendale, Pa.

Society of Automotive Engineers, Human Mechanical Response Task Force. (1985) *Human mechanical response characteristics.* SAE J1460. Society of Automotive Engineers, Warrendale, Pa.

Stalnaker, R.L.; and McElhaney, J.H. (1970) *Head injury tolerance for linear impacts by mechanical impedance methods.* ASME 70-WA/BHF-4. American Society of Mechanical Engineers, New York.

Stalnaker, R.L.; McElhaney, J.H.; Snyder, R.G.; and Roberts, V.L. (1971) *Door crashworthiness criteria.* The University of Michigan, Highway Safety Research Institute, Ann Arbor.

Stalnaker, R.L.; Roberts, V.L.; and McElhaney, J.H. (1973) Side impact tolerance to blunt trauma. *Proc. 17th Stapp Car Crash Conference*, pp. 377–408. Society of Automotive Engineers, New York.

Stalnaker, R.L.; Melvin, J.W.; Nusholtz, G.S.; Alem, N.M.; and Benson, J.B. (1977) Head impact response. *Proc. 21st Stapp Car Crash Conference*, pp. 303–335. Society of Automotive Engineers, Warrendale, Pa.

Swearingen, J.J. (1965) *Tolerances of the human face to crash impact.* Civil Aeromedical Research Institute, Oklahoma City, Ok.

Tabaddor, K. (1982) Emergency care: Initial evaluation. *Head Injury*, pp. 15–26. Edited by P.R. Cooper. Williams and Wilkins, Baltimore, London.

Tarrière, C. (1981) Investigation of brain injuries using the C.T. scanner. *Head and Neck Injury Criteria: A Consensus Workshop*, pp. 39–49. Edited by A.K. Ommaya. U.S. Department of Transportation, National Highway Traffic Safety Administration, Washington, D.C.

Tarrière, C.; Leung, Y.C.; Fayon, A.; Got, C.; Patel, A.; and Banzet, P. (1981) Field facial injuries and study of their simulation with dummy. *Proc. 25th Stapp Car Crash Conference*, pp. 435–468. Society of Automotive Engineers, Warrendale, Pa.

Tarrière, C.; Walfisch, G.; Fayon, A.; Got, C.; Guillon, F.; Patel, A.; and Hureau, J. (1982) Acceleration, jerk and neck-flection angle: Their respective influences on the occurrence of brain injury. ISO Document No. ISO/TC22/SC12/GT6 (USA-13) 118. Also in French in *Impact Injury Caused by Linear Acceleration: Mechanisms, Prevention and Cost, AGARD Conference Proc. No. CP-322*, pp. 12.1–12.23. Advisory Group for Aerospace Research and Development, Neuilly Sur Seine, France.

Thomas, L.M. (1970) Mechanisms of head injury. *Impact Injury and Crash Protection*, pp. 27-42. Edited by E.S. Gurdjian et al. Charles C. Thomas, Springfield, Ill.

Thomas, D.J.; and Jessop, M.E. (1983) Experimental Head and Neck Injury. *Impact Injury of the Head and Spine*, pp. 177-220. Edited by C.L. Ewing et al. Charles C. Thomas, Springfield, Ill.

Tilson, N.B.; McFee, A.S.; and Soudah, H.P. (1972) *The Maxillo-Facial Works of René Le Fort.* University of Texas Dental Branch, Houston, Tx.

Unterharnscheidt, F.J. (1970) Discussion of paper on mechanisms of head injury. *Impact Injury and Crash Protection*, pp. 43-62. Edited by E.S. Gurdjian et al. Charles C. Thomas, Springfield, Ill.

Unterharnscheidt, F.J. (1971) Translational versus rotational acceleration: Animal experiments with measured input. *Proc. 15th Stapp Car Crash Conference*, pp. 767-770. Society of Automotive Engineers, New York.

Unterharnscheidt, F.J. (1983) Neuropathology of Rhesus monkeys undergoing $-G_x$ impact acceleration. *Impact Injury of the Head and Spine*, pp. 94-176. Edited by C.L. Ewing et al. Charles C. Thomas, Springfield, Ill.

Versace, J. (1971) A review of the severity index. *Proc. 15th Stapp Car Crash Conference*, pp. 771-796. Society of Automotive Engineers, New York.

Walker, L.B., Jr.; Harris, E.H.; and Pontius, U.R. (1973) Mass, volume, center of mass, and mass moment of inertia of head and head and neck of human body. *Proc. 17th Stapp Car Crash Conference*, pp. 525-537. Society of Automotive Engineers, New York.

Ward, C.C. (1982) Finite element models of the head and their use in brain injury research. *Proc. 26th Stapp Car Crash Conference*, pp. 71-85. Society of Automotive Engineers, Warrendale, Pa.

Ward, C.C. (1983) Finite element modelling of the head and neck. *Impact Injury of the Head and Spine*, pp. 421-474. Edited by C.L. Ewing et al. Charles C. Thomas, Springfield, Ill.

Ward, C.C.; and Chan, M. (1980) Rotation generated shear strains in the brain. *International Workshop on Human Subjects for Biomechanical Research, Eighth Annual Meeting*, pp. 11-19. No publisher.

Ward, C.C.; and Thompson, R.B. (1975) The development of a detailed finite element brain model. *Proc. 19th Stapp Car Crash Conference*, pp. 641-674. Society of Automotive Engineers, Warrendale, Pa.

CHAPTER 2

SPINE

G.W. Nyquist and A.I. King
Wayne State University
Detroit, Michigan

The human vertebral column is the principal load-bearing structure of the head and torso and provides protection for the spinal cord. The cervical spine also provides the head with mobility relative to the torso, the thoracic spine allows limited mobility of the upper torso and rib cage, and the lumbar segment provides the lower torso with mobility. The protective role of the vertebral column is analogous to the function served by the skull to protect the brain. Anatomical requirements dictate, however, that the spine be flexible and yet strong, so that it can serve a multitude of functions. Like the skull, it is strong, but not strong enough to always withstand mechanical insults of modern day transportation systems. Injuries that affect the function of the spinal cord can result in death, quadriplegia, or paraplegia. Spinal cord injuries almost always cause permanent disabilities.

Huelke et al. (1981) reviewed cervical injury data collected under the National Crash Severity Study (NCSS). Data representing occupants who sustained severe, serious, critical-to-life, and fatal cervical injuries were reviewed. The frequency of such injuries was 0.4% for front seat occupants. This frequency rose to 7% for those who were ejected. Severe to fatal neck injuries were common in frontal and side impacts, and the age group most commonly sustaining these injuries was 16 to 25 years. It was estimated that fatal cervical injuries made up about 20% of all occupant fatalities (5,940 cases) and that about 5,000 cases of quadriplegia per year resulted from automotive accidents.

NCSS files were scanned by King (1984) to sort out those cases in which either the lumbar or the thoracic spine was involved. The NCSS covered 12,050 accidents involving 15,973 vehicles and 26,932 occupants. The principal vehicle types were passenger cars, vans, and light trucks; there were very few motorcycles. Out of these cases, a total of 235 occupants (0.8%) sustained spinal injuries. Approximately 26% of these 235 were involved in rollovers and 20% in frontal impacts with fixed objects. About 22% of these injuries were found in cases of complete or partial ejection from the vehicle. Most of these occupants were unrestrained. Three were lap belted and one wore a three-point belt. Fractures in the lumbar region accounted for about 60% of the spinal injuries. The abbreviated injury scale numbers for all spinal injuries varied from minor to critical (AIS 1 to 5). There were six dislocations and six injuries to the spinal cord.

Although injury to the spine, including the cervical spine, can have serious consequences, the actual incidence of such injuries is relatively low, and thus, according to the Injury Priority Analysis, they probably contribute less than 6% to the total IPR. This figure is uncertain because NASS does not code the spine directly, but rather incorporates it into the neck and back regions.

ANATOMY OF THE SPINE

The normal vertebral column is made up of twenty-four individual bones called vertebrae, that are joined together by several different types of soft tissue. The primary types of soft tissue are the intervertebral discs, ligaments, and skeletal muscle. As shown in Figure 2-1, the seven vertebrae supporting the head constitute the cervical spine, while the twelve vertebrae below it form the thoracic spine. The lumbar spine is the lowest segment and is made up of five vertebrae. The entire column is supported by the sacrum, which is anatomically a part of the pelvic girdle. It is conventional to refer to the individual vertebrae in a numerical order prefixed by the letters C, T, L, or S, indicating the spinal component.

In general, each vertebra consists of a body, neural arches (pedicles, laminae, and two pairs of facets), a spinous process, and transverse processes. The body is a cylindrically shaped bone consisting of a centrum of spongy bone surrounded by a thin layer of cortical (compact) bone. The endplates above and below the centrum are cartilaginous. The sides of the body are usually slightly concave with a narrow waist at midlevel. Figure 2-2 shows a typical lumbar vertebra, viewed from the side. The pedicles arise from the postero-lateral areas of the body and are directed posteriorly. They form the sides of the spinal canal, which surrounds the spinal cord and affords it mechanical protection. The laminae are pieces of bone of quadrilateral cross section that form the back of the spinal canal. At the junction between the pedicles and the laminae are the articular facets. Each vertebra has four facets, two superior and two inferior. A posterior view of the facets of a lumbar vertebra is shown in Figure 2-3. These bony projections articulate with mating projections (facets) of the vertebrae above and below. The joints formed by the facets are diarthrodial (freely moving) joints, enclosed by capsular ligaments. The orientation of the facet joint surfaces varies from vertebra to vertebra and is of biomechanical interest, because the facets form load-bearing junctions between the vertebral bodies. The geometry of the facets will be described below.

Continuing with the general description of a typical vertebra, the transverse and spinous processes complete the posterior structure. They act as attachment points for muscles and ligaments and can be considered as short cantilever beams. The vertebrae gradually increase in size down the spine, roughly in proportion to the weight they support. The lateral view of the entire column in Figure 2-1 shows three principal spinal curves: the lordotic cervical, lordotic lumbar, and kyphotic thoracic curves. The normal spine is straight when viewed frontally. It should also be noted that the thoracic spine supports the posterior section of the rib cage, and a pair of ribs extends from each thoracic vertebra. These ribs articulate with the vertebral bodies near the junction with the pedicles and at the tips of the transverse processes.

A few of the special features of the spine will now be discussed. The first cervical vertebra (C1) is called the atlas. It does not have a vertebral body nor a spinous process but rather is a ring of bone. The superior pair of facets articulate with the skull, allowing a nodding motion of the head. There is thus no intervertebral disc between the skull and C1. The second cervical vertebra (C2) is called the axis, and it articulates with C1 to permit axial rotation of the head (i.e., the "no" gesture). There is no disc between C1 and C2. The body of C2 has a superior projection called the odontoid process (or dens), which is located at the level of C1 and is held in place against the inner anterior aspect of the C1 arch by several short, tough ligaments.

In order to describe the orientation of the facet joint surfaces, it is convenient to use a unit normal vector to establish the approximate orientation of these surfaces. Some of the surfaces are slightly curved, and the description of their orientation assumes the vector

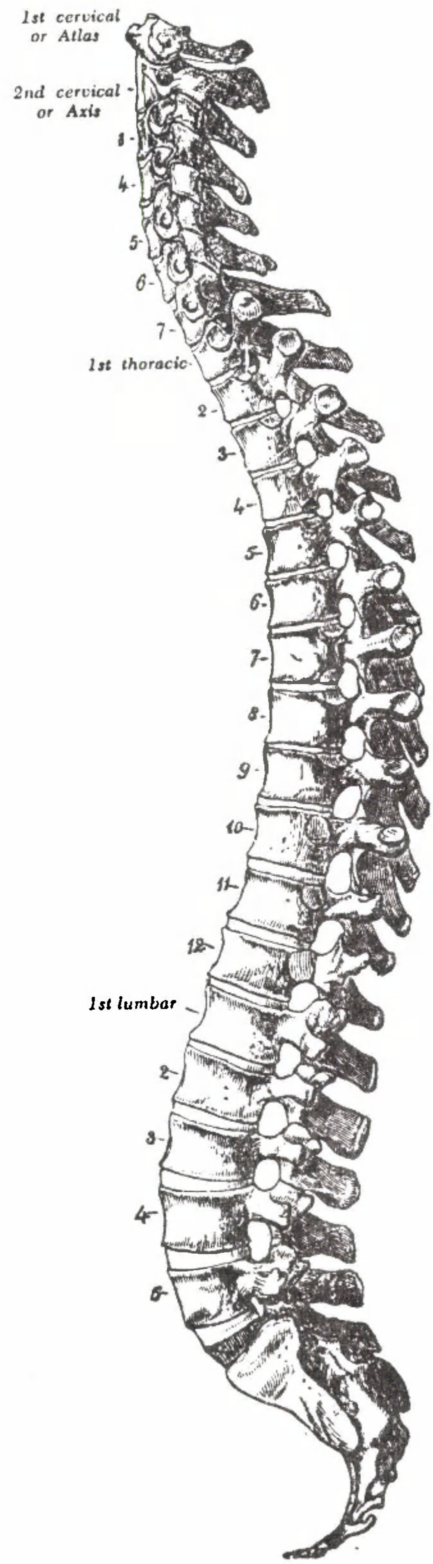

FIGURE 2-1. Lateral view of the spine (*Gray's Anatomy*, American edition).

FIGURE 2-2. Lateral view of a lumbar vertebra.

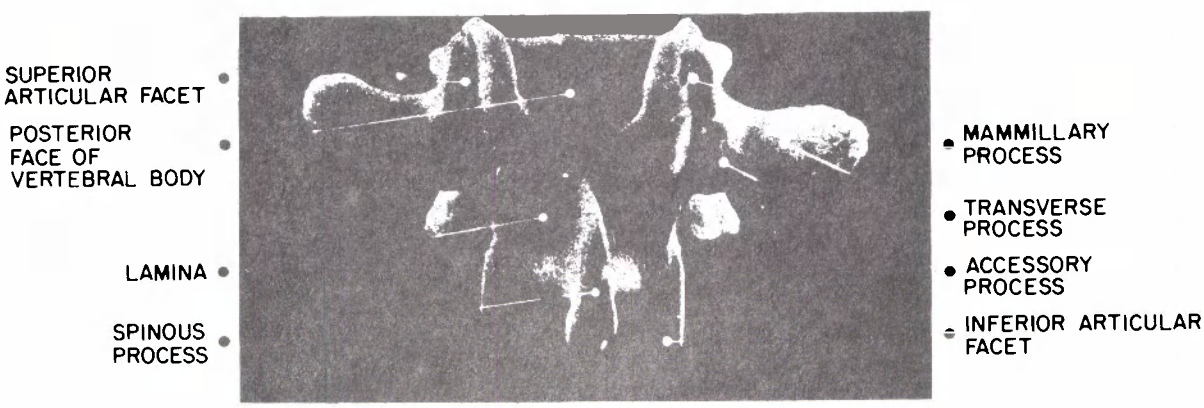

FIGURE 2-3. Posterior view of a lumbar vertebra.

to be located at the center of the surface. For the superior facets of the cervical vertebrae, the vector is directed superiorly and posteriorly, with C1 and C2 having only a slight rearward tilt, while the angle increases to a maximum of about 30° at the level of C4-C5. The tilt is less at the C5-C6 and C6-C7 junction but is again about 30° between C7 and T1, the first thoracic vertebra. The unit normal vector for thoracic superior facets is directed generally posteriorly with a variable lateral component of 10° to 20° and an upward tilt of about 15° to 30° (Gogan et al. 1983). The lumbar surfaces are slightly curved, but the unit normal vector is directed medially. Its orientation tends to shift to a postero-medial direction for the lower lumbar vertebrae, but the vector tends to lie in a horizontal plane. A pictorial description of the orientation of facet surfaces can be found in Gray (1973). Another special feature is the inclination of the fifth lumbar vertebra (L5). The endplates are inclined at the L4-L5 and L5-S1 level due to the lordotic curvature of the lumbar spine. The forward inclination of L5 can be more than 30° in some standing individuals.

The vertebrae are joined together by soft tissue, anteriorly by ligaments and intervertebral discs and posteriorly by ligaments and facet joint capsules. Intervertebral discs are cartilaginous in origin and consist principally of collagen, proteoglycans, and water. The disc can be divided into two main regions, the nucleus pulposus and the annulus fibrosus. The latter is a ring of primarily type I collagen (the type found in skin, tendon, and bone), made up of dense layers of collagen fibers that have an intricacy of pattern that almost defies description. In general, the direction of the fibers in adjacent layers cross each other at an oblique angle, but the direction of the fibers in any given layer can also change, or the fibers can bifurcate and assume more than one direction. In the lumbar region, twelve to sixteen layers can be found anteriorly. Type II collagen (the type found in hyaline cartilage) can be found in the nucleus, which has a higher concentration of proteoglycans, giving it a gel-like characteristic. Proteoglycans have an affinity for water and are responsible for the maintenance of tension in the annular collagen fibers.

The anatomy and function of the disc is affected by age. Disc degeneration begins at a very young age, and normal healthy discs are the exception rather than the rule in spines over the age of 25. The number and size of collagen fibrils increase with age, and the distinguishing features of the nucleus disappear as age transforms the entire disc into fibrocartilage. A detailed description of the anatomy of the disc can be found in Peacock (1952) and in Buckwalter (1982).

Each pair of articular facets are enclosed by a joint capsule and appear to allow the spine to flex freely while acting as motion limiters in spinal extension (or rearward bending). The joint surfaces are lined with articular cartilage and are lubricated by synovial fluid.

There are three spinal ligaments that run along the entire length of the spine. They are the anterior and posterior longitudinal ligaments, which line the anterior and posterior aspects of the vertebral bodies, and the supraspinous ligament, which joins the tips of the spinous processes. The ligamentum flavum (yellow ligament) is a strong band that connects adjacent laminae behind the spinal cord. The interspinous ligament is a thin, tough membrane located between adjacent spinous processes.

The spine is maintained in an erect posture by the skeletal musculature. The extensor muscles of the thoracolumbar spine can be divided into two main groups: the superficial transversocostal and splenius group and the deeper transversospinal group. The former group contains muscles that arise from the pelvic region and insert at various levels from the 6th to the 12th rib. Others arise from the lower ribs and insert at the upper ribs or along the cervical spine. The deeper group contains muscles that join one vertebra to another or span one or more vertebrae. The principal flexors of the thoracolumbar spine are the internal oblique muscles and the rectus abdominus. The cervical spine is extended by muscles that are a continuation of the extensors of the thoracolumbar spine. It also has a group of flexors located anteriorly.

SPINAL INJURY MECHANISMS FROM CLINICAL AND LABORATORY EXPERIENCE

Injuries to the vertebral column are discussed below under two main categories: (1) injuries unique to the cervical spine, and (2) injuries to the spine in general.

Injuries Unique to the Cervical Spine. Injuries to the upper cervical spine (particularly at the atlanto-occipital joint) are considered to be more serious and life threatening than those at a lower level. The atlanto-occipital joint can be dislocated either by an axial torsional load or a shear force applied in the anteroposterior direction, or vice versa. A large axial compression force can also cause the arches of C1 to fracture, breaking it up into two to four sections. The odontoid process of C2 is also a vulnerable area. Extreme flexion of the neck is a common cause of odontoid fractures, and a large percentage of these injuries are related to automotive accidents (Pierce and Barr 1983). Fractures through the pars interarticularis (a narrow isthmus, containing a foramen housing the vertebral artery, between the superior and inferior articular processes) of C2, commonly known as "hangman's" fractures in automotive collisions, are the result of a combined axial compression force and extension (rearward bending) of the cervical spine. Impact of the forehead and face of unrestrained occupants with the windshield can result in this injury. Garfin and Rothman (1983) provide an interesting discussion of this injury and trace the history of execution by hanging. It was estimated by a British judiciary committee that the energy required to cause a hangman's fracture was 1,260 ft•lb (1,708 N•m).

In automotive type accidents, the loading on the neck due to head contact forces is usually a combination of axial compression or tension, shear, and bending. Bending loads are almost always present, and the degree of axial or shear force is dependent upon the location and direction of the contact force. For impacts near the crown of the head, compressive forces predominate. If the impact is principally in the transverse plane, there is less compression and more shear. Bending modes are infinite in number because the impact can come from any angle around the head. To limit the scope of this discussion, the following injury modes will be considered: tension-flexion, tension-extension, compression-flexion, compression-extension in the midsagittal plane, and lateral bending.

Tension-Flexion Injuries. Forces resulting from inertial loading of the head-neck system can result in flexion of the cervical spine while it is being subjected to a tensile force. In experimental impacts of restrained subjects undergoing $-G_x$ acceleration, Thomas and Jessop (1983) reported atlanto-occipital separation and C1-C2 separation occurring in subhuman primates at 120 G. Similar injuries in human cadavers were found at 34 to 38 G by Cheng et al. (1982), who used a preinflated driver airbag system that restrained the thorax but allowed the head and neck to rotate over the bag.

Tension-Extension Injuries. The most common type of injury due to combined tension and extension of the cervical spine is the "whiplash" syndrome. However, a large majority of such injuries involve the soft tissues of the neck. In severe cases, tear drop fractures of the anterior-superior aspect of the vertebral body can occur. Alternately, separation of the anterior aspect of the disc from the vertebral endplate is known to occur. More severe injuries occur when the chin impacts the instrument panel or when the forehead impacts the windshield. In both cases, the head rotates rearward and applies a tensile and bending load on the neck. In the case of windshield impact by the forehead, hangman's fracture can occur. Garfin and Rathman (1983) suggested that it is caused by spinal compression and extension. Hangman's fracture is an injury peculiar to the second cervical vertebra (C2), in which the pars interarticularis is fractured. The pars is located between the superior and inferior facets. It should be noted that the facet joints of C2 are anterior to the pedicles and the spinal canal.

Compression-Flexion Injuries. When a force is applied to the posterior-superior quadrant of the head, or when a crown impact is administered while the head is flexed forward, the neck is subjected to a combined load of axial compression and forward bending. The common fractures seen are anterior wedge fractures of vertebral bodies. With increased load, there may be burst fractures and fracture dislocations of the facets. The latter two conditions are unstable and tend to disrupt and injure the cord. The extent of facet dislocation is dependent upon the magnitude of the posterior-to-anterior component of the applied force.

Recent human cadaveric studies by Nusholtz et al. (1983) involving crown impacts indicate that the injuries observed in accident victims are difficult to reproduce in the laboratory using the unembalmed cadaver as the human surrogate. Hence, the injury mechanisms proposed thus far may be entirely hypothetical, or the unembalmed cadaver may be an inappropriate surrogate of the living human for neck strength studies, since there is no muscle tone to help in supporting bending loads. More research is needed before a full understanding of the mechanisms involved can be achieved.

Compression-Extension Injuries. Frontal impacts to the head with the neck in extension will cause compression-extension injuries. These involve the fracture of one or more spinous processes. There may also be symmetrical lesions of the pedicles, facets, and laminae. If there is a fracture-dislocation, the inferior facet of the upper vertebra is displaced posteriorly and upward and appears to be more horizontal than normal on X-ray.

Injuries Involving Lateral Bending. If the applied force or inertial load on the head has a significant component out of the midsagittal plane, the neck will be subjected to lateral or oblique bending along with axial and shear loads. The injuries characteristic of lateral bending are vertebral-body lateral-wedge fractures and fractures to posterior elements on one side of the vertebral column.

Whenever there is lateral or oblique bending, there is the possibility of twisting the neck. The associated torsional loads may be responsible for unilateral facet dislocations or unilateral locked facets (Moffat et al. 1978). However, the authors postulated that pure torsional loads on the neck are rarely encountered in automotive accidents. It was shown recently by Wismans and Spenny (1983) that, in a purely lateral impact, the head rotated axially about the cervical axis while it translated laterally and vertically and rotated about an anteroposterior axis. These response characteristics were obtained from lateral impact tests performed by the Naval Biodynamics Laboratory on human subjects who were fully restrained at and below the shoulders.

Injuries to the Spine in General. The following injury modes are discussed: anterior wedge fractures, burst fractures, dislocations and fracture-dislocations, rotational injuries, Chance fractures, and hyperextension injuries.

Anterior Wedge Fractures. These injuries occur at all levels of the spine and are common in high-impact-severity automotive accidents. The mechanism of injury is combined flexion and axial compression. It is a relatively mild form of spinal injury, except in cases of very severe wedging. Begeman et al. (1973) have shown that unembalmed human cadaver subjects (no muscle tone) restrained by a lap belt and an upper-torso belt, in a $-G_x$ environment, develop high spinal loads that can cause wedge fractures. Field accident data indicate that this mode of spinal injury is very unusual in the absence of lap-belt submarining (where the belt acts as a fulcrum over which the spine is bent). Automobile occupants can sustain wedge fractures as a result of large vertical accelerations ($+G_z$) that sometimes occur. Aircraft pilot ejections also cause these injuries. Ejection seat research has been an important source of information relative to this type of injury (see Kazarian 1982).

Burst Fractures. These injuries are due to input acceleration or externally applied load that results in high vertebral body compressive loads, causing the body to fracture into multiple segments that tend to move radially outward as a result of the pinching action of the adjacent vertebrae. The integrity of the cord is threatened by the motion of these segments posteriorly into the spinal canal. The cord can also be injured by the retropulsion of the disc into the canal, particularly in the cervical spine.

Dislocations and Fracture-Dislocations. These are generally flexion injuries accompanied by rotation and postero-anterior shear. Unilateral dislocations are thought to require an axial rotational component, while bilateral dislocations can be due solely to flexion. The essential difference between a simple wedge fracture and a fracture-dislocation is, according to Nicoll (1949), in the rupture of the interspinous ligament. This observation is biomechanically significant and will be discussed later. There are varying degrees of dislocation: simple upward subluxation of the facets to a condition of so-called "perching of the facets," forward dislocation with fracture of the facets or the neural arch, and forward dislocation with locking of the facets. There is a high probability of neurological damage in these types of injuries, because the cord is subject to high shearing and stretching displacements. If there is dislocation without vertebral body wedging, the mechanism of injury is thought to be a high shear load in the postero-anterior direction (Kazarian 1982).

Rotational Injuries. If the spine is twisted about its longitudinal axis and is subjected to axial compressive and/or shearing loads, lateral wedge fractures can occur (Nicoll 1949) as a result of localized lateral bending. Other forms of injury include uniform compression of the vertebral body and fracture of the articular facets and lamina. Kazarian (1982) indicated that lateral wedge fractures seem to gravitate to two spinal regions, T2-T6 and T7-T10. The damage to the posterior intervertebral joint is on the concave side of the laterally bent spine, and this injury is often accompanied by fracture of the transverse process on the convex side. Unlike the anterior wedge fracture, this injury can result in neurological deficit as severe as quadraplegia.

Chance Fractures. This injury was first described by Chance (1948) as being a lap-belt related syndrome in which a lumbar vertebra is completely split in a transverse (horizontal) plane. Fracture initiates at the spinous process. Subsequent studies attribute the injury to the improper wearing of the lap belt while involved in a frontal ($-G_x$) collision. The belt rides over the anterior-superior iliac crests of the pelvis (i.e., lap-belt submarining) and acts as a fulcrum for the lumbar spine to flex over, causing a marked separation of the posterior elements without any evidence of wedging (Steckler et al. 1969). When the lap belt is used in conjunction with an upper torso restraint, this injury does not occur.

Hyperextension Injuries. The commonly observed whiplash as a result of rear impact is an example of a hyperextension injury of the cervical spine. Severe hyperextension loading of the spine can result in an avulsion fracture at the anterior aspect of one or more vertebral bodies. This is sometimes termed a tear-drop fracture and occurs as a result of the tensile force in the anterior longitudinal ligament being sufficient to pull a small segment of bone from the vertebra. Kazarian (1977) has reported this type of injury in connection with ejection from high-performance aircraft.

For more detailed treatments of spinal injury mechanisms, the reader is referred to the work of DePalma (1970), Moffat et al. (1978), and Huelke et al. (1978).

BIOMECHANICAL RESPONSE OF THE SPINE

Although spinal injuries are relatively infrequent in automotive accidents, the mechanical response characteristics of the spine are important because of their relationship to central nervous system injuries. In the context of the design of an advanced dummy, the response of the spine can also have a significant effect on head kinematics and, furthermore, on the response of the thorax to impact. Thus, the spine of an anthropomorphic test device is important from the point of view of both response and injury. This spinal response discussion will be divided into two main parts: the response of the cervical spine and that of the thoracolumbar spine. For the cervical spine, there are data for multiple directions of dynamic loading that are relevant to automotive collisions. There is less information of this type available for the thoracolumbar spine, most of it being torso static bending data.

Response of the Cervical Spine. The biomechanics of the cervical spine has been studied by Mertz and Patrick (1967, 1971), Patrick and Chou (1976), Schneider et al. (1975), and Ewing et al. (1978). The latter provided a bibliography of a long series of papers published by these authors over a ten-year period.

Mertz et al. (1973) elected to quantify response in terms of rotation of the head relative to the torso as a function of bending moment at the occipital condyles. Loading corridors were obtained for flexion and extension, as shown in Figures 2-4 and 2-5. An exacting definition of the impact environments to be utilized in evaluating a dummy neck relative to the loading corridors illustrated in these figures is included in SAE J1460 (1985). Furthermore, requirements regarding hysteresis are described there. While specific impact severities are specified in connection with the loading corridors, the authors have indicated that this is only for the purpose of assuring that necks are tested at a reasonable impact severity, and that the response should fall within the corridor regardless of the magnitude of the impact. Mertz et al. (1973) also examined the trajectory of the head center-of-gravity relative to the top of the thoracic spine for a volunteer subject (the data are plotted in the paper) but elected not to define a performance specification, because there appeared to be a lack of uniqueness of head angle as a function of head position.

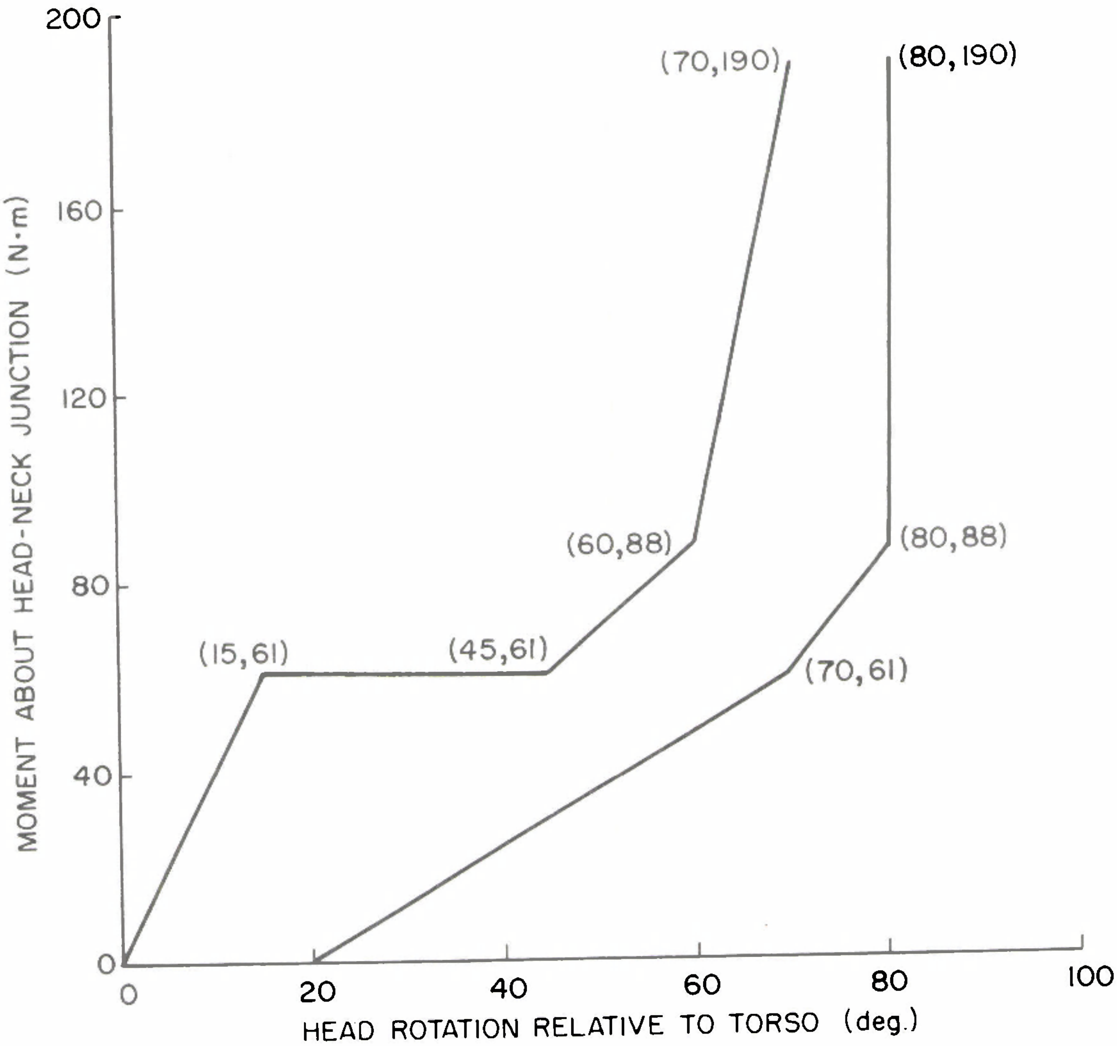

FIGURE 2-4. Loading corridor for neck flexion (forward bending) based on Mertz et al. 1973.

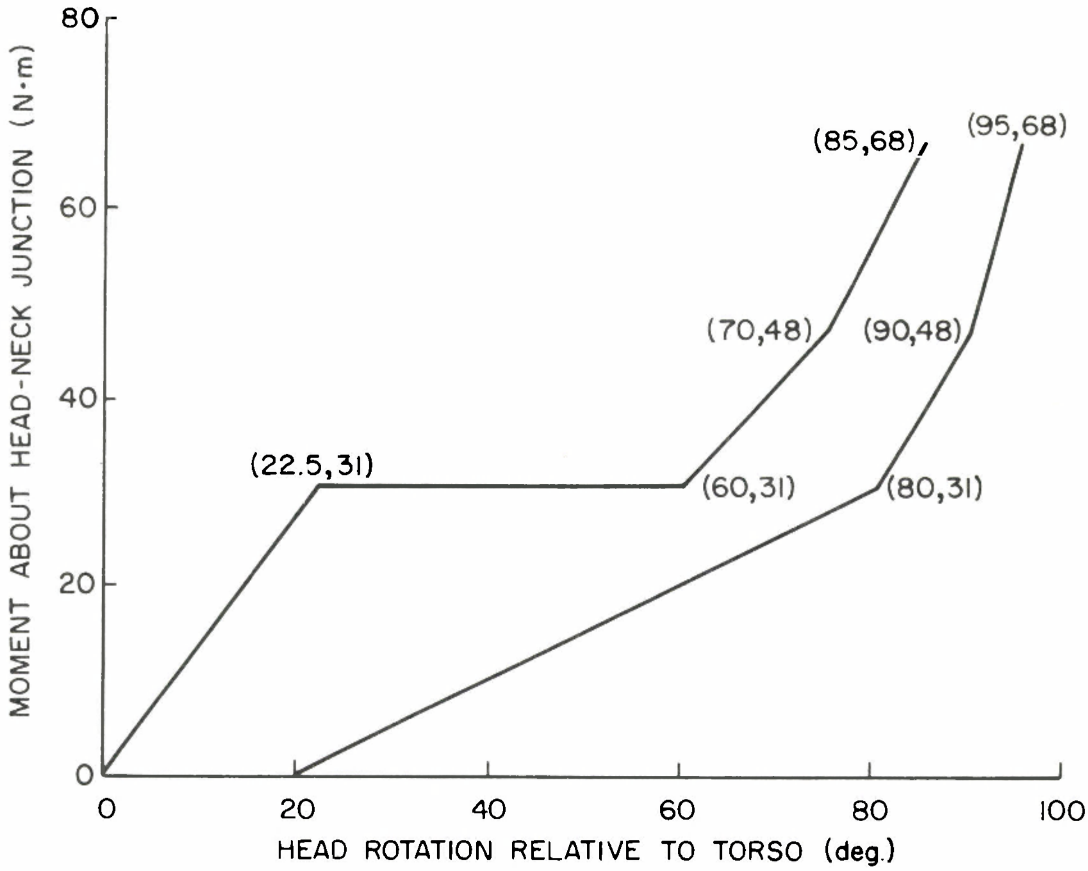

FIGURE 2-5. Loading corridor for neck extension (rearward bending) based on Mertz et al. 1973.

Patrick and Chou (1976) studied the response of the neck in flexion, extension, lateral flexion, and oblique flexion following a testing protocol similar to that of Mertz and Patrick (1967, 1971). Four adult male volunteers were evaluated. Testing was performed using the WHAM III sled facility at Wayne State University. The neck response curves for sagittal flexion and extension were found to fall within the loading and unloading corridors established by Mertz and Patrick (1967, 1971), upon which the loading corridors of Mertz et al. (1973) are based. Figure 2-6 is the preliminary response envelope for lateral flexion proposed by Patrick and Chou (1976) based on their volunteer data. This response envelope could serve as the basis for a more stringent loading corridor following the rationale of Mertz et al. (1973) in defining loading corridors from the envelopes of Mertz and Patrick (1967, 1971). Patrick and Chou (1976) did not provide neck response curves or envelopes for oblique flexion, indicating that further studies were required. However, they did document ranges of static voluntary motion for all of the loading directions studied. These data are reproduced in Table 2-1.

TABLE 2-1

VOLUNTARY RANGE OF STATIC NECK BENDING
(Patrick and Chou 1976)

Volunteer	Flexion	Extension	Total Range
LMP	51°	82°	133°
KJD	65°	73°	138°
SAT	63°	69°	132°
Lateral Flexion			
	Left	Right	
LMP	42°	43°	85°
SAT	35°	39°	74°
45° Mode			
	Toward	Away	
LMP	35°	56°	91°
135° Mode			
	Toward	Away	
LMP	53°	38°	91°

Schneider et al. (1975) have also studied the lateral flexion response properties of the human neck. Ninety-six volunteers were evaluated, including both males and females. Ages ranged from 18 to 74 years, and head and neck anthropometric information was documented. The three-dimensional range-of-motion of the head relative to the torso was

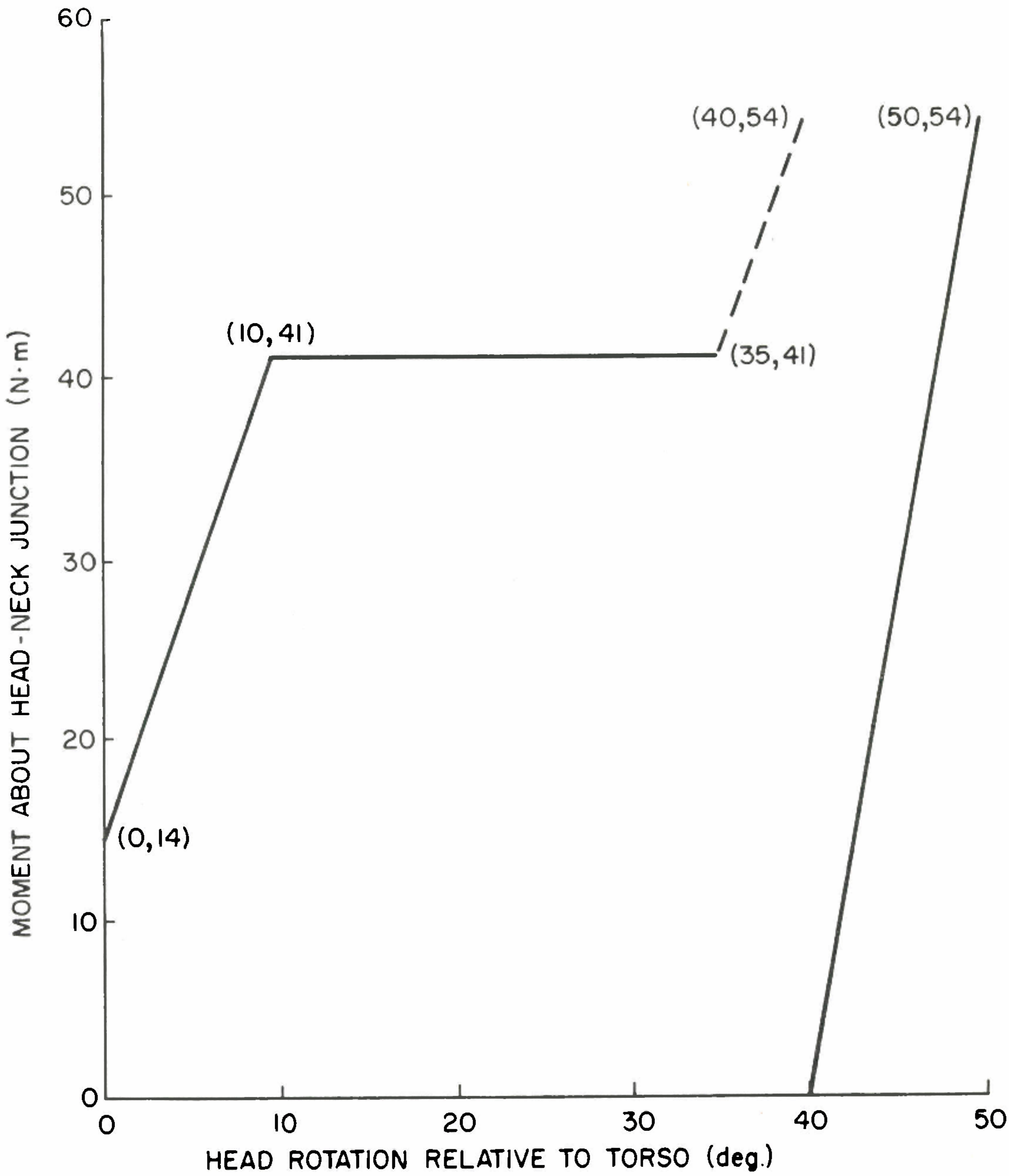

FIGURE 2-6. Lateral flexion response envelope established by Patrick and Chou (1976).

evaluated, and the response of the head/neck to low level acceleration was studied. Data are included regarding the stretch reflex time and voluntary lateral isometric muscle force. Total planar ranges of motion are reported in the form of averages for various age groups for each sex. The overall averages for sagittal and lateral motion were 103.7° and 71.0°, respectively. Rotation of the head (about a superior-inferior axis) had an overall average of 136.5°. Stretch reflex times varied from about 30 to 70 ms. Average isometric lateral pull forces measured for the neck are presented as a function of sex and age group. Males were stronger than females by a factor of about 1.5. The isometric force averages ranged from about 52.5 N (11.8 lb) for elderly females to 142.8 N (32.1 lb) for middle-age males. The authors conclude that, for a complete surprise impact, the total time to maximum muscle force is on the order of 130 to 170 ms and is probably too long to prevent injury in a high-speed collision.

Alem et al. (1984) performed two series of tests where superior-to-inferior impacts to the head were applied to 19 unembalmed male cadavers. A full complement of head and thoracic spine accelerometers were attached to the subjects, enabling computation of loads at the occipital condyles. While fourteen of the cadavers were subjected to sufficiently high levels of impact to generally cause skull fracture or cervical injury, the first five subjects were tested at sub-injury blow severities in order to study the dynamic mechanical response characteristics of the neck. The age, height, and body mass is not reported for these five subjects. The neck and head were positioned relative to the torso to simulate the natural seated or standing spinal curvatures. Impacts were delivered by a 10-kg (22-lb) mass moving at nominally 8 m/s (26 ft/s). There were 51 mm (2 in) of Ensolite® padding on the face of the impactor. The forces applied to the head ranged from 3.9 to 5.1 kN (880 to 1150 lb) with durations of from 12 to 17 ms. Head translational and angular peak accelerations and velocities as well as thoracic spine translational acceleration peak values are tabulated. Furthermore, computed values of triaxial peak forces and bending moments at the occipital condyles are provided.

McElhaney et al. (1983) subjected unembalmed human cervical spines to relaxation, cyclic loading, variable-rate constant-velocity loading (1.3 to 640 mm/s or 0.05 to 25.2 in/s), and constant-velocity loading to failure. The ends of the spines were potted into aluminum caps, using polyester casting resin, and mounted in a MTS servohydraulic testing machine, with the longitudinal axis of the spine flexed to essentially a straight line. A dovetail slide at the proximal end of the spine enabled small levels of anterior or posterior displacement to be introduced. The spines were from males and females that ranged in age from 37 to 77 years. A generalized quasi-linear viscoelastic Maxwell-Weichert model incorporating a continuous relaxation spectrum was developed to predict the relaxation and constant velocity responses. Considerable data are presented. The results of the constant velocity tests to failure are discussed in the section of this literature summary dealing with spinal injury tolerance.

The voluminous data acquired at the Naval Biodynamics Laboratory in New Orleans constitute a valuable resource of neck response data for volunteers who were tested to relatively high G-levels. It will be necessary to analyze the data in detail before they can be fully utilized to define human biomechanical response. Preliminary analyses have been completed recently by Wismans and Spenny (1983, 1984) for sagittal and lateral flexion. A summary of their findings is presented below.

These researchers have developed dynamic performance specifications for human surrogate necks in both sagittal and lateral flexion. The performance specifications include kinematic and dynamic constraints. The kinematic requirements are specified in terms of the length and location (relative to the torso) of an equivalent neck link, pivoted at both ends. The upper pivot point is at the occipital condyles, and the lower pivot is near the first thoracic vertebra. Independent analyses of the sagittal and lateral flexion data bases each resulted in a link length of 125 mm (4.9 in). For sagittal flexion, the lower point is located essentially at the origin of the T1 coordinate system—the point where the midsagittal plane intersects the anterior-superior lip of the vertebral body. For the two volunteers used to define sagittal flexion response, the pivot was at the origin for one subject and 40 mm (1.6 in) below the origin for the other subject, or an average of 20 mm (0.8 in) below. For lateral flexion the lower pivot point is located the same as for sagittal flexion, except it is displaced laterally 20 mm from the midsagittal plane in the direction opposite to that in which the neck flexes. The neck link remains in the midsagittal plane during sagittal flexion; however, in lateral flexion the head rotates about the link (since the head CG is anterior of the occipital condyles). Consequently, while the link representation of the neck has two degrees-of-freedom for sagittal flexion, there are three degrees-of-freedom for lateral flexion.

Wismans and Spenny utilize three angles in quantifying neck response. The angle of rotation of the head and neck relative to vertical axes are denoted by the Greek letters ϕ and θ, respectively. Rotation of the head about an inferior-superior head axis is denoted by the Greek letter ψ (right-hand rule). For dynamic loading conditions comparable to those experienced by the volunteers (specified later), the mechanical response characteristics of the neck have been depicted by specifying moment versus angle plots that are piece-wise linear approximations of responses quantified using a rigid body dynamics analysis of head accelerometer and high-speed cinematography data (along with head inertial characteristics stemming from the anthropometric data that had been recorded for each volunteer). In connection with the use of this analysis to compute loads at the *base* of the neck, it is stated that the errors as a result of neglecting the inertia effects of the neck are expected to be small. Moment-angle plots determined by Wismans and Spenny (1984) for sagittal flexion are reproduced in Figure 2-7. Comparable plots for lateral flexion (Wismans and Spenny 1983) are reproduced in Figure 2-8.

When the authors analyzed the neck response data in terms of torque at the occipital condyles and head rotation relative to the torso, the results fell within the corridor for forward flexion (Figure 2-4) and lateral flexion (Figure 2-6). The dynamic environment in which the above response characteristics should be experienced have been defined based on the acceleration profiles measured at the base of the volunteers' necks (T1 horizontal acceleration). Figures 2-9 and 2-10 are reproductions of these profiles, as presented by Wismans and Spenny for sagittal flexion and lateral flexion, respectively. While the researchers explicitly state that any acceleration profile within or close to the plus-and-minus one-standard-deviation envelope in Figure 2-10 is appropriate for evaluating mechanical necks in lateral flexion, the appropriateness of the profile of Figure 2-9 in evaluating mechanical necks in sagittal flexion is only indirectly implied by the fact that they used it as a basis for their sled pulse when evaluating the performance of dummy necks. Figure 2-9 represents the T1 acceleration profile for only one test run (the most severe frontal flexion test experienced in the program), whereas Figure 2-10 is based on the T1 acceleration profiles for the most severe lateral flexion tests of six different volunteers.

Wismans and Spenny (1983) recognized that, in connection with evaluating mechanical necks, even a simple sled test with the base of the neck experiencing accelerations as described above is a somewhat difficult task, if bending moments must be measured or indirectly computed. Consequently, for lateral flexion they suggest that an alternative is to place a performance requirement on the head CG lateral acceleration profile. More specifically, they presented the data reproduced in Figure 2-11 and indicated

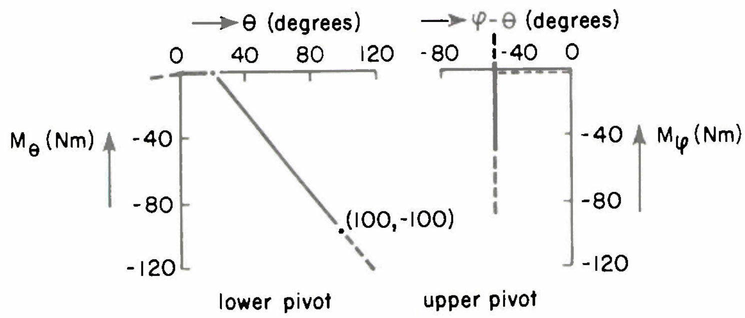

FIGURE 2-7. Moment-angle relationship for sagittal flexion (Wismans and Spenny 1984).

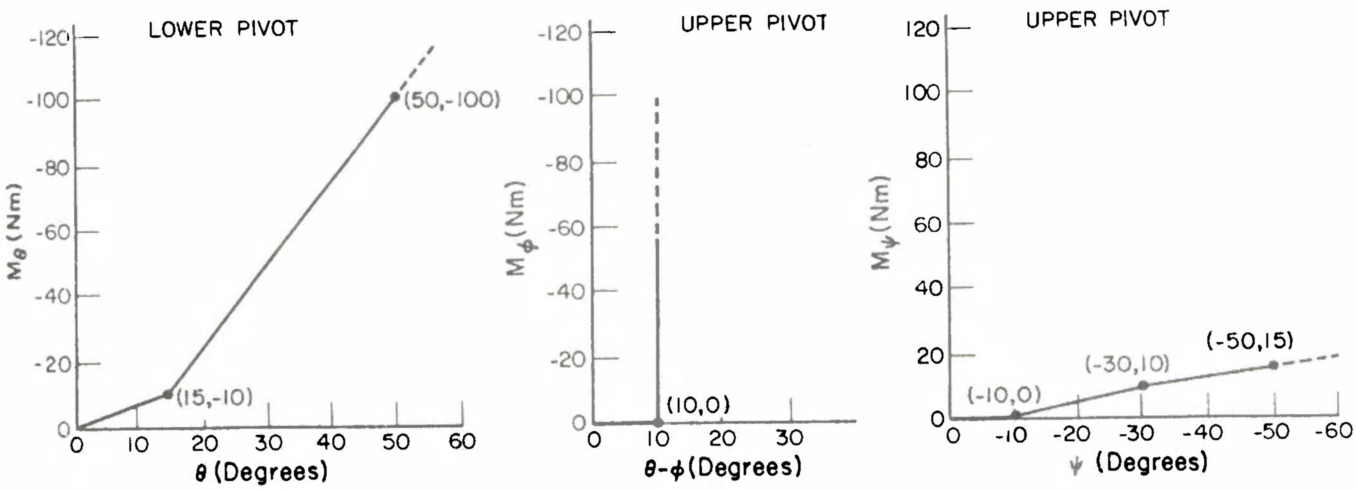

FIGURE 2-8. Moment-angle relationship for lateral flexion (Wismans and Spenny 1983).

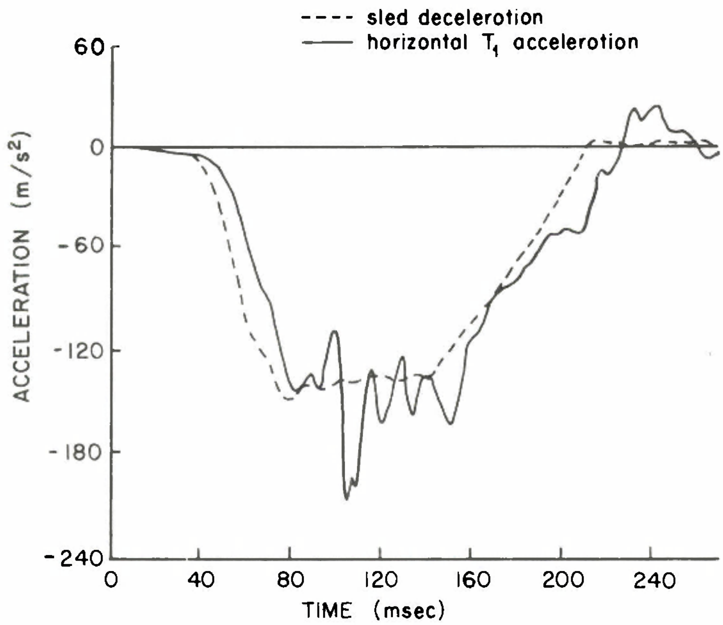

FIGURE 2-9. T1 and sled horizontal acceleration for sagittal flexion tests (Wismans and Spenny 1984).

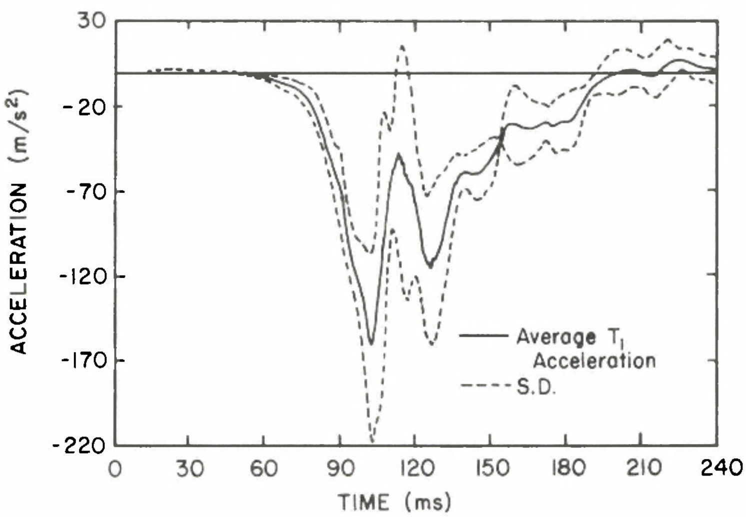

FIGURE 2-10. T1 horizontal acceleration for lateral flexion tests (Wismans and Spenny 1983).

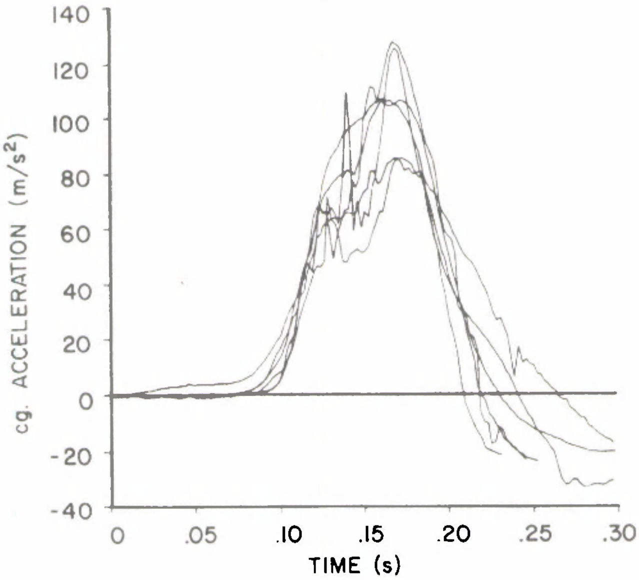

FIGURE 2-11. Lateral acceleration at the center of gravity of the head (Wismans and Spenny 1983).

that the lateral acceleration of a mechanical head could be required to lie in or close to an envelope specified by the results of these six tests. Further kinematic requirements are specified in terms of displacements, as follows:

1. Except for the initial part of the motion, the head should describe a pure rotation ϕ (lateral flexion) in the plane of impact about a fixed center of rotation. The center of rotation is located in the rigid structure, 20 mm (0.8 in) out of a plane equivalent to the torso midsagittal plane in a direction opposite to the head motion. The radius of the trajectory described by the head origin should be about 150 mm (5.9 in).
2. In addition, the head should perform a torsion ψ about the local z-axis, where ψ should be the same order of magnitude as ϕ.
3. The maximum lateral flexion ϕ should be close to 52° (this is the average of the six tests; ϕ was found to vary in these tests between 47° (LX1528) and 58° (LX1510)).

The specification of 150 mm (5.9 in) in item no. 1 above, instead of the neck link length of 125 mm (4.9 in), stems from the fact that the trajectory described is that of the head CG, not the occipital condyles. The CG is 25 mm (1 in) above the occipital condyles.

Wismans and Spenny do not offer an analogous alternative performance specification for sagittal flexion as they have, above, for lateral flexion.

Wismans and Spenny (1983, 1984) have been objective regarding the results of their analyses. While their moment-angle curves are consistent with the corridor developed by Mertz et al. (1973) for frontal flexion, and analytical simulations of the volunteer sagittal flexion tests using the MADYMO computer model provided realistic results with neck parameters based on the above performance specifications, they note that the data bases were of limited size (two volunteers for sagittal flexion and six for lateral flexion) and that the results of their work are only valid for low severity impacts.

Bowman et al. (1984) pursued analytical modeling of tests conducted on volunteer subjects at the Naval Biodynamics Laboratory using the MVMA 2-D and VOM 3-D occupant dynamics models in an effort to quantify the biomechanical properties of the human neck that govern head and neck dynamic response and to establish the mechanisms responsible for primary aspects of response. Preliminary values of model parameters were determined that provided accurate simulations of volunteer responses sustained in $-x$, $+y$, and $-x+y$ sled acceleration environments where direct head impact is not involved. It is suggested that the model can be used to assist in the design plan for the neck of an advanced anthropomorphic dummy.

Response of the Thoracolumbar Spine. The following discussion addresses both static and dynamic bending response.

Static Bending Response of the Thoracolumbar Spine. Data for quantifying the bending characteristics of the lower torso are available from two separate research programs conducted at Wayne State University. The first study was supported by General Motors Corporation and has been described by Nyquist and Murton (1975). The second study was supported by NHTSA and is described in a report by King and Cheng (1984) and in part in publications by Mallikarjunarao et al. (1977), Mital et al. (1978a, 1978b), and Cheng et al. (1979). These two projects will be referred to as the "GM Study" and the "NHTSA Study".

In the GM Study, six male volunteers were evaluated for quasi-static bending response characteristics using a special test fixture. The subject was positioned with his midsagittal plane horizontal, his legs were immobilized, and his shoulders were lashed to a dolly having omnidirectional casters that rolled freely on a sheet of tempered Masonite®. A force was applied to the dolly in a direction nominally perpendicular to the longitudinal (SI) axis of the thoracic spine. The moment of this applied force about the pelvic left-right axis (H-point axis), defined by the two hip-joint centers, was plotted as a function of the thorax-to-pelvis angle and as a function of the pelvis-to-femur angle. Figure 2-12 illustrates the convention used for expressing these angles. Tests were conducted under both relaxed and tensed conditions, both for flexion (forward bending) and extension (rearward bending). Furthermore, all of these tests were conducted both with the legs straight and with a right-angle at the knee. Complete details are given by Nyquist and Murton (1975).

Nyquist and King (1984) have further analyzed the results of the GM Study to provide lower torso bending response performance specifications for the advanced dummy. The results of the analysis are summarized in Figure 2-13 for thorax-to-pelvis response and Figure 2-14 for pelvis-to-femur response. (While the data of Figure 2-14 do not directly involve the spine, the information has been included here for sake of continuity, since it stems from the same test program and required the same types of analysis as the more germane information of Figure 2-13.)

In Figures 2-13 and 2-14, the line segments representing the tensed condition are not unique, since the angle at zero moment simply depended on the test subjects' posture when they tensed their muscles. Because of this fact, the mean lines drawn for tensed extension response start at a zero-moment angle that is different than that of the tensed flexion response. The response lines shown in the figures do not encompass the entire range of possible moment/angle combinations, particularly the large angle/flexion response region and the low angle/extension response region. While no data exist, the extent of these potential regions is indicated in a general manner by the dashed line envelopes shown on the figures. Clearly, if some degree of tensing is to be simulated in a dummy,

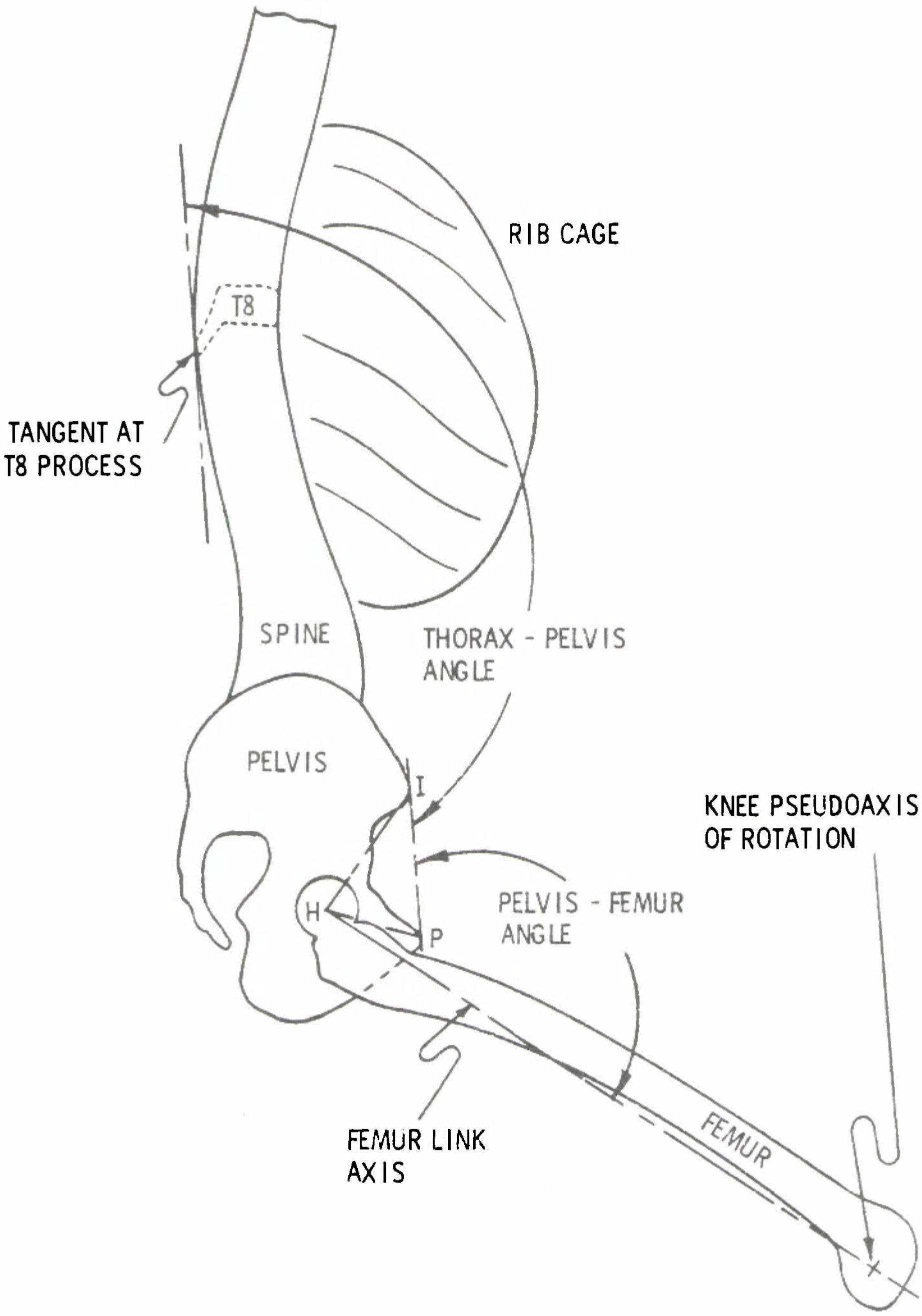

FIGURE 2-12. Definition of bending angles (Nyquist and Murton 1975).

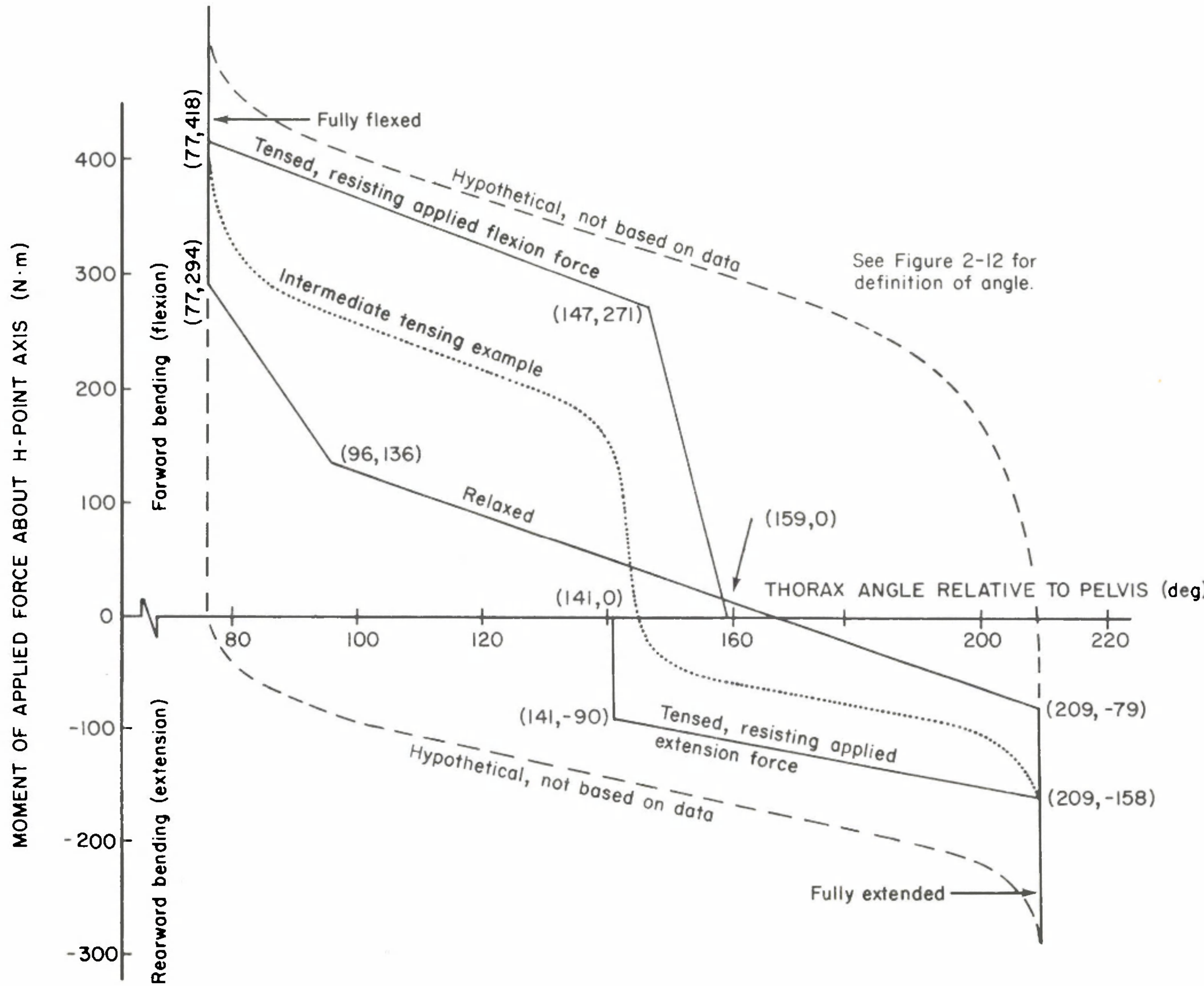

FIGURE 2–13. Static sagittal bending response of the thorax relative to the pelvis.

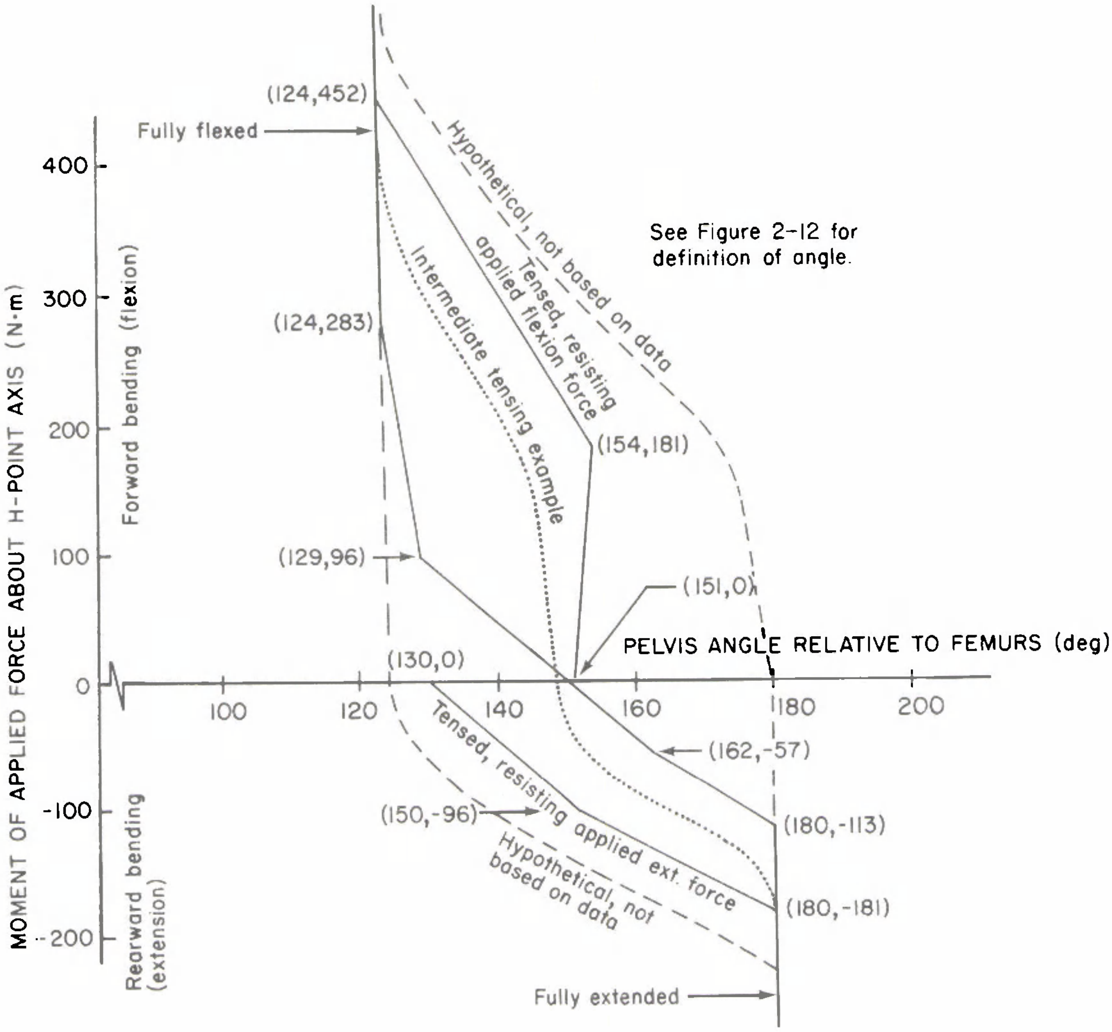

FIGURE 2-14. Static sagittal bending response of the pelvis relative to the femurs.

then there must be a means of adjustment in the lower torso and at the hip joints so that the zero moment conditions can be compatible with a vehicle-seated posture.

The dotted lines in Figures 2-13 and 2-14 represent possible intermediate-level tensed response characteristics. While the line segments crossing the abscissas will do so at angles that depend on the dummy's vehicle-seated posture, it seems logical that the slopes of the lines should always approximate those drawn in the figures, which are averages of the flexion and extension fully-tensed line segments intersecting the abscissa. There should be a gradual stiffening transition of the response line as the limit of articulation is being reached, not a sudden bottoming-out.

The NHTSA Study, entitled *The Kinesiology of the Spine and Shoulder*, (King and Cheng 1984) was carried out to acquire spinal response data during static loading and $-G_x$ acceleration and to design a surrogate spine that was more humanlike in response than current dummy spines but still satisfied the dual conditions of repeatability and reproducibility. A series of static bending tests were performed on cadavers and volunteers (Mallikarjunarao et al. 1977). The test protocol was similar to that of Nyquist and Murton (1975), and there were photo-targets at T1, T12, and the pelvis.

While the GM Study provides torso response data for the T8-to-pelvis region, the NHTSA Study addressed the whole thoracolumbar region of the torso, since targeting spanned from T1 to the pelvis and included a target at T12. The data from the NHTSA Study are thus potentially very important, since there is little information in the literature regarding the bending stiffness of the thoracic region of the torso. A review of the results of the testing and data reduction protocol indicated a need for reevaluation of the basic test data, taking into account the target orientations relative to the skeletal structure, the effective lever arm of the applied force relative to the H-point axis (since the force was not perpendicular to the fixture lever arm as had been assumed), and the location of the force line of action relative to the torso (since it was below the shoulder region). Attention to these issues, together with more discriminating quantitative analyses of the photographic films of the tests, improved accuracy and reduced the spread in results among volunteers sufficiently to enable the development of response descriptions that are representative of the pooled data for each test condition (Nyquist and King 1984). These response descriptions are illustrated in Figures 2-15 and 2-16 for the relaxed and muscles-tensed conditions, respectively.

The relaxed flexion-bending response of the thoracic spine may be examined by subtracting the T1/pelvis curve from the T12/pelvis curve to obtain a result depicting T1/T12 relative angle as a function of applied moment. This is shown in Figure 2-17. Interestingly, the difference is nominally constant at about 42°, except at small moments. This behavior at small moments is thought to be an artifact associated with the curve-fitting procedure (extrapolations to obtain angles at zero moment). Thus, the relaxed flexion data lead to a conclusion that the thoracic spine does not bend in this test environment.

While complete curves for the tensed data could not be developed because of the data scatter, the rough approximations of stop locations (Figure 2-16) that were established for T1/pelvis and T12/pelvis responses have magnitudes such that their difference (130° minus 88°) is 42°, which is the same value observed above for the relaxed data. This is suggestive that the thorax also does not bend during the *tensed* flexion mode of testing. If the thorax is not bending, then in Figure 2-16 the T1/pelvis and T12/pelvis plateaus of 255 and 300 N·m (190 and 220 ft·lb) should be one and the same, since in each case the muscle-yielding phenomenon is taking place in the lumbar spine region. This inconsistency can be attributed to the variability in the data. Since true constant-moment plateaus

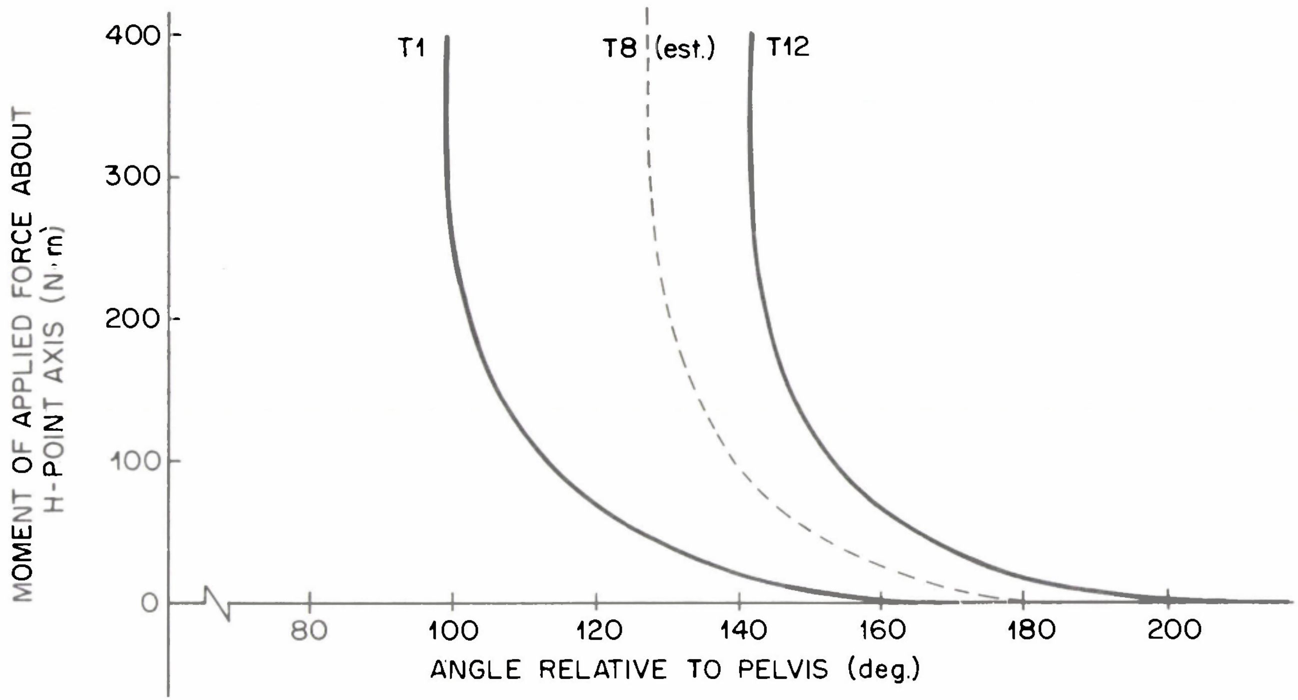

FIGURE 2-15. Relaxed static sagittal bending response of the thorax relative to the pelvis (NHTSA Study).

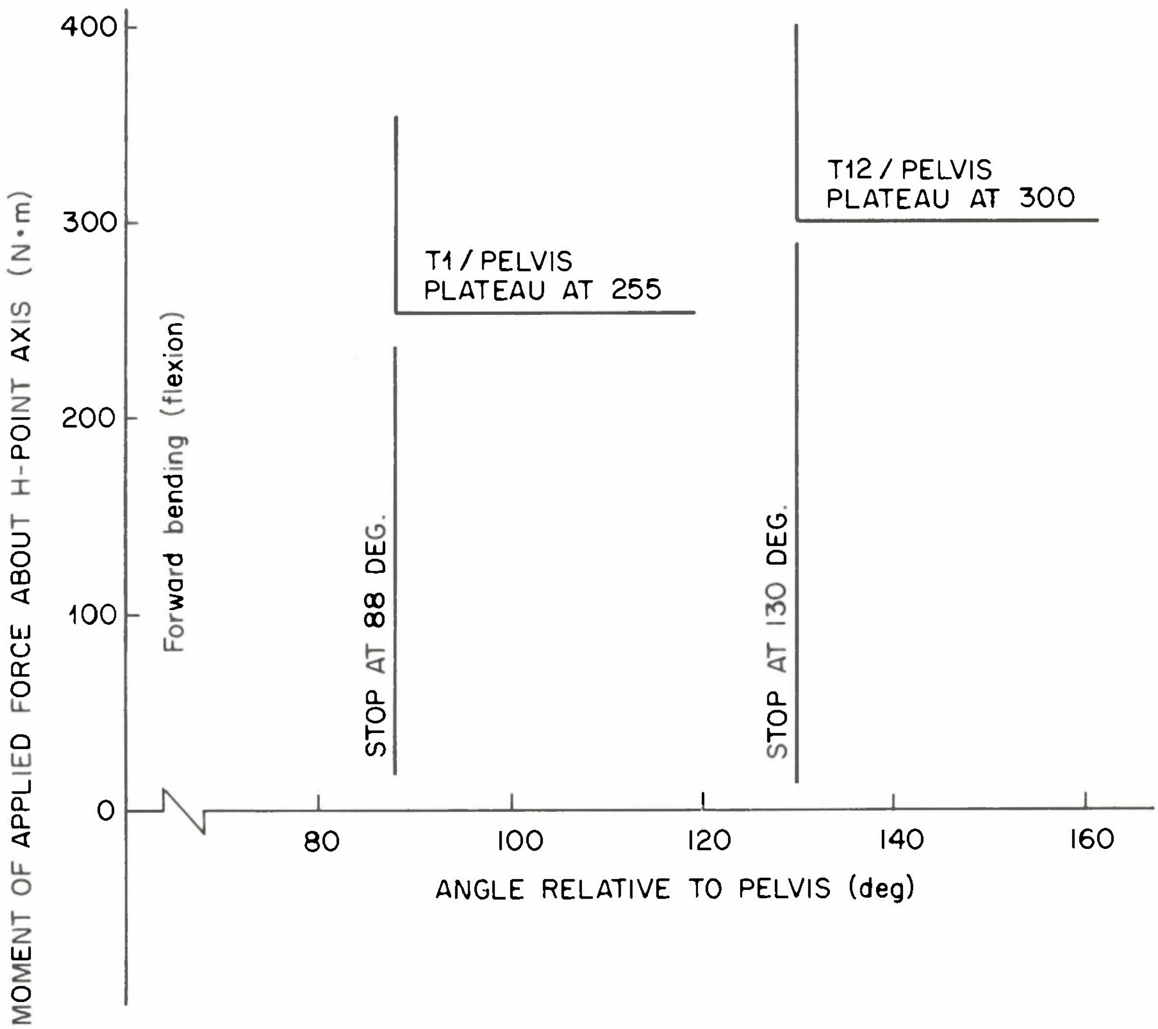

FIGURE 2-16. Tensed static sagittal bending response of the thorax relative to the pelvis (NHTSA Study).

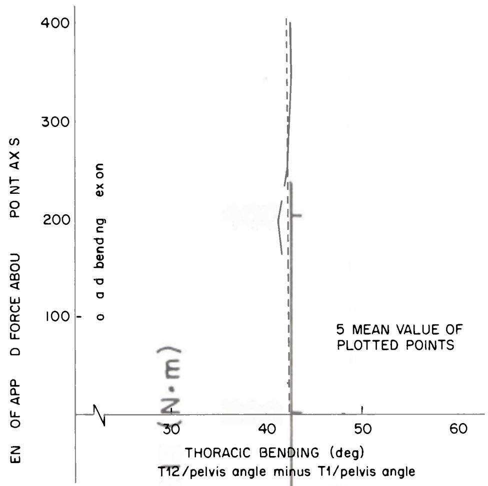

FIGURE 2-17. Difference curve plotted from Figure 2-15, depicting absence of thoracic bending.

generally were not present, it was necessary to pick a representative point on a curved and/or sloped line that appeared to be in a region of muscular yielding. Along with the variability in the data resulting from other sources, it is not surprising that the plateau approximations varied by 45 N•m (33 ft•lb). The slopes of the initial portions of the tensed muscle flexion responses ranged from large positive to large negative values, "large" being greater than 35 N•m/deg (26 ft•lb/deg). This effect is possibly due to large negative values, an effect possibly due to active control of the pelvis angle by the subject during the test. An infinite slope with a smooth, sweeping transition to the plateau appears to be a generally representative approximation.

A possible explanation for the lack of bending of the thoracic spine in the NHTSA Study became apparent upon investigating the location of the bending force line of action. On the average, it was about midway along the thoracic spine; thus, the upper half of the thorax was not loaded, and the bending moment in the lower half was low as a result of the relatively short "lever arms" involved.

The results of the NHTSA Study (depicted in Figures 2-15 and 2-16) may be compared to the results of the GM Study summarized in Figure 2-13. First, it is important to keep in mind that Figure 2-13 deals with angles measured from a film target parallel to the spine at T8, whereas Figures 2-15 and 2-16 deal with angles measured from targets at T1 and T12. These targets are at different orientations, since the thoracic spine is curved. Indeed, Figures 2-15 and 2-16 suggest that the curvature from T1 to T12 leads to an angular difference of 42°. Figures of the spine in Gray (1973) indicate that about one-third of this 42° angular difference stems from the curvature between T8 and T12. This means that in the NHTSA results of Figure 2-15 and 2-16 one must subtract 14° from the T12 data or add 28° to the T1 data before comparing with the GM results of Figure 2-13. Of course, such angular adjustments of the data can only be made because of the above conclusion that the thorax does not bend.

One of the obvious points to be made in comparing the results of the GM and NHTSA studies is that the conclusion regarding lack of thoracic bending under the conditions of load application in the NHTSA data is consistent with the prior assumption in the GM Study that thoracic bending would be small relative to lumbar region bending. It was this assumption that led to targeting only one location (T8) in the GM Study.

Figures 2-13 and 2-15 are in reasonable agreement relative to the angle associated with the neutral configuration (where the bending moment is zero), if one keeps in mind that 14° must be subtracted from the T12 plot and that there is also probably some error as a result of extrapolating the T12 curve to zero.

The shape of the curves in Figure 2-15 is consistent with the break-point or knee of the relaxed response line at location (96,136) in Figure 2-13. Furthermore, the slopes of the curves at small moments compare satisfactorily with the slope of the straight line segment in Figure 2-13. However, in looking at the stop locations, there is a discrepancy. The NHTSA data predict a T8 stop angle of 128° (142° minus 14°), whereas the GM data led to a T8 stop of only 77°, a difference of 51°. No defensible explanation for this lack of correlation has surfaced to date. The 12° shift in stop locations between the relaxed and tensed results for the NHTSA Study (Figures 2-15 and 2-16) is of some concern. However, considering the paucity and variability of the tensed data at high moments compared to the quality of the relaxed data, one must conclude that the relaxed stop locations are of higher credibility. (There is no known mechanism to suggest that tensed and relaxed stops should not be one and the same.)

A tensed flexion plateau in the realm of 225 to 300 N•m (190 to 220 ft•lb) determined from the NHTSA Study (Figure 2-16) is consistent with the sloped plateau of

Figure 2-13 for the GM Study, where the break-point is 271 N·m (200 ft·lb). Furthermore, while the slope of the initial portion of the tensed response in Figure 2-13 has a slope of about 22 N·m/deg (16 ft·lb/deg), and it was earlier concluded that an infinite slope is representative for the NHTSA data, these are both steep slopes compared to the relaxed condition. Considering the variability of the data, this level of correlation is judged to be acceptable.

Since curve fitting has not been completed for the NHTSA extension data, a quantitative discussion of correlation with the GM results for extension cannot be offered. Qualitatively, however, it appears that the initial slopes, plateau magnitudes, and stop locations are in agreement.

Dynamic Response of the Thoracolumbar Spine to Frontal Impact. Under the same NHTSA Study referred to in the previous section, a series of dynamic impacts was carried out using both cadaveric and volunteer subjects. The objective was to acquire response data suitable for the design of a more humanlike vertebral column. The principal direction of impact was in the midsagittal plane, and the configuration of interest was that of spinal flexion. The results have been reported by Mital et al. (1978a, 1978b) and by Cheng et al. (1979).

The test subject was restrained by a three-point belt or by a clamping system, which held the pelvis and the lower extremities firmly to a rigid seat, and the spine was allowed to flex over a protective cushion during $-G_x$ seat acceleration. The latter mode resulted in a substantial amount of spinal flexion data, and results from tests using this mode of restraint will be described. In the clamped mode, the spine was free to flex, but the subject was protected from injury by a soft cushion placed across the lap. There was a slight amount of resistance offered by the cushion, but through the majority of the flexion sequence no external resistance was present. The instrumentation consisted of accelerometer packages at T1, T12, and the pelvis, as well as photo targets at the same locations. The peak sled acceleration for volunteers was 8 G, while that for cadavers was 30 G. The seat pan was equipped with a load cell which could measure applied force and moment about all three axes. After the sled had come to rest, it was possible to use the load cell data to calculate the moment at the hip joint, using equations of static equilibrium. Acceleration data from male volunteers are shown in Figure 2-18. They represent T1 acceleration in the body-fixed z-axis (inferior-superior direction) for runs made in the 5- to 8-G range. Moment-angle curves for male subjects are shown in Figure 2-19 and are compared against data obtained from a 10-G cadaver run.

Rotation data for four male and three female volunteers are given in Table 2-2.

TABLE 2-2

MOBILITY OF THE THORACOLUMBAR SPINE
(Cheng et al. 1979)

Subject	Muscle Tone	Rotation ±1 S.D. T1/T12 (deg)	Rotation ±1 S.D. T12/Pelvis (deg)
Male	Tensed	27.2 ± 6.0	24.8 ± 6.9
Male	Relaxed	38.9 ± 10.4	26.3 ± 5.5
Female	Tensed	24.9 ± 5.4	22.7 ± 6.8
Female	Relaxed	27.9 ± 4.0	28.0 ± 4.3

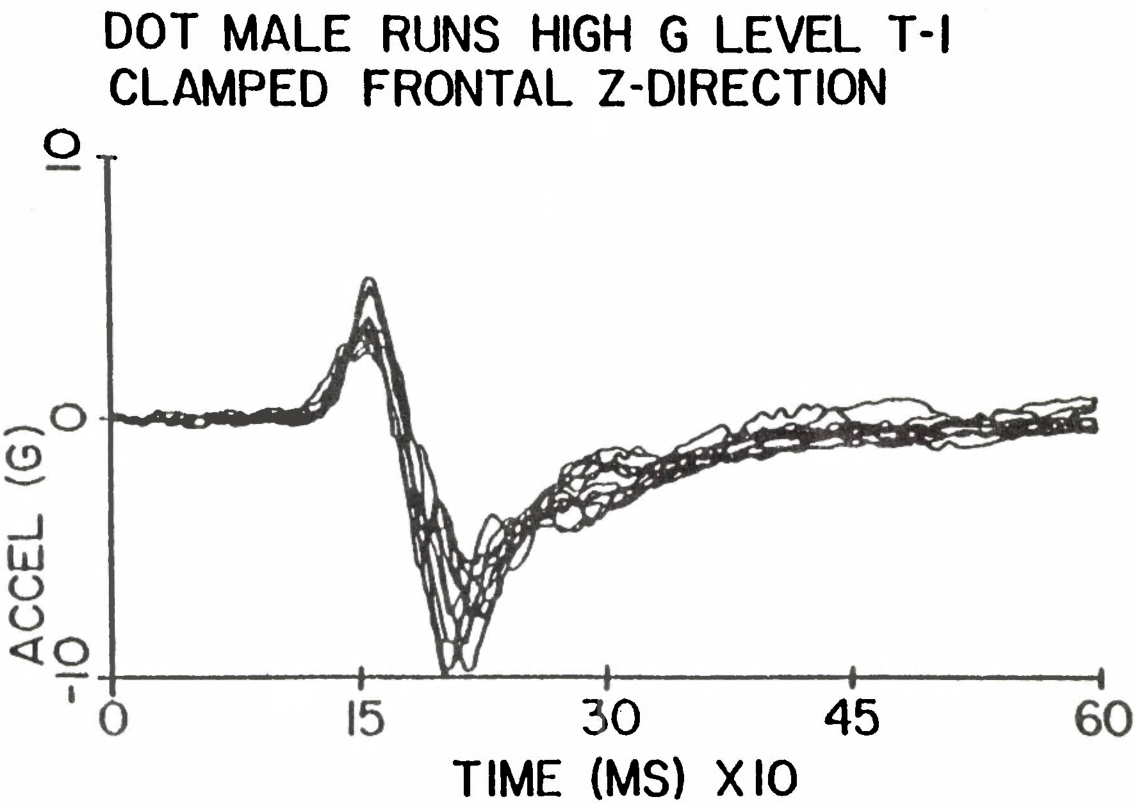

FIGURE 2-18. T1 z-axis acceleration corridor: Male high-G runs.

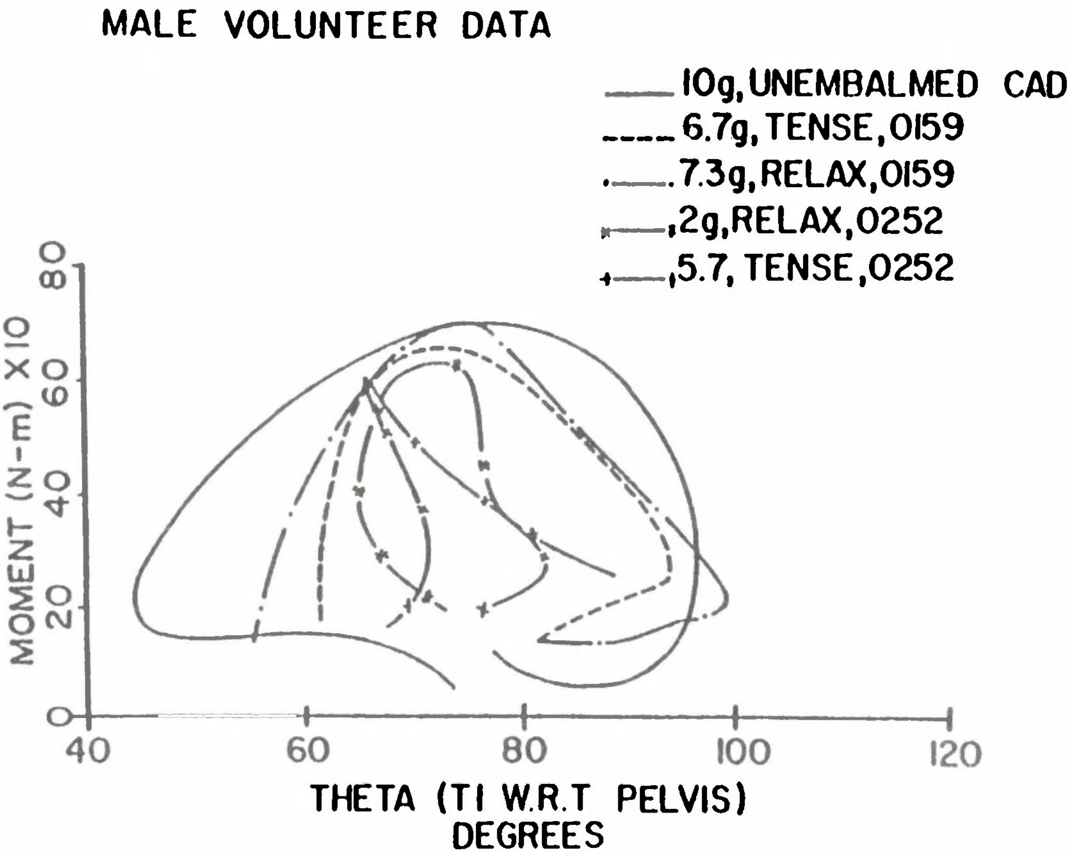

FIGURE 2-19. Moment-angle curves for spinal flexion: Male data.

The total rotation of T1 with respect to T12 was found to be similar to or greater than that of T12 with respect to the pelvis in all cases. In terms of unit rotation (total angle divided by the number of spinal units between the points), the lower spinal units were considerably more flexible (25–80%) than the upper spinal units.

Analyses of the above-discussed dynamic spine response data in connection with this advanced dummy program have led to some questions in connection with the orientations and stabilities of the surface-mounted film targets on the volunteers. These issues should be researched prior to utilizing the data.

The generation of a compressive force in the spinal column during frontal impact, as indicated by seat-pan loads, is a topic of interest. This phenomenon was initially a prediction of a two-dimensional model of the spine formulated by Prasad and King (1974). Cadaver tests were carried out to verify the presence of this force by Begeman et al. (1973). Large seat pan loads were measured if the cadaver was restrained by a shoulder belt, but dummies did not generate such loads. It was concluded that this phenomenon was due to the curvature of the human spine, and that the seat pan load was a manifestation of spinal compression due to the tendency of the spine to straighten during $-G_x$ acceleration. Seat pan loads were found to be generated by volunteer subjects in subsequent studies as reported above and by Begeman et al. (1980).

Dynamic Response of the Thoracolumbar Spine to Vertical Acceleration. Response data from whole-body acceleration have been acquired by a series of investigators using the unique vertical accelerator of Wayne State University. It was designed to simulate ejection from military aircraft and was first installed in 1956 in an elevator shaft of the WSU School of Medicine. Significant results were obtained from the many cadaver experiments performed using this accelerator. The load-bearing role of articular facets was quantified by Prasad et al. (1974) following a careful analysis of strain and load cell data.

Ewing (1968) hypothesized that the facets were motion limiters and that they should play a role in the prevention of wedge fractures. A study was initiated to determine the fracture G-level of the spine in the erect, hyperextended, or flexed configuration. Twelve cadaver subjects were tested in all. The erect mode was designated as the normal seated configuration of the cadaver spine while restrained by a four-point lap-belt/shoulder-harness system. The spine was hyperextended in four of the cadavers tested by placing a block of wood at the level of L1 and by pulling the shoulders back with about 300 N (67.5 lb) of force in each of the shoulder belts. The flexion mode was created in three subjects by a condition of the shoulder restraint system, whereby the belts were left loose during the run, allowing the torso to flex a considerable amount. The results indicated that the fracture level increased 80% between the hyperextended mode (17.75 ± 5.55 G) and the erect model (10.4 ± 3.79 G). A t-test showed that the observed difference was significant at the 95% level (Ewing et al. 1972).

A search for an explanation of this dramatic difference ensued. The accelerator seat was instrumented with seat-pan and seat-back load cells to see if the spine was supported in part by the hyperextension block. The seat pan load was found to be identical for runs made in the erect or hyperextended mode at the same G level. However, vertebral strain data were found to be different. The strain level on the anterior aspect of several vertebrae was found to decrease when the spine was hyperextended. The only logical hypothesis that could be proposed was that the facets acted as a load path and that they became load-bearing elements when the spinal configuration was altered by hyperextension. To prove this hypothesis, a so-called intervertebral load cell (IVLC) was designed and fabricated to measure load transmitted by a lumbar disc. It was capable of measuring the applied compressive load and the location of that load relative to its geometric center. It was designed to fit just above an intervertebral disc after a slice of the vertebral body above it was removed by means of a double bladed saw. In order to estimate the facet load, the total load carried by the spine at the level of the IVLC must be found. It was assumed that this load was proportional to the seat pan load and that it was reduced in proportion to the weight of the torso above the IVLC.

Prasad et al. (1974) computed the facet load, based upon the assumed total load, and found that the vertebral body and the facets were in compression during the initial portion of the acceleration pulse. However, as the head and torso began to flex, the facet load became tensile, and there was confirmation of this fact from strain gages placed on the lamina. These preliminary results were subsequently confirmed by Hakim and King (1976) who performed similar tests on an MTS materials testing machine, using isolated spinal segments. For these experiments, the total load could be measured and need not be assumed. The mechanism of load transmission was hypothesized to be due to the bottoming out of the facets onto the pars interarticularis. The fact that facets could transmit both tensile and compressive loads provided an explanation for the increase in fracture G-level in the hyperextended mode. Furthermore, it provided an explanation for the mechanism of injury. Wedge fractures were caused by excessive compressive load on the vertebral bodies. This load is greater than the axial inertial load, because a flexion moment causes an additional compressive force on the disc and a tensile load in the posterior elements toward the end of the impact. The facets could also remain in compression if the spinal configuration was altered (Ewing et al. 1972). Injury data from subhuman primates, obtained by Kazarian et al. (1971), indicate that derangement of facets was due to locking of the facet joints to act as a load path during $+G_z$ impact acceleration. Although injuries to the posterior elements are rare in pilot ejection, these observations corroborate the load-bearing hypothesis of the facets.

Recently, Patwardhan et al. (1982) measured contact pressure between the articular surfaces of lumbar facets and computed a facet force, purporting it to be the vertical facet force defined by Prasad et al. (1974). This was thought to be erroneous, since the articular surfaces in the lumbar region are almost vertical and are low-friction synovial surfaces quite incapable of transmitting shear forces. Yang and King (1984) performed loading experiments on isolated facet joints and obtained some extremely interesting results. In compression the facets acted as a stiffening spring, while in tension they afforded very little resistance. Most of the tensile resistance was provided by the ligamentum flavum and the interspinous and surpraspinous ligaments.

These results have a significant impact on the understanding of injury mechanisms of the spine. The observation made by Nicoll (1949), that dislocations occur if the interspinous ligaments are ruptured, is equivalent to saying that the capsules of the facets cannot provide much resistance and that subluxation, or the sliding of one over the other, can easily occur if the posterior ligaments are torn. In fact, the geometry of the facet surfaces becomes an important consideration as far as dislocation is concerned. Those with surfaces that are almost horizontal would be easier to dislocate than those that have vertical faces, particularly in the presence of torsional loads and horizontal shear loads.

SPINAL INJURY TOLERANCE AND CRITERIA

Tolerance data for the spine are available from several sources for a variety of loading conditions. These conditions range from static loadings of individual vertebrae to dynamic loading of the whole body in impact tests using human cadaver subjects. While data on the strength of the in-situ spine under dynamic loading are of particular importance in connection with this review, this discussion of tolerance will commence with a brief summary of strength data for individual vertebrae.

Strength of Isolated Vertebrae and Excised Spines. Yamada (1970) provides a summary of the results of Sonoda (1962) for tensile, compressive, and torsional strength characteristics of the cervical, thoracic, and lumbar vertebrae and the intervertebral discs. Data are provided regarding the variation in strength along the column and the dependence of strength on age. Summaries of these data are included in Tables 2-3, 2-4, and 2-5.

McElhaney et al. (1983) subjected unembalmed human cadaver cervical spines to constant velocity loadings to failure as part of the same research program discussed earlier in connection with the response characteristics of the spine. The velocity was 640 mm/s (25.2 in/s). The introduction of small displacements (about 10 mm or 0.4 in) of the proximal end of the spine in the anterior or posterior direction from a nominally straight-spine configuration made a dramatic difference in the failure modes. Failure modes included extension/compression, Jefferson fractures (of the atlas), burst fractures, and anterior wedging. Complete details are provided in the paper.

Myklebust et al. (1983) applied quasi-static compressive loads to individual vertebral bodies, portions of the excised spine (with ligaments intact), and torsos of complete cadavers. Thirty-two isolated thoracic and lumbar vertebral bodies from ten unembalmed male human cadavers were loaded in compression along the superior-inferior direction between parallel plates. The average ultimate forces were 2.638 kN (range 1.557 to 3.470) for ten specimens ranging from T1 through T6. For thirteen vertebrae from T7 through T12 the average was 3.278 kN (range 1.557 to 5.560), and for nine lumbar vertebrae the average was 4.972 kN (range 1.957 to 7.384). The average failure load for fourteen excised thoracolumbar spines was 2.056 kN (range 0.555 to 5.110). Those that sustained failure in the T2-T9 region (n=6) had an average force of 1.224 kN (range 0.555 to 2.220), and those that failed in the T10-L1 region (n=8) had an average of 2.680 kN (range 1.113 to 5.110). The tests on four intact cadavers, however, resulted in an average compressive failure force of 1.788 kN (range 1.110 to 2.750). While this research program generated some useful information, a serious shortcoming is that only vertical loads were measured. The levels of shear force and bending moment that also may have been present at the fixed ends of the spines are unknown.

Strength of the In-Situ Spine. Mertz and Patrick (1971) provide information regarding the upper limits of statically applied neck loads that volunteer subjects were willing to tolerate. The test subjects were restrained in a seated posture, and forces were applied to the head. The applied forces generated bending moments at the occipital condyles, as well as axial and shear forces. Data are included for three postures of the head relative to the neck: normal, neck in extension, and neck in flexion. A summary of the maximum loads documented in this program is provided in Table 2-6.

The same publication addresses the maximum bending moment sustained by a 50th percentile volunteer subject under dynamic conditions. In the flexion mode of loading the onset of pain occurred at an occipital condyle torque of 44 ft·lb (60 N·m) with a maximum rotation of the head relative to the torso of 57°. (The seatback was reclined 15° from the

TABLE 2-3

MEAN BREAKING LOAD (kN) OF SPINAL ELEMENTS
IN TENSION BY AGE GROUP
(Yamada 1970)

Spinal Element	20-39 Yr.	40-79 Yr.
Cervical Vertebrae	1.12	0.89
Cervical Disc	1.03	0.78
Upper Thoracic Vertebrae	1.69	1.31
Upper Thoracic Disc	1.39	1.04
Lower Thoracic Vertebrae	3.29	2.73
Lower Thoracic Disc	2.85	2.15
Lumbar Vertebrae	4.54	3.74
Lumbar Disc	3.86	2.84

TABLE 2-4

MEAN BREAKING LOAD (kN) OF SPINAL ELEMENTS
IN COMPRESSION BY AGE GROUP
(Yamada 1970)

Spinal Element	20-39 Yr.	40-59 Yr.	60-79 Yr.
Cervical Vertebrae	4.09	3.30	1.86
Cervical Disc		3.13	
Upper Thoracic Vertebrae	3.62	3.13	2.31
Upper Thoracic Disc		4.40	
Middle Thoracic Vertebrae	4.22	3.65	2.27
Lower Thoracic Vertebrae	6.30	4.51	2.63
Lower Thoracic Disc		11.25	
Lumbar Vertebrae	7.14	4.67	3.01
Lumbar Disc		14.68	

TABLE 2-5

MEAN BREAKING TORQUE (N·m) OF SPINAL ELEMENTS BY AGE GROUP
(Yamada 1970)

Spinal Element	20-39 Yr.	40-59 Yr.	60-79 Yr.
Cervical Disc	5.5	4.7*	
Upper Thoracic Vertebrae	5.9	4.7	
Upper Thoracic Disc	8.5	8.0*	
Middle Thoracic Vertebrae	10.6	8.9	6.9
Middle Thoracic Disc	17.3	15.7*	
Lower Thoracic Vertebrae	16.1	13.6	11.2
Lower Thoracic Disc	26.7	25.4*	
Lumbar Vertebrae	25.0	20.7	17.1
Lumbar Disc	45.3	41.6*	

*40-69 years.

TABLE 2-6

SUMMARY OF MAXIMUM STATIC NECK
REACTIONS SUSTAINED BY VOLUNTEERS
(Mertz and Patrick 1971)

Neck Posture	Axial Force (kN)		Shear Force (kN), Head Pushing Forward on Neck	Bending Moment (N·m)	
	Tension	Compression		Resisting Flexion	Resisting Extension
Extended	–	–	0.304	33.9	23.7
Normal	1.134	1.112	0.284	31.9	14.2
Flexed	–	–	0.329	35.3	17.0

vertical, and the Frankfort plane of the head was initially horizontal.) The volunteer reached his upper limit of impact severity in a test that resulted in a maximum bending moment of 65 ft·lb (88 N·m) with a maximum head rotation of 70°. He experienced pain at the back of his neck that extended downward. A stiff neck lasting several days was experienced. Human cadaver subjects were also evaluated in this research program. In the flexion mode of loading, a maximum bending moment of 140 ft·lb (190 N·m) and maximum shear force of 450 lb (2 kN) were sustained without evidence of injury on X-ray films. These loads include the equivalent reactions at the occipital condyles resulting from chin-to-chest contact. Neck extension experiments were also conducted. The volunteer subject sustained an extension bending moment of 17.5 ft·lb (24 N·m) but was apprehensive about being subjected to any higher level of impact. The authors indicate that 35 ft·lb (47 N·m) is a non-injurious magnitude for an average-size male. One of the cadaver subjects sustained minor ligamentous damage between C3 and C4 in a test that resulted in a peak extension moment of 24.6 ft•lb (33 N•m). This cadaver was small, however, and scaling techniques were used to illustrate that this moment equates to 42 ft•lb (57 N•m) for an average size male. These researchers indicated that the angle of the head relative to the torso is not an adequate physical measurement for expressing flexion and extension tolerance limits, since a small error in angle measurement equates to a relatively large change in occipital condyle bending moment. Moment, therefore, is claimed to be a better measure.

Mertz et al. (1978) studied the tolerance of the neck in dynamic axial compressive loading indirectly by utilizing the Hybrid III dummy in reconstructions of injury-producing high school football "spearing" maneuvers involving a mechanical tackling machine. Compressive forces registered by the load cell at the occipital condyles of the dummy were correlated with the injuries sustained. Following considerable analyses, the results presented in Figure 2-20 were offered for judging the severity of such loads to the normal adult population (as opposed to high school football players). One criticism of this work that has been voiced is that the Hybrid III neck is probably less compliant in axial compression than is the human neck. Accordingly, while the results may provide a useful calibration of the Hybrid III neck, the forces may not be equivalent to those a human would experience in the same impact environment.

The Hybrid III dummy has also been utilized in reconstructions of Volvo field accidents involving frontal impacts with occupants restrained by lap/shoulder belts and documented not to have sustained head impact with the vehicle interior. The field accident data suggested that frontal collisions of about 48 km/h (30 mph) barrier equivalent velocity for the particular vehicle design studied correlated to approximately a 14% probability of a maximum neck injury severity of AIS 1. In this impact environment the following neck loads were measured on the dummy at the occipital condyles: 153 N•m (113 ft•lb) flexion bending moment, 2.97 kN (668 lb) shear force (head pushing from posterior to anterior on neck), and 3.29 kN (740 lb) axial tensile force. To the extent that the Hybrid III neck response is representative of that of the human, these results should provide measures of human tolerance.

Mertz (1984) has used the above results of Mertz and Patrick (1967, 1971), Mertz et al. (1978), and Nyquist et al. (1980) in formulating injury assessment guidelines for interpreting neck loads measured using the Hybrid III dummy. The reference value for neck flexion bending moment is 190 N•m (140 ft•lb). The implication is that, if the moment is less than 190 N•m, then significant neck injury due to flexion bending is unlikely. For neck extension the reference value is a bending moment of 57 N•m (42 ft•lb). The implication of not exceeding this value is analogous to that for flexion. The injury assessment guideline for neck axial compressive force was taken directly from Mertz et al. (1978) which has already been discussed (see Figure 2-20). The assessment guidelines for neck shear and axial tension forces are the result of further analyses by Mertz of the data collected by Nyquist et al. (1980). These guidelines are illustrated in Figures 2-21 and 2-22. As noted earlier, while such injury assessment guidelines are based on biomechanical data, in the instances where they stem from correlations of Hybrid III loads and human injuries, the loads reflect those that can be tolerated by a human only to the extent that the dummy responded in a humanlike manner.

While 190 N•m (140 ft•lb) has been suggested as a reference value for neck flexion, below which significant neck injury is unlikely, Cheng et al. (1982) have reported on a human cadaver experiment where the peak flexion moment at the occipital condyles was 340 N•m (250 ft•lb), and a catastrophic separation occurred at the upper cervical spine. This was a case of combined loading, however, with an axial tensile force in excess of 6.5 kN (1460 lb) at the instant of failure.

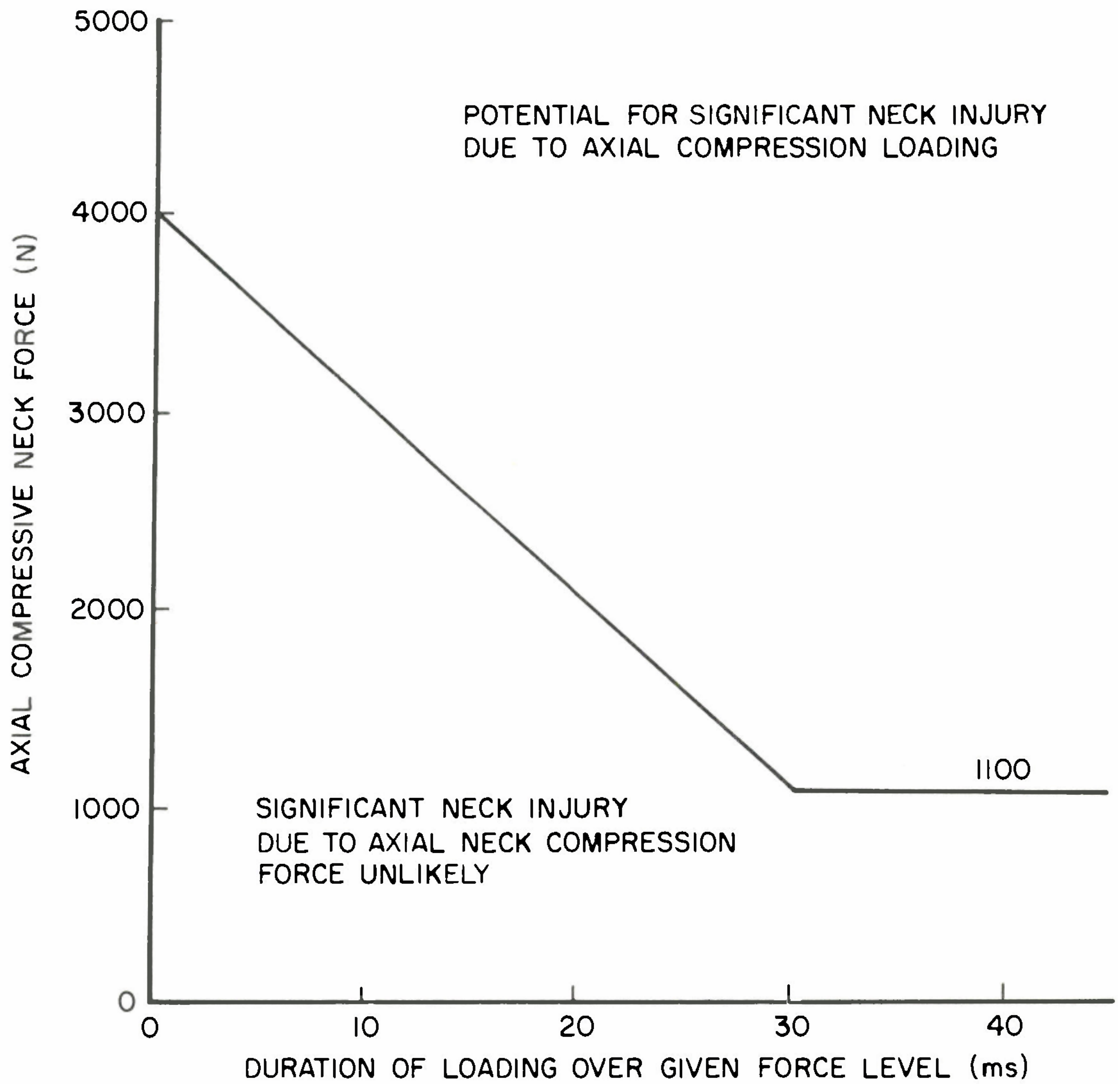

FIGURE 2-20. Injury assessment criterion for neck axial compression loading (Mertz et al. 1978).

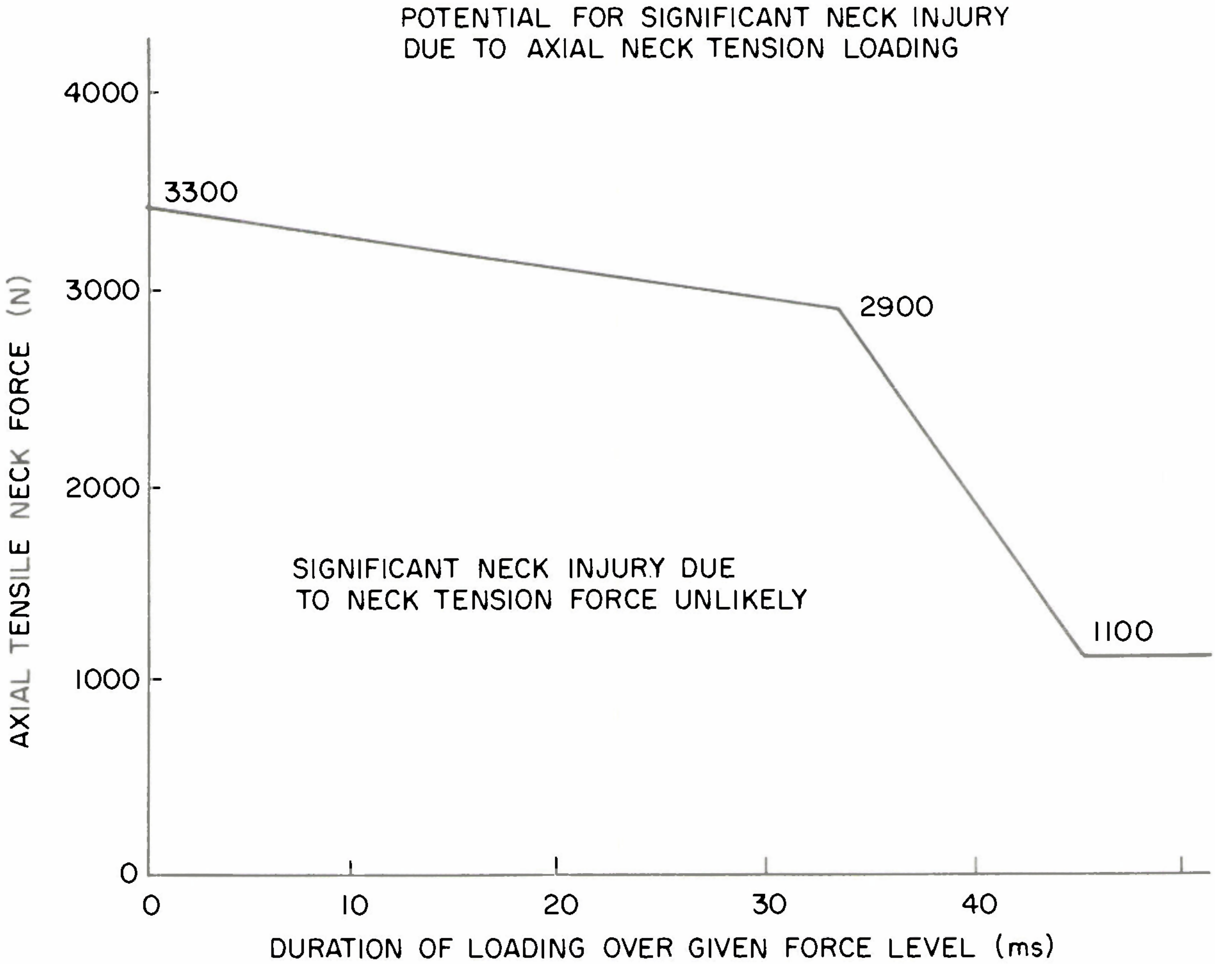

FIGURE 2-21. Injury assessment criterion for neck axial tension loading (Mertz 1984).

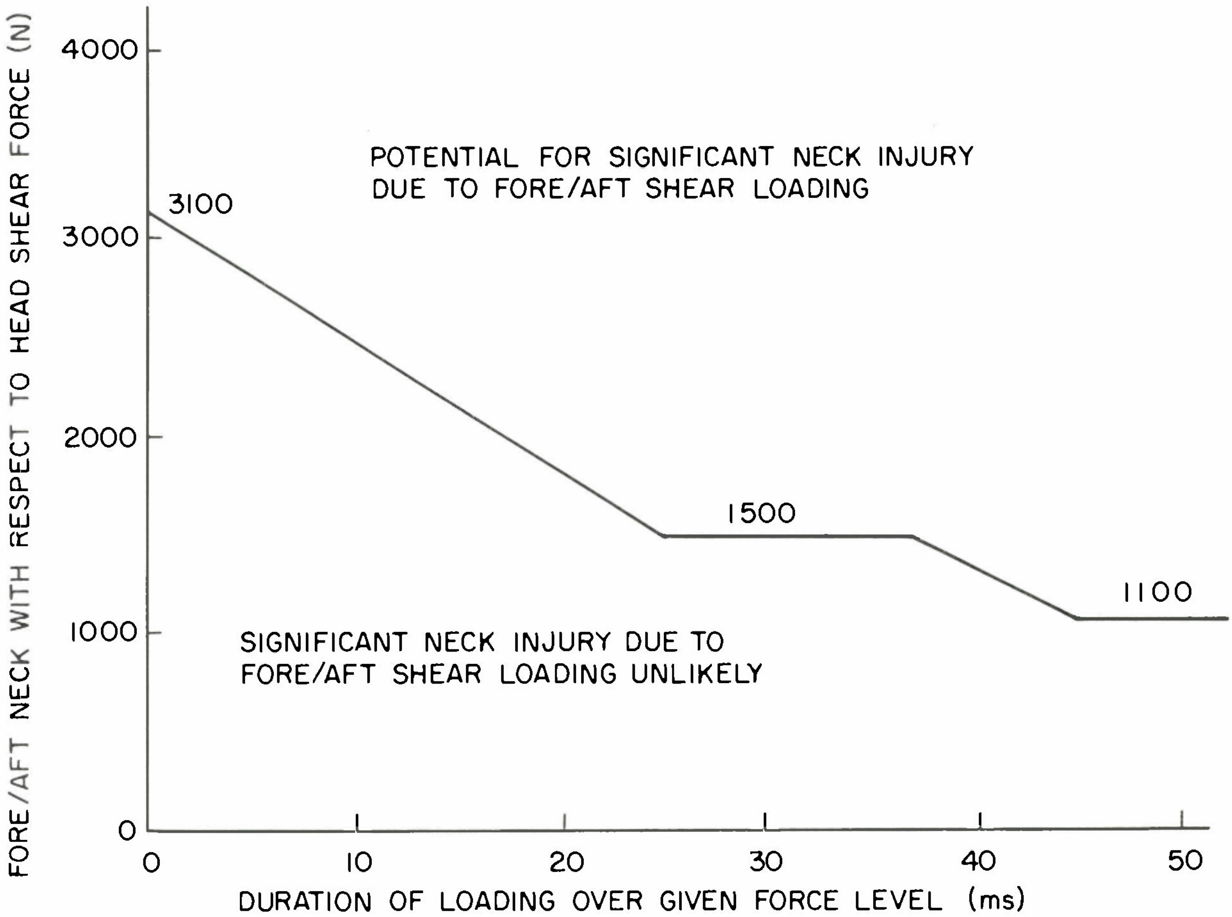

FIGURE 2-22. Injury assessment criterion for anterior-posterior shear force at the head-neck junction (Mertz 1984).

Neck injury tolerance related to impacts to the crown of the head have been studied by Culver et al. (1978), Hodgson and Thomas (1980), and Nusholtz et al. (1981, 1983). Both embalmed and unembalmed human cadavers were tested in these studies. Mechanisms of failure were various forms of combined axial compression and bending. The initial curvature of the cervical spine, its position relative to the head and torso, and the precise direction of impact were found to have a strong influence on the type of injury sustained.

Culver et al. (1978) applied superior-to-inferior impacts to the heads of eleven unembalmed cadavers using a 10-kg (22-lb) padded impactor. Peak forces varied from 4.7 kN (1050 lb) to 8.9 kN (2000 lb) with initial input energies ranging from 260 J to 645 J (192 to 475 ft•lb). Cervical vertebral fractures, primarily in the posterior elements, were produced.

Hodgson and Thomas (1980) tested embalmed human cadavers wearing protective helmets. Static and dynamic loads were applied to the head in the superior-to-inferior direction. Strain gages were attached at the vertebral bodies and facets of the cervical spine in some cases. Furthermore, some subjects had the cervical spine sectioned to enable high-speed photographic analyses of the vertebrae during impact. These authors concluded that the head's freedom to rotate about the atlanto-occipital junction, the location of impact, and the alignment of the impact force relative to the spine are influential factors on injury site and level.

Nusholtz et al. (1981) tested a series of twelve unembalmed human cadavers, applying superior-to-inferior impacts to the top of the head. The guided impactor had a mass of 56 kg (123 lb) and had pre-impact velocities ranging from 4.6 to 5.6 m/s (15 to 18 ft/s). Instrumentation included head, T8, and sternum accelerometers, impactor biaxial force transducer, and high-speed cameras. The face of the impactor was padded. Damage to the cervical spine was produced in all but one test. There were fractures of spinous processes, laminae, transverse processes, and bodies of the cervical vertebrae. Torn ligaments and ruptured discs also occurred. Damage occurred at sites ranging from C2 to T4. Peak forces ranged from 1.8 to 11.1 kN (405 to 2495 lb). While it was stated that specific conclusions with regard to cervical spine tolerance levels could not be made based on this limited study, other noteworthy conclusions were reached. Initial orientation of the spine was said to be a critical factor in influencing the type of damage produced. Flexion-type damage was observed in some tests where extension motion of the neck occurred, and vice versa. A two-dimensional description of the bending of the neck was thought to be inadequate to characterize the bending mechanisms of damage in the cadaver. Energy absorbing materials were found to be effective in reducing peak impact forces, but they did not necessarily reduce the energy transferred through the neck nor the damage produced.

Nusholtz et al. (1983) performed a series of drop tests to study cervical spine tolerance where eight unembalmed cadavers were released from heights ranging from 100 mm to 1.8 m (3.9 in to 5.9 ft). Several of the subjects were subjected to multiple low-energy drops prior to a final high-energy injury-producing drop. The subjects ranged in age from 51 to 70 years, in mass from 50 to 83 kg (110 to 183 lb), and in height from 1.60 to 1.81 m (5.25 to 5.94 ft). The crown of the head impacted a rigidly mounted force transducer that was padded with from 6 to 25 mm (0.25 to 1.0 in) of Ensolite® foam. Two series of tests comprising a total of fifteen impacts were conducted. In the first series the midsagittal plane of the head was aligned with the midsagittal plane of the thorax. Only the force applied to the head was monitored in these tests. The second series of tests involved pre-positioning the head by rotating it about the lateral, anterior-posterior, and superior-inferior axes. These latter tests included a full complement of head and thoracic spine accelerometers. The researchers concluded that flexion-type cervical spine damage appears to be unlikely when the head-neck is constrained to move in the midsagittal plane during crown impacts. In contrast, flexion-type damage was observed when the head-neck-thorax was prepositioned to produce non-midsagittal plane motion. Cervical spine injury is thought to be a three-dimensional phenomenon in general, although the thoracic spine response in these events may be two-dimensional. Thoracic spine response is thought to be a critical factor influencing cervical spine response and damage pattern.

Alem et al. (1984) reported on two series of superior-to-inferior head impacts to nineteen unembalmed human cadavers. While the first series of tests was for the purpose of generating dynamic response data for sub-injurious impacts, the second series of tests (fourteen impacts to fourteen cadavers) was intended for studying neck injury tolerance. A 10-kg (22-lb) impactor moving at from 7 to 11 m/s (23 to 36 ft/s) was utilized in the second series. Parameters quantified included impact velocity, force and energy, and head three-dimensional kinematics. The accelerations at T1, T6, and T12 were also monitored. The cadavers evaluated in the tolerance study were all males and had body masses ranging from 44.7 to 81.5 kg (98.3 to 179.3 lb) and statures from 1.66 to 1.84 m (5.45 to 6.04 ft). Their ages ranged from 41 to 72 years. Peak forces applied to the head ranged from 3 to 17 kN (675 to 3820 lb). In these tests there was no attempt to align the cervical spine longitudinal axis with that of the impactor. Rather, the curvature of the neck was allowed to simulate the natural attitude of a normally standing or seated subject. It is reported that when skull fracture occurred (at the point of force application or basal skull fracture), neck injuries were absent. In all other tests, when there was sufficient input energy to cause the neck to "buckle," there were injuries to one or more cervical vertebrae. Attempts to assign a threshold peak applied force value necessary to cause neck injury were elusive. While 4 kN (900 lb) seemed to have some merit, injury occurred at a force as low as 3 kN (675 lb), and one test resulted in 16 kN (3600 lb) without injury. The authors concluded that, of the parameters examined, head velocity seemed to be the best injury predictor. However, none of the potential predictors of injury were infallible. It was recognized that the sample size was too small for stating these conclusions with confidence.

The first five cadavers tested by Alem et al. (1984) were subjected to non-injurious impacts for the purpose of studying neck response characteristics. The neck reaction moments were listed as high as 170 N•m (125 ft•lb) about the posterior-to-anterior axis, 107 N•m (79 ft•lb) about the right-to-left axis, and 68 N•m (50 ft•lb) about the inferior-to-superior axis. Since these were moments exerted by the neck in reaction to head motion, they represent bending moments during head leftward lateral flexion, rearward extension in the sagittal plane, and rightward axial twisting, respectively. These peak values are associated with short durations in the range of 5 to 10 ms, which occurred during the head impact-loading phases of the dynamic time-histories. The lateral bending value is near the forward flexion limit of 190 N•m (140 ft•lb), suggested by Mertz et al. (1973), while the rearward extension value greatly exceeds the suggested limit of 57 N•m (42 ft•lb). It must be noted that this peak value occurred early in the test, before significant head/neck extension took place, and may represent an increased tolerance to such bending moments for short durations and small bending angles. Significant peak magnitudes for the other five force and moment components are listed for this test. While all peaks may not have been experienced simultaneously, in all probability there was substantial combined loading present.

As early as 1959, human tolerance limits to caudocephalad ($+G_z$) acceleration were described by Eiband (1959). He summarized all available data from humans and animals and indicated that the U.S. Army Air Force had proposed a 20-G limit for ejection seats. The limit assumed a trapezoidal acceleration pulse acting on a subject fully restrained by a lap belt and shoulder straps. An alternate criterion was proposed by Stech (1963) in the form of an index called the Dynamic Response Index (DRI). It is based on the response of Latham's (1957) spring-mass model and is principally a function of the rate of onset. The limiting value was said to correlate to a 5% probability of spinal injury.

There are several problems with these $+G_z$ tolerance limits. They apply to accelerations in the $+G_z$ direction only and are meant to be used in aircraft ejection seat design. That is, the torso is assumed to be fully restrained and subjected to a trapezoidal pulse that has relatively low rate of onset. From research studies of whole-body acceleration, it was established that tolerance to injury is closely tied to the mechanism of injury and of load transmission along the spine. The fracture level was shown to be extremely sensitive to spinal configuration (Ewing et al. 1972), and vertebral body strain along the anterior aspect was a function of the position of the head just prior to impact (Vulcan et al. 1970). Anterior wedge fracture of a vertebral body can occur when there is a combined axial compression and flexion bending load on the spine. If the $+G_z$ acceleration is accompanied by a small $-G_x$ acceleration component, the fracture G-level is lower due to increased spinal flexion. This phenomenon was observed in simulated helicopter crashes conducted by King and Levine (1982). Anterior wedge fractures and ruptures of the supraspinal and interspinous ligaments were observed. The addition of an axial torque to an applied flexural load appears to facilitate dislocations and fracture-dislocations of the spine. The orientation of the facet joint surfaces may be a determining factor as far as the susceptibility to subluxation is concerned. Griffith et al. (1966) indicated that T5-T7 injuries were often more severe than T11-L1 injuries.

Vertebral strength is known to decrease with age. Osteoporosis is a common cause of vertebral fractures in the absence of impact loads. Various investigators have reported on this decrease in strength with age. Perey (1957) tested eighty-one vertebral bodies (posterior elements removed) and found that there was a dramatic decrease in compressive strength after the age of 60. He also found that the decrease in strength of vertebral endplates was over 50% between the second and sixth decade of life. Similar results were reported by Bell et al. (1967), Bartley et al. (1966), and Weaver (1966). For impact loading upward through the buttocks, the average fracture level of acceleration for well restrained cadaveric subjects aged 57 to 63 was approximately 10 G. This value is consistent with the 20-G limit set by Eiband (1959) for young pilots. However, if the $+G_z$ acceleration is coupled with a $-G_x$ component by adding a 10° forward pitch, the fracture level appears to drop to 8.5 G for cadavers in the age range of 47 to 63. This statement is based on unpublished data acquired recently at Wayne State University. The principal reason for this decrease in tolerance level is an increase in flexion moment.

Defining a limited set of injury criteria for the spine, particularly since the failure of the spinal components is not restricted to the bony portions of the spine, is extremely difficult. Much of the spinal resistance to bending and torsional loads is provided by soft tissues—ligaments, muscles, and cartilage (disc). For each set of loading conditions, injury criteria need to be formulated. Such a task is indeed formidable.

SUMMARY AND CONCLUSIONS

The vertebral column is the principal load-bearing structure of the head and torso and provides a flexible protective pathway for the spinal cord. Injuries that affect the function of the spinal cord can result in death, quadriplegia, or paraplegia. Despite these potentially serious consequences, the actual incidence of such injuries is relatively low, and thus they contribute less than 6% to the total IPR.

The static and dynamic response of the head/neck system to indirect inertial loading at low crash severities has been studied extensively in volunteers and, to a lesser extent, in cadavers. These studies have included frontal, lateral, and oblique impacts. A limited data base exists for rear impacts. Specifications for suitable neck linkage systems, ranges of motion, and joint resistance characteristics are available from the published literature. Direct crown loading experiments have also produced data on the superior-inferior compliance of the cervical spine in cadavers.

The static midsagittal bending response of the thoracolumbar spine has been studied in volunteers for flexion and extension. Specifications in terms of overall rotation ranges and bending resistance characteristics of the rotation of the thorax relative to the pelvis have been produced. The equivalent dynamic data are quite limited but are suggestive of the presence of upper thoracic spine mobility.

The status of knowledge on the tolerance of the neck to loading is limited. Of necessity, all volunteer data are below the injury threshold. Additionally, injury mechanisms can be quite different than those mechanisms controlling response. Most injury threshold data are either based on cadaver tests or on reconstructions of accidents with instrumented dummies. As such, the threshold values are subject to the limitations associated with the surrogate used to obtain the data. These data sources have been used to develop limiting tolerance values for neck bending moments in midsagittal flexion and extension, axial compressive and tensile neck forces, and neck shear forces. No efforts have been made at this time to develop limit values associated with combinations of the various forces and moments. Corresponding studies of the tolerance of the thoracolumbar spine are not available. The only tolerance studies done on the thoracolumbar spine are those related to vertical accelerations.

REFERENCES

Alem, N.M. (1980) *Helmet impact test system development.* Report no. UM-HSRI-80-72-1. The University of Michigan, Highway Safety Research Institute, Ann Arbor.

Alem, N.M.; Nusholtz, G.S.; and Melvin, J.W. (1984) Head and neck response to axial impacts. *Proc. 28th Stapp Car Crash Conference*, pp. 275-281. Society of Automotive Engineers, Warrendale, Pa.

Bartley, M.H.; Arnold, J.S.; Haslam, R.K.; and Jee, W.S.S. (1966) The relationship of bone strength and bone quantity in health, disease and aging. *Journal of Gerontology*, 21:517-521.

Begeman, P.C.; King, A.I.; and Prasad, P. (1973) Spinal loads resulting from $-G_x$ acceleration. *Proc. 17th Stapp Car Crash Conference*, pp. 343-360. Society of Automotive Engineers, New York.

Begeman, P.C.; King, A.I.; Levine, R.S.; and Viano, D.C. (1980) Biodynamic response of the musculoskeletal system to impact acceleration. *Proc. 25th Stapp Car Crash Conference*, pp. 477-509. Society of Automotive Engineers, Warrendale, Pa.

Bell, G.H.; Dunbar, O.; Beck, J.S.; and Gibb, A. (1967) Variation in strength of vertebrae with age and their relation to osteoporosis. *Calcified Tissue Research*, 1:75-86.

Bowman, B.M.; Schneider, L.W.; Lustick, L.S.; Anderson, W.R.; and Thomas, D.J. (1984) Simulation analysis of head and neck dynamic response. *Proc. 28th Stapp Car Crash Conference*, pp. 173–194. Society of Automotive Engineers, Warrendale, Pa.

Buckwalter, J.A. (1982) The fine structure of human intervertebral disc. *Idiopathic Low Back Pain*, pp. 108–143. Edited by A.A. White and S.L. Gordon. C.V. Mosby, St. Louis.

Chance, G.O. (1948) Note on a type of flexion fracture of the spine. *British Journal of Radiology*, 21:452–453.

Cheng, R.; Mital, N.K.; Levine, R.S.; and King, A.I. (1979) Biodynamics of the living human spine during $-G_x$ impact acceleration. *Proc. 23rd Stapp Car Crash Conference*, pp. 721–763. Society of Automotive Engineers, Warrendale, Pa.

Cheng, R.; Yang, K.H.; Levine, R.S.; King, A.I.; and Morgan, R. (1982) Injuries to the cervical spine caused by a distributed frontal load to the chest. *Proc. 26th Stapp Car Crash Conference*, pp. 1–40. Society of Automotive Engineers, Warrendale, Pa.

Culver, R.H.; Bender, M.; and Melvin, J.W. (1978) *Mechanisms, tolerances and responses obtained under dynamic superior-inferior head impact, a pilot study*. Report no. UM-HSRI-78-21. University of Michigan, Highway Safety Research Institute, Ann Arbor.

DePalma, A.F. (1970) *The management of fractures and dislocations*, pp. 272–295. Saunders, Philadelphia.

Eiband, A.M. (1959) *Human tolerance to rapidly applied accelerations: A summary of the literature*. NASA Memorandum No. 5-19-59E. NASA Lewis Research Center, Cleveland.

Ewing, C.L. (1968) Personal communication to A. King.

Ewing, C.L.; King, A.I.; and Prasad, P. (1972) Structural considerations of the human vertebral column under $+G_z$ impact acceleration. *Journal of Aircraft*, 9:84–90.

Ewing, C.L.; Thomas, D.J.; Lustick, L.; Muzzy, W.H.; Willems, G.C; and Majewski, P. (1978) Effect of initial position on the human head and neck response to +Y impact acceleration. *Proc. 22nd Stapp Car Crash Conference*, pp. 101–138. Society of Automotive Engineers, Warrendale, Pa.

Garfin, S.R.; and Rothman, R.H. (1983) Traumatic spondyloisthesis of the axis (hangman's fracture). *The Cervical Spine*, pp. 223–232. Edited by R.W. Baily. Lippincott, Philadelphia.

Gogan, W.; Knight, G.; Patwardhan, A.; Plioplys, A.; and Vanderby, R. (1983) Three-dimensional orientation of the thoracic spine facets. *Advances in Bioengineering*, pp. 48–49. Edited by D. Bartel. American Society of Mechanical Engineers, New York.

Gray, H. (1973) *Anatomy of the human body*, pp. 109–111. Lea and Febiger, Philadelphia.

Griffith, H.B.; Gleave, J.R.W.; and Taylor, R.G. (1966) Changing patterns of fracture in the dorsal and lumbar spine. *British Medical Journal*, 1:891–894.

Hakim, N.S.; and King, A.I. (1976) Programmed replication of in-situ (whole-body) loading conditions during in vitro (substructure) testing of a vertebral segment. *Journal of Biomechanics*, 9:629-632.

Hodgson, V.R.; and Thomas, L.M. (1980) Mechanisms of cervical spine injury during impact to the protected head. *Proc. 24th Stapp Car Crash Conference*, pp. 15-42. Society of Automotive Engineers, Warrendale, Pa.

Huelke, D.F.; Mendelsohn, R.A.; and States, J.D. (1978) Cervical fractures and fracture dislocations sustained without head impact. *Journal of Trauma*, 18:533-538.

Huelke, D.F.; O'Day, J.; and Mendelsohn, R.A. (1981) Cervical injuries suffered in automobile crashes. *Journal of Neurosurgery*, 54:316-322.

Kazarian, L.E. (1977) *Escape injury mechanism assessment.* AMRL-TR-77-60. Aerospace Medical Research Laboratory, Wright-Patterson AFB, Ohio.

Kazarian, L.E. (1982) Injuries to the human spinal column: biomechanical and injury classifications. *Exercise and Sports Sciences Review*, 9:297-352.

Kazarian, L.E.; Boyd, D.; and von Gierke, H. (1971) The dynamic biomechanical nature of spinal fractures and articular facet derangement. *Linear Acceleration of Impact Type, AGARD Conference Proc. No. CP-88-71*, pp. 19.1-19.25. Advisory Group for Aerospace Research and Development, Neuilly Sur Seine, France.

Kazarian, L.E.; Beers, K.; and Hernandez, J. (1979) Spinal injuries in the F/FB-111 crew escape system. *Aviation, Space, and Environmental Medicine*, 50:948-957.

King, A.I. (1984) The spine: Its anatomy, kinematics, injury mechanisms and tolerance to impact. *The Biomechanics of Impact Trauma*, pp. 191-226. Edited by A. Chapon and B. Aldman. Elsevier, Amsterdam.

King, A.I.; and Cheng, R. (1984) *Kinesiology of the human shoulder and spine.* Final Report, DOT Contract No. DOT-HS-5-01232. Wayne State University, Detroit (in press).

King, A.I.; and Levine, R.S. (1982) Human cadaveric response to simulated helicopter crashes. *Impact Injury Caused by Linear Acceleration: Mechanisms, Prevention and Cost, AGARD Conference Proc. No. CP-322*, pp. 7.1-7.8. Advisory Group for Aerospace Research and Development, Neuilly Sur Seine, France.

Latham, F. (1957) A study in body ballistics: Seat ejection. *Proc. Royal Society (B)*, 147:121-139.

Mallikarjunarao, C.; Padgaonkar, A.J.; Levine, R.S.; Gurdjian, E.S.; and King, A.I. (1977) Kinesiology of the human spine under static loading. *1977 Biomechanics Symposium*, pp. 99-102. American Society of Mechanical Engineers, New York.

McElhaney, J.H.; Paver, J.G.: McCrackin, H.J.; and Maxwell, G.M (1983) Cervical spine compression responses. *Proc. 27th Stapp Car Crash Conference*, pp. 163-178. Society of Automotive Engineers, Warrendale, Pa.

Mertz, H.J. (1984) *Injury assessment values used to evaluate Hybrid III response measurements.* General Motors Corp. NHTSA Docket Submission VSG 2284 Part III, Attachment I, Enclosure 2.

Mertz, H.J.; and Patrick, L.M. (1967) Investigation of the kinematics and kinetics of whiplash. *Proc. 11th Stapp Car Crash Conference,* pp. 267–317. Society of Automotive Engineers, New York.

Mertz, H.J.; and Patrick, L.M. (1971) Strength and response of the human neck. *Proc. 15th Stapp Car Crash Conference,* pp. 207-255. Society of Automotive Engineers, New York.

Mertz, H.J.; Neathery, R.F.; and Culver, C.C. (1973) Performance requirements and characteristics of mechanical necks. *Human Impact Response: Measurement and Simulation,* pp. 263–288. Edited by W.F. King and H.J. Mertz. Plenum Press, New York.

Mertz, J.H.; Hodgson, V.R.; Thomas, L.M.; and Nyquist, G.W. (1978) An assessment of compressive neck loads under injury-producing conditions. *The Physician and Sports Medicine,* 6:95–106.

Mital, N.K.; Cheng, R.; King, A.I.; and Eppinger, R.H. (1978a) A new design for a surrogate spine. *Proc. 7th Experimental Safety Vehicle Conference,* pp. 427–438. U.S. Government Printing Office, Washington, D.C.

Mital, N.K.; Cheng, R.; Levine, R.S.; and King, A.I. (1978b) Dynamic characteristics of the human spine during $-G_x$ acceleration. *Proc. 22nd Stapp Car Crash Conference,* pp. 139–165. Society of Automotive Engineers, Warrendale, Pa.

Moffat, E.A.; Siegel, A.W.; and Huelke, D.F. (1978) The biomechanics of automotive cervical fractures. *Proc. 22nd Conference of American Association for Automotive Medicine,* pp. 151–168. AAAM, Morton Grove, Ill.

Myklebust, J.; Sances, A.; Maiman, D.; Pintar, F.; Chilbert, M.; Rauschning, W.; Larson, S.; Cusick, J.; Ewing, C.; Thomas, D.; and Saltzberg, B. (1983) Experimental spinal trauma studies in the human and monkey cadaver. *Proc. 27th Stapp Car Crash Conference,* pp. 149–161. Society of Automotive Engineers, Warrendale, Pa.

National Center for Health Statistics. (1965) Weight, height and selected body dimensions of adults, United States, 1960–1962. *Vital and Health Statistics,* Series 11, No. 8. U.S. Public Health Service, Washington, D.C.

Nicoll, E.A. (1949) Fractures of the dorso-lumbar spine. *Journal of Bone and Joint Surgery,* 31B:376–393.

Nusholtz, G.S.; Melvin, J.W.; Huelke, D.F.; Alem, N.M.; and Blank, J.G. (1981) Response of the cervical spine to superior-inferior head impact. *Proc. 25th Stapp Car Crash Conference,* pp. 195–237. Society of Automotive Engineers, Warrendale, Pa.

Nusholtz, G.S.; Huelke, D.F.; Lux, P.; Alem, N.M.; and Montalvo, F. (1983) Cervical spine injury mechanism. *Proc. 27th Stapp Car Crash Conference,* pp. 179–197. Society of Automotive Engineers, Warrendale, Pa.

Nyquist, G.W.; and King, A.I. (1984) *Sagittal plane static bending response of the torso.* Subcontractor report on DTNH22-83-C-07005. Wayne State University, Detroit.

Nyquist, G.W.; and Murton, C.J. (1975) Static bending response of the human lower torso. *Proc. 19th Stapp Car Crash Conference*, pp. 513–541. Society of Automotive Engineers, Warrendale, Pa.

Nyquist, G.W.; Begeman, P.C.; King, A.I.; and Mertz, H.J. (1980) Correlation of field injuries and GM Hybrid III responses for lap-shoulder belt restraint. *Journal of Biomechanical Engineering*, 102:103–109.

Patrick, L.M.; and Chou, C. (1976) *Response of the human neck in flexion, extension, and lateral flexion.* Vehicle Research Institute Report No. VRI-7-3. Society of Automotive Engineers, Warrendale, Pa.

Patwardhan, A.; Vanderby, R.; and Lorenz, M. (1982) Load bearing characteristics of lumbar facets in axial compression. *1982 Advances in Bioengineering*, pp. 155–160. American Society of Mechanical Engineers, New York.

Peacock, A. (1952) Observations on the postnatal structure of the intervertebral disc in man. *Journal of Anatomy*, 86:162–179.

Perey, O. (1957) Fracture of the vertebral end-plate in the lumbar spine. *Acta Orthopedics Scandinavia*, 25.

Pierce, D.A.; and Barr, Jr, J.S. (1983) Fractures and dislocations at the base of the skull and upper spine. *The Cervical Spine*, pp. 196–206. Edited by R.W. Baily. Lippincott, Philadelphia.

Prasad, P.; and King, A.I. (1974) An experimentally validated dynamic model of the spine. *Journal of Applied Mechanics*, 41:546–550.

Prasad, P.; King, A.I.; and Ewing, C.L. (1974) The role of articular facets during $+G_z$ acceleration. *Journal of Applied Mechanics*, 41:321–326.

Schneider, L.W.; Foust, D.R.; Bowman, B.M.; Snyder, R.G.; Chaffin, D.B.; Abdelnour, T.A.; and Baum, J.K. (1975) Biomechanical properties of the human neck in lateral flexion. *Proc. 19th Stapp Car Crash Conference*, pp. 455–486. Society of Automotive Engineers, Warrendale, Pa.

Society of Automotive Engineers, Human Mechanical Response Task Force. (1985) *Human mechanical response characteristics.* SAE J1460. Society of Automotive Engineers, Warrendale, Pa.

Sonoda, T. (1962) Studies on the strength for compression, tension, and torsion of the human vertebral column. *Journal of the Kyoto Prefectural University of Medicine, Medical Society*, 71:659–702.

Stech, E.L. (1963) *The variability of human response to acceleration in the spinal direction.* Frost Engineering Development Corp., Englewood, Co.

Steckler, R.M.; Epstein, J.A.; and Epstein, B.S. (1969) Seat belt trauma to the lumbar spine: An unusual manifestation of the seat belt syndromes. *Journal of Trauma*, 9:508–513.

Thomas, D.J.; and Jessop, M.E. (1983) Experimental head and neck injury. *Impact Injury of the Head and Spine*, pp. 177-217. Edited by C.L. Ewing et al. Charles C. Thomas, Springfield, Ill.

Vulcan, A.P.; King, A.I.; and Nakamura, G.S. (1970) Effects of bending on the vertebral column during $+G_z$ acceleration. *Aerospace Medicine*, 41:294-300.

Weaver, J.K. (1966) Bone: Its strength and changes with aging and an evaluation of some methods for measuring its mineral content. *Journal of Bone and Joint Surgery*, 41A:935.

Wismans, J.; and Spenny, D.H. (1983) Performance requirements for mechanical necks in lateral flexion. *Proc. 27th Stapp Car Crash Conference*, pp. 137-148. Society of Automotive Engineers, Warrendale, Pa.

Wismans, J.; and Spenny, D.H. (1984) Head-neck response in frontal flexion. *Proc. 28th Stapp Car Crash Conference*, pp. 161-171. Society of Automotive Engineers, Warrendale, Pa.

Yamada, H. (1970) *Strength of biological materials*, pp. 75-80. Edited by F.G. Evans. Williams and Wilkins, Baltimore.

Yang, K.H.; and King, A.I. (1984) Mechanism of facet load transmission as a hypothesis for low back pain. *Spine*, 9:557-565.

CHAPTER 3

THORAX

J.W. Melvin, R.L. Hess, and K. Weber
The University of Michigan
Ann Arbor, Michigan

The thorax houses most of the body's vital organs and is thus the next most critical region, after the head, to protect from injury. Injuries to the chest constitute nearly 19% of the cost to society of injuries sustained by automobile occupants, as calculated using the Injury Priority Rating scheme. The nature of thoracic injury, however, is such that there are few long-term disabilities. In general, the victim either dies soon after impact or recovers completely.

ANATOMY OF THE THORAX

The thorax, as referred to here, consists of the rib cage and the organs surrounded by it, but not the overlying tissue.

Rib Cage. The cage structure consists of the twelve thoracic vertebrae, the sternum, and twelve pairs of ribs. The upper seven pairs articulate with the sternum directly through cartilaginous extensions of the ribs. The next two pairs articulate indirectly, and the lower three pairs are not connected to the sternum at all. The rib cage covers some of the upper abdominal organs. The diaphragm, a dome-shaped, thin muscle, is the lower thoracic boundary separating the thoracic and abdominal contents. Portions or all of the ribs from the seventh pair to the twelfth are thus well below the diaphragm and enclose, to a variable degree, the liver, stomach, spleen, pancreas, and kidneys.

Lungs. The lungs are covered by a membrane (the visceral pleura) that quite closely fits the lungs' contours. Another membrane (the parietal pleura) lines the inner surface of the chest wall, covers the diaphragm, and encloses the structures in the middle of the thorax. These two sacs, left and right, are separate from each other. Each sac has potential space between the visceral and the parietal pleura that is known as the pleural cavity. Air or blood may fill this potential space when thoracic injury occurs, causing respiratory arrest.

Mediastinum and Heart. The space between the right and left pleural sacs is known as the mediastinum. It is limited in the front by the sternum and in the back by the thoracic vertebrae. The mediastinum can be crudely pictured on a plane X-ray plate. Fluid filling this space leads to an observed "widening of the mediastinum" and serves as a primary diagnostic signal of possible distress of the heart or the great vessels. These vessels are the pulmonary arteries (left and right), the pulmonary veins (left and right), the thoracic aorta, and the vena cava (superior and inferior). The inferior vena cava receives blood from the lower parts of the body and the superior receives blood from the head, neck, and upper extremities.

The heart is divided into four parts, the left and right atria and ventricles. The heart is encased in a two-layered sac (the pericardium), the inner layer of which is continuous with that of the heart surface. The two layers of the sac are completely separate and thus form the pericardial space. This sac also extends along the first inch of the great vessels. Fluid build-up in the pericardial sac puts pressure on the heart, constricting it and reducing cardiac output. This condition is referred to as a pericardial tamponade.

A partial tracing of a plate illustrating the relative position of the above structures and organs at about the mid-height of the thorax is shown as Figure 3-1.

THORACIC INJURY FROM CLINICAL EXPERIENCE

To provide some background on and insight into the mechanisms of actual thoracic injuries, clinical literature was selected and reviewed. These articles, included in an appendix to this chapter, are not concerned with creating a statistical basis for analysis of injury types or degrees, but rather are primarily concerned with matters of diagnosis and treatment in order to reduce mortality and morbidity among those who reach medical treatment facilities. In addition, injuries generated in an automotive environment are often combined with non-automotive injury cases. Finally, this literature treats the development of secondary ailments triggered by the original trauma, an aspect of injury development that is largely absent from the biomechanics literature.

The clinical literature can be very instructive, in that it provides the basis for a mechanistic description of the thoracic structure and an appreciation for its failures under blunt loading. This literature does not, however, directly establish any well-founded hypotheses regarding injury mechanisms or tolerances such as could be related to location, distribution, direction, or time-history of external loading. It does serve to establish a background against which the biomechanics researcher might create hypotheses.

Generally, we shall divide our discussion of thoracic injury among injury of the ribs, injury of the lungs, and injury of the heart. Rib fracture by itself was not included in the clinical literature reviewed, so this injury will not be discussed except to the extent that rib fracture can be used as a diagnostic indicator.

Flail Chest. The flail chest is a condition of instability or flapping of the chest wall due to multiple rib fracture. This results in chest motion opposite to that occurring during normal breathing. The literature indicates that it is common for the flail chest either not to have developed by the time of first diagnosis in an emergency room, or to be missed in the emergency room diagnosis. Neither the existence of head injury or unconscious state nor the number of ribs fractured seems to differentiate between early and late flailing development. Although flail chest is directly related to trauma-induced instability of the thoracic cage, a change in pulmonary compliance due to airway injury, an accumulation of secretions, or artery-to-vein shunting due to lung contusions may develop in a few hours after the trauma and lead to increased effort in breathing. Oxygen levels in the arterial blood may fall below required levels, carbon dioxide tensions may rise with cardiac arrest, or radical pH changes of body fluid may result. Tracheal injury or rupture may also be a contributing factor leading to the flail chest.

The flail chest is not directly an injury in its own right and thus cannot be related to a specific class of blow other than blunt trauma to the front or side of the rib cage. As a matter of interest, immediate treatment requires placing a breathing tube into the airway and providing mechanical respiratory assistance. It is also generally advantageous for the surgeon to later cut an opening into the trachea to facilitate breathing. However important these treatments may be, the development of bacterial infection of the bronchial

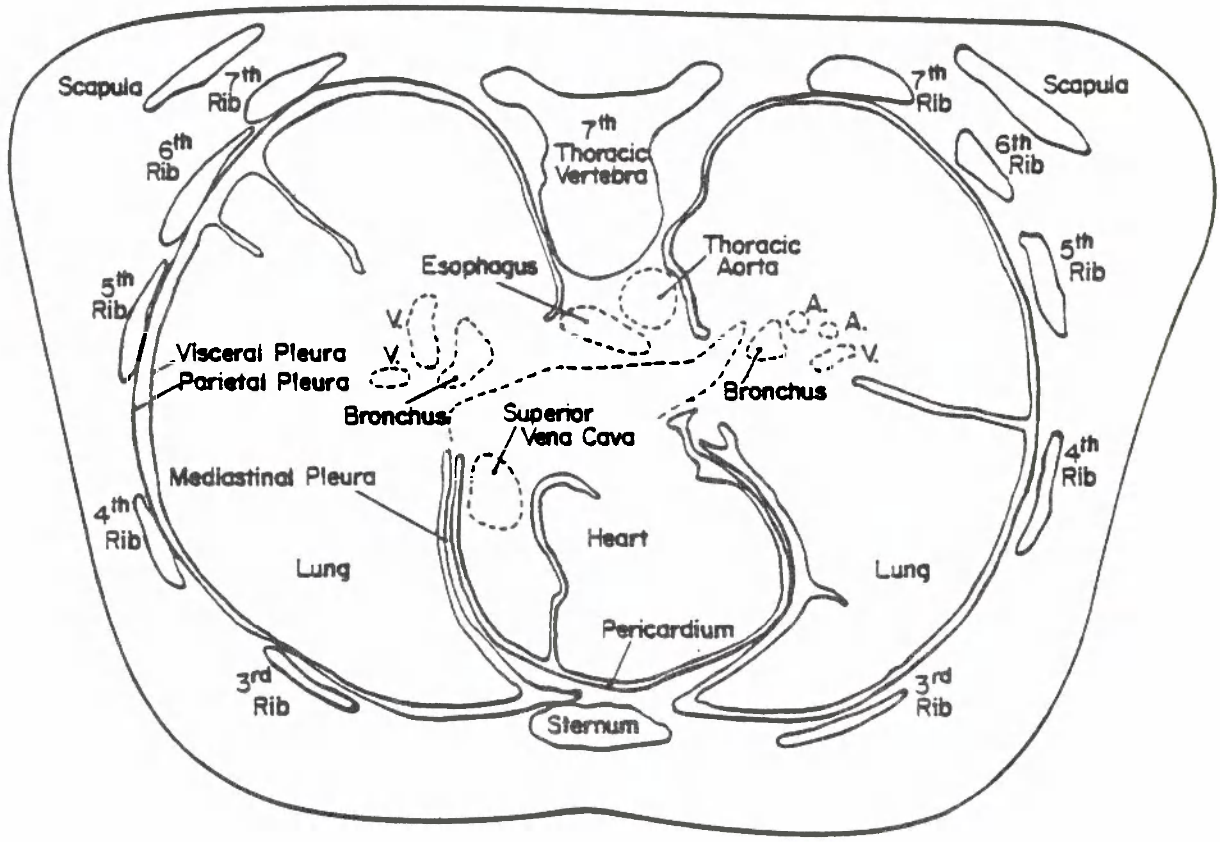

FIGURE 3-1. Cross section at mid-height of thoracic cage (adapted from Eycleshymer and Shoemaker 1911).

tubes, the trachea, or the lungs follows in the majority of cases. Furthermore, mechanically-assisted ventilation causes pulmonary blood volume and left atrial pressure to decrease. In turn, there is a reflex of the vagus nerve that results in an increased release of an antidiuretic hormone, causing water retention and leading to pulmonary edema.

Lung Contusion. It appears that lung bruising (contusion) occurs in over half of the cases having flail chests. Lung contusion commonly occurs in cases with no rib fracture and is also commonly associated with abdominal injury. Clinical evidence of lung contusion appears to be masked by the presence of rib fractures, air or blood in the pulmonary pleural cavity, collapse of a lung, or inflammation of the lungs due to sucking in of fluids. Lung contusion can be inferred in the second or third day after injury by blood gas studies. Comparison of the time history of the oxygen partial pressures between the air in the lung and the arterial blood provides a basis for the diagnosis of a contusion. In the absence of a contusion, the oxygen partial-pressure difference will fall by the end of twenty-four hours, and in the presence of contusion it will rise to a large difference at about forty-eight hours after trauma.

Lung contusion may double the probability of the development of pneumonia, which is said to be the most serious problem and most common cause of death in cases involving severe thoracic trauma, given survival beyond one to two days. The development of pneumonia prolongs the use of respirators and calls for increased oxygen levels (100 percent for prolonged periods). Oxygen toxicity added to pneumonia and contusion is considered uniformly fatal in its consequences. Further, the contused lung is more susceptible to simple "blowout." Lung contusion is also likely to lead to local areas being left airless with a resulting artery-to-vein shunting and local pneumonitis occurring. The shunting apparently leads to increased strain on the heart and an ultimate decrease in arterial oxygen.

Hemothorax or Pneumothorax. The pleural cavity represents "potential" space. When blood or air enters this space, the situation is described as hemothorax or pneumothorax. The combined hemopneumothorax case also exists. Treatment is by entubing the area and often physically cutting into the cavity to remove clotted blood. In either the hemo- or pneumothorax case, it is important to prevent compression or collapse of the lung by draining the cavity. Neither is properly an "injury," although each is reported on both accident and medical reports. Original pneumothorax would most likely result from a fractured rib cutting through the pulmonary pleura. Late-developing pneumothorax seems to be the result of a "blowout" of the lung at a contused location when on mechanical respiratory assistance. Hemothorax could result from several different blood vessel injury locations. It need not be accompanied by rib fracture, but usually occurs when vessels tear at the same time that adjacent ribs are fractured.

Heart and Great Vessels. Contusion of the muscle wall of the heart frequently occurs in the same cases in which severe contusion of the lung(s) is found. Diagnosis at the time of admission is seldom made. Since oxygen shortage in the arterial blood would result from the lung injury and contribute to the ECG pattern characteristic of reduced blood supply to the heart muscle, the heart contusion would not be distinguishable. Contusion of the heart is generally discovered at the time of autopsy. It is not considered a primary cause of death in the short run but does seem to add to the overall set of problems of a lung-injured case, sometimes in the form of oxygen shortage in the brain and cardiac arrest. Treatment for and the general course of heart muscle contusion are similar to those associated with myocardial infarction, except that coronary vasodilators and anticoagulants are of little benefit.

Among heart injuries, rupture of the muscle wall is the lesion quite frequently found at autopsy following fatalities from nonpenetrating chest trauma. Rupture of the right ventricle is most common, followed by the left ventricle, the right atrium, and the left atrium. Survival is seldom over thirty minutes, and successful surgical treatment is rare. Survival long enough to reach a medical facility corresponds to the pericardial tamponade situations. Interventricular wall (septum) perforation is a less acute form of rupture. Congestive heart failure in the first two weeks is common if this rupture is not diagnosed and surgically repaired. Animal studies have suggested that this perforation is more likely when the blow is delivered late in the dilation of the ventricles or early in the contraction period.

Late true aneurysm, i.e., the thinning or stretching of the heart's muscle wall, or late pseudoaneurysm, i.e., the dilation of an artery at a nearby site, are further complications of heart trauma. Morbidity and mortality are high in these instances.

Heart valve rupture, particularly the left side aortic valve in people with pre-existing disease conditions, is not rare in blunt chest and abdominal trauma. Rapid progression of congestive heart failure in one or two years is the expected outcome of untreated cases.

Pericardial disruption, the rending of the double layered sac containing the heart and the beginning of the great vessels, is found in a significant portion of those cases examined at autopsy following blunt chest trauma. The tears are typically transverse and extend across the upper base of the heart near the reflection of the visceral (inner) and parietal (outer) pericardium. Naturally, such a tear in the presence of heart muscle injury and bleeding can produce fatal, gross loss of blood from the heart. Smaller tears may allow a sufficient tamponade to occur to control bleeding adequately and long enough to allow treatment. In the absence of pericardial rending of any great extent, the pericardium "potential" space may be filled with blood creating a cardiac tamponade with serious results. Surgical puncture of the pericardium and removal of this blood is required but is a dangerous procedure. An inflammatory reaction in the pericardium following blunt trauma is ordinarily well resolved.

Aneurysms of the aorta are not uncommon among people suffering blunt thoracic trauma sufficient to cause bony injury and a widened mediastinum. Aortography is required to confirm the aneurysm. Aortic aneurysms appear to be associated most frequently with upper sternal and/or upper rib fractures. To physically visualize the aorta, consider this image. From the left ventricle, a single great vessel (the ascending aorta) rises upward. This vessel arches above the heart and then turns down, rearward, and to the left, becoming the thoracic aorta (the descending aorta). From the top of the arch of the aorta, the brachiocephalic trunk artery, the left common carotid artery, and the left subclavian artery arise. The brachiocephalic trunk branches in a few centimeters into the right common carotid and right subclavian arteries. The coronary arteries originate at the base of the ascending aorta.

Ruptures of the aorta appear to occur in several regions. Because clinical literature is being reviewed, one must suspect that there is case selection being performed according to the author's specialty or interest, and one should not therefore accept sweeping statements that indicate preferred locations for rupture. However, it appears that the site of the rupture is ordinarily just distal (most outboard) to the left subclavian artery. It is estimated that only ten to twenty percent of thoracic aortic rupture cases live long enough for operative care to be achieved, and that even these cases often show few signs of external injury.

Finally, impact to the thorax can cause a disruption in the heart conducting system, which can most seriously result in ventricular fibrillation. This condition is characterized by rapid but incomplete contractions of the ventricles and is generally fatal unless there is medical intervention. Further discussion of this mechanism can be found in Viano and Artinian (1978).

BIOMECHANICAL RESPONSE OF THE THORAX

This section is divided into research on biomechanical response to two types of thoracic loading: flat impactor and diagonal belt.

Response to Flat Impactor. Static and dynamic thoracic stiffness measurements have been reported by Patrick et al. (1966) for several embalmed cadaver subjects. Static loading in the anterior-posterior direction by a 4-inch (10.2-cm) wide bar yielded force-deflection values from 185 to 400 lb/in (822 to 1780 N/cm). Chest impacts at 16.5 mph (26.6 km/h) against a 6-inch (15.2-cm) diameter padded target, however, resulted in approximately constant spring rates of 1000 lb/in (4.45 kN) for loads up to 900 lb (4.0 kN) for two different subjects. Rib fractures apparently occurred at this point and stiffness dropped markedly, but it then increased again to about 500 lb/in (2.22 kN) as the internal organs began to be compressed. Peak forces of 1400 lb (6.2 kN) and 1600 lb (7.1 kN) were reached in these tests, and chest deflection was about 1.5 in (3.8 cm) and 2.5 in (6.4 cm), respectively. Deflection was measured by way of film analysis of a rod inserted through the thorax and protruding from the back of the test subject. The authors pointed out the fundamental difference between the stiffness characteristics of the thorax under gradual vs. sudden loading conditions. The stiffer response in the latter case was explained as being due to the inertial force gradients developed in the thoracic cavity during impact and the viscous behavior of the thoracic viscera.

Nahum et al. (1971) reported on a limited number of static load-deflection tests of embalmed and unembalmed cadavers prior to dynamic testing with a 6-in (15.2-cm) impactor. The static stiffnesses of the unembalmed cadavers ranged from 36 to 62 lb/in (63 to 109 N/cm). Using dynamic load-deflection data based on impacts to the thoraxes of unembalmed cadavers, published previously by Nahum et al. (1970) and Kroell et al. (1971), Lobdell et al. (1973) developed recommended chest response corridors for these two velocity/impactor-mass conditions as performance guidelines for the design of dummy chest structures. Basically, for a 16-mph (25.8 km/h) impact with a 51-lb (112-kg) mass, forces up to 1200 lb (5.3 kN) and deflections up to 3 in (7.6 cm) were considered acceptable. These corridors included adjustments of the load level upward by 150 lb (667 N) to account for the lack of muscle tone in the cadaver test subjects. This adjustment was based on estimates from static load-deflection tests on seven volunteers. The mean stiffness of the volunteers in a relaxed state was 40 lb/in (70 N/cm), and the mean stiffness in the tensed state was 135 lb/in (236 N/cm). Deflections up to 1.5 in (3.8 cm) were obtained with loading by a 6-in (15.2-cm) diameter surface.

Impact tests of ten cadaver chests, using a 22-lb (10-kg), 6-in (15.2-cm) diameter impactor at 13 mph (21 km/h), were performed by Stalnaker et al. (1973a), and force-deflection curves were reported. The most consistent finding was the relationship between rib fracture and rib cage deflection, no fractures being associated with deflections up to 2.1 in (5.3 cm) in this study. Static compression tests using both human volunteers and cadavers confirmed that chest stiffness varied upward relative to the following conditions: (1) unembalmed cadaver, (2) embalmed cadaver, (3) relaxed volunteer, and (4) tense volunteer. The middle two, however, overlapped to a large extent. The average static stiffness for the unembalmed cadavers in the study was found to be 70 lb/in

(123 N/cm) with rib fractures occurring at loads of approximately 500 lb (2224 N) with deflections of about 3 in (7.6 cm). The average static stiffness for the two volunteers was 230 lb/in (403 N/cm) relaxed and 650 lb/in (1138 N/cm) tensed. The apparent initial dynamic stiffness of the thorax in the cadaver tests ranged from 2000 to 4500 lb/in (3500 to 7900 N/cm).

A mathematical model of a thorax and impactor was developed (Lobdell et al. 1973) that was based on a 3-mass, 4 degree-of-freedom mechanical analog. The model simulations were found to correlate well with actual cadaver frontal impact tests. The authors suggested this model could be used as a tool for improving dummy thorax design and was simplified for those purposes (Neathery and Lobdell 1973), with the primary structural response being represented by a spring and damper in parallel between a sternal mass and a torso mass. The spring constant was double-valued at 150 lb/in (263 N/cm) for deflections less than 1.25 in (3.18 cm) and 450 lb/in (788 N/cm) for larger deflections. The damper was bidirectional with damping coefficients of 3.00 lb•s/in (5.25 N•s/cm) for compression and 7.00 lb•s/in (12.3 N•s/cm) for expansion. The sternal mass was 1.0 lb (0.45 kg) and the torso mass was 60.0 lb (27.2 kg).

Stalnaker et al. (1973b) reported on lateral impact tests with six unembalmed cadavers struck on the left side by a 6-in (15.2-cm) diameter flat impactor with a mass of 22 lb (10 kg). Two impact velocity levels, 20 and 29 ft/s (6.1 and 8.8 m/s), were used. The range of apparent initial dynamic stiffnesses for the 20 ft/s (6.1 m/s) impacts (four tests) was 1563 to 2500 lb/in (2736 to 4378 N/cm). At the higher velocity, the values were 2500 lb/in and 4500 lb/in (4378 and 7900 N/cm).

Patrick (1981) described a series of eight chest impacts conducted in 1970 with himself as the test subject. He used a moving-mass impactor weighing 22.1 lb (10 kg) with a 6-in (15.2-cm) diameter impact surface that was padded with 15/16-in (2.4-cm) thick Rubatex® R310V padding. Impact velocities ranged from 8.0 to 15.0 ft/s (2.4 to 4.6 m/s). The subject was seated in an upright position with the center of the impact at about the nipple level. Impact force was measured with a strain gage load cell, and chest deflection was measured by analysis of high-speed movies using impactor motion and motion of a back target conforming to the back of the subject and held in place with surgical tubing around the torso. Tests at 8.0 ft/s (2.4 m/s) and 11.3 ft/s (3.4 m/s) were conducted with the subject tensed and relaxed. Tests at higher velocities were with the subject tensed only. The rate of loading in the tests ranged from 22 to 50 lb/ms (100 to 222 N/ms).

The apparent initial dynamic thoracic stiffnesses for the subject were found to be 325 lb/in (570 N/cm) at 8 ft/s (2.4 m/s) relaxed and 450 lb/in (790 N/cm) tensed at the same velocity. At 15 ft/s (4.6 m/s) the stiffness rose to 1400 lb/in (2500 N/cm) tensed. The maximum force level reached in the high velocity test was 376 lb (1670 N), while the largest skeletal deflection was 1.8 in (4.57 cm), which occurred in the 11.3-ft/s (3.4 m/s) relaxed test. All of the peak skeletal deflections were on the order of 1.7 to 1.8 in (4.42 to 4.55 cm), which correspond to approximately 16-17% deflection of the thoracic rib cage.

The limited impact energy and momentum represented by the motion of the relatively low impact mass used in this study served to limit the chest deflections to approximately the same level for all tests. Higher momentum impacts would have likely produced greater deflections at the higher velocities. Within the range of impact velocities used, the rate sensitivity of the thorax response accounted for the fact that the maximum deflection was relatively constant.

Tsitlik et al. (1983) reported on chest compression experiments on living human patients using an instrumented cardiopulmonary resuscitation (CPR) chest compression device. The pneumatic device compressed the chest of the patient through a 1.9- by 2.5-in (4.8- by 6.4-cm) rubber loading pad. Force and sternal deflection were recorded during the cyclic compression (1 Hz with a duration of 0.5 s). The loading rate was 0.7 lb/ms (3 N/ms), and the peak forces for ten subjects ranged from 70 to 118 lb (312 to 524 N) with a deflection range of 1.23 to 2.36 in (3.12 to 6.00 cm). The force-deflection curves were found to be best described by a second degree polynomial, but the authors did calculate a best-fit linear relation that gave a mean stiffness of 52.4 lb/in (91.7 N/cm) and a range of 30 to 91 lb/in (52.9 to 158.9 N/cm).

Investigations into thoracic response and its measurable indicators had, in the previous studies, concentrated on localized impacts to human surrogates instrumented with one or perhaps two sensing devices. A new approach, described by Robbins et al. (1976), used ten accelerometers located on the sternum, spine, and ribs at prescribed points around the thorax. This array of sensors allows the measurement of the kinematic response of this flexible, ellipsoidal body, subject to blunt impact in various test modes and including different impact directions. From these acceleration measurements, the magnitude and velocity of deformations could be inferred. These data describing global thoracic motion would then be correlated with observed injuries. The system was designed to be usable both with cadavers and with dummies.

Side impact experiments using the above system were reported by Melvin et al. (1978). These tests compared the kinematic response of cadavers to that of the Part 572 dummy and the British Transport and Road Research Laboratory (TRRL) side impact dummy. (The TRRL dummy had no arms; design details can be found in Harris 1976.) The ten-accelerometer system was used on the thoraxes of the seven cadavers, but the two dummies were instrumented according to Part 572 requirements. The subjects were seated sideways on the sled next to either a rigid wall structure or a padded, contoured surface representing a vehicle side interior. At impact, the subjects slid into these structures. The differences in whole-body kinematics were significant and were due primarily to the very compliant shoulder structures of the cadavers compared to the fairly rigid dummy structures. The visually obvious consequence of this difference was the response of the head/neck system. The side of the cadaver heads impacted the wall with considerable force, while the dummy heads rotated laterally and barely touched the wall, if at all. Further implications were apparent, however, for determining thoracic injury potential, if indeed existing dummies did not deform as humans do. It was clear that these dummies were totally inappropriate for side impact testing. It should also be noted that, in the 20-mph lateral impact using the padded structure, the Part 572 dummy recorded a peak left-right chest acceleration of 102 G, while the cadaver recorded 19 G.

Stalnaker et al. (1979) presented the results of a series of lateral impacts to the thoraxes of unembalmed cadavers. The tests were conducted by dropping the test subjects on their sides against rigid or padded surfaces containing load cells. The drop heights were 3.3 ft (1 m) for rigid impacts and 6.6 ft (2 m) for padded impacts. Triaxial acceleration of the fourth thoracic vertebra and thoracic deflection were measured. Both total thoracic deflection and spinal motion were measured, total deflection being obtained by a rod passing through the thorax. The data were analyzed to produce load-deflection curves based on the relative deflection of the half-thorax. Walfisch et al. (1982) presented additional data in the same form and summarized the lateral response of the half-thorax. The data presented in that paper, when analyzed for the differences between whole-thorax deflection and half-thorax deflection, indicate that the deflections of the struck-side half-thorax were approximately 63% of the total thoracic deflection. Based on that relation and assuming an average thorax width of 13.8 in (35 cm), the following apparent stiffness ranges can be obtained: for the whole thorax 553 to 1457 lb/in (968 to 2552 N/cm) and for the half thorax 878 to 2313 lb/in (1537 to 4051 N/cm).

Eppinger and Chan (1981) developed a dynamic characterization of the human thorax in lateral impact using digital convolution theory. They applied a numerical analysis process involving discrete-time system theory and assumptions of linearity and time invariance to generate an approximate impulsive response that can relate an input sequence to an output sequence. The process used experimentally-observed input and output sequences from a variety of lateral impact tests with cadavers to obtain an "averaged finite impulse response" (AFIR). This characterization of the human thorax related the acceleration response of the struck side to the far side response. The AFIR technique was shown to produce excellent agreement with experimental data in predicting far-side acceleration response and the differential acceleration, velocity, and displacement of the far side with respect to the struck side over a large range of dynamic test conditions. The AFIR exhibited the vibratory response characteristics of a second order damped system subjected to an impulsive input.

Morgan et al. (1981) addressed the problem of comparing acceleration-time responses from different human surrogates by using a cumulative variance analysis that was similar to a root-mean-square analysis. They analyzed the results of seven identical lateral impact test conditions involving 34 cadaver test subjects (28 sled tests and 6 side pendulum impacts). Comparison tests were performed with two lateral impact ATDs, the Side Impact Dummy (SID), and the APR dummy. The authors concluded that the cumulative variance approach allowed an objective comparison of the response of each dummy design with respect to the cadaver data.

The results of ten cadaver tests that were incorporated into the analysis were reported separately by Kallieris et al. (1981). These ten tests were lateral impact sled tests conducted under four different conditions: 15- and 20-mph (24- and 32-km/h) lateral impacts into a rigid wall and 20-mph lateral impacts into two different types of padding. Detailed injury information was also provided in the paper.

Nusholtz et al. (1983) reported on a test series using unembalmed cadavers to investigate thoracic response differences in low- and high-energy impacts. Repeated tests at low energy (no rib fractures produced) were conducted at 6.6 ft/s (2 m/s) for different impact directions (frontal, 45° oblique, and lateral) using a 55-lb (25-kg) impactor mass. Single high-energy (rib fractures produced) left lateral impacts were conducted at either 15 ft/s (4.6 m/s) with a 123-lb (56-kg) impactor mass with no padding or at 28 ft/s (8.5 m/s) with a 55-lb (25-kg) impactor with various padding thicknesses. Accelerations were measured on the thoracic spine and rib cage with triaxial measurements at the upper and lower sternum, right and left fourth ribs, and T1 and T12 vertebrae. Uniaxial measurements were made laterally at the right and left eighth ribs.

The point-of-impact impedance was calculated for the low-energy impacts and for all three directions. These produced similar impedance vs. frequency plots with a spring-like behavior from 10 to 30 Hz, followed by one or two local minima and a subsequent mass-like behavior at higher frequencies. In frontal impacts the minima occurred at 32 to 38 Hz and 65 to 80 Hz; in lateral impacts they occurred at 42 to 48 Hz and 80 to 100 Hz; and in the oblique 45° impacts they occurred at 27 to 32 Hz and 57 to 66 Hz. The spring-like behavior was indicative of stiffnesses in the range of 171 to 457 lb/in (300 to 800 N/cm), although the phase angles of the impedance were not indicative of such elastic behavior. The apparent thoracic stiffness when the arm was involved in the lateral impacts was higher than when direct loading was applied to the thorax.

The high-energy unpadded lateral impacts produced responses that were indicative of increased thoracic stiffness at the higher test velocities. It was pointed out, however, that the velocity of the impact mass was changing throughout the impact event, and variations in the energy management of the thoracic structure for a given impact mass may be more responsible for the velocity sensitivity effects than material rate sensitivity alone.

Figures 3-2 and 3-3 summarize the frontal impact response of the chest to flat impactor loading. Data from the human volunteer tests of Patrick (1981) and the unembalmed cadaver tests of Kroell et al. (1974), from which detailed load-deflection data are available, have been analyzed to determine the apparent initial stiffness of the force-deflection curve as well as the force plateau values characteristic of flat impactor loading. Figure 3-2 shows the rate sensitivity of the thoracic structural response, with the apparent initial stiffness, S_{AI}, being directly proportional to impactor velocity at speeds above 1.3 m/s (4.3 ft/s), as indicated by the equation given in that figure. Figure 3-3 displays the plateau force (defined as the force at 3.8 cm (1.5 in) total deflection) versus the impactor velocity. The cadaver data are shown as a range from the direct experimental values to the values adjusted upward by Kroell et al. by 667 N (150 lb) for muscle effects. The unadjusted data, however, have better agreement with the Patrick volunteer data. These data demonstrate a linear dependence of plateau force on velocities above 4 m/s (13 ft/s), as indicated by the equation given in Figure 3-3.

Response to Belt Loading. The diagonal strip loading of the thorax that is characteristic of the shoulder-belt portion of a three-point-belt restraint system presents a significantly different load distribution condition than that of a flat 6-in (15.2-cm) diameter impactor. This fact was known qualitatively from whole-body cadaver tests and from accident investigation. Schmidt et al. (1974) reported on shoulder belt tests with forty-nine cadavers. The rib fracture patterns followed the asymmetry of the diagonal belt. Patrick et al. (1974) reported similar results from detailed investigations of crashes in which the occupants were wearing three-point belts. They found that all of the fractures were in the sternum or lower inboard rib cage.

The first study to investigate the load-deflection behavior of the thorax due to shoulder belt loading was reported by Fayon et al. (1975). The authors conducted sled tests with cadavers in three-point-belt systems with sternal deflection measurements made by rods passing through the thorax. Belt spatial geometry was analyzed to provide the resultant normal force on the thorax. Static tests were made with volunteers and cadavers using belt loading and flat disc loading. Only one good dynamic cadaver load-deflection curve (Test 53) was obtained for a cadaver tested at 27 mph (43 km/h) with a stopping distance of 17.7 in (450 mm). Three other tests were reported, but one (Test 54) produced a spurious deflection response and the other two (Tests 44 and 47) were conducted with pyrotechnic belt pretensioners that loaded the chest at a rate that was much greater than that associated with conventional belt/occupant interaction. The apparent thoracic stiffness (in Tests 44 and 47) was ten times greater than the stiffness of 950 lb/in (1664 N/cm) found in Test 53.

The static tests on volunteers produced sternal force-deflection stiffness values in the range of 100 to 150 lb/in (175 to 263 N/cm) for belt loading and 50 to 100 lb/in (88 to 175 N/cm) for disc loading. Static sternal deflection levels ranged up to 1 in (2.5 cm) for belt loading and up to 1.5 in (3.8 cm) for disc loading. Deflections were also measured at the second and ninth ribs under the belt. The resulting apparent stiffnesses were found to lie in the 100 to 200 lb/in (175 to 350 N/cm) range for the second rib and in the 50 to 100 lb/in (88 to 175 N/cm) range for the ninth rib. These tests were performed with the subjects laying supine on a flat surface.

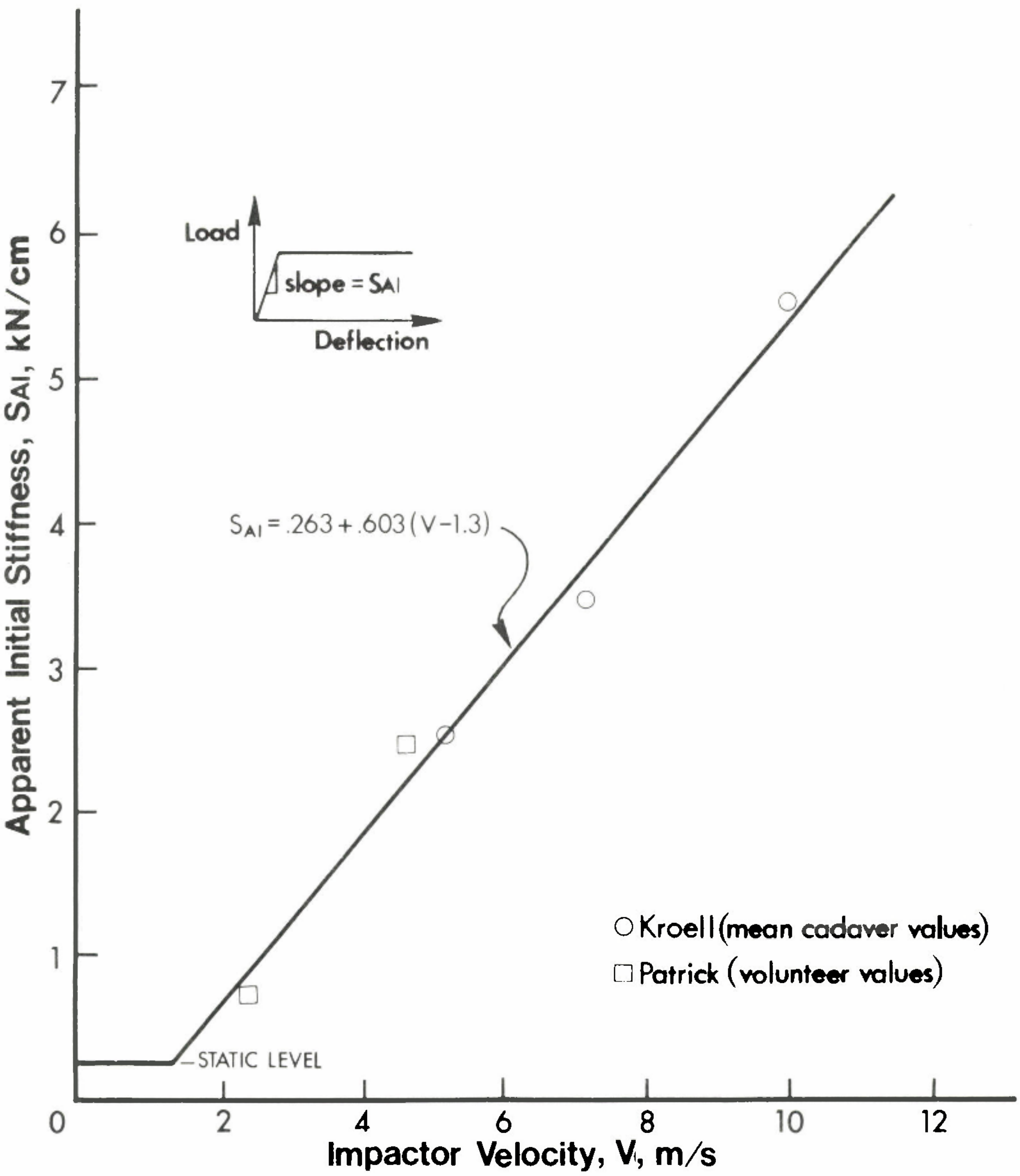

FIGURE 3-2. Apparent initial stiffness of the load-deflection response of the chest to frontal impact with a flat, circular impactor.

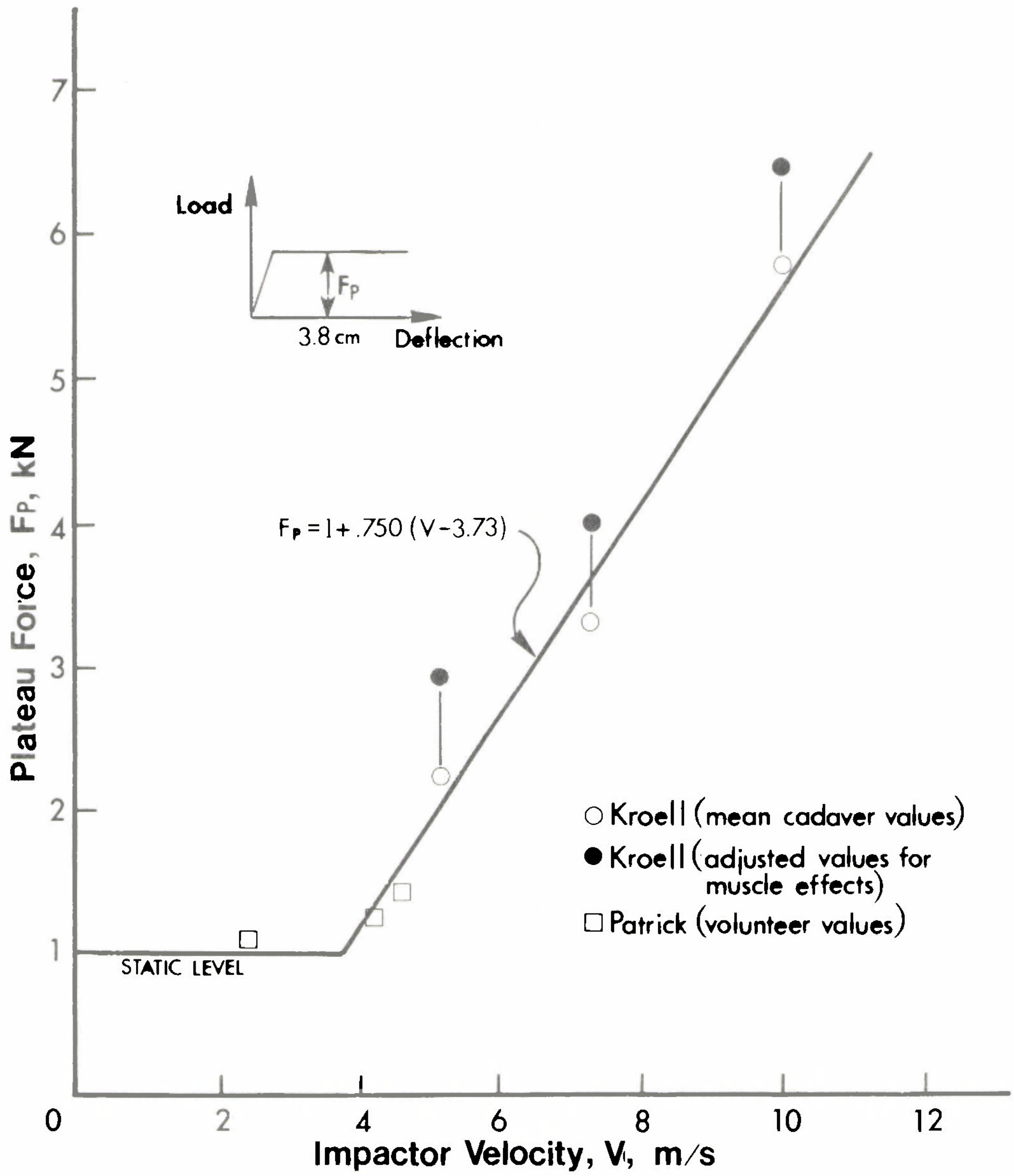

FIGURE 3-3. Plateau force versus impactor velocity for frontal chest impacts with a flat, circular impactor.

In a later summary paper, Walfisch et al. (1982) report the results of five more dynamic sled tests with belted cadavers. The resulting normal-force/sternal-deflection loading curves were generally linear in nature. The authors suggested a response corridor based on the loading curves. The range of stiffnesses included by the corridor is approximately 400 to 920 lb/in (700 to 1226 N/cm) assuming an average chest depth of 9 in (23 cm), since the authors plotted the corridor based on relative thoracic deflection rather than absolute deflection. The characterization of a linear force-deflection response appeared to be appropriate up to deflections of at least 2 in (5 cm). The mean stiffness was 682 lb/in (1194 N/cm).

Verriest et al. (1981) studied the mechanical response of the pig thorax using belt loading conditions for living and dead test subjects. Tests were conducted at velocity levels of 25 to 34 mph (40 to 55 km/h). The test subjects were mini pigs with a mean weight of 96 lb (43.6 kg) and a range of 73 to 170 lb (33 to 77 kg). The thoracic dimensions were similar to those of man except that the pigs' chest depths were relatively larger than the widths, whereas man is just the opposite. The mean chest depth was 11.9 in (30.3 cm) with a range of 9.1 to 14.8 in (23 to 37.5 cm). The mean chest breadth was 10.0 in (25.4 cm) with a range of 8.3 to 12.6 in (21 to 32 cm). Chest deflections were measured photographically and were reported as the variation of the distance between the back column and the maximum crush point of the belt inside the thorax. The resultant normal force on the chest due to the belt webbing forces was also determined from the photographic data. All the thoracic force-deflection curves exhibited an initial low stiffness behavior with a concave-upward stiffening behavior up to about 1 to 2 in (2.5 to 5 cm) deflection. This was followed by a generally linear high stiffness behavior up to maximum deflection of 4 to 6 in (10 to 15 cm). The average apparent initial dynamic thoracic stiffness for the dead animals was 204 lb/in (357 N/cm), while the corresponding value for the living animals was 113 lb/in (198 N/cm), 55% of the value for the dead animals. The high stiffness regions were about three times as stiff as the corresponding low stiffness regions, 661 lb/in (1157 N/cm) dead and 370 lb/in (648 N/cm) living. The mean high stiffness of the dead animals was remarkably close to that found by Walfisch et al. (1982) for human cadavers. The rate of loading in the tests was on the order of 30 lb/ms (133 N/ms).

L'Abbé et al. (1982) reported on static and dynamic shoulder belt loading of ten human volunteer subjects. The subjects lay on their backs, but with their legs flexed into a simulated seated position rather than supine. A shoulder belt was placed diagonally from the left shoulder across the thorax for load application, and the deflections of the thorax were measured at eleven points on the thorax. Static normal forces of up to 150 lb (650 N) were applied to the subjects. The static load-deflection curves at locations under the belt were linear in form. Deflections up to 0.4 in (1 cm) were produced at the sternum. The apparent stiffnesses were 386 lb/in (676 N/cm) at the mid-sternum, 228 lb/in (400 N/cm) at the right seventh rib, and 541 lb/in (948 N/cm) at the left clavicle.

The dynamic tests applied total loads up to 810 lb (3.6 kN) over a 60-ms duration and produced about twice the deflections of the static tests. The loading rate was not reported, but it was probably on the same order as that of the Verriest et al. animal tests, that is, about 30 lb/ms (135 N/ms). The average apparent stiffnesses of the dynamic force-deflection curves were 785 lb/in (1375 N/cm) at the mid-sternum, 703 lb/in (1232 N/cm) at the right seventh rib, and 1142 lb/in (2000 N/cm) at the left clavicle. The sternal value is comparable to the stiffnesses reported for belted cadavers and dead pigs but twice as great as that for living pigs. The static volunteer tests of Fayon et al. (1975) produced greater deflections and much lower stiffnesses than were found in this study. The reason for this is not clear. One possible explanation is that the supine posture of the

Fayon et al. subjects produced a curved spinal shape that could have lowered the apparent stiffness by introducing additional whole-body thoracic motions under load.

L'Abbé et al. also examined the response of the Hybrid III ATD under the same loading conditions as the volunteers experienced. They observed that the ATD tended to be stiffer and deformed less than the volunteers, and the ATD response to load was more localized than the global response of the volunteers. The largest variations appeared to occur in the deformations of the left side of the thorax, where the volunteers responded asymmetrically and produced upward deflections while the ATD produced downward deflections.

THORACIC INJURY MECHANISMS, TOLERANCE, CRITERIA, AND PREDICTIVE MODELS

Injuries to the thorax include skeletal damage in the form of rib and sternal fractures as well as soft tissue damage to the organs contained in the chest. This section will discuss the early research on thoracic injury in general and then review the more recent work in terms of the proposed injury criteria. These criteria include spinal acceleration, chest deflection, rate of chest deflection, load on the chest, and global thoracic accelerations.

Much of the early research is summarized in a review paper by Mertz and Kroell (1970), and therefore only selected work, including some whole-body acceleration research, is discussed here.

Bierman et al. (1946) reported on tests in which young male volunteers received chest impacts through a restraining harness attached to a dropped-weight device. With a standard lap/double-shoulder harness configuration (76 in^2 or 490 cm^2), load "tolerance," defined as producing a painful reaction and various minor injuries, was found to be about 2000 lb (8.9 kN). These tests led to the development of a vest-type restraining harness that distributed loads over a larger area (156 in^2 or 1006 cm^2) and absorbed some of the energy through controlled stretching. With this harness, peak loads in the range of 1800 to 3000 lb (8.0 to 13.3 kN), the peaks being reached at 50 to 70 ms, were sustained without injury. The experiments also confirmed that rate of onset affected load tolerance, with peaks reached within less than 30 ms being "very uncomfortable."

Whole-body rocket-sled data provided by Stapp (1951) and summarized by Eiband (1959) indicated that harnessed thoracic accelerations up to 40 G were tolerable as long as the duration of acceleration at this level did not exceed 0.1 s. The maximum voluntary tolerance observed was 45 G for 44 ms, with a pressure under the restraining harness calculated to be 36.5 psi (252 kPa). Rate of onset was again found to affect tolerance to maximum accelerations, with peaks of 30 G reached at 1000 G/s becoming debilitating.

The behavior of the internal organs during blunt impact to the chest without rib fracture and the mechanism of resulting injuries to the arterial system were studied by Roberts et al. (1966). Anesthetized dogs were struck at midsternum by a 3-inch (7.6-cm) diameter impactor. The authors found that tears in the aorta and great vessels were in the transverse rather than the longitudinal direction and therefore postulated that these tears were caused by the displacement of the heart into the left side of the chest, rather than by pressure surges within the vascular system during impact. This reasoning was probably invalid, however, because later work (e.g. Yamada 1970) has shown that arterial tissue is significantly stronger in the hoop-stress direction of the vessel than along its length and is thus more likely to experience transverse tears when stressed. This finding is confirmed by Mohan and Melvin (1983) who found that descending mid-thoracic aortas, under conditions of uniform biaxial stretch, consistently failed in a direction perpendicular to the long axis.

Chest impacts with a human cadaver were reported by Patrick et al. (1967). Tests were run at increasing velocities for the same specimen and were aimed at determining rib fracture threshold. Findings were consistent with earlier experiments (Patrick et al. 1966), in that rib fracture apparently occurred at about 900 lb (4.0 kN) of load during a 16.8 mph (27.0 km/h) impact, and deflection was measured at 1.7 in (4.3 cm) for a peak load of 1340 lb (6.0 kN). Impactor geometry problems precluded measurement of initial chest stiffness, but deflection of 1 in (2.54 cm) occurred at about 1000 lb (4.4 kN) load.

Design evaluation of the General Motors EA (energy absorbing) steering assembly during this period was guided by Patrick's data and was reported by Gadd and Patrick (1968). Two embalmed, lap-belted cadavers were used in sled tests at 24.4 mph (39.3 km/h), and one subject was used in a second test at 29.4 mph (47.3 km/h). As the cadavers rotated around the lap belts into contact with the EA systems, the columns crushed from 4 to 5-3/4 in (10.2 to 14.6 cm), and the force developed on the upper body ranged from 1630 to 1810 lb (7.3 to 8.1 kN). No skeletal damage resulted from the lower speed tests, but rib fractures did occur after the higher velocity test on the repeated subject.

The state of understanding of cardiovascular injury mechanisms during thoracic impact was summarized in the introduction to a medical-engineering study of sixty-seven accident cases in which such injury might be expected. Lasky et al. (1968) identified three possible occurrences: (1) shearing of vessels at their attachments to the heart, (2) direct compression causing bruising and other damage, particularly when heart displacement is restricted, and (3) development of fluid pressure waves within this closed system. The authors promoted the latter concept by introducing the idea of a "third collision" between the internal organs and the thoracic skeletal structure, during which "the sudden deceleration of the blood can produce a water hammer effect," or a large increase in pressure. Results of the study confirmed the value of EA steering assemblies and brought the problem of side impact injuries to light:

> The mechanisms of cardiovascular injury in side impact collisions appear to be caused both by direct impact with the side door and arm rest.... They present an increasing problem and will require rather specific design solutions that at least reduce interior penetration.

Nahum et al. (1970) conducted tests of both embalmed and unembalmed cadavers and compared the results to those of Patrick et al. (1966, 1967). Subjects were struck at known velocities by a 6-in (15.2-cm) diameter, 42.5-lb (19.3 kg), rigid-surface impactor. This test method effected impact conditions similar to those of the earlier tests. Load-deflection curves and rib fracture data, both from X-ray diagnosis and dissection, indicated that the fracture threshold occurred at about 2 in (5.1 cm) deflection, a value consistent with Patrick et al.'s findings, but that thoraxes were less stiff and damage occurred at lower loads than in the earlier studies. The unembalmed specimens in the current study sustained larger deflections and more fractures at lower force levels than did the embalmed cadavers in any of the studies. Rib fractures occurred in five of six unembalmed subjects under maximum loads ranging from 350 to 680 lb (1.6 to 3.0 kN). The authors postulated that the differences in gross chest stiffness might be related to differences in embalming procedures, as well as the lack thereof, but they cautioned that an unembalmed, aged cadaver subject might not in fact be a good representation of the living vehicle occupant population. The authors also suggested that thoracic injury criteria should be based on actual internal injury to the lungs, liver, aorta, etc., rather than on rib fracture only.

Spinal Acceleration Tolerance and Criteria. By 1970, the Severity Index (SI)[7] had become generally accepted as a fruitful step in the direction of calculating head injury potential, but there were no corresponding index and threshold values for the chest. Brinn and Staffeld (1970) proposed a damage index, based index, based on the relative displacement of body organs and structures, that could replace the SI for head acceleration tolerance and could also be used to predict thoracic injury from whole-body acceleration and blunt impact. This Effective Displacement Index (EDI) used a simple spring-mass model for the body part of interest to determine displacement as a result of input pulses of various shapes and durations. For whole-body rocket-sled data (Stapp 1951), the authors calculated not only the EDI but also the SI, noting that the latter had been employed for chest impacts by "some safety testers." The tolerable 45-G run, referred to previously, resulted in an SI of 972, a value very close to the head injury threshold of 1000. No SIs were calculated, however, for blunt chest impact experiments. For assessment of the latter type of injury, the one found most commonly in the automotive environment, the authors recommended obtaining the EDI from a direct measurement of sternal deflection. In their closure, however, they commented that the crushing injuries now seen might change to the inertial-type injuries of the rocket-sled tests if broad, soft surfaces, such as air bags, proved practical in the future.

Mertz and Gadd (1971) described an interesting case related to chest acceleration tolerance. An instrumented stunt man jumped from 57 ft (17.4 m) to land on his back on a thick foam mattress and registered a resultant acceleration at midsternum of 49.2 G without discomfort. After additionally reviewing human tolerance literature, the authors concluded that there was no evidence that "even a 60-G chest acceleration level would not be tolerable with an adequate restraint system" for pulse durations less than 100 ms. They recognized, however, that frontal chest impacts were characterized by compression, and that "internal organ tolerance to trauma produced by chest compression should be specified in terms of a thoracic compression limit and not an acceleration limit."

Deflection Tolerance and Criteria. Tolerance to lateral impact was the subject of a paper by Stalnaker et al. (1973b). The 22-lb (10-kg), 6-in (15.2-cm) diameter impactor, used in previous frontal experiments (Stalnaker et al. 1973a), was again used here, but both a flat surface and one simulating an armrest were employed. The impact device could be preset to stop within a range of 1.8 to 3.8 in (4.6 to 9.7 cm) and could maintain a constant velocity up to 3 in (7.6 cm) of penetration. Impacts were made to both human cadavers and live infrahuman primates. Data from the latter tests were scaled relative to chest depths and breadths (called an aspect ratio) to estimate human side impact tolerance. Results of both series led to a deflection criterion for predicting chest injury. The authors suggested that a lateral deflection of 2.65 in (6.73 cm), achieved during a 21.6-mph (34.8 km/h), 25-ms impact, would result in a 900 lb (4.0 kN) load and a serious, but reversible injury, or level 3 on the Abbreviated Injury Scale (AIS).[8] (The deflection

---

[7]The SI is a weighted-impulse criteria obtained by integrating the acceleration-time waveform over time, with the acceleration raised to the power 2.5, and is described in SAE J885a (1966).

[8]This 6-point injury scale is briefly: 0 none, 1 minor, 2 moderate, 3 serious, 4 severe, 5 critical, 6 unsurvivable. At this time, rib fractures were coded as AIS-2 or 3. In 1980, the scheme was revised, and rib fractures alone are currently considered AIS-1 or 2. Further internal injury results in a higher AIS. For details see both *Abbreviated Injury Scale, 1976 Revision* and *1980 Revision*, AAAM, Morton Grove, Ill.

value was later corrected by Melvin et al. (1975) to 3.72 in (9.45 cm) for an AIS-3 injury, while 2.65 in (6.7 cm) was estimated to be a non-fracture deflection level for the average male.)

Commenting on the various parameters that might be used to evaluate chest injury, the authors eliminated acceleration as being "very awkward because of the different accelerations encountered throughout the chest during impact," and force as being "cumbersome because of its dependence upon the weight of the upper torso." They concluded that, "Since most chest injuries were found to be related to the deflections of the rib cage, chest displacement was chosen for this study as the indicator for thoracic injury." The findings of this and the previous frontal-impact study were later conveniently summarized and integrated by Stalnaker and Mohan (1974), but this paper should be used in conjunction with the corrected figures found in Melvin et al. (1975). Basically, however, the conclusion was that, for either frontal or lateral impact, a chest deflection in the range of 30% to 35% of the corresponding chest dimension would result in an AIS-3 level injury, while a deflection of up to 20% to 23% would probably not result in any fracture.

Kroell et al. (1974) reported data from twenty-three additional cadaver tests, integrated the data with previous results (Nahum et al. 1970 and Kroell et al. 1971), and provided full documentation of test procedures and results. After impact, the cadavers in this series were subjected to complete thoracic and abdominal necropsy, and AIS values were assigned. Correlation coefficients were then calculated for AIS vs. both peak load and chest deflection, the latter being expressed as a percentage of chest depth. Correlation with force was poor ($r=0.524$), but deflection again proved to be a reasonable predictor of injury ($r=0.772$), with AIS-3 injuries being associated with chest deflections in the range of 28% to 33%, although the regression line indicated 34% deflection for AIS-3 when all injury levels were analyzed. The authors suggested that further parameters, such as cadaver age and size, would contribute to an even better correlation. Although further analysis was indicated, this work was significant in that enough data of a similar type existed to allow such models of injury potential to be developed.

Neathery (1974) was motivated to perform such a multivariate analysis of the available chest impact data, because these data applied to subjects of widely varying physical characteristics but were being used to predict the response of a 50th percentile male. The author therefore wished to find an appropriate means of scaling these data to determine thoracic response corridors for a range of dummy sizes. Using dimensional analysis methods, six dimensionless terms were devised based on cadaver characteristics (mass, height, chest depth, age), test conditions (impactor mass, impact velocity, gravity), and test results (peak plateau force, maximum impactor penetration).

Neathery's intent was to use data from both the Kroell group and the Stalnaker group, but detailed analysis indicated that impact responses in the two series were not similarly related to the variables chosen. Male and female data also were not apparently comparable. Regression equations to predict various impact response values were therefore developed only for the ten male cadavers from the early series of Kroell et al. These cadaver equations were then manipulated to produce dummy response prediction equations (the age factor being dropped), and scaling rules were developed for determining biomechanically acceptable force-deflection corridors for 5th, 50th, and 95th percentile dummies. These dummy equations and associated corridors were then revised in an appendix to take the later data of Kroell et al., just discussed, into account and went on to specify appropriate biomechanical response corridors for the three dummy sizes in terms of sternal deflection, which is approximately 0.5 in (1.3 cm) less than maximum chest penetration. Nahum et al. (1975) compared sternal and spinal accelerations and resulting SIs for eighteen of the unembalmed cadaver experiments reported above. The authors concluded that $SI < 1000$ is meaningless for either measurement location, the sternal SIs sometimes exceeding 20,000 and the spinal SIs usually being under fifty. Although the spinal SI did correlate well with AIS ($r = 0.720$), normalized chest deflection was still recommended as the best predictor of injury for blunt impacts. The authors also attempted to calculate chest deflections by taking the difference between the second integrals of the sternal and spinal accelerations. These values were consistently high, however, and the technique was determined to be unreliable unless more precise acceleration measurements could be made.

Neathery et al. (1975) carried forward the previous dimensional analysis work (Neathery 1974) to develop equations predicting AIS for cadavers, using data from both the Kroell and Stalnaker series, and then to establish recommended chest deflection limits for dummy test criteria. Dummy "age" was set at 45, and the corresponding penetration-to-depth ratio (or percent deflection) associated with AIS-3 injuries was determined to be 38.68%. Allowable penetration for a 50th percentile male dummy was thus 3.48 in (8.84 cm) based on a chest depth of 9.0 in (22.86 cm). The allowable percent deflection recommended here is greater than those suggested by Melvin et al. (1975) and Kroell et al. (1974), because the latter did not adjust for age.

Viano (1978) cautioned against emphasizing thoracic skeletal damage to the exclusion of organ and vascular injury, which is in fact more serious. After reviewing the Kroell et al. series of cadaver data, he concluded that deflection and injury potential have a linear relationship only to a point, and that beyond that point the rib cage collapses and the likelihood of "life-threatening" injury increases dramatically. He suggested that this stability limit for frontal chest loading was a penetration-to-depth ratio of about 32%, which is consistent with previous estimates. The important point to note, however, is the critical need to stay below this level of compression lest serious injury result.

Eppinger and Chan (1981) used their AFIR technique, described previously, to develop injury predictive relationships through the use of single and multiple linear regression techniques employing the synthetic response parameters derived from the AFIR technique. They developed a relationship for the number of fractured ribs in a lateral impact, which suggested that the magnitude of the resulting trauma is not only the result of the maximum deflection of the thorax but also depends upon the rate at which the thoracic deflection occurs. They indicated that this process could be extended to be used with an ATD, provided that the device has demonstrated biofidelity of lateral response of the rib cage on the struck side.

The question of age and associated bone condition was addressed by Sacreste et al. (1982) for the case of side impact. Various physical measures (mechanical properties, mineral content, etc.) were combined to create an index of thoracic resistance to impact. Although related to age, the correlation was only 0.60. Test results indicated that both thoracic deflection and rib fractures were related to this index.

High Velocity Impact. The rate sensitivity of the thoracic response to load has been noted by many researchers. It is natural to expect that the rate of loading and subsequent rate of deformation might also be related to thoracic injury mechanisms and tolerance to impact. This section summarizes those studies found to have relevance to such a concept. Many of the conditions under which experiments have been performed to study the effect of loading rates on thoracic injury involve impact velocities that are significantly higher than those currently found in typical automotive impacts. However, the findings of these studies provide an additional understanding of potential injury mechanisms and tolerance criteria for thoracic impact.

Early interest in high velocity loading of the thorax was generated by "blast biology" studies conducted some twenty-five years ago in relation to nuclear explosions. Bowen et al. (1965) described a fluid-mechanical model of the thoraco-abdominal system and used it to estimate human responses to blast overpressures from those measured and known to be hazardous in several species of animals of different sizes. Although blast exposures represent a type of loading that is not seen in automotive impact environments in terms of the rapid pressure rise of the shock wave as it strikes the body, nuclear explosions do produce a long duration pressure waveform following the rapid rise. Using scaling techniques based on the modeling effort, the authors estimate the reflected blast wave maximum overpressure for 50% mortality of 70-kg (154-lb) mammals (man) to be 62 psi (427 kPa) for overpressure durations of 30 to 500 ms (square wave) at an ambient pressure of 14.7 psi (101 kPa). The corresponding overpressure for shorter durations was estimated to increase significantly with decreasing durations as high as 290 psi (2000 kPa) at 2 ms. The authors attributed this increased tolerance to overpressure to the effect of the nonlinear "air spring" represented by the lungs. They estimated that stiffness to be much greater than the stiffness of the chest wall and abdomen. Their concern appeared to be related to lung injury exclusively. No mention of cardiovascular injury was made. Later work reported by Bowen et al. (1968) estimated the free-stream 50% survival overpressure for man to be in the range of 40 to 50 psi (276 to 345 kPa) for durations of 10 to 100 ms. Increasing lung volume and decreasing lung density both served to increase the survivable pressure for mammalian species.

Viano and Artinian (1983) analyzed the electrocardiograms (ECG Lead II) taken following blunt thoracic impacts conducted on twelve anesthetized pigs. All animals developed some degree of trauma to the heart conducting system, although later studies (Kroell et al. 1981) with pigs oriented in a prone rather than an upright position did not produce the same dysfunctions of the heart. The authors indicated a correlation between the occurrence of ventricular fibrillation and high levels of sternal acceleration (930 G) and high impact velocity (35 ft/s or 10.7 m/s). A lack of correlation of this dysfunction with other biomechanical impact parameters, such as thoracic deflection, spinal acceleration, or applied force, was also noted. The authors criticized the AIS rating system for not coding myocardial conducting system dysfunctions (MCD) and subsequently developed an MCD severity score.

Jonsson et al. (1979) reported on a study of lateral blunt impact on the right chest wall of anesthetized rabbits using a captive piston driven by a falling weight. The animals were lying with their left side supported on a large flat-plate load cell. Chest wall deflections and, in some cases, diaphragm deflections were recorded to study the effects of magnitude and rate of deformation of the thorax on the resulting lung injury. Tests were conducted at impact velocities ranging from 2 to 22 m/s (6.6 to 72.2 ft/s). Lung injuries typical of primary blast injuries began to occur above the 9-m/s (29.5-ft/s) impact level. Below 5 m/s (16.4 ft/s) the lung injuries were not typical of primary blast. The authors observed that a normalized deformation of the chest of about 30% (relative to total chest width) produced no pulmonary injury when the rate of deformation was less than 4.5 m/s (14.8 ft/s). Similarly, a normalized deformation of about 7% produced over 50% mortality when the rate of deformation exceeded 19.5 m/s (64.0 ft/s). For velocities in the range of 15 m/s (49.2 ft/s), normalized deformations of not more than 15% to 20% produced lethal injuries. The motion of the chest wall at the impact site was observed to be very much like that of the mass of a critically damped visoelastic system. The intrathoracic pressure maximum was found to coincide with maximum chest deflection for impacts of 5 m/s

(16.4 ft/s) and below, while for higher velocity impacts (on the order of 20 m/s or 65.6 ft/s) it occurred earlier than the peak deflection.

Cooper et al. (1982) reported on a study of the biomechanical response of the chest wall to the nonpenetrating impact of small (0.14 to 0.38 kg or 0.242 to 0.836 lb), fast (20 to 74 m/s or 65.6 to 242.8 ft/s), cylindrical impactors with effective diameters of 3.7 and 10.0 cm (1.5 to 4 in). The test subjects were pigs (19 to 86 kg or 42 to 190 lb) supported in a prone position. Injuries produced in this series of thirty-eight mid-sternum impacts included sternal fractures and a range of cardiac injuries, including bruising and rupture of the cardiac tissues and acute ventricular fibrillation (VF). The authors concluded that the sternal fractures and gross myocardial injuries were significantly correlated to the degree of chest compression, whereas cardiac dysrhythmias following impact could not be quantitatively correlated with any of the measured biomechanical parameters. Acute ventricular fibrillation was found to be initiated by blows to the mid-sternum, particularly during a vulnerable period associated with the T-wave of the electrocardiogram. Acute VF occurred at impact velocities as low as 28.4 m/s (93.2 ft/s), with an associated chest wall compression of 27.4% and was accompanied by undisplaced sternal fractures. Pressure changes within the right ventricle of the heart showed a positive correlation with chest wall displacement. Analysis of the data produced a mathematical relation that demonstrated that the degree of chest wall displacement from a strike by a free-flying impactor is dependent upon impactor kinetic energy, impactor diameter, and animal weight.

Tests with animal subjects by Kroell et al. (1981) indicated the importance of considering the rate at which thoracic compression occurs as well as its extent. Swine impacted at high velocity (14.5 m/s or 47.6 ft/s) received more varied and severe injuries, including pulmonary contusion, rib fracture, and cardiovascular rupture, than did those impacted at low velocity (9.7 m/s or 31.8 ft/s), even though some of the latter tests included greater thoracic compression than the former (22-29% vs. 15-24%). Only pulmonary contusions, ranging from moderate to critical, were produced during the low-velocity higher-compression impacts.

Viano and Lau (1983) presented the results of controlled frontal thoracic impact tests on 123 anesthetized rabbits. Both impact velocity (held constant at 5 to 22 m/s or 16.4 to 72.2 ft/s) and degree of compression (4% to 55%) were directly controlled. Myocardial and major vascular injury increased from contusion to rupture with cardiac tamponade and sudden death as either impact velocity or chest compression was independently increased. The authors suggested a relationship for impact severity (IS) that combined the effects of impact velocity, V, and normalized chest compression, C, in the form IS=VC/1-C. Probit analysis of the frequency of critical/fatal injury gave an IS=6.4 m/s (21.0 ft/s) as an estimate of the 50% level of critical/fatal injury in the experimental model.

Load Tolerance and Criteria. During the mid-1970s, a number of programs combining accident investigation and laboratory simulation were undertaken. Gloyns and Mackay (1974) reported that not all steering systems complying with FMVSS 203 actually provided protection for their drivers from serious chest and abdominal injury. Further, the authors observed that the damage sustained by certain systems under standard test conditions did not resemble that seen in the field. They found that a criterion of peak load alone could not distinguish between protective and nonprotective designs, but that differences could be shown if effective loaded area was also taken into account.

Patrick et al. (1974) analyzed the injury experience of 169 Volvo occupants restrained by three-point belts and compared this to results of 72 sled simulations using instrumented pre-Part-572 dummies in a standard Volvo interior environment. Belt loads and accelerations were measured during the tests, and SI values were calculated with the goal of determining reasonable injury threshold parameters. Among the actual accident victims, chest injuries were the most prevalent. The authors calculated that there was a 50% chance that these occupants would receive at least an AIS-3 injury at a barrier equivalent velocity (BEV) of 45 mph, which, for a dummy in the Volvo system, would result in a peak chest acceleration of 85 G, an SI of 560, and a load at the upper end of the shoulder belt of 1930 lb (8.6 kN). The authors suggested therefore that the 60-G limit (even with the 3-ms exclusion) was too restrictive, and that the SI< 1000 criterion left too much leeway. The SI was also found not to be a suitable predictor of rib fracture, these fractures occurring when the SIs were estimated to range from essentially zero to 710. Belt load at the upper end of the shoulder harness was found to be "the most sensitive parameter to thoracic injury" because of its direct association with forces on the chest. Even so, rib fractures occurred in crashes ranging from 10 to 53 mph (16 to 85 km/h), which, when simulated, resulted in belt loads on the dummies ranging from 800 to 2310 lb. Even at the higher velocities, fewer than 40% of the occupants did indeed sustain fractures. The injury tolerance variability shown by these data emphasizes the difficulties inherent in trying to establish meaningful injury threshold parameters.

Three papers comparing experimental injuries to cadavers with injuries observed in actual crashes include Cromack and Ziperman (1975), Patrick and Levine (1975), and Tarriére et al. (1975). All three investigations dealt with cadavers and occupants restrained by three-point lap/shoulder belts, and all found that the cadavers received more severe chest injuries in similar crash environments than did their living counterparts, although the nature of the injuries was the same.

Patrick and Levine (1975) measured upper torso belt loads on the nine on the nine cadavers tested. (The horizontal load component was also calculated, these being generally 10% to 15% lower than the measured load at typical shoulder belt angles, but only the latter loads will be cited to facilitate comparison with other studies.) For tests ranging from 20 to 40 mph (32.2 to 64.4 km/h) BEV, loads resulting in rib fracture ranged from 1020 to 1930 lb (4.5 to 8.6 kN), while the range for non-fracture was 560 to 1560 lb (2.5 to 6.9 kN). Although the two 20-mph runs did not result in rib fracture, three of the four 40-mph runs did produce fractures. In contrast, rib fracture did occur among the Volvo occupants at speeds under 20 mph, but a lower percentage of living occupants received fractures at the higher speeds than did the cadavers. The authors also pointed out that the average number of ribs fractured per subject was much higher for the cadavers (5.6) than for the Volvo occupants (0.9) at BEVs of 30 mph (48.3 km/h) or more. Although age can be a factor, it was probably not significant here, the cadavers in this series ranging in age at death from 32 to 61 years. Despite the range of tolerance displayed in these as in other tests, the authors suggested that the threshold for cadaver rib fracture corresponded to a horizontal upper shoulder belt force of about 1000 lb (4.45 kN).

Fayon et al. (1975) also found that when adjusted for subject weight, the load on the thorax correlated fairly well ($r=0.71$) with the number of rib fractures in 31 dynamic tests using three-point-belted cadavers. The authors also showed that the relationship between deflection and injury was dependent on the rate of loading and on the nature of the load application (i.e., belt or disk impactor). The correlation between chest acceleration and injury was found to be poor.

Eppinger (1976) reported his analysis of 108 experimental impact tests with cadavers, restrained by three-point-belt systems, that had been conducted in recent years. He found that the number of ribs fractured was a statistically significant function of cadaver weight, age at death, and maximum upper torso belt force. Using dimensional analysis to scale the weight factor and statistical analysis to account for age, a relationship between thoracic fractures and shoulder belt load was developed. This relationship was applied to the driver/passenger population for a 30-mph (48.3-km/h) frontal barrier impact to derive an optimum load limit, given certain belt slack, that would minimize rib fracture. The optimum level for 2 in (5.1 cm) of slack was 1300 lb (5.8 kN), and for 3 in (7.6 cm) of slack the level rose to 1500 lb (6.7 kN). Eppinger also suggested that further analysis was needed to address the problem of life-threatening internal organ injuries.

Foret-Bruno et al. (1978) were able to relate vehicle occupant injuries to shoulder belt loads, in frontal crashes involving Peugeot and Renault vehicles, because of an energy absorbing belt system in which several ribbons of fabric tear successively as the force increases. No rib fractures were received by occupants less than 30 years old under loads up to about 1630 lb (7.3 kN). After age 50, however, fractures began to occur at about 950 lb (4.2 kN). Comparing these results to Eppinger's predictions of rib fractures in cadavers of the same ages, the authors found that cadavers could be expected to sustain from three to five more rib fractures than did the living occupant.

A means of possibly reducing rib fractures by spreading the load using wider (100 mm vs. 50 mm or 4 in vs. 2 in) belt webbing was investigated by Kallieris et al. (1980). Shoulder belt forces ranging from 5.7 kN (1279 lb) to 7.4 kN (1654 lb) were measured. Although AIS was not significantly different between the two belt widths, fewer rib fractures occurred with the wider belts. Age, however, was the overriding factor in predicting rib fracture. Because these fractures were located at the edges of the belts, the assumption was made that a loading surface as wide as the chest itself could eliminate rib fracture. The authors further suggested that the number of rib fractures is a better descriptor of thoracic injury severity than AIS.

Schmidt et al. (1981) tested 212 fresh cadavers restrained by three-point belts in 30-to-60-km/h (18.6-to-37.3-mph) and 10-to-25-G frontal sled impacts. While age and bone constitution were still the major determinants of injury, the authors found that sled deceleration was the best predictor of injury severity among test-condition variables. A matrix of impact conditions vs. age was developed that would limit injury severity to AIS 3. If impact speed is held at 49 km/h (30.4 mph) and deceleration at 14 G, allowable shoulder belt loads could range from more than 1800 lb (8 kN) for a 20-year-old cadaver to less than 450 lb (2 kN) for a 60-year-old cadaver. Corresponding limits for impact speed, ranging from 60 to 30 km/h, and sled deceleration, ranging from 25 to 10 G, were given for the same age range when the other two variables were held constant.

Results of nineteen oblique sled impact tests were reported by Kallieris et al. (1981). Angles of 15°, 30°, and 45° were used, and the deceleration ranged from 9 to 12 G. Shoulder belt loads ranged from 450+ lb (2.0 kN) for the smallest female to 1210 lb (5.4 kN) for the largest male. Rib fractures (range 0 to 9) and thoracic AIS (range 0 to 3) were more dependent on age than on belt load or thoracic acceleration (range 15 to 28 G). As in the frontal tests, fractures tended to occur at the edges of the initial belt location in the 15° and 30° impacts. In the 45° tests, however, the fracture pattern shifted upward on the side opposite the restrained shoulder, following the shifting of the belt itself.

An interesting factor in side impacts is the presence or absence of the arm. Cesari et al. (1981) found that, for cadavers impacted with a 23-kg (10.5 lb) mass, loads resulting in rib fracture were lower (1.75 to 2.90 kN or 393 to 652 lb) if the impact was directly into the side of the thorax than if the arm were placed between the impactor and the torso (average 2.96 kN or 665 lb). With the arm in the way, less deformation of the thorax occurred, and greater velocity was required to achieve the same load as when there was no arm.

Global Approaches. Using a ten-accelerometer array, Robbins et al. (1976) conducted frontal impacts using thirteen cadaver and twenty baboon subjects retrained by three-point belts, EA steering assemblies, and/or airbags. AIS was used as the indicator of injury level, rather than number of fractures, because the former addressed the full range of thoracic injuries. Various combinations of anthropometric and accelerometer measurements were used to try to develop linear regression models that would predict injury levels. With the limited number of subjects and the many possible parameters, the modeling effort was not as successful as had been hoped. The baboon series, however, in which the subjects were more similar to each other, yielded better predictions than the cadaver series, the former having an average error of less than 0.13 AIS.

The Robbins et al. series of frontal and side impact experiments with cadavers was increased to 51, the additional tests being primarily controlled frontal and lateral tests with a 51.5-lb (113.3-kg) flat-faced impactor. For these tests, two additional accelerometers were added to the spinal locations. With these data, a new approach to injury-predictive modeling, using a nonlinear Adaptive Learning Network (ALN) program, was tried and reported by Eppinger et al. (1978). With the goal of eventually being able to duplicate as much of the kinematic response of cadavers as possible in a dummy structure, models were exercised with increasingly fewer parameters to reach an optimum set that might be mechanically feasible while still adequately predicting injury. Both AIS and number of ribs fractured were used as injury measures.

The parameters chosen for analysis included measured accelerations, first and second integrals of these, and differences between accelerations at two points. Data from both frontal and lateral impacts were included, as well as cross-products of values for each to create "oblique" parameters. Age and sex were also used. The maximum number of parameters was thirteen, and, with the full set, high predictive capabilities were achieved for both AIS and rib fractures. However, the AIS model using only seven parameters was nearly as good ($R^2 = 0.911$), and, for rib fractures, nine parameters were adequate ($R^2 = 0.946$). It is interesting that age did not prove to be a significant variable, perhaps because the "structural response" parameters actually reflected the effects of age on injury potential.

This modeling approach selected key parameters that could theoretically be used as a basis for designing and constructing a "universal" dummy with valid responses when impacted from any direction. A word of caution is in order, however, regarding the use of multiple acceleration measurements, their integrals, differences, and cross-products, to arrive at a known value (AIS). While it may be possible to achieve a reasonable end result, the relationships among parameters that the model must use to achieve these results may not themselves be reasonable. Further analysis may be needed to validate this approach.

Robbins et al. (1980) presents an analysis of only the lateral cadaver tests, both sled and flat impactor. To differentiate among the many subjects with identical AIS ratings, a modified AIS that introduced a rib fracture bias was proposed but not used in the final analysis. Some adjustments on data processing procedures were made, so that the first and second integrals of acceleration (similar to, but not exactly velocity and deformation, because the vector direction was not precisely known) could be more accurately calculated. Using regression techniques, injury prediction models were developed using various acceleration-based parameters. The first integral of the left upper rib acceleration (impact forces were on the left side) proved to have the highest correlation with injury ($R^2 = 0.778$). Other significant parameters came from measurements on the right upper rib, the spine (laterally oriented accelerometers), and the lower sternum (accelerometer oriented perpendicular to impact). The authors concluded that, if the instrumentation system used in the cadaver tests were integrated into a dummy design, and if the dummy could exhibit the same responses as the cadavers at these accelerometer locations, it was reasonable to assume that this dummy could be used as a valid test device to predict injury.

SUMMARY AND CONCLUSIONS

The most critical injuries are those to the internal organs. In most experimental studies using cadavers, however, injury rating has been based on skeletal damage. As thoracic skeletal deflection increases under dynamic loading, the force resisting the motion remains somewhat constant. Further deflection begins to produce rib fractures, which can be followed by the sudden appearance of internal soft tissue injuries as the skeletal structure collapses. It is necessary, therefore, to be conservative in defining thoracic injury criteria in terms of deflection levels related only to rib fracture, because of the instability of the thoracic structure under such conditions. Applied load by itself is also inadequate as an injury criterion, because of its insensitivity to increasing deflection in the force-plateau region characteristic of dynamic thoracic response.

Another factor that must be considered in defining thoracic injury criteria is the fact that thoracic response to impact loading is highly rate-sensitive. Viscous and inertial forces dominate the initial response, and elastic forces become significant only as large deflections of the system occur. Some forms of pulmonary and cardiac injuries have been found to occur only in conditions of high impact velocities with very little chest deflection. The rate of thoracic deflection as well as the degree of deflection can both be important parameters in describing the injurious effects of an impact to the chest, and they should both be considered in the development of general thoracic injury criteria.

In terms of response, the sensitivity of the thoracic structure to the rate of loading makes it difficult to interpret the findings from different types of experiments without accounting for this variable. For instance, the strip loading produced by the shoulder belt may produce an apparent stiffness that is lower than that produced by a flat circular impactor, due to differences in shape and area of loading. The rate of loading in shoulder belt tests, however, is usually much lower than that of the typical impactor test, thereby confounding the interpretation of shoulder belt interactions with the thorax. Impactor mass is a variable that can also strongly affect the apparent response of the thorax and must be accounted for when comparing experimental results.

Flat circular impactor tests tend to produce a characteristic thoracic force-deflection response that consists of an initial linear region, followed by a plateau region of almost constant force, and finally, if the impact has sufficient severity, a third region of increasing stiffness. This general form of response has been shown to be true for both frontal and side impact and with volunteers as well as cadavers. Thoracic structural rate sensitivity appears to be responsible for much of the initial stiffness and for the subsequent plateau in force as the rate of loading decreases during the impact. However, the distribution of load by the flat impactor surface must play some role in determining the response, since shoulder belt loading does not appear to produce the plateau region (Walfisch et al. 1982), even when loading rates are taken into account. Such local loading effects are not, however, well documented.

Because of the complexities of thoracic response, simple elastic structural representations are inadequate to guide the designer of mechanical analogues of the thorax. Instead, representation by means of spring-mass-damper models, such as Lobdell et al. (1973), and/or transfer function approaches (Eppinger and Chan 1981) are necessary to provide the designer with the proper insight into the relative contributions of elastic, viscous, and inertial forces to the overall system response.

The three-dimensional structure of the thoracic skeleton and its contents requires deformation descriptors that are global in nature to provide an omnidirectional description of response. In the cadaver, this has been accomplished to some degree by the use of arrays of accelerometers on the periphery of the thorax. Similar or alternative methods of global response measurement would be necessary in a mechanical model to ensure adequate capability to assess injury potential in different directions and under different types of loads and loading rates.

REFERENCES

Bierman, H.R.; Wilder, R.M.; and Hellems, H.K. (1946) *The physiological effect of compressive forces on the torso.* Report no. 8. Naval Medical Research Institute Project X-630, Bethesda, Md.

Bowen, I.G.; Holladay, A.; Fletcher, E.R.; Richmond, D.R.; and White, C.S. (1965) *A fluid-mechanical model of the thoraco-abdominal system with applications to blast biology.* Lovelace Foundation for Medical Education and Research, Albuquerque, N.M.

Bowen, I.G.; Fletcher, E.R.; and Richmond, D.R. (1968) *Estimate of man's tolerance to the direct effects of air blast.* Lovelace Foundation for Medical Education and Research, Albuquerque, N.M.

Brinn, J.; Staffeld, S.E. (1970) Evaluation of impact test accelerations: A damage index for the head and torso. *Proc. 14th Stapp Car Crash Conference*, pp. 188–220. Society of Automotive Engineers, New York.

Brinn, J.; Staffeld, S.E. (1971) The effective displacement index: An analysis technique for crash impacts of anthropometric dummies. *Proc. 15th Stapp Car Crash Conference*, pp. 817–824. Society of Automotive Engineers, New York.

Cesari, D.; Ramet, M.; and Bloch, J. (1981) Influence of arm position on thoracic injuries in side impact. *Proc. 25th Stapp Car Crash Conference*, pp. 271–297. Society of Automotive Engineers, Warrendale, Pa.

Cooper, G.J.; Pearce, B.P.; Stainer, M.C.; and Maynard, R.L. (1982) The biomechanical response of the thorax to nonpenetrating impact with particular reference to cardiac injuries. *The Journal of Trauma*, 22(12):994–1008.

Cromack, J.R.; and Ziperman, H.H. (1975) Three-point belt induced injuries: A comparison between laboratory surrogates and real-world accident victims. *Proc. 19th Stapp Car Crash Conference*, pp. 1–24. Society of Automotive Engineers, Warrendale, Pa.

Eiband, A.M. (1959) *Human tolerance to rapidly applied accelerations: A summary of the literature.* NASA Memorandum 5-19-59E. NASA Lewis Research Center, Cleveland.

Eppinger, R.H. (1976) Prediction of thoracic injury using measurable experimental parameters. *Report 6th International Technical Conference on Experimental Safety Vehicles*, pp. 770–779. National Highway Traffic Safety Administration, Washington, D.C.

Eppinger, R.H.; and Chan, H. (1981) Thoracic injury prediction via digital convolution theory. *Proc. 25th Stapp Car Crash Conference*, pp. 369–393. Society of Automotive Engineers, Warrendale, Pa.

Eppinger, R.H.; Augustyn, K.; and Robbins, D.H. (1978) Development of a promising universal thoracic trauma prediction methodology. *Proc. 22nd Stapp Car Crash Conference*, pp. 209–268. Society of Automotive Engineers, Warrendale, Pa.

Eycleshymer, A.C.; and Shoemaker, D.M. (1911) *A cross-section anatomy*. Appleton, New York.

Fayon, A.; Tarrière, C.; Walfisch, G.; Got, C.; and Patel, A. (1975) Thorax of 3-point belt wearers during a crash (experiments with cadavers). *Proc. 19th Stapp Car Crash Conference*, pp. 195–223. Society of Automotive Engineers, New York.

Foret-Bruno, J.Y.; Hartemann, F.; Thomas, C.; Fayon, A.; Tarrière, C.; Got, C.; and Patel, A. (1978) Correlation between thoracic lesions and force values measured at the shoulder of 92 belted occupants involved in real accidents. *Proc. 22nd Stapp Car Crash Conference*, pp. 271–292. Society of Automotive Engineers, Warrendale, Pa.

Foster, J.K.; Kortge, J.O.; and Wolanin, M.J. (1977) Hybrid III: A biomechanically-based crash test dummy. *Proc. 21st Stapp Car Crash Conference*, pp. 975–1014. Society of Automotive Engineers, Warrendale, Pa.

Gadd, C.W.; and Patrick, L.M. (1968) *System versus laboratory impact tests for estimating injury hazard.* Society of Automotive Engineers, New York.

Gloyns, P.F.; and McKay, G.M. (1974) Impact performance of some designs of steering assembly in real accidents and under test conditions. *Proc. 18th Stapp Car Crash Conference*, pp. 1–27. Society of Automotive Engineers, Warrendale, Pa.

Harris, J. (1976) The design and use of the TRRL side impact dummy. *Proc. 20th Stapp Car Crash Conference*, pp. 77–106. Society of Automotive Engineers, Warrendale, Pa.

Hess, R.L.; Weber, K.; and Melvin, J.W. (1981) *Review of literature and regulation relating to thoracic impact tolerance and injury criteria.* Report no. UM-HSRI-81-38. The University of Michigan, Highway Safety Research Institute, Ann Arbor.

Jonsson, A.; Clemedson, C.; Sundqvist, A.; and Arvebo, E. (1979) Dynamic factors influencing the production of lung injury in rabbits subjected to blunt chest wall impact. *Aviation, Space, and Environmental Medicine*, 50(4):325–337.

Kallieris, D.; Barz, J.; and Schmidt, G. (1980) Influence of the belt width in regard to the injury severity and injury pattern at the thorax. *Proc. 8th International Conference of the International Association for Accident and Traffic Medicine*, pp. 120–126. Danish Society for Traffic Medicine, Arhus.

Kallieris, D.; Mattern, R.; Schmidt, G.; and Eppinger, R.H. (1981) Quantification of side impact responses and injuries. *Proc. 25th Stapp Car Crash Conference*, pp. 329–366. Society of Automotive Engineers, Warrendale, Pa.

Kallieris, D.; Schmidt, G.; and Schuler, F. (1982) Thorax load and pattern of injury in oblique collisions. *Beitrage zur Gerichtlichen Medizin*, 40:275–281.

Kroell, C.K.; Schneider, D.C.; and Nahum, A.M. (1971) Impact tolerance and response of the human thorax. *Proc. 15th Stapp Car Crash Conference*, pp. 84–134. Society of Automotive Engineers, New York.

Kroell, C.K.; Schneider, D.C.; and Nahum, A.M. (1974) Impact tolerance of the human thorax II. *Proc. 18th Stapp Car Crash Conference*, pp. 383–457. Society of Automotive Engineers, Warrendale, Pa.

Kroell, C.K.; Pope, M.E.; Viano, D.C.; Warner, C.Y.; and Allen, S.D. (1981) Interrelationship of velocity and chest compression in blunt thoracic impact to swine. *Proc. 25th Stapp Car Crash Conference*, pp. 549–579. Society of Automotive Engineers, Warrendale, Pa.

L'Abbé, R.J.; Dainty, D.A.; and Newman, J.A. (1982) An experimental analysis of thoracic deflection response to belt loading. *Proc. 7th International Conference on the Biomechanics of Impacts*, pp. 184–194. IRCOBI, Bron, France.

Lasky, I.I.; Siegel, A.W.; and Nahum, A.M. (1968) *Automotive cardio–thoracic injuries: A medical-engineering analysis.* SAE Paper No. 680052.

Lau, V.; and Viano, D.C. (1981) Influence of impact velocity and chest compression on experimental pulmonary injury severity in rabbits. *The Journal of Trauma*, 21(12):1022–1028.

Lobdell, T.E.; Kroell, C.K.; Schneider, D.C.; Hering, W.E.; and Nahum, A.M. (1973) Impact response of the human thorax. *Human Impact Response: Measurement and Simulation*, pp. 201–245. Plenum Press, New York.

McElhaney, J.H.; Stalnaker, R.L.; Roberts, V.L.; and Snyder, R.G. (1971) Door crashworthiness criteria. *Proc. 15th Stapp Car Crash Conference*, pp. 489–517. Society of Automotive Engineers, New York.

McElhaney, J.H.; Mate, P.I.; and Roberts, V.L. (1973) A new crash test device: "Repeatable Pete." *Proc. 17th Stapp Car Crash Conference*, pp. 467–507. Society of Automotive Engineers, New York.

Melvin, J.W.; Mohan, D.; and Stalnaker, R.L. (1975) *Occupant injury assessment criteria.* SAE Paper No. 750914. Society of Automotive Engineers, Warrendale, Pa.

Melvin, J.W.; Robbins, D.H.; and Stalnaker, R.L. (1978) Side impact response and injury. *Report 6th International Technical Conference on Experimental Safety Vehicles*, pp. 681–689. National Highway Traffic Safety Administration, Washington, D.C.

Melvin, J.W.; Robbins, D.H.; and Benson, J.B. (1980) Experimental application of advanced thoracic instrumentation techniques to anthropomorphic test devices. *Report 7th International Technical Conference on Experimental Safety Vehicles*, pp. 416–427. U.S. Government Printing Office, Washington, D.C.

Mertz, H.J.; and Gadd, C.W. (1971) Thoracic tolerance to whole-body deceleration. *Proc. 15th Stapp Car Crash Conference*, pp. 135-157. Society of Automotive Engineers, New York.

Mertz, H.J.; and Kroell, C.K. (1970) Tolerance of thorax and abdomen. *Impact Injury and Crash Protection*, pp. 372-401. Charles C. Thomas, Springfield, Ill.

Mohan, D.; and Melvin, J.W. (1983) Failure properties of passive human aortic tissue II: Biaxial tension tests. *Journal of Trauma*, 16:31-44.

Morgan, R.M.; Marcus, J.H.; and Eppinger, R.H. (1981) Correlation of side impact dummy/cadaver tests. *Proc. 25th Stapp Car Crash Conference*, pp. 301-326. Society of Automotive Engineers, Warrendale, Pa.

Nahum, A.M.; Gadd, C.W.; Schneider, D.C.; and Kroell, C.K. (1970) Deflection of the human thorax under sternal impact. *1970 International Automobile Safety Conference Compendium*, pp. 797-807. Society of Automotive Engineers, New York.

Nahum, A.M.; Gadd, C.W.; Schneider, D.C.; and Kroell, C.K. (1971) The biomechanical basis for chest impact protection: I. Force-deflection characteristics of the thorax. *Journal of Trauma*, 11(10):874-882.

Nahum, A.M.; Schneider, D.C.; and Kroell, C.K. (1975) Cadaver skeletal response to blunt thoracic impact. *Proc. 19th Stapp Car Crash Conference*, pp. 259-293. Society of Automotive Engineers. Warrendale, Pa.

Neathery, R.F. (1974) An analysis of chest impact response data and scaled performance recommendations. *Proc. 18th Stapp Car Crash Conference*, pp. 459-493. Society of Automotive Engineers. Warrendale, Pa.

Neathery, R.F.; and Lobdell, T.E. (1973) Mechanical simulation of human thorax under impact. *Proc. 17th Stapp Car Crash Conference*, pp. 451-466. Society of Automotive Engineers, New York.

Neathery, R.F.; Mertz, H.J.; Hubbard, R.P.; and Henderson, M.R. (1974) The Highway Safety Research Institute dummy compared with General Motors biofidelity recommendations and the Hybrid II dummy. *Proc. 3rd International Conference on Occupant Protection*, pp. 357-383. Society of Automotive Engineers, New York.

Neathery, R.F.; Kroell, C.K.; and Mertz, H.J. (1975) Prediction of thoracic injury from dummy responses. *Proc. 19th Stapp Car Crash Conference*. pp. 295-316. Society of Automotive Engineers, Warrendale, Pa.

Nusholtz, G.S.; Melvin. J.W.; and Lux, P. (1983) The influence of impact energy and direction on thoracic response. *Proc. 27th Stapp Car Crash Conference*, pp. 69-94. Society of Automotive Engineers, Warrendale, Pa.

Patrick, L.M. (1981) Impact force-deflection of the human thorax. *Proc. 25th Stapp Car Crash Conference*, pp. 471-496. Society of Automotive Engineers, Warrendale, Pa.

Patrick, L.M.; Kroell, C.K.; and Mertz, H.J. (1966) Forces on the human body in simulated crashes. *Proc. 9th Stapp Car Crash Conference*. pp. 237-259. University of Minnesota, Nolte Center for Continuing Education, Minneapolis.

Patrick, L.M.; Mertz, H.J.; and Kroell, C.K. (1967) Cadaver knee, chest, and head impact loads. *Proc. 11th Stapp Car Crash Conference*, pp. 106–117. Society of Automotive Engineers, New York.

Patrick, I.M.; Bohlin, N.I.; and Andersson, A. (1974) Three-point harness accident and laboratory data comparison. *Proc. 18th Stapp Car Crash Conference*, pp. 201-282. Society of Automotive Engineers, Warrendale, Pa.

Patrick, L.M.; and Levine, R.S. (1975) Injury to unembalmed belted cadavers in simulated collisions. *Proc. 19th Stapp Car Crash Conference*, pp. 79–115. Society of Automotive Engineers, Warrendale, Pa.

Robbins, D.H.; Melvin, J.W.; and Stalnaker, R.L. (1976) The prediction of thoracic impact injuries. *Proc. 20th Stapp Car Crash Conference*, pp. 697–729. Society of Automotive Engineers, Warrendale, Pa.

Robbins, D.H.; Lehman, R.J.; and Augustyn, K. (1980) Prediction of thoracic injuries as a function of occupant kinematics. *Report 7th International Technical Conference on Experimental Safety Vehicles*, pp. 374–383. U.S. Government Printing Office, Washington, D.C.

Roberts, V.L.; Moffat, R.C.; and Berkas, E.M. (1966) Blunt trauma to the thorax: Mechanism of vascular injuries. *Proc. 9th Stapp Car Crash Conference*, pp. 3–12. University of Minnesota, Nolte Center for Continuing Education, Minneapolis.

Sacreste, J.; Brun-Cassan, F.; Fayon, A.; Tarrière, C.; Got, C.; and Patel, A. (1982) Proposal for a thorax tolerance level in side impacts based on 62 tests performed with cadavers having known bone condition. *Proc. 26th Stapp Car Crash Conference*, pp. 155–171. Society of Automotive Engineers, Warrendale, Pa.

Schmidt, G.; Kallieris, D.; Barz, J.; and Mattern, R. (1974) Results of 49 cadaver tests simulating frontal collision of front seat passengers. *Proc. 18th Stapp Car Crash Conference*, pp. 283–291. Society of Automotive Engineers, Warrendale, Pa.

Schmidt, G.; Kallieris, D.; Barz, J.; Mattern, R.; Schulz, F.; and Schuler, F. (1981) *Load tolerance of belt-wearing vehicle occupants on frontal impact.* Forschungsvereinigung Automobiltechnik eV, Frankfurt, Germany.

Society of Automotive Engineers. (1966) *Human tolerance to impact conditions as related to motor vehicle design.* SAE J885a. Society of Automotive Engineers, New York.

Stalnaker, R.L.; McElhaney, J.H.; Roberts, V.L.; and Trollope, M.L. (1973a) Human torso response to blunt trauma. *Human Impact Response: Measurement and Simulation*, pp. 181–198. Plenum Press, New York.

Stalnaker, R.L.; Roberts, V.L.; and McElhaney, J.H. (1973b) Side impact tolerance to blunt trauma. *Proc. 17th Stapp Car Crash Conference*, pp. 377-408. Society of Automotive Engineers, New York.

Stalnaker, R.L.; and Mohan, D. (1974) Human chest impact protection criteria. *Proc. 3rd International Conference on Occupant Protection*, pp. 384–393. Society of Automotive Engineers, New York.

Stalnaker, R.L.; Tarriere, C.; Fayon, A.; Walfisch, G.; Baltlazard, M.; Masset, J.; Got, C.; and Patel, A. (1979) Modification of Part 572 dummy for lateral impact according to biomechanical data. *Proc. 23rd Stapp Car Crash Conference*, pp. 843–872. Society of Automotive Engineers, Warrendale, Pa.

Stapp, J.P. (1951) *Human exposure to linear deceleration. Part 2. The forward-facing position and the development of a crash harness.* AFTR 5915, pt. 2. Wright-Patterson AFB, Dayton, Ohio.

Tarriere, C.; Fayon, A.; Hartemann, F.; and Ventre, P. (1975) The contribution of physical analysis of accidents towards interpretation of severe traffic trauma. *Proc. 19th Stapp Car Crash Conference*, pp. 965–993. Society of Automotive Engineers, Warrendale, Pa.

Tennant, J.A.; Jensen, R.H.; and Potter, R.A. (1974) GM-ATD 502 anthropomorphic dummy: Development and evaluation. *Proc. 3rd International Conference on Occupant Protection*, pp. 394–420. Society of Automotive Engineers, New York.

Tsitlik, J.E.; Weisfeldt, M.L.; Chandra, N.; Effron, M.B.; Halperin, H.R.; and Levin, H.R. (1983) Elastic properties of the human chest during cardiopulmonary resuscitation. *Critical Care Medicine*, 11:685–692.

Verriest, J.P.; Chapon, A.; and Trauchessec, R. (1981) Cinnephotogrammetrical study of porcine thoracic response to belt applied load in frontal impact: Comparison between living and dead subjects. *Proc. 25th Stapp Car Crash Conference*, pp. 499–545. Society of Automotive Engineers, Warrendale, Pa.

Viano, D.C. (1978) Thoracic injury potential. *Proc. 3rd International Meeting on the Simulation and Reconstruction of Impacts in Collisions*, pp. 142–156. IRCOBI, Bron, France.

Viano, D.C. (1983) Biomechanics of nonpenetrating aortic trauma: A review. *Proc. 27th Stapp Car Crash Conference*, pp. 109–114. Society of Automotive Engineers, Warrendale, Pa.

Viano, D.C.; and Artinian, C.G. (1983) Myocardial conducting system dysfunctions from thoracic impact. *The Journal of Trauma*, 18:452–459.

Viano, D.C.; and Lau, V. (1983) Role of impact velocity and chest compression in thoracic injury. *Aviation, Space, and Environmental Medicine*, 54(1):16–21.

Walfisch, G.; Chamouard, F.; Lestrelin, D.; Fayon, A.; Tarriere, C.; Got, C.; Guillon, F.; Patel, A.; and Hureau, J. (1982) Tolerance limits and mechanical characteristics of the human thorax in frontal and side impact and transposition of these characteristics into protection criteria. *Proc. 7th International Conference on the Biomechanics of Impacts*, pp. 122–139. IRCOBI, Bron, France.

Yamada, H. (1970) *Strength of biological materials.* Williams and Wilkins, Baltimore.

APPENDIX: BIBLIOGRAPHY OF THORACIC CLINICAL LITERATURE

1. Blair, E.; Topuzlu, C.; and Davis, J. (1971) Delayed or missed diagnosis in blunt chest trauma. *The Journal of Trauma*, 11:129–145.

2. Bricker, D.; and Hallman, G. (1970) Complete transection of the thoracic aorta: Management of a case associated with massive total body injury. *The Journal of Trauma*, 10:420–426.

3. Conn, J.; Hardy, J.; Chavez, C.; and Fain, W. (1971) Challenging arterial injuries. *The Journal of Trauma*, 11:167–177.

4. Irving, M.; and Irving, P. (1967) Associated injuries in head injured patients. *The Journal of Trauma*, 7:500–511.

5. Laasonen, E.; Penttila, A.; and Sumuvuori, H. (1980) Acute lethal trauma of the trunk: Clinical, radiologic, and pathologic findings. *The Journal of Trauma*, 20:657-662.

6. Liedtke, A.; and DeMuth, W. (1973) Nonpenetrating cardiac injuries: A collective review. *American Heart Journal*, 86:687–696.

7. Naccarelli, G.; Haisty, W.; and Kahl, F. (1980) Left ventricular to right atrial defect and tricuspid insufficiency secondary to nonpenetrating cardiac trauma. *The Journal of Trauma*, 20:887–891.

8. Noon, G.; Boulafendis, D.; and Beall, A. (1971) Rupture of the heart secondary to blunt trauma. *The Journal of Trauma*, 11:122–128.

9. Olson, R.; and Johnson, J. (1971) Diagnosis and management of intra-thoracic tracheal rupture. *The Journal of Trauma*, 11:789–792.

10. O'Sullivan, M.; Spagna, P.; Bellinger, S.; and Doohen, D. (1972) Rupture of the right atrium due to blunt trauma. *The Journal of Trauma*, 12:208–214.

11. Paton, B.; Elliott, D.; Taubman, J.; and Owens, J. (1971) Acute treatment of traumatic aortic rupture. *The Journal of Trauma*, 11:1–14.

12. Pellegrini, R.; Layton, T.; DiMarco, R.; Grant, K.; and Marrangoni, A. (1980) Multiple cardiac lesions from blunt trauma. *The Journal of Trauma*, 20:169–173.

13. Relihan, M.; and Litwin, M. (1973) Morbidity and mortality associated with flail chest injury: A review of 85 cases. *The Journal of Trauma*, 13:663–671.

14. Shackford, S.; Virgilio, R.; Smith, D.; Rice, C.; and Weinstein, M. (1978) The significance of chest wall injury in the diagnosis of traumatic aneurysms of the thoracic aorta. *The Journal of Trauma*, 18:493–496.

15. Sutorius, D.; Schreiber, J.; and Helmsworth, J. (1973) Traumatic disruption of the thoracic aorta. *The Journal of Trauma*, 13:583–590.

16. Weisz, G.; Schramek, A.; and Barzilai, A. (1974) Injury to the driver. *The Journal of Trauma*, 14:212–215.

CHAPTER 4

ABDOMEN

A.I. King
Wayne State University
Detroit, Michigan

In spite of the fact that there is little bony structure to protect abdominal organs from blunt impact, injuries to this region contribute only 7.5% to the total IPR. Like the thorax, the abdomen can be the site of injuries induced by restraint systems themselves. Although beyond the scope of the current program, the abdominal region is also of special interest with regard to pregnant occupants and their fetuses, and thus the topic is included in this review.

ANATOMY OF THE ABDOMEN

The classical definition of the abdomen includes all organs and viscera below the diaphragm, above the pelvic girdle, and surrounded by the peritoneum. However, for the purposes of this study, organs of the urogenital system will also be considered as part of the abdomen. Mechanically, they can be roughly divided into two main groups, solid organs and hollow organs. The principal solid organs are the liver, spleen, kidneys, and pancreas, while the principal hollow organs are the stomach, the small and large intestine, the bladder, and the uterus. The other structures that make up the abdomen are muscle, blood vessels, and skin. The thoracolumbar spine is generally not considered part of the abdomen and neither are the ribs, which extend below the dome of the diaphragm and provide a certain degree of mechanical protection to the upper organs. In fact, the location of some of the organs of the abdominal viscera are given in terms of rib levels. For a complete description of the position of the various organs, it is necessary to define a series of bony landmarks and planes of orientation.

Bony Landmarks. The upper border of the abdomen is defined by the xiphoid process, the cartilages of the 7th through the 10th ribs, and the ends of the 11th and 12th ribs. This border is shown in Figure 4-1, which is an anterior (front) view of the abdomen, and in Figure 4-2, a posterior (back) view. The lower borders are based on the bony pelvis and are visible and/or palpable. They are the crests of the ilium, the anterior superior iliac spines (ASIS), and the pubic tubercle in the region of the mons pubis.

Planes of Orientation. For convenience of describing organ locations and for the purpose of providing a frame of reference for the abdomen, it is divided into nine regions by a series of imaginary planes (two horizontal and two sagittal) as shown in Figure 4-3 . The two transverse planes (transpyloric and transtubercular) divide the abdomen into three zones, named, in descending order, the subcostal, umbilical, and hypogastric zones. The transpyloric plane is located midway between the jugular notch and the upper border of the symphysis pubis. The transtubercular plane is at the level of the iliac tubercles and cuts through the body of the 5th lumbar vertebra. Each of the resulting three zones is further subdivided into three regions by right and left sagittal planes located half way between the ASISs and the torso midsagittal plane.

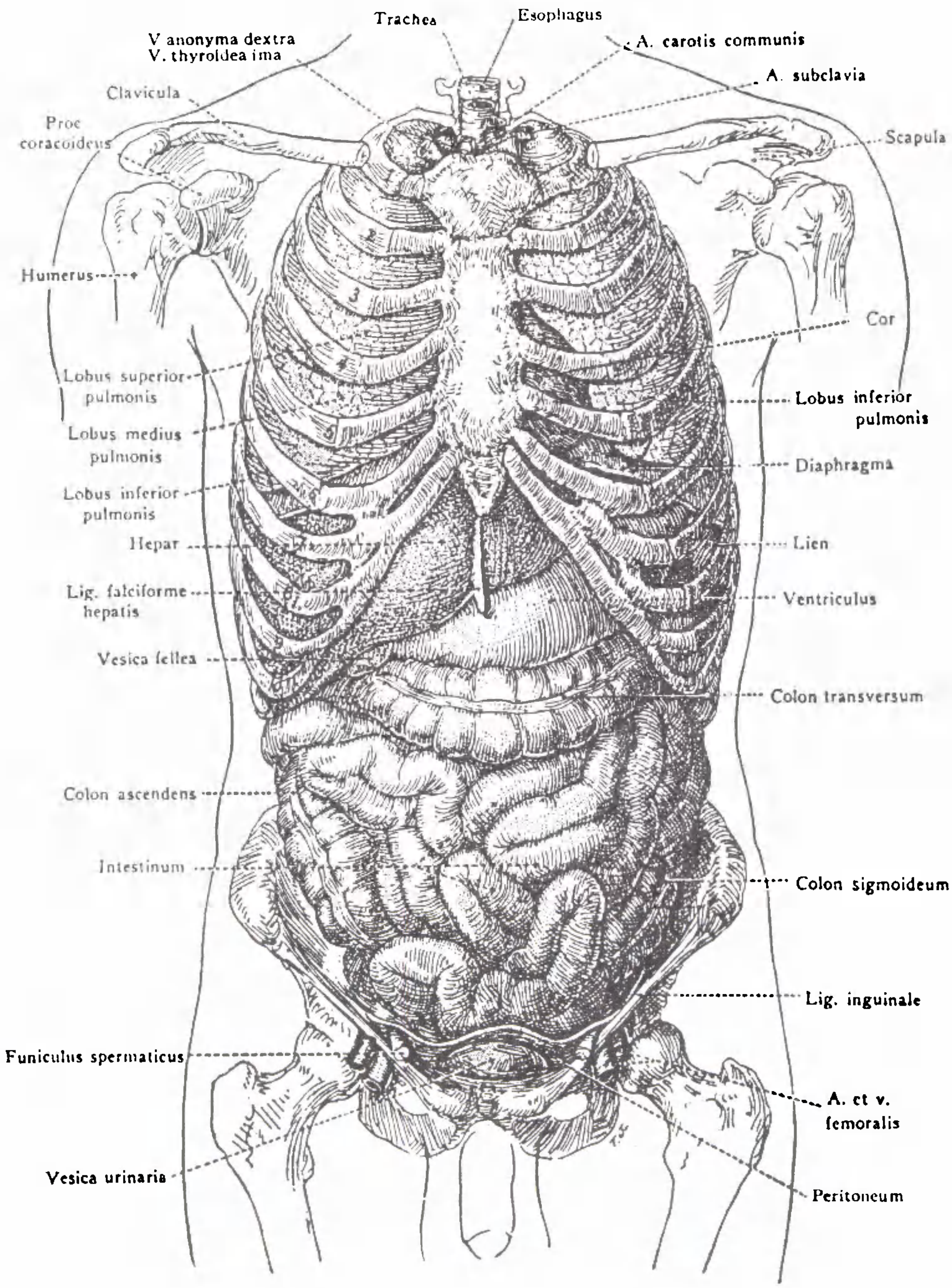

FIGURE 4–1. Thoracic and abdominal viscera shown in their normal relations to the skeleton, anterior view (*Gray's Anatomy*, American edition).

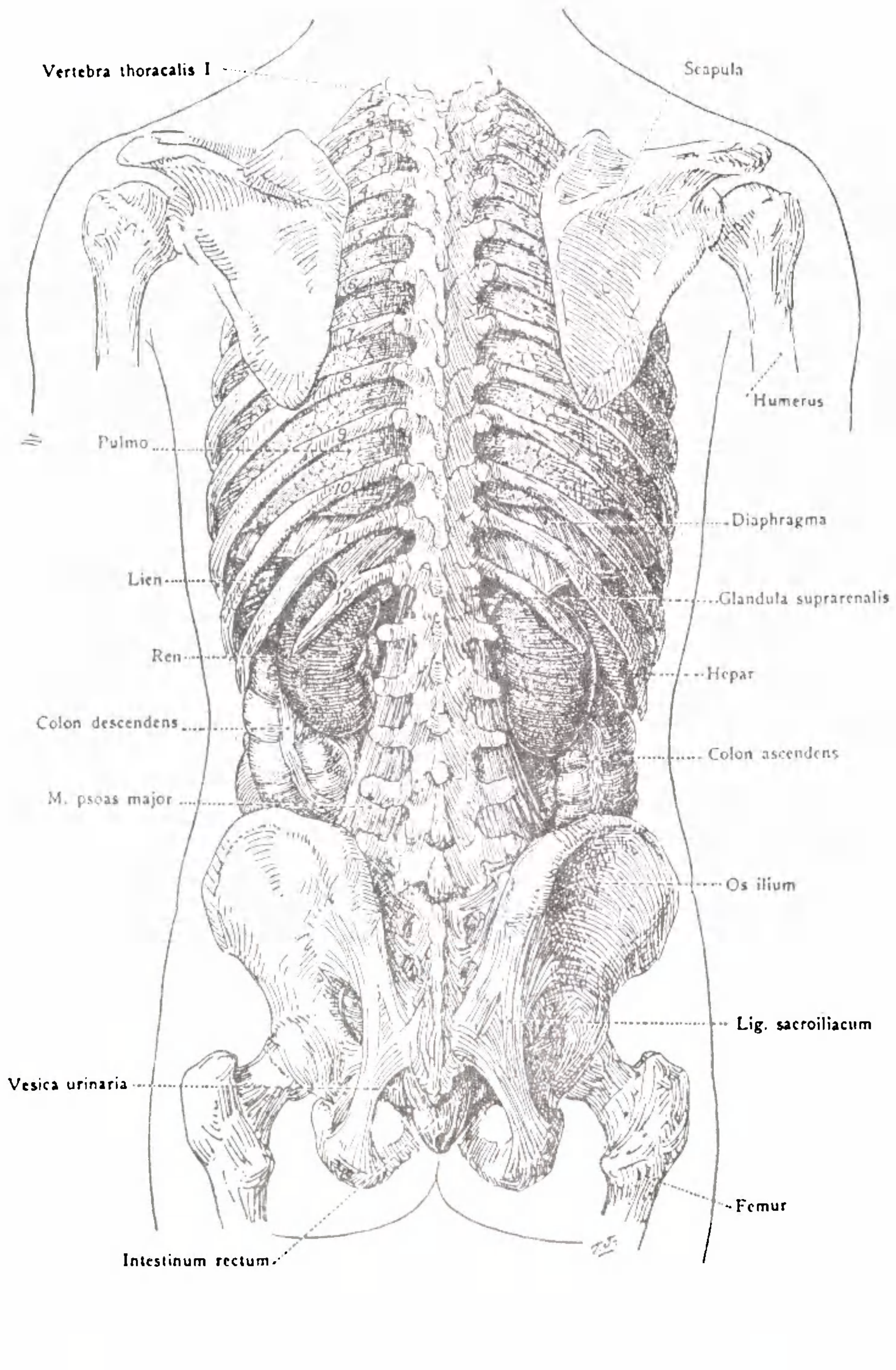

FIGURE 4-2. Thoracic and abdominal viscera shown in their normal relations to the skeleton, posterior view (*Gray's Anatomy*, American edition).

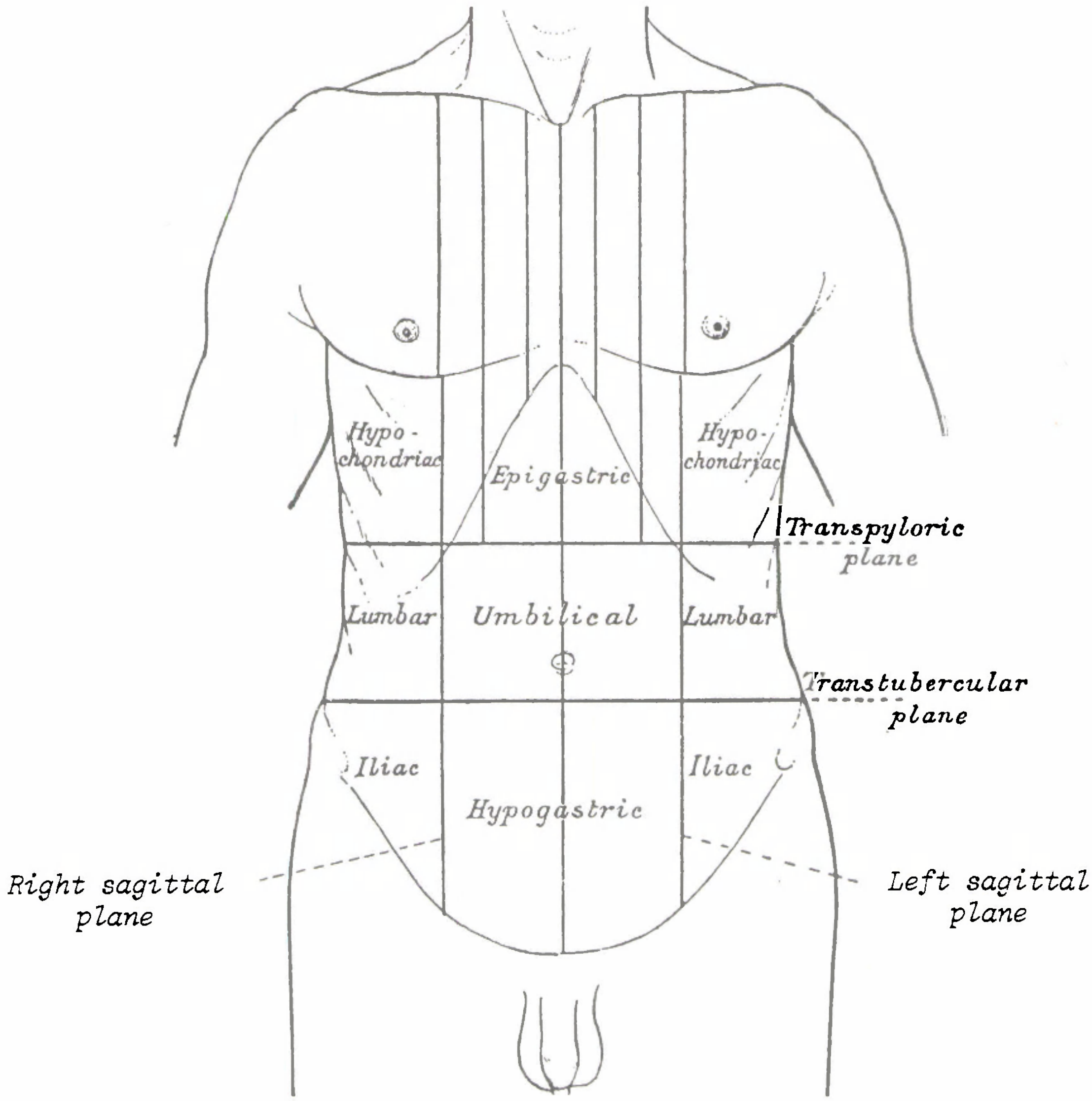

FIGURE 4-3. Regions of the abdomen (*Gray's Anatomy*, American edition).

The lateral regions of the upper zone are the right and left hypochondrium. They are located on both sides of the epigastric region. The middle zone has the umbilical region in the center, flanked by the right and left lumbar regions. The middle region of the lower zone is called the hypogastric or pubic region, and the lateral regions are the right and left iliac or inguinal regions.

The Liver. The liver is the largest gland in the body. It occupies almost the whole of the right hypochondrium, as well as the greater part of the epigastrium, and commonly extends into the left hypochondrium. It weighs approximately 1.5 kg (3.3 lb) in the male and 1.3 kg (2.9 lb) in the female and is divided into two lobes, the right lobe being about six times as large as the left. It is supported by five ligaments from the diaphragm. These are the falciform ligament, the coronary ligament, the left and right triangular or lateral ligaments, and the round ligament. The last four are weight-bearing ligaments, while the lax falciform ligament serves to limit lateral displacement.

The antero-lateral portion of the right lobe is covered by the 6th to the 10th ribs and their cartilaginous connections to the sternum. The lower portion of the sternum and the cartilage of the right ribs also cover the greater portion of the liver anteriorly.

The Spleen. The spleen is located in the left hypochondrium, but its cranial extremity extends into the epigastric region. It lies between the diaphragm and the fundus of the stomach, along the left posterior wall of the upper abdomen, at the level of the 7th to the 9th ribs. It can weigh from 40 to 400 g (1.4 to 14.1 oz) and is a quadrilaterally shaped organ with approximate dimensions of 120 by 70 mm (4.7 by 2.8 in) and 30 to 40 mm (1.2 by 1.6 in) thick. It receives its blood supply from the splenic artery, which is relatively large in diameter in proportion to the size of the spleen.

The Kidneys. The kidneys are located in the dorsal part of the abdomen, one on either side of the vertebral column, posterior to the peritoneum and surrounded by a mass of fat and loose areolar tissue. The superior border of the kidney is at the level of the superior endplate of T12, and the inferior border is at the level of L3. The right kidney is usually slightly lower than the left due to the size of the liver on that side. The kidney is ellipsoidal in shape, and the three diameters are approximately 115, 65, and 25 mm (4.5, 2.6, and 1.0 in). Its weight varies from 130 to 150 g (4.6 to 5.3 oz), and it is not supported by a ligamentous structure. It is held in position by the renal fascia and is in contact with the diaphragm, causing it to move up and down with respiration. The two main blood vessels are the renal artery and vein. The blood supply is estimated to be approximately 12% of the cardiac output to each kidney. The kidneys are strictly part of the urogenital system and lie outside of the peritoneum. However, for the purposes of impact biomechanics, they are a pair of important organs in the abdominal cavity. Like the liver and spleen, they are considered to be solid organs as opposed to the stomach and intestines, which are called the hollow organs.

The Pancreas. It is an elongated gland situated transversely across the posterior wall of the abdomen in the epigastric and left hypochondriac region. It is approximately 140 mm (5.5 in) long and weighs about 90 g (3.2 oz). The wider end (head) lies in the curve of the duodenum, and the narrower end (tail) extends laterally leftward almost to the medial border of the spleen.

The Stomach. It is a hollow organ situated in the epigastric and left hypochondriac regions. It is bounded by the diaphragm and the anterior abdominal wall between the liver and the spleen. It has the general shape of the letter "J," and its size is variable, depending upon the amount of its contents and the stage of digestion. The walls of the stomach consist of several layers of muscular coats. Food from the esophagus enters the superior opening just below the fundus and exits via the pylorus, which is a muscular sphincter connecting the stomach to the duodenum.

The Small Intestine. The small intestine is about 7 m (23 ft) long and is located in the central and lower part of the abdominal cavity. Anatomically, it is divided into three segments, the duodenum, the jejunum, and ileum. The duodenum is about 250 mm (9.8 in) long and is the widest of the three segments. There is no morphological difference between the jejunum and ileum. The diameter is about 40 mm (1.6 in) and the lengths are respectively 3 and 4 m (10 and 13 ft). This tubular organ forms arbitrary coils within the confines of the abdomen

The Large Intestine. The large intestine extends from the ileum to the anus and is about 1.5 m (5 ft) in length. It is largest at the ileocecal junction and decreases in diameter at the anal canal. The four principal segments are the ascending, transverse, descending, and sigmoid colon. The ascending colon extends from the cecum upward along the right abdominal wall to the lower surface of the liver. Then it becomes the transverse colon, which goes across the upper abdominal zone from the right hypochondrium to the left hypochondrium. The descending colon extends from the left hypochrodriac region to the lumbar region along the lateral border of the left kidney. The terminal portion of the colon is the sigmoid colon, which is about 400 mm (16 in) long and lies within the pelvis. It forms one or two loops before it ends in the rectum.

The Urinary Bladder. It is a musculomembranous sac located behind the pubic symphysis and is symmetric with respect to the midline. The lower portion extends forward and down from the behind and pubic bones. When moderately full it is oval in shape, and its major diameter is about 120 mm (4.7 in) long. When empty it has the shape of a flattened tetrahedron.

The Uterus. In the female, the uterus is a thick-walled muscular organ located in the pelvis between the bladder and the rectum. It is somewhat pear-shaped with its long axis parallel to the median plane. It is about 75 mm (3 in) long, 50 mm (2 in) wide, and 30 mm (1.2 in) thick. It weighs about 35 g (1.2 oz). The principal ligaments of the uterus are the broad ligaments, the round ligaments, the uterosacral ligaments, and the cardinal ligaments. The cardinal, broad, and uterosacral ligaments hold the uterus in place, while some mechanical support is provided by the pelvic diaphragm below the muscular floor of the pelvis.

ABDOMINAL INJURIES FROM CLINICAL EXPERIENCE

The clinical literature on abdominal injuries summarizes case histories of penetrating and nonpenetrating blunt trauma to the abdomen. Four papers were identified that dealt with large series of traffic accident victims, including pedestrians. None of the four papers was limited to vehicular occupants. There was one survey from Australia, one from the United Kingdom, and two from the United States. The Australian series by Ryan (1967) contained the largest number of cases (1315 cases) and covered the period 1963-64. There were 1029 vehicular occupants, 508 of whom were injured and 2 were killed. Only 18 victims (3.6%) sustained abdominal injuries and 5 of these (1%) had a moderate to severe injury, which is probably in the AIS 3 to 6 range, as there was one fatality due to an abdominal injury. The direction of impact was not given, but the door was responsible for six of the injuries and the front seat for two. The specific abdominal organs injured were not described, since the paper was concerned with all traffic accidents in Adelaide, South Australia. The steering system was not implicated in any of the 18 abdominal injuries.

The other three surveys of traffic injuries dealt only with fatalities. The British study discussed 289 road fatalities involving 172 car occupants. Eleven of these died from abdominal injuries (6.4%), and a total of 64 sustained abdominal injuries. The paper was published by Grattan and Clegg (1973), who did not specify the period during which these fatalities occurred. The principal abdominal injuries for all road users were 35 liver ruptures, 11 splenic ruptures, 12 combined liver, and splenic ruptures and 2 ruptures of the abdominal aorta. The steering system was responsible for 13 fatal injuries, and the door and/or the A or B post for nine more. One fatal injury was attributed to the seat belt, and there were three fatal injuries due to ejection, resulting in a total of 26 fatal abdominal injuries for the 11 fatalities. It should be noted that, in many cases, injury to the abdomen was not the only cause of death and that the same vehicle systems, such as the steering system and the side interior surface, caused both fatal thoracic as well as abdominal injuries.

In the United States, Gertner et al. (1972) provided a survey of 33 abdominal deaths in the Baltimore area from 1964 to 1969. There were 17 drivers, 8 passengers, and 8 pedestrians, ranging in age from 7 to 82. There were 16 solid organ injuries, 7 hollow organ injuries, and 10 involving both types of organs as well as other viscera and blood vessels. Six of the 16 solid organ injuries involved more than one organ. Of the other 10, two were liver injuries, seven were splenic, and one was a kidney injury. Of the seven hollow organ injuries, five were intestinal and two were bladder injuries. The paper concluded that 21 of the 33 were not treated adequately, and that 17 of these could have been saved with proper care.

The second U.S. study was in Vermont. It dealt with 127 fatalities due to abdominal injuries sustained in automobile accidents during the period of 1969–1974. Seventy were killed at the scene, 43 expired en route to the hospital, and 43 were treated. In the last group, 23 died in the emergency room, and the remaining 17 died at a later date after surgery and/or treatment. Of the 84 who died before reaching the hospital, hemorrhage of the liver occurred in 17 cases and of the spleen in one case. The cause of these injuries was not discussed, and the number of pedestrians was not revealed.

In eleven other general surveys of blunt abdominal trauma, seven were from the U.S., two from the United Kingdom, one each was from Sweden and Canada. Two of the papers investigated injuries associated with head injuries. One of the seven U.S. surveys was limited to pancreatic injuries, while another was a survey of military injuries. There was a total of 1246 civilian cases and 1175 military cases of abdominal injury in the U.S. surveys by Walt and Grifka (1970), Barnett et al. (1966), DiVincenti et al. (1968), Olinde (1960), Perry (1965), Fitzgerald et al. (1960), and Mueller (1970). In the civilian surveys, about one-half of the cases were traffic related. The exact number of vehicular occupants cannot be determined. The most frequently injured organs were the spleen, liver, kidney, and intestines. Only one survey reported a higher incidence of liver than splenic injuries. The order of injuries for military accidents was liver, spleen, kidney, intestines, and pancreas. Multiple injuries were commonly seen, and liver injuries were found to be most threatening to life because of the prevalence of massive hemorrhage and the need for immediate medical and surgical intervention.

There were 394 British cases reported by Bates (1973) and Wilson (1963). In Bates' series of 129 cases, 50 were vehicular occupants. The three most frequently injured organs for all 129 cases were the kidney (57%), the spleen (41%), and the liver (13%). These injuries were responsible for 17 of the 25 fatalities. Injury to the thorax in the form of rib fracture or something more severe was associated with abdominal injury 30% of the time. Wilson (1963) reported 40% kidney injuries, 26.3% splenic injuries, 17.9% injuries to the hollow organs, and 15.8% liver injuries. He had a total of 256 cases, 36.2% of which were traffic related. The mortality rate was 5.9% (15 cases out of 256). However, 13 of these 15 deaths were traffic related.

The Swedish series of 291 cases was reported by Solheim (1963). There was a total of 164 traffic accident cases and 60 traffic fatalities. The total number of abdominal injuries was 366. The frequency of injury was again in the order of kidney (36.6%), spleen (21.3%), liver (19.7%), and hollow organs (12.3%). There were 69 cases with injuries to the left kidney, and 10 of them had a coexistent splenic rupture. The overall mortality rate was 27.8%. This rate was 19.7% if there was injury to only one abdominal organ, but it jumped to 64.2% if there were injuries to two or more organs. In the Canadian study of 100 cases of splenic rupture by Willox (1965), 42% involved unrestrained vehicular occupants, 10% of whom were ejected from the car. The overall mortality rate was 17%, but the existence of associated head and chest injuries made it impossible to ascertain a mortality rate due to splenic rupture alone.

Incidence of Abdominal Injury. Bondy (1980) provided detailed statistics of abdominal injuries sustained by vehicular occupants during the period 1977 to 1979 from the National Crash Severity Study (NCSS). There was a total of 1516 injuries from AIS 1 to 5, representing 2.6% of all injuries. From AIS 3 to 5, there were 653 injuries which represented 14.6% of all injuries. That is, although the frequency of abdominal injuries was low, there was an over-representation of severe injuries in the abdominal area.

Considering now the 1516 abdominal injuries for AIS ratings of 1 to 5, 32% of the injuries were sustained by the solid organs and 8.6% by the hollow organs. The corresponding statistics for AIS 3 to 5 are 73.8% and 15.3%. The liver injury rate was 30.3%, while the kidney and spleen were both slightly under 22% in the AIS 3 to 5 range.

Frontal Impact. The total number of injuries (AIS 1-5) in this mode is 739. Of these, 304 (41%) were in the AIS 3 to 5 range. In this range, there were 120 liver injuries, 76 splenic injuries, and 43 kidney injuries. Injuries to the hollow organs numbered 58 (50 digestive and 8 urogenital). The preponderance of injuries to the solid organs is quite obvious. In fact, the minimum possible rating for injuries to solid organs is AIS 3, and liver injuries were generally AIS 4 or higher.

Side Impact. Of the 419 injuries (AIS 1-5) sustained in side impacts, 226 (54%) were in the AIS 3 to 5 range. There were 54 liver injuries, 62 kidney injuries, and 46 splenic injuries. The total number of AIS 3 to 5 injuries to the hollow organs was 41, equally divided between the intestines and the urogenital system. Again, there were no liver injuries less than AIS 4, and most of the splenic injuries were rated as AIS 4.

Contact Areas. For all impact directions and all injuries in the AIS 1 to 5 range, the steering system was most frequently involved (456 injuries or 30%). The areas were broken down rather finely, and, if certain ones were combined, the frequency of contact would be as shown in Table 4-1 for all injuries in the AIS 1 to 5 and AIS 3 to 5 ranges. Injuries due to the armrest were combined with the side interior surface, and those due to the instrument panel and the glove compartment area were also combined.

Injuries by Organ and Contact Area (AIS 1-5). An analysis was made of injuries to the principal solid and hollow organs of the abdomen as a function of the vehicle systems that apparently caused these injuries. Since there were very few injuries less than AIS 3 to these principal organs, the information given in Table 4-2 is representative of moderate to life-threatening injuries.

TABLE 4-1

MOST FREQUENTLY CONTACTED AREAS
FOR ABDOMINAL INJURIES

Area Contacted	AIS 1-5 Injuries	AIS 3-5 Injuries
Steering System	456	187
Side Interior Surface	149	95
Instrument Panel	119	61
Restraint System Webbing	72	4
Front Seat Back	34	20

TABLE 4-2

INJURIES BY ORGAN AND CONTACT AREA
(AIS 1-5)

Contact Area	Liver	Spleen	Kidney	Digestive	Urogenital
Steering System	68	39	24	36	10
Side Surface	19	19	30	6	12
Instrument Panel	20	15	10	7	6
Belt Webbing	0	0	0	3	1

It can be seen from Table 4-2 that the steering system is associated with a large percentage of the injuries to these organs. The fact that the spleen and kidneys are situated toward the sides of the abdominal cavity explains the relatively high frequency of injury associated with the side interior surface, including armrests. The fact that the restraint system webbing caused no injuries to the solid organs is also significant.

General Comments. The following comments are made for two purposes. First they serve to point out additional observations that can be made from the data provided. Second, they indicate that additional computer runs to configure the data in different ways could bring out other facts.

1. Restraint systems reduce injury severity quite substantially. However, only 7% of the sample were restrained by any kind of a belt system, and only 3.5% used a three-point-belt system. Restrained occupants sustained 2.6% of the injuries, and the rate for those using the three-point system was 0.4%.

2. Distribution by age, sex, seating position, and direction of impact were not provided. If the mechanism of injury is to be studied, such information could be helpful.

3. Associated injuries to other body regions were not given. In particular, the severity of thoracic injuries (number and location of rib fractures) would be helpful in correlating solid organ injuries to damage to the rib cage.

4. Occupants with multiple abdominal injuries were not identified. For example, the simultaneous occurrence of splenic and left kidney injuries would be an important data point.

5. A detailed description of the injuries to the individual organs is not available. Such descriptions are necessary for a better understanding of the mechanisms of injury to the major abdominal organs.

Belt-Induced Abdominal Injuries. Although there is overwhelming evidence to show that the seat belt is effective in reducing the frequency of death and injury, there exists a long list of clinical reports that attribute a large variety of lower torso injuries to the seat belt. Most of the injuries occurred to occupants wearing of a single lap belt, and there were occasional references to other types of belt restraints, such as the three-point belt and the full-double shoulder harness. These reports in the clinical literature are generally sporadic, individual, and anecdotal. Huelke and Lawson (1976) listed 26 of these reports, and 11 more reports in the same vein were also identified. These references are listed in an appendix to this chapter.

Huelke and Lawson (1976) performed a search of the Collision Performance and Injury Report (CPIR) file to study the effect of lap belts on lower torso injuries. The search was restricted to front-seat, lap-belted, outboard occupants involved in frontal crashes. The 1976 AIS scale was used to quantify the injuries. The study concluded that the "no-injury" category increased by 50% in belt users over unbelted occupants. About 20% of the belted occupants sustained lower torso injuries, and, of these, approximately 70% were rated as minor. Belts reduced the occurrence of serious injuries in all lower torso regions except in the lumbar spine area. The more serious injuries occurred at impact speeds of over 30 mph (50 km/h). Only 5% of the lap-belted occupants had critical to life-threatening injuries in the lower torso area. The angle of the seat belt did not appear to be related to the severity of lower torso injury.

There is now some information regarding the injury potential of three-point-belt systems, as far as the abdominal area is concerned. The first paper with a respectable series of cases was written by Williams and Kirkpatrick (1971), who discussed injuries to 63 individuals that were injured as a result of wearing a three-point restraint. It was not clear from the paper how many of the 63 cases were treated by the authors. In any event, intra-abdominal injuries were rare. There were only four known cases of rupture to the small intestine, even though the impact speeds were all in excess of 30 mph (50 km/h).

Because of the mandatory belt law in Ontario, Canada, recent statistics regarding three-point-belt injuries have become available. Gallup et al. (1982) reviewed abdominal injuries sustained by a total sample of 314 occupants in Transport Canada's Fully Restrained Occupant Study (FROS). A total of 65 occupants sustained an abdominal injury, 25 in frontal collisions and 40 in non-frontal collisions. In the AIS range of 3 to 5, there were 8 frontal injuries (32%) and 14 non-frontal injuries (35%). For the frontal collision occupants, there were 12 drivers and 13 front seat passengers. The total number of drivers and passengers involved in frontal collisions was 91 and 30, respectively. Thus, the incidence of injury to the right-front-seat passenger is considerably higher than that to the driver (43.3% vs. 13.2%).

Life-threatening injuries were principally sustained by the hollow organs, which were perforated, ruptured, lacerated, and torn. The only solid organ identified was the spleen. The injuries were attributed to the lap belt buckle and the steering wheel rim. It was also stated that individuals in the back seat who were restrained by a single lap belt had a very high incidence of abdominal injuries, and in most cases these were more severe. The authors were of the opinion that the abdominal injuries sustained by three-point-belted occupants were not the result of submarining but rather due to poor positioning of the occupant relative to the lap belt. The fact that more front seat occupants were injured than drivers points to the likelihood that the former were more often out of position.

Factors that contributed to abdominal injuries were obesity, sex, and age. Females and older people tended to have more injuries as well as those who were obese. Other factors included belt geometry, seat geometry and stiffness, clothing, and seat material. It is difficult to assess the importance of these factors, however, in the absence of any indication of crash severity.

Leung et al. (1982) had access to French accident data and reported on injuries to 1423 front seat occupants who were all wearing three-point restraints at the time of their accident. There were 35 abdominal injuries that had a severity of AIS 3 or higher. They attributed 68% of these abdominal injuries to lap belt submarining, because there were associated lumbar spine injuries. Contributing factors included poor geometry of the lap belt, a slackly worn belt, and impact speeds in excess of 50 km/h (30 mph). The shoulder harness could be responsible for the initiation of submarining if the buckle was placed too far forward. The authors had a recommendation for lap belt angles to prevent submarining. The angle in the vertical plane should be 50° or higher, and the angle in the horizontal plane should be 100° or less. A more detailed treatment of this topic is given by Leung et al. (1981).

Snyder et al. (1969) carried out baboon experiments to study the effect of lap belts on the abdominal viscera during frontal ($+G_x$ and $-G_x$) and lateral ($+G_y$) impacts. There were sixteen right-lateral impacts, four forward-facing ($-G_x$) impacts, and four rearward-facing ($+G_x$) tests. The impact speeds varied from 36.4 ft/s (11.1 m/s) at 15 G to 88.2 ft/s (26.9 m/s) at 44 G for the lateral impacts. Pathology was found to be significantly higher in lateral impact. Ruptured bladders and uteri, adrenal hemorrhage, and intracranial subdural and epidural hemorrhage occurred frequently. Pancreatic hemorrhage, due to lateral impact, had an unexplained etiology. Under these test conditions, both survival and tolerance levels were found to be lowest in the lateral ($+G_y$) direction, indicating that lap belt restraint alone was not adequate for side impact protection.

Lau and Viano (1981) impacted beagles with a scaled-down lap belt across the upper abdomen, just below the xiphoid process, and with a similar diagonal belt, running from the left shoulder across the sternum. There were six animals in each loading experiment. Four types of liver injuries similar to those seen in the field were observed. The dynamic applied pressure necessary to cause a liver surface injury was 350 kPa (51 psi) at an impact speed of 1.7 m/s (5.6 ft/s). The tolerance information was considered valid, but the beagle was thought to be more susceptible to liver injury than the human because of increased exposure of the abdomen to the belt webbing. The postulated mechanisms of injury were pressure, bending of the lobes, and shear forces.

Obstetric Injuries in Vehicular Accidents. Several papers exist dealing with obstetric injuries as a result of automotive accidents. An excellent series of papers was written by Crosby, who presented clinical as well as experimental evidence that pregnant occupants should wear a three-point-restraint system. In one of his early papers, Crosby (1970) reported on 168 cases in which pregnant car occupants were involved in vehicular accidents. Thirty-eight of these occupants were restrained by a lap belt and the rest were unrestrained. The data were collected from a variety of sources, including clinical literature, case reports, and a series of 79 cases collected in cooperation with the California Highway Patrol. The conclusion was that the single leading cause for fetal death was maternal death. However, the lap belt caused the mother to jackknife over the uterus, resulting in fetal injuries and increased intra-uterine pressure. Thus, fetal survival rate was not significantly improved by the use of the lap belt alone. This was confirmed by a subsequent paper by Crosby and Costiloe (1971), who studied 208 pregnant occupants involved in severe accidents. Crosby et al. (1968, 1972) also performed controlled experiments on pregnant baboons that were restrained by either a lap belt or a three-point belt. In their second study, a comparison of fetal survival was made between lap-belted and three-point-belted baboons. This survival rate was 50% with the lap-belt restraint and 92% with the three-point-belt restraint. The observed difference was statistically significant at the 95% level.

Other clinical papers discuss various aspects of abdominal trauma to a gravid uterus. In a limited study of 27 cases by Pepperell et al. (1977), in which all fetuses were killed due to vehicular impacts, there were 18 cases of placental separation, 6 of which occurred despite the fact that a three-point belt was worn. There were five maternal deaths in this series with two cases of placental separation. None of the five mothers was restrained. Other causes of fetal distress were listed by Buchsbaum (1968). They included maternal hypotension, hypoxia, and psychological shock.

Summary of Clinical Experience. Data from NCSS files indicate that abdominal injuries account for 14.6% of all severe injuries (AIS 3–5). An earlier Australian survey by Ryan (1967) was as large as the NCSS survey and showed only one fatality attributable to abdominal injuries. Surveys of traffic fatalities resulting from abdominal injuries indicate that the cause of death was attributed to massive hemorrhage, and in many cases the victims died before they reached the hospital. The literature review was extended to clinical reports of blunt abdominal trauma in an attempt to acquire more information regarding the probability of fatalities resulting from such injuries. Unfortunately, most of the reports do not single out traffic fatalities as a percentage of the cases seen by the clinical authors. In one case, Wilson (1963) reported an overall fatality rate of 5.9% for a total of 256 cases. The majority of the deaths were traffic related (5% of all cases), but the statistics included pedestrians as well as vehicular occupants. However, this fatality rate compares well with the survey by Grattan and Clegg (1973), who reported a 6% fatality rate from traffic related accidents in the same country (UK). In any case, the fatality rate is low and appears to be dropping with improved emergency medical services and diagnostic techniques.

ABDOMINAL INJURY MECHANISMS, TOLERANCE, AND RESPONSE

Although the injury mechanisms of the various abdominal organs are not well understood, much research has been done to duplicate blunt abdominal trauma in the laboratory, in both animals and cadavers. The early work of Windquist et al. (1953) was followed by that of Williams and Sargent (1963), Baxter and Williams (1961), Mays (1966), Hellstrom (1965), Nickerson et al. (1967), Trollope et al. (1973), Melvin et al. (1973), Gogler et al. (1977), Nusholtz et al. (1980) , Walfisch et al. (1980), and Leung et al. (1982), as well as previously cited work of Snyder et al. (1969) and Lau and Viano (1981). The following descriptions of the more recent of these studies is intended to bring out the salient points in abdominal research.

Melvin et al. (1973) performed some basic strength studies on the liver and kidney of Rhesus monkeys by exposing them to direct impact while they were being perfused by their original blood supply. The organs were impacted at loading rates of 50, 2500, and

5000 mm/s (2, 100, and 200 in/s), and the peak strain level was controlled to vary the severity of injury. In the 17 liver impacts, the strain was from 40% to 75%, while, in the six kidney tests, the strain was from 35% to 67%. Stress–strain curves were obtained for both organs. A difference in response due to strain rate was evident from the liver data, but there were insufficient kidney data to bring out a similar difference. The onset of liver injury during dynamic loading occurred at 310 kPa (45 psi). This tolerance value is approximately the same as that reported by Lau and Viano (1981) for belt-induced liver injuries. The paper also gave a description of the common forms of liver injury seen in accident victims. They vary from subcapsular hematomas and superficial lacerations to severe crushing and bursting type injuries with star-shaped lacerations and gross destruction of the tissue. However, no attempt was made to correlate the observed injuries to the impact load.

Trollope et al. (1973) impacted 100 animals in the abdominal area, using over ten different types of impactors. There were four different species of animals of varying size and body weight, and the impact location was also varied to cause injury to different abdominal organs. Because of the large number of experimental conditions, the results could not be analyzed statistically. However, a few general remarks can be made regarding this study.

1. The upper abdomen was more vulnerable than the lower abdomen.
2. To produce the same injury to an organ, a higher pressure was required for a rigid bar impactor than that for a large surface impactor.
3. A small change in velocity of an impactor produced a large change in the severity of the injury.
4. Relatively high lap belt forces produced few injuries.
5. The estimated severity of impact was found to be a logarithmic function of the peak force, the impact duration, animal mass, and area of contact.

Williams and Sargent (1963) attempted to determine the mechanism of injury to the intestines. Anesthetized dogs were subjected to impacts by a 50-lb (23-kg) weight that was dropped from a height of 8 ft (2.4 m). The abdomen was covered by a board placed across the supine animal. Pressures were recorded from the peritoneum and the gastrointestinal tract. A total of 45 animals was used. The impact conditions were the same for all animals, but, in ten of the tests, the board was prevented from crushing the abdomen completely by the use of steel stops. In twenty tests, the ileum was sutured transversely across the spine to test the "fixed-point" hypothesis, which attributes the observed intestinal tears to fixed points along the intestinal tracts. Their results are summarized below.

1. The 45 dogs sustained 35 mesenteric tears and 33 intestinal tears.
2. Eighteen of the twenty animals with a sutured ileum sustained intestinal tears. Ten of these also sustained mesenteric injury.
3. When the board was arrested, there were three mesenteric injuries and two intestinal tears among the ten animals tested in this mode.
4. Intraperitoneal pressures were always higher than intra-intestinal pressures.
5. All injuries occurred in the midline.

The authors concluded that the mechanism of injury was shear and compression between opposing surfaces. This conclusion was based on the fact that (1) the observed pressure differences between the intestines and peritoneum tended to compress the hollow organ, and (2) fixation of the intestine resulted in more frequent injuries, which were principally at the midline.

Nusholtz et al. (1980) performed lateral impacts on 12 subhuman primates, 10 canine subjects, and 3 cadavers. Five of the primates and one dog were post-mortem subjects. A pneumatic impactor was used to deliver blows to the right side of each subject. For the cadaver, the impact location was at the level of the center of gravity of the liver. That for the primates and canines was variable. The human cadavers sustained peak forces of 3.2, 4.5, and 4.8 kN (720, 1012, and 1080 lb) with a liver injury occurring in the test with a peak force of 3.2 kN (720 lb) and no injury at the other levels. The peak force for the subhuman primates averaged 1.9 kN (427 lb) for the live subjects and 2.4 kN (540 lb) for the post-mortem subjects. Ten primates sustained liver injuries in the AIS range of 2 to 5. Eight had kidney injuries. Seven were on the impacted side, one had bilateral injuries, and one was injured on the right side. The average peak force for the canine subjects was 3.4 kN (773 lb). All dogs sustained liver injuries in the range of AIS 3 to 6. One had a right kidney injury. Injury location in the primates was thought to be due to differential organ motion, and there was a trend of increasing injury level with increasing rate of abdominal deformation.

Walfisch et al. (1980) performed a series of side impacts on human cadavers by dropping them on their right side from a height of 1 or 2 m (3.28 or 6.56 ft). The subjects impacted a 70-mm (2.7-in) wide rigid protrusion that simulated an armrest. The surface of the protrusion was a piece of wood, 25 mm (1 in) thick and rounded at the edges. In some tests the rest of the protrusion varied in height and was made from different padding materials. Although 11 cadavers were tested, the results were limited to eight of the subjects, because three of them suffered from cirrhosis of the liver, and the high fiber content of the diseased liver increased its tolerance to impact. Six of the eight cadavers with normal livers sustained an AIS 3 to 5 hepatic injury. There were also rib injuries, but they were not an aggravating factor, as far as liver injuries were concerned. The livers did not burst, and their ligaments were not torn. The authors normalized the force and pressure data, using the method proposed by Eppinger (1976) for rib fractures. The normalized force for an AIS 3 injury to the liver was 4.5 kN (1012 lb). The corresponding pressure was 260 kPa (38 psi).

Walfisch et al. also presented the load-deflection response of the abdomen to these lateral impacts. These data have been further analyzed by Brinn, whose analysis is presented here. Figure 4-4 shows the resulting responses of five of the cadavers tested against the rigid armrest. The ordinate scale is the actual measured force, while the abscissa is the actual penetration plus deflection of the lower rib-cage/abdomen, normalized by the ratio of cadaver torso depth to a 50th percentile depth of 245 mm (9.6 in).

Leung et al. (1982) made a survey of belt-induced injuries to cadaveric subjects in tests carried out at the sled lab of Association Peugeot-Renault (APR) and at the University of Heidelberg. These were frontal impacts of belted subjects. In the APR survey, there was a total of 70 runs that resulted in 43 cases with injuries. Twenty-three of the subjects submarined. If the injuries were limited to those of the liver, spleen, and spine, the number of cases was reduced to 24, eighteen of whom submarined. Two of the seven liver injuries, and two of the four splenic injuries were not attributable to submarining. There were no intestinal injuries in non-submarining cases. In the Heidelberg survey, there were 81 frontal impacts below 16 G, and 132 impacts above 16 G. In the latter group, there were 46 drivers and 84 front seat passengers. The liver injury rate was 3.5% for drivers and 16% for passengers for impacts above 16 G.

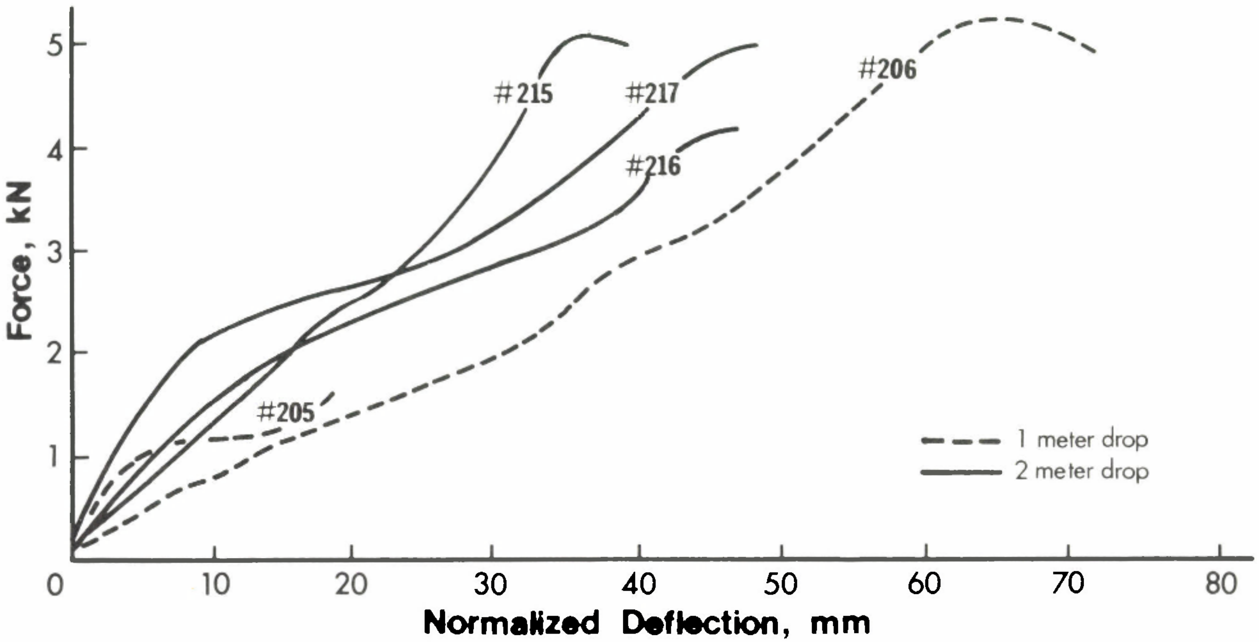

FIGURE 4-4. Load/deflection of the lower rib cage at the 9th rib level
(Analysis by Brinn, after Walfisch et al. 1980, with deflection normalized to torso depth of 245 mm).

SUMMARY AND CONCLUSIONS

The abdomen includes the organs and viscera below the diaphragm and above the pelvic girdle. Although there is little bony structure to protect these organs from blunt impact, injuries to this region contribute only 7.5% to the total IPR. Like the thorax, the abdomen can be the site of injuries induced by restraint systems themselves, including belts and steering systems. As far as the crucial organs are concerned, the liver, spleen, and kidneys are most frequently injured, and these injuries tend to be the most serious and life-threatening.

Injury mechanisms in the abdomen are thought to be primarily the result of deformation or penetration of the abdominal contents along with significant force or pressure generation in the deformed organs. In addition, solid organs, such as the liver, may undergo severe damage due to pressure generation alone at high impact velocities. There is evidence to show that these organs are viscoelastic, that the rate of loading is a crucial factor in injury causation, and that a compressive stress of 300 kPa (43 psi) will cause a superficial liver injury. Regarding dynamic response of the abdomen, the problem is complicated by the fact that there is a variety of surface geometries and component materials that can impact the upper abdominal area in a vehicle crash environment. In side impacts, however, the surfaces such as doors and armrests are somewhat well-defined, and dynamic load-deflection response curves do exist to a limited extent for lateral impact. Much more research data are needed, however, before abdominal response to impact can be fully quantified.

REFERENCES

Barnett, W.O.; Hardy, J.D.; and Yelverton, R.L. (1966) Pancreatic trauma: Review of 23 cases. *Annals of Surgery*, 163:892-901.

Bates, T. (1973) Abdominal trauma: A report of 129 cases. *Postgraduate Medical Journal*, 49:285-292.

Baxter, C.F.; and Williams, R.D. (1961) Blunt abdominal trauma. *Journal of Trauma*, 1:241-248.

Bondy, N. (1980) Abdominal injuries in the National Crash Severity Study. *National Center for Statistics and Analysis Collected Technical Studies, Vol. II: Accident data analysis of occupant injuries and crash characteristics*, pp. 59-80. National Highway Traffic Safety Administration, Washington, D.C.

Buchshaum, H.J. (1968) Accidental injury complicating pregnancy. *American Journal of Obstetrics and Gynecology*, 102:752-769.

Crosby, W.M. (1970) Pathology of obstetric injuries in pregnant automobile-accident victims. *Accident Pathology: Proceedings of an International Conference*, pp. 204-207. U.S. Government Printing Office, Washington, D.C.

Crosby, W.M.; and Costiloe, J.P. (1971) Safety of lap-belt restraint for pregnant victims of automobile collisions. *New England Journal of Medicine*, 284(12):632-636.

Crosby, W.M.; Snyder, R.G.; Snow, C.C.; and Hanson, P.G. (1968) Impact injuries in pregnancy I: Experimental studies. *American Journal of Obstetrics and Gynecology*, 101:100-110.

Crosby, W.M.; King, A.I.; and Stout, L.C. (1972) Survival following impact: Improvement with shoulder harness restraint. *American Journal of Obstetrics and Gynecology*, 112:1101-1106.

DiVincenti, F.C.; Rives, J.D.; Laborde, E.J.; Fleming, I.D.; and Cohn, I., Jr. (1968) Blunt abdominal trauma. *Journal of Trauma*, 8:1104-1013.

Eppinger, R.H. (1976) Prediction of thoracic injury using measurable experimental parameters. *Proc. 6th Experimental Safety Vehicle Conference*, pp. 770-780. National Highway Traffic Safety Administration, Washington, D.C.

Fitzgerald, J.B.; Crawford, E.S.; and DeBakey, M.E. (1960) Surgical considerations of non-penetrating abdominal injuries. An analysis of 200 cases. *American Journal of Surgery*, 100:22-29.

Foley, R.W.; Harris, L.S.; and Pilcher, D.B. (1976) Abdominal injuries in automobile accidents: Review of care of fatally injured patients. *Journal of Trauma*, 17:611-615.

Gallup, B.M.; St-Laurent, A.M.; and Newman, J.A. (1982) Abdominal injuries to restrained front seat occupants in frontal collisions. *Proc. 26th Conference of American Association of Automotive Medicine*, pp. 131-148. AAAM, Morton Grove, Ill.

Gertner, H.R.; Baker, S.P.; Rutherford, R.B.; and Spitz, W.U. (1972) Evaluation of the management of vehicular fatalities secondary to abdominal injury. *Journal of Trauma*, 12:425-431.

Grattan, E.; and Clegg, N.G. (1973) Clinical causes of death in different categories of road user. *Proc. International Conference on the Biokinetics of Impacts*, pp. 73-81. IRCOBI, Bron, France.

Gogler, E.; Best, A.; Braess, H.H.; Burst, H.E.; and Laschet, G. (1977) Biomechanical experiments with animals on abdominal tolerance levels. *Proc. 21st Stapp Car Crash Conference*, pp. 711-751. Society of Automotive Engineers, Warrendale, Pa.

Hellstrom, G. (1965) Intravascular pressure response to closed liver injury: An experimental study in dogs. *Upsala Journal of Medical Sciences*, 70:152-166.

Huelke, D.F.; and Lawson, T.E. (1976) *Lower torso injuries and automobile seat belts.* SAE Paper No. 760370. Society of Automotive Engineers, Warrendale, Pa.

Lau, V.K.; and Viano, D.C. (1981) An experimental study of hepatic injury from belt-restraint loading. *Aviation, Space, and Environmental Medicine*, 52:611-617.

Leung, Y.C.; Tarrière, C.; Fayon, A.; Mairrese, P.; and Banzet, P. (1981) An anti-submarining scale determined from theoretical and experimental studies using three-dimensional geometric definition of the lap-belt. *Proc. 25th Stapp Car Crash Conference*, pp. 685-729. Society of Automotive Engineers, Warrendale, Pa.

Leung, Y.C.; Tarrière, C.; Lestrelin, D.; Got, C.; Buillon, G.; Patel, A.; and Hureau, J. (1982) Submarining injuries of three-point belted occupants in frontal collisions: Description, mechanisms and protection. *Proc. 26th Stapp Car Crash Conference*, pp. 173-205. Society of Automotive Engineers, Warrendale, Pa.

Mays, E.T. (1966) Bursting injuries of the liver. *Archives of Surgery*, 93:92–103.

Melvin, J.W.; Stalnaker, R.L.; Roberts, V.L.; and Trollope, M.L. (1973) Impact injury mechanisms in abdominal organs. *Proc. 17th Stapp Car Crash Conference*, pp. 115-126. Society of Automotive Engineers, Warrendale, Pa.

Mueller, W.F. (1970) Nonpenetrating injuries of the abdomen in landcraft accidents. *Accident Pathology: Proceedings of an International Conference*, pp. 196–203. U.S. Government Printing Office, Washington, D.C.

Nickerson, J.L.; Drazic, M.; Johnson, R.; Udesen, H.; and Turner, K. (1967) A study of internal movements of the body occurring on impact. *Proc. 11th Stapp Car Crash Conference*, pp. 129–135. Society of Automotive Engineers, Warrendale, Pa.

Nusholtz, G.S.; Melvin, J.W.; Mueller, G.; Mackenzie, J.R.; and Burney, R. (1980) Thoraco-abdominal response and injury. *Proc. 24th Stapp Car Crash Conference*, pp. 187–228. Society of Automotive Engineers, Warrendale, Pa.

Olinde, H.D.H. (1960) Nonpenetrating wounds of the abdomen: A report of 47 cases with review of the literature. *Southern Medical Journal*, 53:1270–1282.

Pepperell, R.J.; Rubinstein, E.; and MacIsacc, I.A. (1977) Motor-car accidents during pregnancy. *Medical Journal of Australia*, 1:203–205.

Perry, J.F., Jr. (1965) A five-year survey of 152 acute abdominal injuries. *Journal of Trauma*, 5:53–61.

Ryan, G.A. (1967) Injuries in traffic accidents. *New England Journal of Medicine*, 276:1066–1076.

Snyder, R.G.; Snow, C.C.; Young, J.W.; Price, C.T.; and Hanson, P. (1969) *Experimental comparison of trauma in lateral* ($+G_y$), *rearward-facing* ($+G_x$), *and forward-facing* ($-G_x$) *body orientations when restrained by lap belt only*. FAA report no. AM69-13. Federal Aviation Agency, Office of Aviation Medicine, Washington, D.C.

Solheim, K. (1963) Closed abdominal injuries. *Acta Chirurgica Scandinavica*, 126:579-592.

Trollope, M.J.; Stalnaker, R.L.; McElhaney, J.H.; and Frey, C.F. (1973) The mechanism of injury in blunt abdominal trauma. *Journal of Trauma*, 13:962–970.

Walfisch, G.; Fayon, A.; Tarrière, C.; Rosey, J.P.; Guillon, F.; Got, C.; Patel, A.; and Stalnaker, R.L. (1980) Designing of a dummy abdomen for detecting injuries in side impact collisions. *Proc. 5th International Conference on the Biomechanics of Impacts*, pp. 149–164. IRCOBI, Bron, France.

Walt, A.J.; and Grifka, T.J. (1970) Blunt abdominal injury: A review of 307 cases. *Impact Injury and Crash Protection*, pp. 101–124. Edited by E.S. Gurdjian et al. Charles C. Thomas, Springfield, Ill.

Williams, J.S.; and Kirkpatrick, J.R. (1971) The nature of seat belt injuries. *Journal of Trauma*, 11:207–218.

Williams, R.D.; and Sargent, F.T. (1963) The mechanism of intestinal injury in trauma. *Journal of Trauma*, 3:288–294.

Willox, G.L. (1965) Nonpenetrating injuries of abdomen causing rupture of spleen: Report of 100 cases. *Archives of Surgery*, 90:498–502.

Wilson, D.H. (1963) Incidence, aetiology, diagnosis, and prognosis of closed abdominal injuries: A study of 265 consecutive cases. *British Journal of Surgery*, 50:381–389.

Windquist, P.G.; Stumm, P.W.; and Hansen, R. (1953) *Crash injury experiments with the monorail deceleration.* Report no. AFFTC 53-7. Air Force Field Technical Center, Edwards AFB, Calif.

APPENDIX: BIBLIOGRAPHY OF CLINICAL LITERATURE ON BELT-INDUCED ABDOMINAL INJURIES

1. Anon. (1974) Seat belt injuries to the colon. *British Medical Journal*, 1:85–86.

2. Backwinkel, K. (1968) Injuries from seat belts. *Journal of the American Medical Association*, 205:305–308.

3. Bouillot, J.L.; Gayral, F.; Alasseur, F.; and Larrieu, H. (1983) Traumatismes coliques par ceinture de sécurité. *Journal de Chirurgie*, 120(2):109–110.

4. Braun, P.; and Dion, Y. (1973) Intestinal stenosis following seat belt injury. *Journal of Pediatric Surgery*, 8:549–550.

5. Cocke, W.; and Meyer, K. (1963) Splenic rupture due to improper placement of automobile safety belt. *Journal of the American Medical Association*, 183:693.

6. Dajee, H; and MacDonald, A.C. (1982) Gastric rupture due to seat belt injury. *British Journal of Surgery*, 69:436–437.

7. Dardik, H.; Warren, A.; and Dardik, I. (1973) Diaphragmatic, visceral, and somatic injuries. *New York State Journal of Medicine*, 73:577–580.

8. DeHaven, H.; Tourin, B.; and Macri, S. (1953) *Aircraft safety belts: Their injury effect on the human body*. Automotive Crash Injury Research of Cornell University, Ithaca, New York.

9. Dehner, J.R. (1971) Seat belt injuries of the spine and abdomen. *American Journal of Roentgenology*, 3:833–843.

10. Denis, R.; Allard, M.; Atlas, H.; and Farkouh, E. (1983) Changing trends with abdominal injury in seatbelt wearers. *Journal of Trauma*, 23:1007–1008.

11. DiFiore, F.R.; and Gin, D.M. (1968) Injuries due to automobile seat belts. *American Surgeon*, 34:828–830.

12. Dominguez, J.; and deWardener, H.E. (1972) Stock car kidney. *Lancet*, 1:125–126.

13. Engberg, A. (1961) Injuries caused by safety belts: A contribution to the discussion with reference to an unusual case. *Svensk Lakartidningen*, 58:884–886.

14. Fish, J.; and Wright, R.H. (1965) The seat belt syndrome: Does it exist? *Journal of Trauma*, 5:746–750.

15. Herbert, D.C. (1964) Injury reduction by diagonal and other vehicle safety belts. *Medical Journal of Australia*, 1:61–72.

16. Hudson, I.; and Kavanagh, T.G. (1983) Duodenal transection and vertebral injury occurring in combination in a patient wearing a seat belt. *Injury*, 15(1):6–9.

17. Huelke, D.F.; and Chewning, W.A. (1969) *Comparison of occupant injuries with and without seat belts*. SAE Paper No. 690244. Society of Automotive Engineers, Warrendale, Pa.

18. Kulowski, J.; and Rost, W.B. (1956) Intra-abdominal injury from safety belt in auto accident. *Archives of Surgery*, 73:970–971.

19. Lister, R.D.; and Milson, B.M. (1963) Car seat belts: An analysis of the injuries sustained by car occupants. *Practitioner*, 191:332–340.

20. McBoyle, M.F.; Schiller, W.R.; and Hurt, A.V. (1984) Massive gastrointestinal bleeding following blunt abdominal trauma: An unusual case presentation. *Journal of Trauma*, 24:1057–1059.

21. MacLeod, J.H.; and Nicholson, D.M. (1969) Seat belt trauma to the abdomen. *Canadian Journal of Surgery*, 12:202–205.

22. Michelinakis, E. (1971) Safety-belt syndrome. *Practitioner*, 207:77–80.

23. Myers, J.W.; Schmidt, C.; and Draft, R.O. (1972) An unusual seat belt injury: Case report. *Journal of Trauma*, 12:529–533.

24. Payne, D.D.; Resnicoff, S.A.; States, J.D.; and Williams, J.S. (1973) Seat belt abdominal wall muscular avulsion. *Journal of Trauma*, 13:262–266.

25. Porter, S.D.; and Green, E.W. (1968) Seat belt injuries. *Archives of Surgery*, 96:242–246.

26. Ritchie, W.P.; Ersek, R.A.; Bunch, W.L.; et al. (1970) Combined visceral and vertebral injuries from lap-type seat belts. *Surgery, Gynecology, and Obstetrics*, 131:431–435.

27. Rouse, T.; Collin, J.; and Daar, A. (1984) Isolated injury to the intestine from blunt abdominal injury. *Injury*, 16(2):131–133.

28. Schneider, R.C.; Smith, W.S.; Grabb, W.C.; et al. (1968) Lap seat belt injuries: The treatment of the fortunate survivor. *Michigan Medicine*, 67:171–186.

29. Shamblin, J.R. (1968) Seat belt injuries. *Archives of Surgery*, 97:474–477.

30. Shennan, J. (1973) Seat-belt injuries of the left colon. *British Journal of Surgery*, 60:673–675.

31. Snyder, C.J. (1972) Bowel injuries from automobile seat belts. *American Journal of Surgery*, 123:312–316.

32. Stevenson, J.H. (1979) Severe thoracic intra-abdominal and vertebral injury in combination with patient wearing a seat belt. *Injury*, 10:321–323.

33. Sube, J.; Ziperman, H.; and McIver, W. (1967) Seat belt trauma to the abdomen. *American Journal of Surgery*, 113:346–350.

34. Tolins, S. (1964) An unusual injury due to the seat belt. *Journal of Trauma*, 4:397-399.

35. Tourin, B.; and Garrett, J.W. (1960) *Safety belt effectiveness in rural California Automotive Accidents.* Automotive Crash Injury Research of Cornell University, Ithaca, New York.

36. Towne, J.B.; and Coe, J.D. (1971) Seat belt trauma of the colon. *American Journal of Surgery*, 122:683–685.

37. Traylor, F.A.; Morgan, M.W.; Licero, J.I.; et al. (1969) Abdominal trauma from seat belts. *American Surgeon*, 35:313–316.

38. Von Bahr, V.; and Erickson, E. (1961) Injuries caused by safety belts. *Svensk Lakartidningen*, 58:141–143.

39. Wagner, A.C. (1979) Disruption of abdominal wall musculature: Unusual feature of seat belt syndrome. *American Journal of Roentgenology*, 133:753–754.

40. Williams, J.S.; Lies, B.A.; and Hale, H.W., Jr. (1966) The automotive safety belt: In saving a life may produce intra-abdominal injuries. *Journal of Trauma*, 6:303–315.

41. Williams, J.W.; and Kirkpatrick, J.R. (1971) The nature of seat belt injuries. *Journal of Trauma*, 11:207–218.

42. Witte, C.L. (1968) Mesentery and bowel injury from automotive seat belts. *Annals of Surgery*, 176:486–492.

43. Woelfel, G.F.; Moore, E.E.; Cogbill, T.H.; and Van Way, C.W., III (1984) Severe thoracic and abdominal injuries associated with lap-harness seatbelts. *Journal of Trauma*, 24:166–167.

CHAPTER 5

PELVIS

A.I. King
Wayne State University
Detroit, Michigan

The pelvis is a bony structure that transmits the weight of the torso to the lower extremities during normal locomotion and supports the torso in the seated position. In an automotive impact environment, it can sustain injury from both frontal and side impact, and, during aircraft ejection or vertical falls, it is called upon to take the entire inertial load from seat-to-head acceleration. Injuries to the pelvis, however, contribute only about 1% to the total IPR. This structure is important in this discussion, therefore, primarily for its response during load transmission.

ANATOMY OF THE PELVIS

The pelvis (Latin for "basin") is a ring of bone interposed between the flexible spinal column, which it supports, and the movable lower limbs, upon which it rests. Mechanically, it is the only load path for the transmission of the weight of the head, arms, and torso to the ground. Thus, the pelvic structure is more massive than that of the cranial or thoracic cavities. The pelvic ring or girdle is composed of four bones. Two hip bones form the side and front walls of the ring, while the sacrum and coccyx make up the rear wall. Figure 5-1 shows a frontal view of the male and female pelvis. There are many differences between the male and female pelvis, but the principal functional difference is the shape of the inner cavity that is completely surrounded by bone. This aperture is almost circular in the female, while it is wider in the side-to-side direction in the male. In the female, this aperture is the birth canal through which the fetus must pass. The orientation of the pelvis is less variable in the standing posture than that of the seated posture. A method for defining pelvic orientation will be discussed below.

The Hip Bone. The hip bone is a large, relatively flat, and irregularly shaped bone that forms the greater part of the pelvic girdle. It is formed by three fused bones called the ilium, ischium, and pubis. The fusion occurs around a cup-shaped articular cavity called the acetabulum (hip socket), which is situated near the middle of the outer surface of the bone. The ilium makes up the flank of the hip bone and is the upper broad and expanded portion which extends upward from the acetabulum. The ilium is divided into two parts, the large wing-like ala and the body of the ilium that forms a part of the acetabulum. Most of the landmarks and surface features are of little biomechanical significance and will not be discussed. However, it is necessary to point out the anterior-superior iliac spine (ASIS), which acts as an anatomical anchor point to prevent the lap belt from slipping over the top of the pelvis, a phenomenon called "submarining." The ilium is attached to the sacrum along its medial (inside) surface called the auricular surface. This surface is covered with cartilage, but the joint is not synovial. It is therefore postulated that only a limited amount of relative motion can occur here.

The ischium forms the lower and rearward part of the hip bone and is divided into two parts, a body and a ramus. The former constitutes the rearward third of the

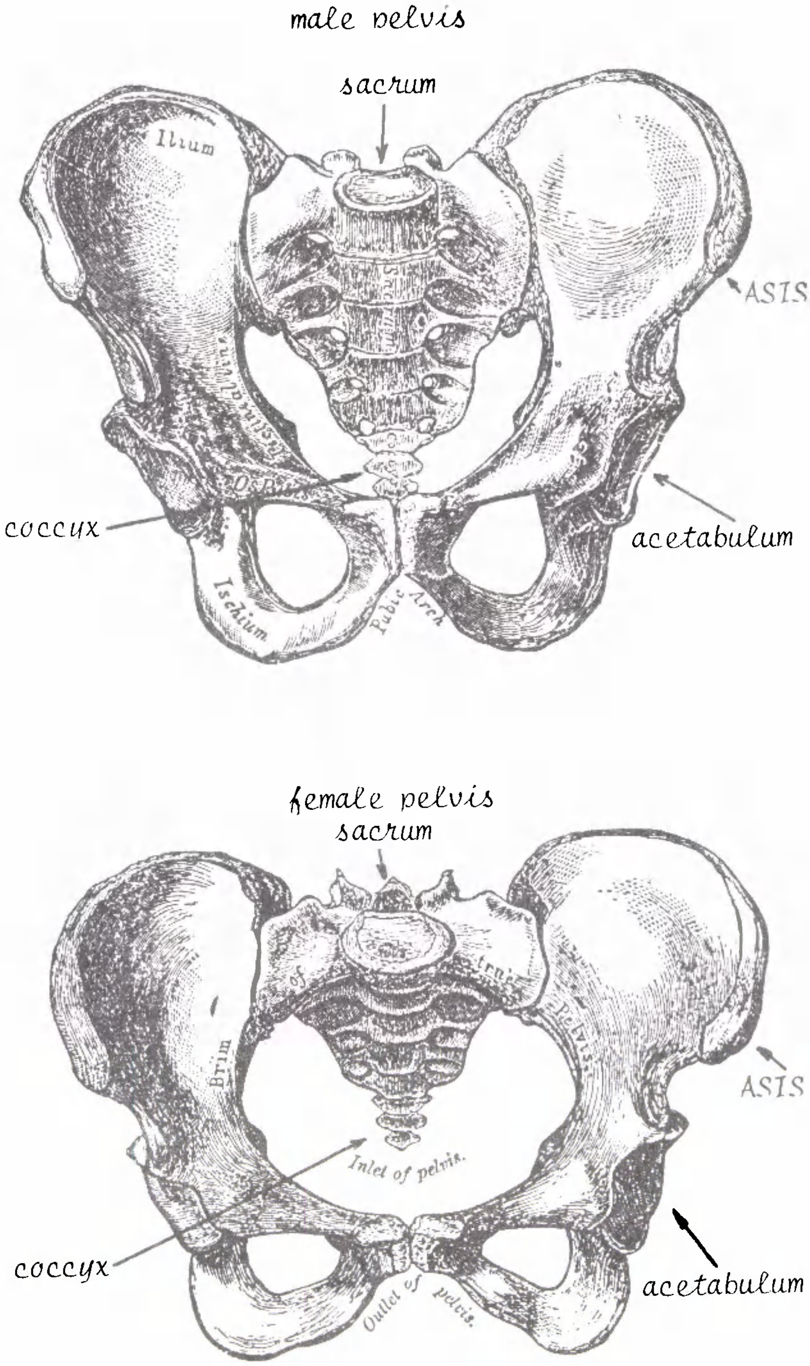

FIGURE 5–1. Frontal view of the male and female pelvis (*Gray's Anatomy*, American edition).

acetabular cup. The lowest portion of the body is the ischial tuberosity, which supports the upper torso in a seated posture. The ramus is a thin flattened part of the ischium that joins with the inferior pubic ramus. The pubic bone is an irregularly shaped bone composed of a body and two rami, the superior and inferior pubic rami. The body forms the front third of the acetabulum. The upper ramus extends from the body to the midsagittal plane, where it articulates with the corresponding ramus on the opposite side. The joint formed by the two superior pubic rami is called the pubic symphysis, which is a slightly movable joint containing a cartilaginous disc between the two bones. The lower pubic ramus joins with the ramus of the ischium to form the bottom arch of the obturator foramen. The inferior pubic rami likewise join each other through the pubic symphysis.

The Sacrum and Coccyx. The rear wall of the pelvic girdle is composed of the sacrum and the coccyx. The former is a fusion of five sacral vertebrae and is triangular in shape. Its auricular surfaces form a solid joint with the pelvis through which the weight of the upper torso is transmitted to the legs or the ischial tuberosities. The bone is concave towards the front and supports the lumbar spine at the top.

The coccyx is a vestigial tail made up of three to five fused vertebra. The vertebrae do not have all of the features of normal vertebrae, in as much as they are devoid of all the posterior structures and the last vertebra is a mere nodule of bone. The sacral-coccygeal joint is a slightly movable joint, interposed by a thin disc of cartilage that is stiffer than a normal intervertebral disc.

Orientation of the Pelvis. This orientation varies from person to person and is different for the standing and seated posture. Quantification of orientation requires a plane of reference that appears as a straight line when the pelvis is viewed laterally. Nyquist and Murton (1975) proposed that the plane formed by the two ASIS and the pubic symphysis can be used as a reference. The three landmarks are palpable, and X-ray is not needed to identify them. Although a method exists to define pelvic orientation, it is not known whether a large body of data exists for either the standing or seated posture. According to Gray (1973), the variation in pelvic orientation in the standing posture is about 10°.

The Proximal Femur. Since the femur articulates with the pelvis and injuries are often located in the vicinity of the hip joint, it is necessary to discuss briefly the anatomy of the proximal femur. The femur is the longest and strongest bone in the body and is roughly cylindrical in shape along its shaft. However, the shape of the two ends is different from that of the shaft. In particular, the proximal or upper portion of the femur is made up of a head, neck, and trochanteric region. A view of the proximal femur from the rear is shown in Figure 5-2.

The head of the femur has a spherical shape, forming a synovial joint with the acetabulum. This joint is commonly known as the hip joint. The surface of the head is lined with a layer of hyaline cartilage, typical of a synovial joint. Its blood supply comes through the neck of the femur, which is the structure below the head.

The neck of the femur is shaped like a truncated cone and connects the head with the rest of the femur. It is almost cylindrical at the base of the head, and its axis is at an angle of about 125° with the femoral shaft. In the female, this angle can be as low as 90°. The lower boundary of the neck is defined by the intertrochanteric crest in the rear and by the intertrochanteric line in the front. Both boundaries are well defined ridges that act to demarcate the neck from the trochanteric region.

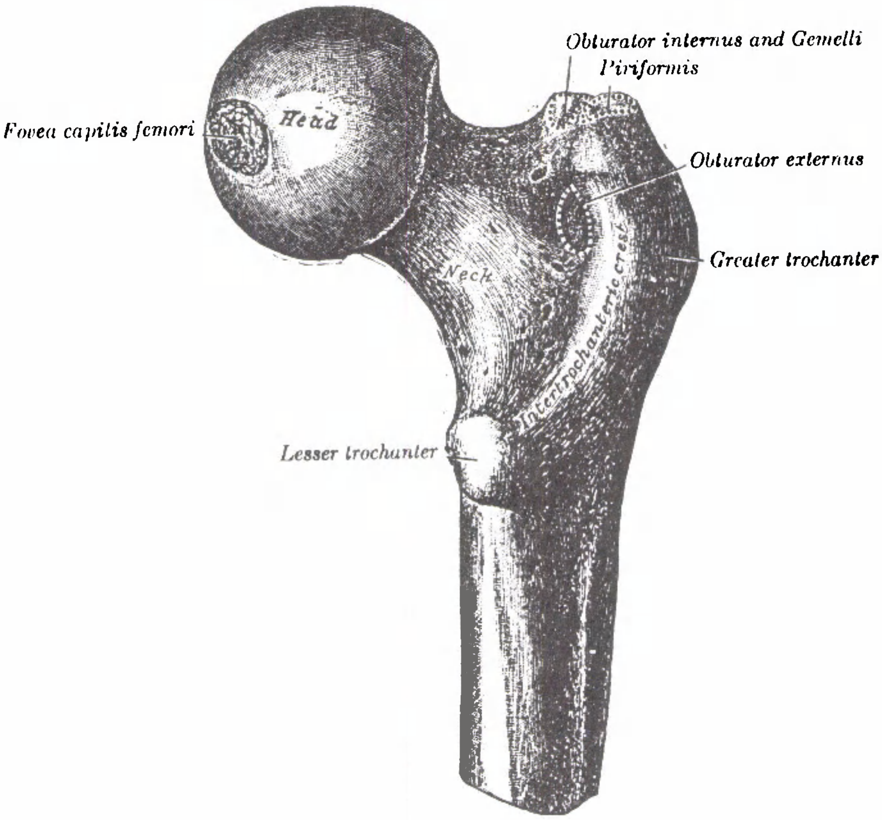

FIGURE 5–2. Rear view of the proximal (upper) femur (*Gray's Anatomy*, American edition).

The trochanteric region is an enlarged portion of the proximal femoral shaft distinguished by two landmarks, the greater and lesser trochanter. The former is a prominence that extends laterally from the base of the neck and is easily palpable in most people. The level of its upper boundary corresponds to the center of the femoral head or the center of the hip joint. The lesser trochanter is a smaller prominence on the inside of the femur. It is visible on X-ray but not palpable.

The proximal femur is covered by a layer of cortical or compact bone and contains spongy or cancellous bone within. The strength and density of the spongy bone varies with age and sex. Impact trauma can cause fractures to the head, neck, or trochanter. As the fracture line moves downward from the head, the fracture type changes from subcapital to transcervical to intertrochanteric and pertrochanteric.

PELVIC INJURIES FROM CLINICAL EXPERIENCE

A survey of pelvic injury patterns as reported in the clinical literature was made in an effort to understand the various types of injuries to this bony structure. Although the more recent clinical literature tends to report injuries to the pelvis due to auto-related accidents, the reports generally cover pelvic injuries from all causes, such as crushing injuries to miners, falls, and excessive muscular activity. Many of the papers describe injuries to the hip joint and the proximal femur along with those of the bony pelvis. The extension into the hip joint has a sound clinical basis, since the treatment of the hip and upper femur involves the pelvis, and the hip and pelvis are frequently injured simultaneously. This discussion will therefore include injuries to the hip joint and the upper femur.

This review is divided into pelvic injury types, hip injury types, and clinical incidence. A comprehensive summary of injuries sustained by the entire anatomical region was found in Watson-Jones (1976), and that classification is presented here.

Pelvic Injuries. Injuries to the pelvis, not involving the hip joint, can be classified under four distinct headings: avulsions of muscle insertions, isolated fractures of the pelvic ring, double or multiple fracture of the pelvic ring, and fractures of the sacrum and coccyx.

Avulsions of Muscle Insertions. Due to excessive muscular activity, a portion of the pelvis can be avulsed or separated from the main bone at the point of muscle insertion. For example, the ASIS can be avulsed by the sartorius muscle, or the hamstrings can avulse the ischial tuberosity. These injuries occur in young adults who are engaged in athletic activities, and they are not the result of impact-type accidents.

Isolated Fractures of the Pelvic Ring. If there is a single fracture around the pelvic ring, significant displacement of the fractured segments does not arise. Unilateral fractures of the superior or inferior pubic rami, or of both rami, are examples of isolated fractures that do not require surgical intervention. Other isolated fractures include single fractures of the ilium with minor separation of the pubic symphysis, separation of the pubic symphysis, and sacroiliac subluxation (slippage). These injuries appear to be the result of minor impacts.

Multiple Fractures or Fracture-Dislocations. With multiple fractures, the pelvic ring becomes unstable. Large displacements of the fragments are possible. The two main types of injury are fractures of the pubic segments only and fractures of the pubic bone associated with fractures of the ilium.

Multiple injuries of the pubis consist of two or more fractures of the rami with dislocation of the pubic symphysis. They occur in pedestrians struck on the side of the pelvis by an automobile. In general, fractures of the rami occur on the non-impacted side. If there are bilateral multiple fractures of the rami, the impacted side cannot be firmly established. Although surgical intervention is not required, the patient can suffer urinary tract injuries, such as rupture of the urethra, a duct which conducts urine out of the body from the bladder (Wiggishoff and Kiefer 1968).

The most common type of combined injuries of the iliac and pubic segments is the dislocation of the pubic symphysis with dislocation of the sacroiliac joint. Other types of injury include the fracture of the ilium accompanied by a dislocation of the pubic symphysis or fracture of both rami on one side with sacroiliac dislocation on the same side. Bladder and urethral injuries are common in these cases. The mechanism of injury is a force applied from the front to the back as opposed to a sideward force in the previous case.

Injuries to the Sacrum and Coccyx. Extensive injuries to the pelvis can result in fractures of the sacrum. These usually occur in regions of stress concentration; that is, across the foramina or holes through which the sacral nerves pass. There may be associated nerve injury. Vertical acceleration can cause compression of the sacrum with a loss in height. Coccygeal injuries are sustained in falls in a sitting position. The injury can be a contusion, fracture, or dislocation of the coccyx. Although it is not a serious injury, it can be extremely painful.

Associated Soft-Tissue Injuries. The most serious soft-tissue injury associated with pelvic fractures is hemorrhage. It comes from large blood vessels in the pelvic wall as well as from the fracture surfaces themselves. The amount of blood loss can be large, and one of the methods to stop the hemorrhage is to ligate the internal iliac arteries. Injuries to the bladder and urethra and to the abdominal viscera are also common. These injuries will be discussed in detail below.

Hip Injuries. These injuries occur in and around the hip joint. They involve one or more of the following structures: acetabulum, femoral head, and proximal femur. In the adolescent, damage to the epiphysis in the proximal femur can occur, and in the aged injuries to the hip are the result of bone loss and decreased resilience. Hip injuries can be grouped under three main headings: avulsions of the proximal femoral epiphysis, traumatic hip dislocations, and fractures of the neck of the femur.

Avulsions of the Epiphysis. These injuries occur in adolescents due to powerful muscular exertions. The greater and lesser trochanter can be avulsed by muscular violence during athletic competition.

Traumatic Hip Dislocations and Fracture-Dislocations. These injuries are described below according to whether the dislocations are accompanied by injuries to the pelvis (acetabulum), femoral head, femoral neck, and femoral shaft.

The easiest way to dislocate a hip is to flex and adduct the hip and to apply a force along the femur rearward. In this position the hip joint is not supported by any bony structure. Automobile occupants who undergo a frontal impact with their legs crossed are liable to sustain this dislocation injury. If the hip is not fully adducted, fracture of the lip of the acetabulum along the back of the hip joint can occur together with a backward dislocation of the hip joint. Central dislocation with fracture of the acetabulum occurs when the hip is struck from the side, such as in a side impact collision. The near-side occupant is struck by the door at the level of the greater trochanter, causing the femoral head to punch through the thin wall of the acetabulum. The mechanism of a central acetabular fracture due to a side impact to the greater trochanter has been reproduced in a series of cadaveric experiments by Pearson and Hargadon (1962), who used 56-lb (25.5-kg) and 150-lb (68.2-kg) pendulums to cause these fractures. Grattan and Hobbs (1969) reported that six out of seven cases of central acetabular fracture were due to side impact, while Eichenholtz and Stark (1964) asserted that the mechanism was a blow to the greater trochanter. This injury can also occur in the standing posture with the hip joint in a neutral position. A heavy blow to the shoulders or back can cause the hip to abduct, forcing the head of the femur into the acetabulum. If the hip is abducted, a rearward impact to the femur can cause an anterior (forward) dislocation. A rear seat passenger in a frontal crash can be forced into the seat back with the thighs abducted and suffer such a dislocation (Beaupre 1973). If the knee is wedged between the front seat back and the wall of the vehicle, separation of the sacroiliac joint can result (Markham 1972).

In rearward dislocations of the hip joint involving fracture of the rim of the acetabulum, the femoral head can also be fractured. There is the prospect of developing a long-term disability in the form of traumatic arthritis. According to Armstrong (1948), the incidence is as high as 60%.

Hip dislocations accompanied by injuries to the femoral neck are rarely seen and occur in the elderly group. Necrosis of the head of the femur due to loss of blood supply (avascular necrosis) tends to result from these injuries. The mechanism of injury is a high tensile bending stress applied to the femoral neck causing it to fracture as the joint is dislocated.

Dislocations with fracture of the femoral shaft are also rare and are easy to miss on X-rays (Schoenecker et al. 1978). The mechanism of injury is unknown, but bending of the shaft is involved because the fractures tend to be transverse.

Fractures of the Neck of the Femur. There are two major classes of femoral neck fractures, intracapsular and extracapsular. The hip joint capsule, or the fibrous tissues enclosing the joint, extends from the pelvis to the intertrochanteric line of the femur. If a fracture occurs within the capsule, it can be a subcapital fracture of the head or a transcervical fracture of the neck. Extracapsular fractures can be either intertrochanteric or pertrochanteric.

Clinical Incidence of Pelvic Injuries. Six large series of clinical studies involving pelvic injuries are summarized. Three of the six were concerned with skeletal injuries, one with massive hemorrhage, and two with abdominal injuries.

Ryan (1971) surveyed 713 patients between 1956 and 1967 with fractures and fracture-dislocations of the pelvis. X-ray films of 387 patients admitted between 1958 and 1963 were studied in detail. A large majority (321) of these 387 patients were traffic accident victims, including 154 pedestrians and a large group of 140 of unknown status. Only twenty were known to be occupants. The most common fracture was that of the pubic ramus (305), followed by the acetabulum (89), and the ilium (79). There were a total of 116 dislocations divided approximately equally among those of the hip, pubic symphysis, and sacroiliac joint.

Conolly and Hedberg (1969) reported on 200 patients with pelvic injuries. They classified them as being major or minor. Injuries that involve the line of weight transmission and bilateral fracture of the pubic rami were considered major. A total of 109 patients sustained major injuries. The four major injuries were acetabular fracture (49), bilateral pubic rami fracture (34), multiple fracture of the hemipelvis (21), and separation of the pubic symphysis (5). Among the minor injuries there were 82 cases of unilateral fracture of rami and an occasional case of isolated fracture of the ilium. In the third study by Kulowski (1962), he reported on 145 cases of hip, femur, and knee injuries sustained by automotive occupants. There were a total of 184 lesions, with 23 patients having multiple injuries. Twelve cases of hip injury were associated with femoral shaft fractures or knee injuries, and there were only three cases of pelvic fractures.

Hauser and Perry (1966) looked at 196 patients with pelvic fractures and analyzed the role played by hemorrhage. About two-thirds of the patients were traffic accident victims. The total mortality rate was 19.4%. However, those with significant blood loss suffered a mortality rate of 30% (19 out of 63 patients). There was more blood loss in the more severely injured patients who required more transfusions. There was a high mortality rate among patients who received transfusions. It was suggested that ligation of the hypogastric arteries saved three of four patients so treated.

As far as associated abdominal injuries are concerned, there were two surveys. Levine and Crampton (1963) reported on a series of 425 patients with pelvic girdle fractures. Only 35 patients had severe or major abdominal injuries (8.2%). This is much lower than the 22% to 29% rate reported previously. Thirty-three of the 35 patients had traffic-related injuries. A total of fifteen types of complicating injuries were listed. They can be grouped under the following categories:

- Injuries to the bladder, urethra, and vagina with or without vascular injuries
- Injuries to the hard abdominal organs (liver, spleen, and kidney)
- Injuries to the small intestine, mesentery, and diaphragm
- Hemothorax
- Retroperitoneal hemorrhage
- Nerve injuries (frequently to the sciatic nerve)

This survey shows a low percentage of urinary tract injuries (3.5%) compared to 9% to 21% in other surveys. This may be due to the heavy concentration of cases related to automotive trauma. In the other survey of 1309 cases by Moore (1966), there were only twenty-six cases of intra-abdominal injuries not involving the urogenital organs. The paper was concerned with perforation of the large and small intestines and laceration of the mesentery. There were 11 patients with perforation of the intestines and no other injuries. Ten of the twenty-six patients had multiple intra-abdominal injuries, including perforations and lacerations. No mechanisms of injury were proposed.

PELVIC IMPACT RESPONSE AND TOLERANCE TO INJURY

Research on pelvic response to static and dynamic loads and associated injury thresholds can be categorized in terms of direction of loading: vertical, frontal, and lateral. Early work on pelvic response to vertical loading constituted a significant contribution to the literature, but, when viewed from current perspectives, it appears to be largely qualitative due to the lack of instrumentation at that time. Pelvic response to frontal loads applied via the femur was studied by several investigators. Although the data are rather sparse, it is possible to determine a response relationship between knee load and pelvic acceleration. In side impact, there are recent data that can be used to establish injury tolerance of the pelvis as a function of age and body weight.

Vertical Loading. Data on pelvic response to vertical loads were provided by Evans and Lissner (1955) and Fasola et al. (1955), who performed vertical loading tests on human pelves. In the former study, stresscoat lacquer was used to determine the areas of high tensile strain during the application of static and dynamic loads to the pelvis. Input energies from 33 to 113 in•lb (3.7 to 12.8 N•m) were applied to the ischial tuberosities of 22 isolated pelves, sixteen of which were embalmed. Tensile strain patterns were found on both surfaces of the iliac wing, around the acetabulum, and on the pubic rami. In a second series of tests, the entire body was dropped vertically onto the ischial tuberosities resulting in input energy levels of 200 to 450 in•lb (22.6 to 50.9 N•m). Fracture of the ischiopubic ramus occurred in a 79-year-old male pelvic at 240 in•lb (27.1 N•m). The strain pattern was similar to that observed in the first series.

The study by Fasola et al. (1955) involved the dropping of a weight onto the lumbar spine of cadaveric specimens. The lower portion of the pelvis, including the proximal femur, was imbedded in cement to hold the pelvis upright. A force of 830 lb (3.7 kN) was necessary to cause a bilateral dislocation of the sacroiliac joint. The disjunction was due to avulsion of the bone at sites of ligamentous attachment near the joint. Static loading resulted in a fracture dislocation of the joint at a load of 775 lb (3.5 kN).

Frontal Loading. Evans and Lissner (1955) also carried out stresscoat studies on the pelvis, which was loaded frontally at the pubic symphysis, and identified regions of tensile strain. Fasola et al. (1955) produced bilateral fracture of the superior and inferior pubic rami with a load of 595 lb (2.7 kN).

Sled tests to elicit the response of the knee-thigh-pelvis complex to frontally applied impact loads were carried out by Patrick et al. (1966) using embalmed cadavers. Most of the study was concerned with the tolerance of the knee and femur, but there were data on the fracture loads of the proximal femur and the pelvis. The hip sustained fractures at loads ranging from 950 to 3850 lb (4.2 to 17.1 kN) among the ten cadavers tested. The load range for pelvic fractures was 1400 to 2650 lb (6.2 to 11.8 kN). The authors considered these load limits to be conservative because of the age of the cadavers. However, the wide range over a limited number of tests renders statistical analysis difficult. A normalization procedure for cadaver data needs to be formalized before these data can be used.

In a more recent study, Melvin and Nusholtz (1980) performed six sled tests on unembalmed cadavers during which knee loads and pelvic accelerations were measured. Two knee load cells were used, but they were tied together by a rigid plate to minimize errors due to excessive bending. Impact load peaks varying from 8.9 to 25.6 kN (2000 to 5760 lb) resulted in hip and/or pelvic fractures. There were also femoral shaft fractures and injuries to the patella and condyles. There was only one case in which the hip or pelvis was not involved, and, in a lightweight individual, the loads generated were insufficient to cause any fracture (6.2 to 8.1 kN, 1400 to 1820 lb). Pelvic accelerations were indicative of load transfer to the pelvis, and abrupt changes in the acceleration signal were representative of pelvic fractures occurring. Acceleration traces were provided in the report by Melvin and Nusholtz (1980), but their peaks were not listed or correlated with injury. It is also interesting to note that the knee force curves showed a double peak if there was fracture of the femoral neck followed by that of the shaft. There was only a single peak if the shaft fractured first.

In another study by Nusholtz et al. (1982), 37 knee impacts were carried out on 16 cadavers, using a pendulum impactor. The test subject was suspended in a restraint harness and impacted frontally at the knee or laterally at the level of the greater trochanter. Only the frontal impacts are discussed here. The impactor surface was either rigid or padded by three different types of foam: 25 mm (0.5 in) of Styrofoam® or 25 to 100 mm (0.5 to 4 in) of Ensolite®. Impactor velocity varied from 3.4 to 21.3 m/s (11.2 to 69.9 ft/s). Pelvic and trochanteric acceleration were monitored along with impactor force. No pelvic or hip fractures occurred at force levels as high as 37 kN (8300 lb). Response data in the form of pelvic linear and angular acceleration were provided. However, acceleration data were difficult to analyze. For example, the magnitudes of the three components of angular acceleration of the pelvis were inconsistent in that the component about the spinal axis (z-axis) was not always predominant. Initial rotation of the pelvis appeared to be about the contralateral trochanter, but subsequent motion of the pelvis and femur were rather complex. Peak pelvic accelerations were less than those of the greater trochanter and were found to lag the trochanteric acceleration. Mechanical impedance was used as an analytical tool, and resonance was estimated to occur between 180 and 280 Hz. Impedance corridors were plotted for both the pelvis and the trochanter. However, because of the large scatter in the data, it was difficult to obtain average values of mass and spring rate for the pelvis.

Brun-Cassan et al. (1982) conducted ten whole-body impacts on unrestrained and unembalmed cadavers at collision speeds of 49.5 to 67.1 km/h (30.7 to 41.7 mph). Peak knee loads ranged from 3.7 to 11.4 kN (830 to 2560 lb). There was only one fracture injury noted, that of the right patella and iliac crest at a knee load of 8.8 kN (1980 lb). Finally, Doorly (1978) impacted isolated pelves with a dropping weight causing acetabular and hip injuries. The impact force was not measured but was computed from energy considerations. The computed average force could not be correlated to the observed injuries.

Lateral Loading. Cadaveric research on lateral impact response of the pelvis was performed at Organisme National de Securite Routiere (ONSER), Association Peugeot-Renault (APR), University of Michigan Transportation Research Institute (UMTRI), and the University of Heidelberg. Results from each laboratory will be discussed separately without regard to chronology. Repeated impacts were carried out on ONSER test subjects, while the APR studies were single drop tests on a variety of surfaces. The UMTRI lateral tests were single impacts. At the University of Heidelberg, whole-body sled tests were conducted in the side-impact mode.

ONSER. Pendulum impacts on cadaveric subjects were reported by Ramet and Cesari (1979), Cesari et al. (1980), and Cesari and Ramet (1982). The latest report was given by Cesari et al (1983), which contains all of the results reported since 1979. A total of 22 cadavers were used in this effort by ONSER. There were a total of 60 tests, using a 17.3-kg (38-lb) pendulum impactor with a 175-mm (6.9-in) diameter impact face having a spherical radius of curvature of 600 mm (23.6 in). In 55 of these tests, a rigid impactor was used. The remaining tests were padded impacts. All impacts were aimed at the greater trochanter. Impact force and pelvic acceleration were measured. Peak force data as well as force and acceleration data, except for cumulative durations less than 3 ms (the so-called 3-ms clip), were provided.

Most of the injuries were multiple fractures of the pubic rami. In order of frequency of occurrence, these were followed by fractures of the proximal femur, dislocation of the sacroiliac joint, fractures of the iliac wing, and fractures of the acetabulum. The authors stated that this pattern of injury compared favorably with data from fourteen accidents, the source of which was not given. In general, the experimental injuries were less severe because the tests were suspended when an injury occurred. It was noted that seated subjects tend to sustain fractures of the rami while standing subjects (pedestrians) are more prone to acetabular fractures. No reason was given for the observed difference in injury pattern.

In terms of quantitative data, the results were separated into two groups by sex. For males, the force for fracture with the 3-ms clip, ranged from 4.9 to 12.9 kN (1100 to 2900 lb). The corresponding range for females was 4.4 to 8.2 kN (1000 to 1840 lb). The average force for an AIS-2 or 3 pelvic injury was 8.6 kN (1930 lb) for males and 5.6 kN (1260 lb) for females. The age range for males was 54 to 85 years, and that for females was 54 to 84. An index was introduced to correct for the body weight and height of the test subjects. It was termed the Livi Index, which is the ratio of the cube root of the body weight in kg and 10 times the standing height in meters. The Livi Index is used to obtain a corrected body weight. The Livi Index for a 50th percentile male is 23.5. Thus, the correction factor is the ratio of 23.5 to the computed Livi Index of the test subject. The corrected weight of the subject is the product of the correction factor and its actual weight. By plotting the fracture-producing force at 3 ms against actual body weight, the correlation coefficient was found to be 0.75. It increased to 0.89 if the corrected weight was used. The least squares line for impact force as a function of corrected body weight is given by

$$\text{Impact Force} = 193.85\ Wc\ - 4710.6$$

where Wc is the corrected body weight. For a 50th percentile male weighing 75 kg (165 lb), the impact force for fracture is 9.8 kN (2210 lb), which is higher than that of the average of the male cadaver data. The measured acceleration values with the 3-ms clip were less than 100 G. The authors defended their multiple impact procedure vigorously, stating that the force-time histories were consistent in pattern for multiple impacts and that the impact force increased consistently with increasing impactor speed.

The effect of using a padded impactor was studied in five tests on three cadavers. Two of them sustained AIS-3 injuries while one had AIS-2 injuries. The force required to cause fracture was about the same as that for a rigid impactor, but the speed of the impactor could be increased by 40%.

Following dynamic testing, the non-impacted hemipelvis was instrumented with nine strain gages and subjected to a static lateral load. High strains were measured in the pubic rami followed by strains in the ischiopubic rami. Strains were low in the acetabulum and ilium. Section moduli of the iliopubic rami were measured and plotted against the impact force at fracture. The resulting least squares line had a correlation coefficient of 0.96.

The proposed tolerance force with the 3-ms clip is 10 kN (2250 lb) for a 75-kg (165-lb) person. This reduces to 4.6 kN (1030 lb) for a 5th percentile female. The authors recommended that side impact dummies should be fitted with a lateral force transducer. This transducer should be located in the anterior region of the pelvis, such as near the pubic rami where many injuries occur.

In a later paper presenting the development of an improved ATD pelvis for lateral impact, Cesari et al. (1984) discussed the use of the ATD pelvic acceleration with the 3-ms clip as an injury criterion. They concluded that injury does not correlate with impactor maximum force as well as it does with maximum pelvic acceleration ($r=0.891$ versus $r=0.986$). However, their pelvis design was also shown to produce higher accelerations than those obtained with cadavers. A linear regression analysis of cadaver maximum pelvic lateral acceleration versus impactor force produced a correlation coefficient of 0.77.

APR. The bulk of the APR data are contained in reports by Fayon et al. (1977) and Tarrière et al. (1979). The latter contains all of the side impact data acquired at APR via a series of 26 cadaveric drop tests. The subjects ranged in age from 25 to 71 years and in weight from 41 to 75 kg (90 to 165 lb). Each subject was dropped only once, but there was a variety of test configurations and impact surfaces for the thorax as well as the pelvis. The subject was suspended with cables and dropped on its side onto a load-measuring plate. The arm was either at a 45° angle or was pulled out of the way during thoracic impact. The impact surfaces were rigid planes or padded surfaces. Some supported the shoulder at impact while others did not. When energy absorbing pads were used, the thorax and pelvis impacted separate blocks. The thoracic impact load was measured by a load cell. Pelvic response was given in terms of pelvic acceleration, measured at the sacrum in the midsagittal plane, 90 mm (3.5 in) distal to the iliac crests. The condition of the bone was characterized by its ash content given as a percentage of wet weight (C/M) and ash content in 10 mm (0.4 in) of rib given in g/cm (C/L). Undamaged ribs were also subjected to standard bending and shear tests.

The drop height ranged from 0.5 to 3 m (20 to 118 in). Fractures of the pubic rami were observed in four subjects. There were multiple injuries in one subject who sustained fractures of the iliac wing and acetabulum in addition to the fractures of the rami. In the other 22 subjects, there were no pelvic or hip injuries. If data from a 68-year-old female subject are ignored, the lowest fracture level is 50 G with the 3-ms clip and the highest is 90 G with the 3-ms clip. The proposed tolerance level is 80 to 90 G with the 3-ms clip. Note that this is pelvic acceleration and not that of the impactor.

UMTRI. Published UMTRI data consist of twelve tests reported by Nusholtz et al. (1982) using a flat pendulum impactor. Most of the impacts were aimed at the greater trochanter of a cadaver suspended in a restraint harness. Impact force and pelvic acceleration were measured. The peak force ranged from 3.2 to 14 kN (720 to 3150 lb), and the peak linear acceleration varied from 38 to 135 G. Six of the twelve cadavers sustained pelvic fractures. Four of them had fractures of the pubic rami, and one sustained fractures to the ilium. These injuries did not occur at high force or acceleration levels. The lack of correspondence between observed injuries and measured data was attributed to variation among subjects. It was also concluded that these data were not comparable to those of ONSER, since the test set-up and impactor configuration were all different.

University of Heidelberg. Marcus et al. (1983) presented data from eleven cadaver tests carried out at the University of Heidelberg. They were whole-body side impact tests in which the thoracic and pelvic impact surfaces were instrumented with load cells to measure contact force. Eight of the eleven tests were rigid wall impacts at 15, 20, and 25 mph (24, 32, and 4 km/h). The other three were padded impacts at 20 mph, using foam developed by APR. Subjects ranged in age from 17 to 61 years and in weight from 50 to 99 kg (110 to 218 lb). The body weight was corrected in the same manner as that proposed by Cesari and Ramet (1982), using the Livi Index. The pelvic impact force was then plotted against corrected body weight. Among the nine data points, there was one with pelvic fracture and three with pelvic injuries with AIS ratings of 2 or 3. The range of pelvic forces at 3 ms was 800 to 6500 lb (3.6 to 28.9 kN). It was concluded from this study that the tolerance limits proposed by Cesari and Ramet (1982) may be too conservative. It was also determined that 28% of the inertial force of impact was transmitted via the pelvis.

Pelvic Response to Frontal and Lateral Impacts. If pelvic response is defined as an acceleration output at the pelvis for a force input to either the knee, for frontal response, or the greater trochanter, for lateral response, the only published data that can provide this information are found in Nusholtz et al. (1982). For frontal response, the peak force and acceleration data in Table 7 of Nusholtz et al. (1982) were analyzed by linear regression techniques. (Run 80L098 was considered to be an "outlier," and the data from this run were not used in the regression analysis.) For all 15 data points, including both rigid and padded knee impacts, the correlation coefficient is 0.78. If only rigid impacts are used, the result is a correlation coefficient of 0.80, a value similar to that obtained by Cesari et al. (1984) for lateral impacts. There is thus not a strong relationship between pelvic acceleration and knee loads.

A similar analysis was performed for all available lateral impact data provided by Nusholtz et al. (1982). A meaningful linear regression line could not be drawn for the lateral impact data. Its slope was almost zero, and the correlation coefficient was less than 0.1. The low correlation of maximum pelvic acceleration and peak input load may reflect the highly variable response of the system to the point of load application and pelvis/leg orientation at the time of impact.

SUMMARY AND CONCLUSIONS

As a major load-bearing structure between the upper torso and the lower extremities, the pelvis plays an important role in controlling body kinematics. Injuries to the pelvis contribute only about 1% to the total IPR. Lateral response of the pelvis has been studied for both impactor and flat-wall impacts and has been described in terms of force-time histories and pelvic acceleration-time histories. Lateral loading tolerances for the pelvis are available in terms of force limits and peak acceleration limits.

REFERENCES

Armstrong, J.R. (1948) Traumatic dislocation of the hip joint. *Journal of Bone and Joint Surgery*, 30B:430–445.

Beaupre, A. (1973) Trochanteric fractures. *Proc. 10th Traffic Injury Research Foundation of Canada Annual Meeting*, pp. 15–18. TIRF, Ottawa.

Brun-Cassan, F.; Leung, Y.C.; Tarrière, C.; Fayon, A.; Patel, A.; Got, C.; and Hureau, J. (1982) Determination of knee-femur-pelvis tolerance from the simulation of car frontal impacts. *Proc. 7th International Conference on the Biomechanics of Impacts*, pp. 101–115. IRCOBI, Bron, France.

Cesari, D.; and Ramet, M. (1982) Pelvic tolerance and protection criteria in side impact. *Proc. 26th Stapp Car Crash Conference*, pp. 145–154. Society of Automotive Engineers, Warrendale, Pa.

Cesari, D.; Ramet, M.; and Clair, P.Y. (1980) Evaluation of pelvic fracture tolerance in side impact. *Proc. 24th Stapp Car Crash Conference*, pp. 229–253. Society of Automotive Engineers, Warrendale, Pa.

Cesari, D.; Ramet, M.; and Bouquet, R. (1983) Tolerance of human pelvis to fracture and proposed pelvic protection criterion to be measured on side impact dummies. *Proc 9th International Technical Conference on Experimental Safety Vehicles*, pp. 261–269. U.S. Department of Transportation, National Highway Traffic Safety Administration, Washington, D.C.

Cesari, D.; Bouquet, R.; and Zac, R. (1984) A new pelvis design for the European side impact dummy. *Proc. 28th Stapp Car Crash Conference*, pp. 1–11. Society of Automotive Engineers, Warrendale, Pa.

Conolly, W. B.; and Hedberg, E. A. (1969) Observations on fractures of the pelvis. *Journal of Trauma*, 9:104–111.

Doorly, T.P.G. (1978) Forces imposed on the hip-joint in car collisions. *Journal of Traffic Medicine*, 6:44–46.

Eichenholtz, S. N.; and Stark, R. M. (1964) Central acetabular fractures a review of thirty-five cases. *Journal of Bone and Joint Surgery*, 46:695–714.

Evans, F.G.; and Lissner, H.R. (1955) Studies on pelvic deformations and fractures. *Anatomical Record*. 121: 141-165.

Fasola, A.F.; Baker, R.C.; and Hitchcock, F.A. (1955) *Anatomical and physiological effects of rapid decelerations*. WADC-TR 54-218. Wright-Patterson AFB, Ohio.

Fayon, A.; Tarrière, C.; Walfisch, G.; Got, C.; and Patel, A. (1977) Contributions to defining the human tolerance to perpendicular side impact. *Proc. 3rd International Conference on Impact Trauma*, pp. 297–309. IRCOBI, Bron, France.

Grattan, E.; and Hobbs, J. A. (1969) Injuries to hip joint in car occupants. *British Medical Journal*, 11:71–73.

Gray, H. (1973) *Anatomy of the Human Body*. Lea and Febiger, Philadelphia.

Haffner, M. (1983) Personal communication.

Hauser, C. W.; and Perry, J. F., Jr. (1966) Massive hemorrhage from pelvic fractures. *Minnesota Medicine*, 49:285–290.

Kulowski, J. (1962) Interconnected motorist injuries of the hip, femoral shaft and knee. *Proc. 5th Stapp Automotive Crash and Field Demonstration Conference*, pp. 105–124. University of Minnesota, Minneapolis.

Levine, J. I.; and Crampton, R. S. (1963) Major abdominal injuries associated with pelvic fractures. *Surgery, Gynecology and Obstetrics*, 11:223–226.

Marcus, J.H.; Morgan, R.M.; Eppinger, R.H.; Kallieris, D.; Mattern, R.; and Schmidt, G. (1983) Human response to and injury from lateral impact. *Proc. 27th Stapp Car Crash Conference*, pp. 419–432. Society of Automotive Engineers, Warrendale, Pa.

Markham, D. E. (1972) Anterior-dislocation of the hip and diastasis of the contralateral sacroiliac joint: the rear-seat passenger's injury? *British Journal of Surgery*, 59:296–298.

Melvin, J.; and Nusholtz, G. (1980) *Tolerance and response of the knee-femur-pelvis complex to axial impacts*. UM-HSRI-80-27. The University of Michigan, Highway Safety Research Institute, Ann Arbor.

Moore, J. R. (1966) Pelvic fractures: Associated intestinal and mesenteric lesions. *Journal of Surgery*, 9: 253-261.

Nusholtz, G.; Alem, N.M.; and Melvin, J.W. (1982) Impact response and injury to the pelvis. *Proc. 26th Stapp Car Crash Conference*, pp. 103–144. Society of Automotive Engineers, Warrendale, Pa.

Nyquist, G. W.; and Murton, C. J. (1975) Static Bending Response of the Human Lower Torso. *Proc. 19th Stapp Car Crash Conference*, pp. 513-542. Society of Automotive Engineers, Warrendale, Pa.

Patrick, L.M.; Kroell, C.K.; and Mertz, H.J., Jr. (1966) Forces on the human body in simulated crashes. *Proc. 9th Stapp Car Crash Conference*, pp. 237–259. University of Minnesota, Minneapolis.

Pearson, J. R.; and Hargadon, E. J. (1962) Fractures of the pelvis involving the floor of the acetabulum. *Journal of Bone and Joint Surgery*, 44B:550–561.

Ramet, M.; and Cesari, D. (1979) Experimental study of pelvis tolerance in lateral impact. *Proc. 4th International Conference on the Biomechanics of Trauma*, pp. 243–249. IRCOBI, Bron, France.

Ryan, P. (1971) Traffic injuries of the pelvis at St. Vincent's Hospital, Melbourne. *Medical Journal of Australia*, 1:475–479.

Schoenecker, P. L.; Manske, P. R.; and Sertl, G. O. (1978) Traumatic hip dislocation with ipsilateral femoral shaft fractures. *Clinical Orthopaedics and Related Research*, 130:233–238.

Tarriére, C.; Walfisch, G.; Fayon, A.; Rosey, J.P.; Got, C.; Patel, A.; and Delmas, A. (1979) Synthesis of human tolerance obtained from lateral impact simulations. *Proc. 7th International Technical Conference on Experimental Safety Vehicles*, pp. 359-373. U.S. Department of Transportation, National Highway Traffic Safety Administration, Washington, D.C.

Watson–Jones, R. (1976) *Fractures and joint injuries*. Churchill Livingston, London.

Wiggishoff, C.C.; and Kiefer, J.H. (1968) Urethral injury associated with pelvic fracture. *Journal of Trauma*, 8:1042–1048.

CHAPTER 6

LOWER EXTREMITIES

G.W. Nyquist and A.I. King
Wayne State University
Detroit, Michigan

The lower extremities provide the primary means of locomotion for the human body. Injuries to this region are rarely fatal, but they often require significant periods of hospitalization and lost working days. In addition, severe injuries can result in degenerative arthritis, particularly if a joint is involved. Even so, injuries to the lower extremities constitute only a little more than 5% of the total IPR.

ANATOMY OF THE LOWER EXTREMITIES

The lower extremities, or the lower limbs, constitute approximately one-third of the body weight and are required to withstand large dynamic loads, even during normal locomotion. For example, the joint load at the hip or knee during normal gait is estimated to be about three to four times body weight.

Each limb consists of three segments: the thigh, shank (lower leg), and foot. The bone of the thigh is the femur, and the principal bone in the shank is the tibia. The foot is made up of a collection of irregularly shaped bones as well as long bones that constitute the toes. There are at least 29 muscles in each lower extremity. The majority are one-joint muscles, i.e., they span only one joint. However, there are several two-joint muscles and a few with more than one origin or insertion point. Each of the three major joints (hip, knee, ankle) is unique and quite different from each other. The only common denominator is that they are all weight-bearing synovial joints surrounded by a ligamentous joint capsule.

Thigh. The thigh is shaped like an inverted truncated cone. The muscles of the thigh are surrounded by a circumferential layer of fat and skin. Figures 6-1 and 6-2 show cross sections of the thigh at the upper end and mid-shaft. The femur is the only bone of this body segment. It runs along its long axis, almost through the center of the segment. In terms of impact injury and response, the femur is of primary interest because it is the major load-bearing member. It is the strongest and longest bone of the skeleton and is roughly cylindrical along its shaft. However, the shape of the two ends is different from that of the shaft. The proximal or upper end of the femur is described in the chapter on the pelvis. The distal or lower end is much larger than the shaft as it expands into two condyles to form the proximal portion of the knee joint. The condyles are separated by an intercondylar fossa as shown in Figure 6-3. The anterior portion of bone between the condyles is depressed to accommodate the patella, which is a large sesamoid bone, acting as a "pulley" to allow the quadriceps tendon to slide over the knee joint and attach itself on the tibia. An overall view of the anterior and posterior femur are shown in Figure 6-4.

In terms of its architecture, the femur has a layer of compact bone throughout its outer surface. This layer is relatively thin at the two ends and quite thick mid-shaft. The thin cortex is reinforced, however, by a dense core of spongy bone at each end. The

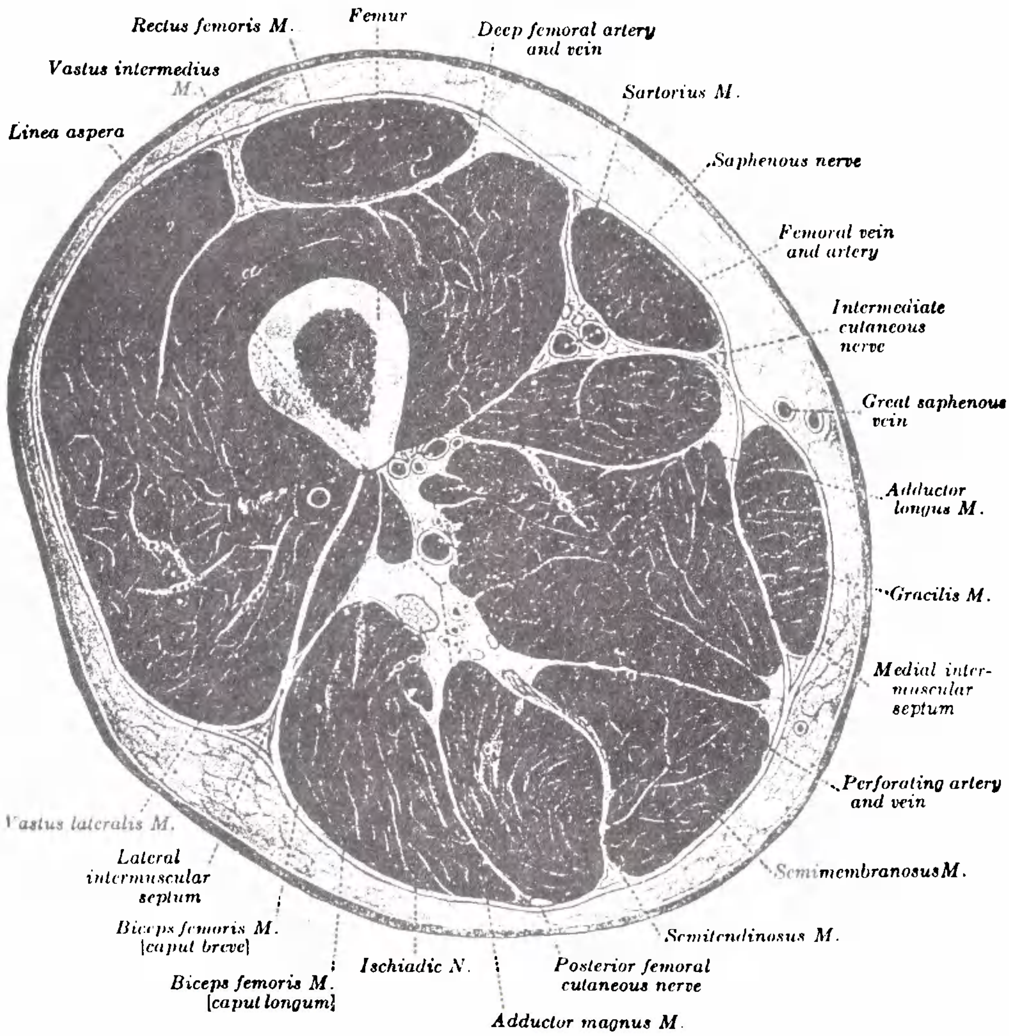

FIGURE 6-1. Cross section through the proximal end of the thigh (*Gray's Anatomy*, American edition).

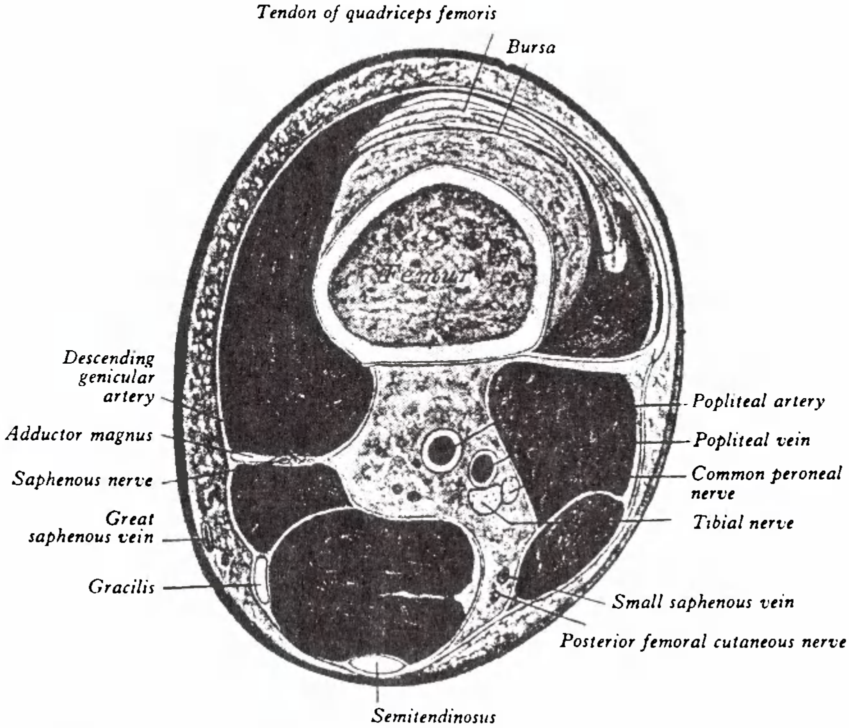

FIGURE 6-2. Cross section through the middle of the thigh (*Gray's Anatomy*, British edition).

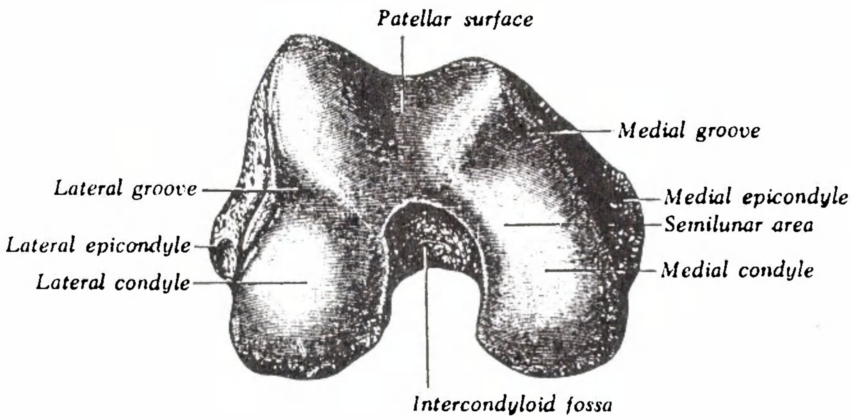

FIGURE 6-3. End view of the distal end of the femur (*Gray's Anatomy*, American edition).

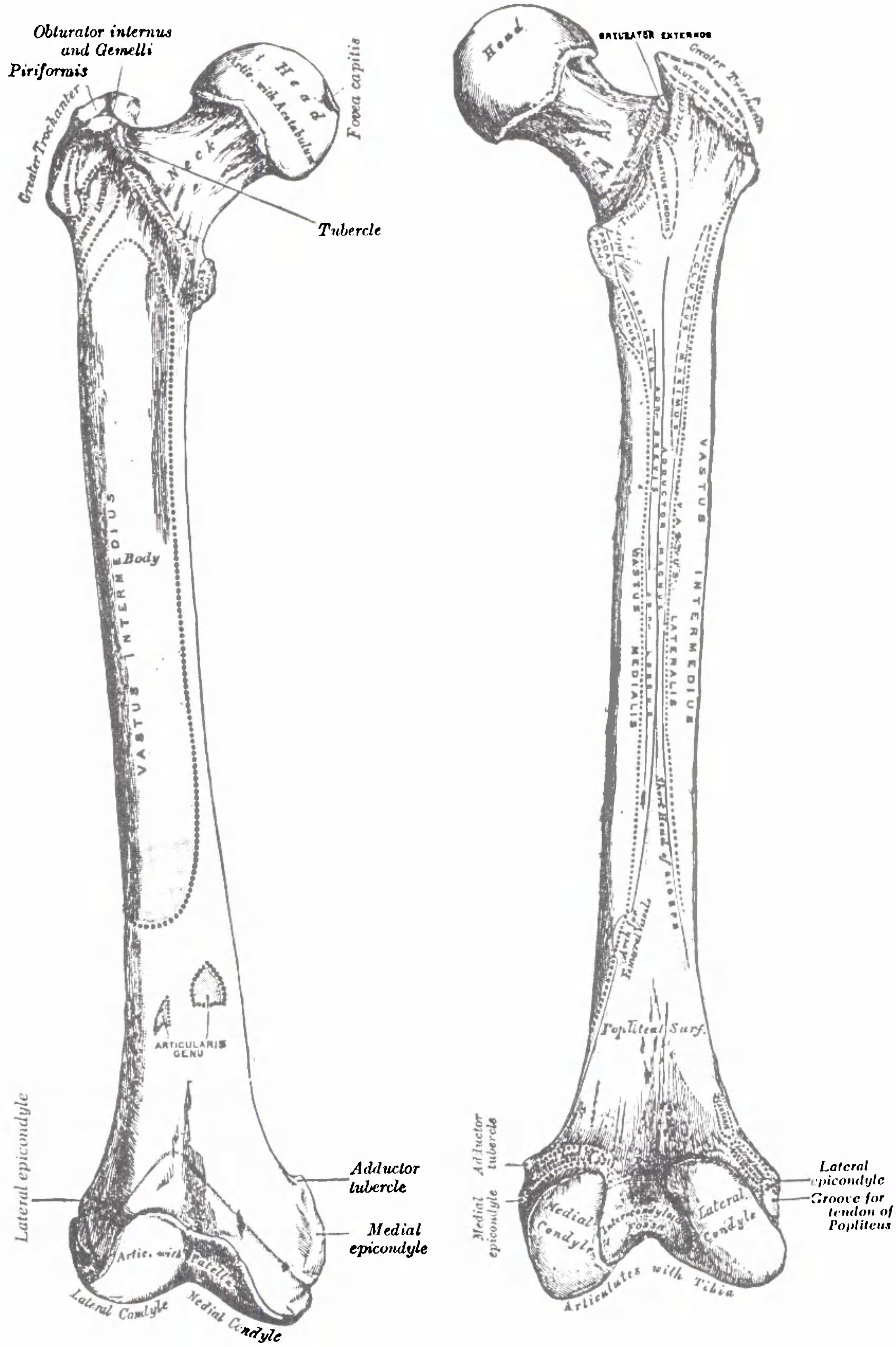

FIGURE 6–4. Anterior and posterior views of the femur (*Gray's Anatomy*, American edition).

trabecular pattern appears to be oriented along directions of principal stresses, particularly in the proximal femur, but, this theory of adaptation has not been shown to be true.

Shank. The shank is roughly cylindrical in shape, with its lower end smaller in diameter than that of the upper end. The layer of circumferential fat is generally thinner in the shank than in the thigh. The principal bone of the shank is the tibia. It runs longitudinally along the shank's long axis but is situated in the anteromedial (inner front) quadrant. Figures 6–5 and 6–6 show cross-sectional views of the shank near the two ends. The fibula is a smaller bone that is found along the outer side of the tibia. The two bones are in contact with each other at both ends and are joined along the shaft by the interosseous membrane. Anterior and posterior views of the tibia–fibula complex are shown in Figure 6–7.

The tibia is the second longest bone of the skeleton. The shaft is roughly trapezoidal in shape while the two ends are expanded to form the knee and ankle joints. At the upper end, the tibia expands into two condyles to mate with those of the femur. They are known as the medial and lateral plateaus, since their surfaces are relatively flat in comparison with the femoral condyle, as shown in Figure 6–7. They form the lower half of the knee joint. This joint is held together by a large variety of ligaments. For the purposes of this discussion it is sufficient to list the major groups responsible for joint integrity. The collateral ligaments are located along the sides of the joint and provide lateral stability. They tend to prevent rotation of the joint about an anteroposterior axis and also restrict relative lateral motion of the femur and tibia. The cruciate ligaments control relative motion in the anteroposterior direction, the anterior cruciate preventing anterior motion and the posterior cruciate preventing posterior motion of the tibia with respect to the femur. Figure 6–8 is a dissected view of the right knee showing the major ligaments. There are two menisci separating the tibia and the femur. They are crescent-shaped fibrocartilaginous semi-circles that form a peripheral band of support between the femoral condyles and the tibial plateaus. As shown in Figure 6–9, the top surfaces of the menisci are concave to conform to the surfaces of the condyles. Their bottom surface is flat as they are in contact with the tibial plateaus. It is estimated that the menisci carry about half the knee load, and, if the load is low, they may carry the entire load.

The shaft of the tibia is trapezoidal in cross section, but its anatomic topography consists of three surfaces and three borders. These features are shown in Figure 6–7. It can also be seen from this figure that the lower end of the tibia is enlarged, but not to the same extent as the upper end. On the inner side, the bone ends in a strong and prominent projection, called the medial malleolus. The bottom surface of the malleolus articulates with the talus to form the ankle joint. Behind the medial malleolus is a rough depression that serves as an attachment point for ligaments joining the tibia to the fibula.

The fibula is on the outer side of and is smaller than the tibia. Its cross section is slender and approximately triangular in shape. The head is located below the knee joint and is in contact with the tibia. The shaft has three surfaces and three borders as shown in Figure 6–7. The lower end is slightly enlarged and is termed the lateral malleolus. It articulates with the talus. Above this articulation, there is a tibiofibular articulation.

Foot. The skeletal part of the foot consists of three parts, the tarsus, metatarsus, and the phalanges. There are seven tarsal bones of which the largest is the calcaneus followed by the talus. Figure 6–10 is a top view of the bones of the right foot. The superior surface of the talus is convex and articulates with the tibia and fibula to form the ankle joint. Its inferior and posterior surfaces articulate with the calcaneus, which is the heel bone. The other five tarsal bones are relatively small and are interposed between the talus and calcaneus and the five metatarsal bones. As shown in Figure 6–10, the

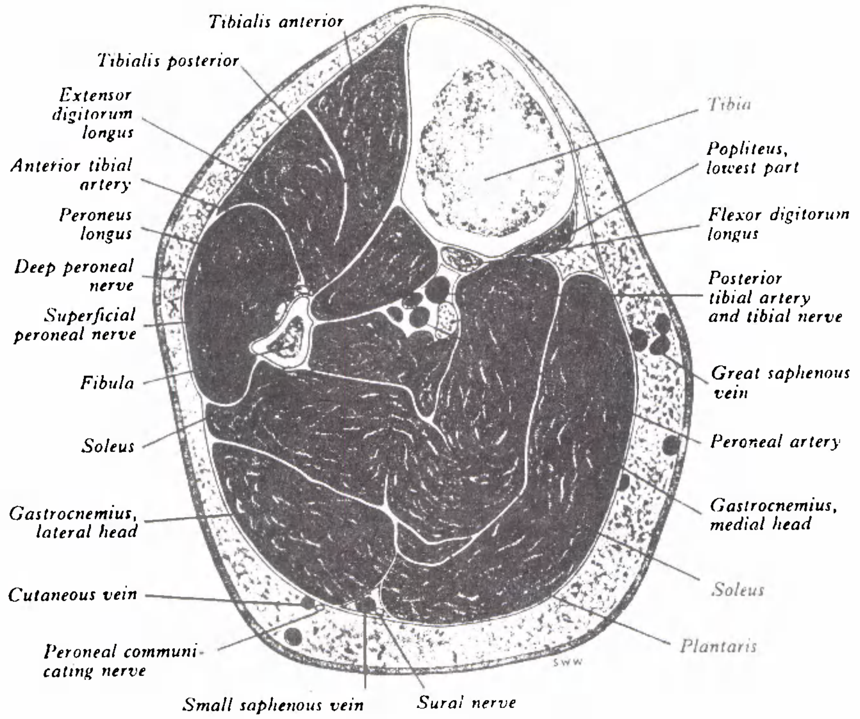

FIGURE 6–5. Cross section through the proximal end of the shank (*Gray's Anatomy*, British edition).

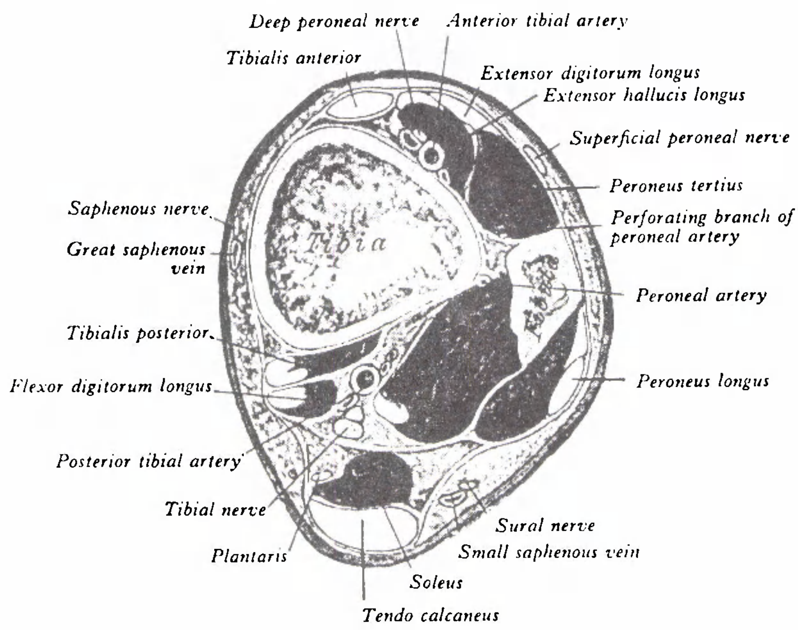

FIGURE 6–6. Cross section through the distal end of the shank (*Gray's Anatomy*, British edition).

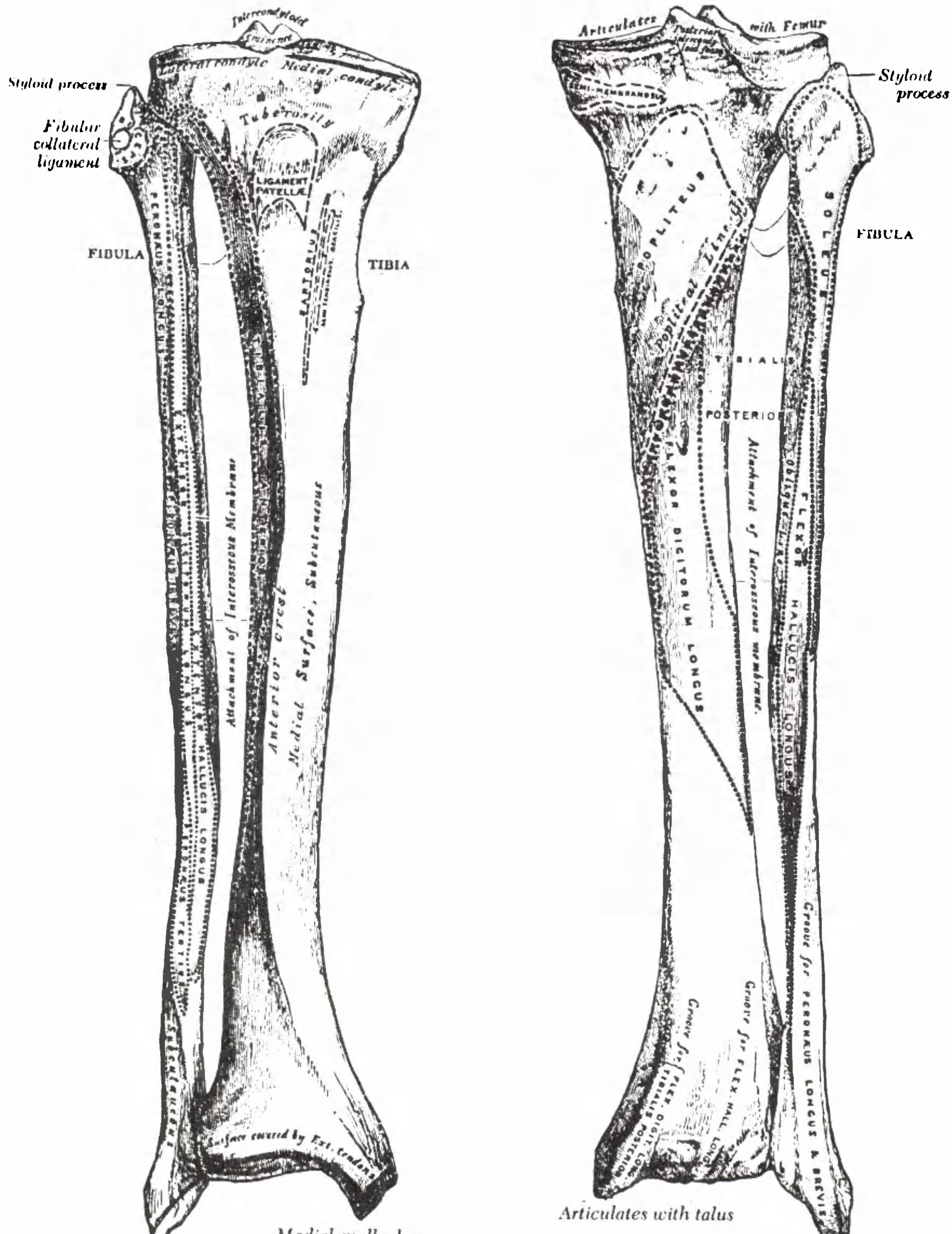

FIGURE 6–7. Anterior and posterior views of the tibia and fibula (*Gray's Anatomy*, American edition).

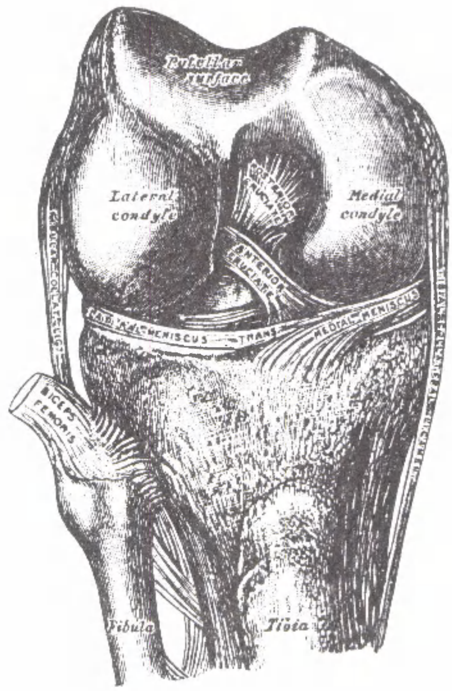

FIGURE 6-8. The right knee joint, flexed and dissected (*Gray's Anatomy*, American edition).

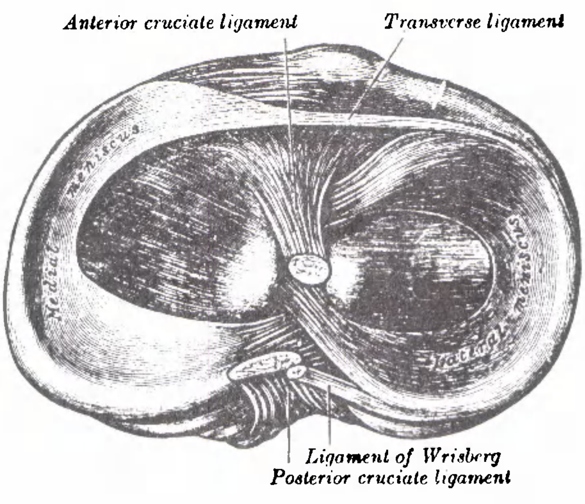

FIGURE 6-9. Top view of the right tibia, showing the menisci and ligamentous attachments (*Gray's Anatomy*, American edition).

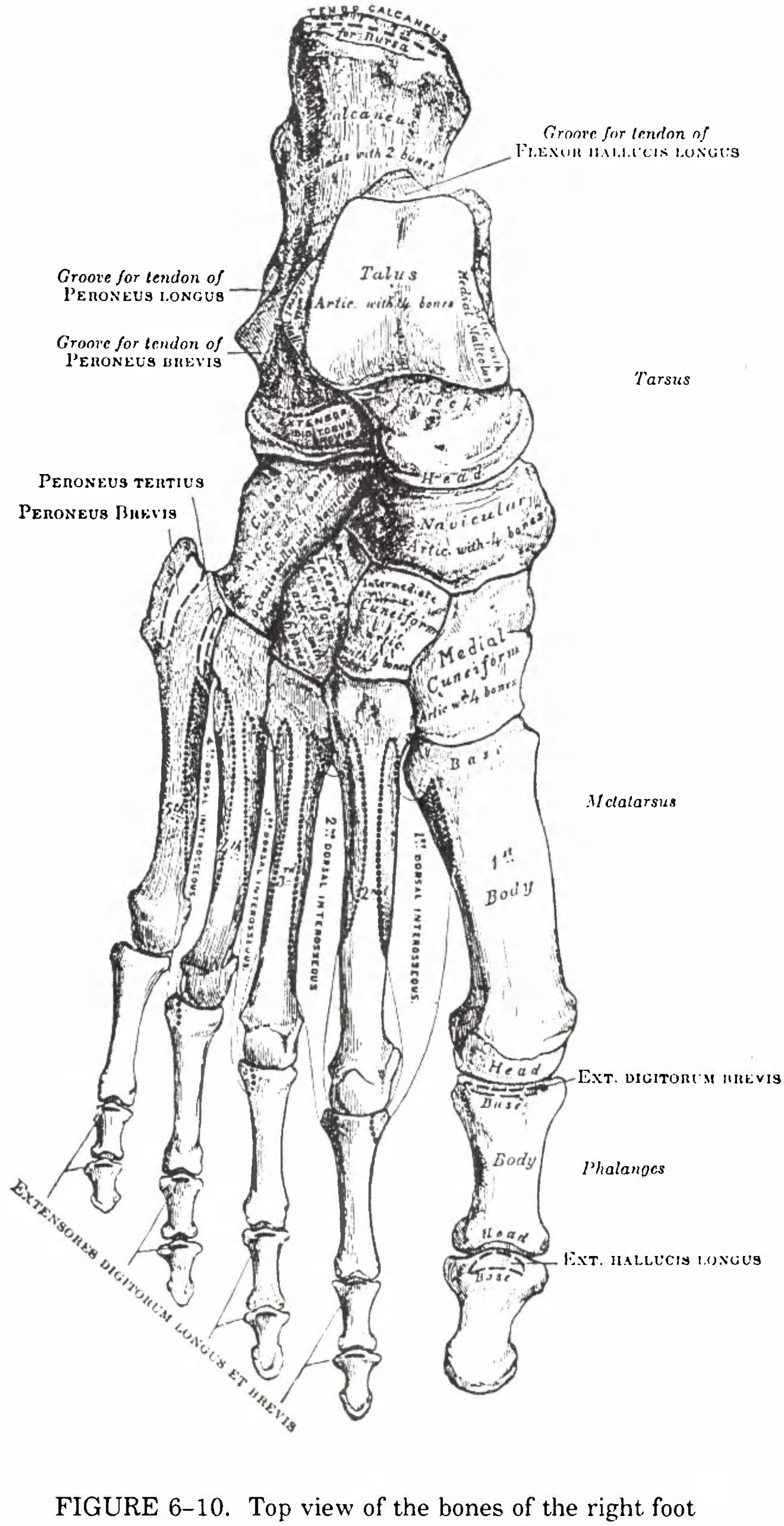

FIGURE 6–10. Top view of the bones of the right foot (*Gray's Anatomy*, American edition).

metatarsals are relatively long and slender and are tapered. From the side, they are convex upward. They are numbered sequentially from one to five from the inside outward so that the big toe is attached to the first metatarsal bone. The proximal end of the metatarsals articulate with the tarsal bones, while their lower ends articulate with the phalanges or the bones of the toes. There are in general three rows of phalanges, named proximal, middle, and distal. However, the big toe has only two rows. Their size and length vary considerably, as shown in Figure 6–10.

LOWER EXTREMITY INJURIES FROM CLINICAL EXPERIENCE

Types of Injuries. Grattan and Hobbs (1968) have stated that the total number of named lower extremity injuries is 167 for unrestrained front seat occupants. This number resulted from an analysis of 355 occupants who sustained serious lower extremity injuries in a variety of accidents. The aim of the study was to determine the mechanism of injury and the direction of the applied force to eight common types of injury. The mechanisms described below were proposed by Grattan and Hobbs (1968). Note that these were deduced from observations of the vehicle interior rather than from laboratory experiments.

Posterior Dislocation of the Hip Joint. This injury is caused by an axial impact to the knee, via the patella. The force is transmitted through the femur to the hip joint, producing a fracture of the posterior aspect of the acetabulum and dislocation of the hip. In a frontal impact, the hip is flexed 90°, and the impacting surface is generally the instrument panel. Patellar fracture can occur concomitantly with this injury.

Central Fracture–Dislocation of the Hip. The head of the femur is pushed medially into the acetabulum by a lateral force, causing fracture of the acetabulum. The force is generally applied to the greater trochanter. In a side impact, the near-side occupant is vulnerable to this injury. However, large deformation of the door is generally required to cause this fracture.

Fracture of the Roof of the Acetabulum. If the thigh is flexed less than 90° and the knee receives an axial impact, the femur transmits a rearward as well as an upward force to the hip joint. The upward component can cause the bone in and around the top of the acetabulum to fracture. In a frontal impact, this injury can occur if the knee is impinged against the dashboard and the torso rotates forward and is lifted from the seat.

Transverse Fracture of the Femoral Shaft. This type of fracture can be a single clean fracture or a comminuted fracture of the femoral shaft. It is caused by a load applied to the top (anterior) surface of the femur in the mid-shaft area. In a frontal impact, the occupant's knee submarines under the dashboard and the torso rotates forward and is lifted from the seat. Thus, the thigh is flexed less than 90° when the injury occurs. If only the knee goes under the dashboard, the result can be a supracondylar fracture. There can easily be another injury mechanism to explain shaft fractures. Viano and Stalnaker (1980) attributed mid-shaft fractures to anteroposterior bending of the femur, due to an axial knee impact. Single transverse fractures can also occur in a side impact. The near-side occupant can be struck by the door along the shaft of the femur, causing this injury.

Double Fracture of the Femoral Shaft. This injury is caused by two forces acting simultaneously on the shaft of the femur. In a frontal impact, the knee can slide below the dashboard and the thigh can contact the steering assembly as the torso rotates forward and is lifted from the seat, resulting in a supracondylar fracture and an intertrochanteric fracture. Double comminuted fractures of the shaft are caused by dual contact of the shaft with interior vehicular surfaces or a distributed load on the femur. Again, bending failure due to a knee impact is a more likely injury mechanism.

Oblique Fracture of the Femoral Shaft. In an oblique impact, the knee can be pocketed in the dashboard and the torso forced laterally into the door. This motion applies a twist to the femur, resulting in a spiral or oblique fracture. Of course, other means of applying torsional loads to the femur are possible.

Patellar Fractures. In a frontal impact, the patella generally impacts the dashboard. If it hits a stiff portion of the dashboard, such as the edge of a tray, the patella can fracture.

Plateau Fracture of the Tibia. Contact of the proximal tibia with a stiff portion of the dashboard can result in fracture of the proximal tibia, involving one or both plateaus. The fibula can also be fractured.

Incidence to Lower Extremity Injury. Nahum et al. (1968) reviewed lower extremity injury data from 290 crashes in which at least one occupant received a moderate or more severe injury. There were a total of 405 occupants who sustained 1,112 injuries. Of these injuries, 375 or 34% were sustained by the lower extremities. In terms of injured occupants, 186 received lower extremity injuries and 141 or 76% sustained these injuries by striking the instrument panel. There was a preponderance of knee injuries for front-seat occupants, while a previous study showed more lower-leg injuries for rear-seat occupants (Nahum et al. 1967). The parameters that were used in the analysis of the data were occupant age, impact speed, vehicle model year, and vehicle weight. Injuries decreased with newer models and with vehicle weight. They increased with occupant age from 28% in the first decade of life to 38% in the seventh decade. The frequency of injury also increased with vehicular speed, for both the lower extremities as well as for the occupant.

Melvin et al. (1975) presented lower extremity injury data extracted from Collision Performance and Injury Report (CPIR) files. By restricting the impacts to frontal crashes involving unrestrained occupants over 12 years of age, they found 382 cases of lower extremity injuries with an AIS of 2 or higher. There were a total of 2,024 cases which satisfied their search conditions. The frequency rate was thus only 19%. In another study by Nagel and States (1977), the injury rate was 37%, since 57 of 153 occupants sustained 80 knee injuries. The dashboard was responsible for 69 of these injuries.

Results of a survey of British accident data is given by Gloyns et al. (1979). In this study, 258 cases were selected from a data bank of 2,200 cases, which had been collected by the Accident Research Unit of the University of Birmingham. Of the 258 occupants, 197 were male and 61 female. There were 164 male drivers and 17 female drivers. The overall injury rate for AIS 2 lower extremity injuries was 39% or 101 occupants. This can be broken down to 82 drivers and 19 front-seat passengers. The data include 47 drivers and 19 front passengers who were wearing a restraint system. In addition to the AIS, two other injury scales were used: the Treatment Period (TP) and Permanent Impairment (PI), as defined in the Comprehensive Research Injury Scales (CRIS) proposed by States (1969) and States et al. (1971). The severity ranking of lower extremity injuries among all body regions for each scaling system, as well as the frequency (in percent) that lower extremity injuries were given the highest rating in each system, are given in Table 6-1. The distribution of injuries for the five regions of the lower extremity is shown in Table 6-2. The 39 injuries sustained by the 66 restrained occupants are shown in Table 6-3.

TABLE 6–1

RANKING AND HIGHEST-RATING FREQUENCY OF LOWER EXTREMITY INJURIES
(Gloyns et al. 1979)

Injury Scale	Drivers		Front Passengers	
	Ranking	Freq. %	Ranking	Freq. %
AIS	2nd	30	4th	12
TP	1st	50	3rd	22
PI	1st	51	3rd	18

TABLE 6–2

DISTRIBUTION OF INJURIES IN UNRESTRAINED OCCUPANTS
(Gloyns et al. 1979)

Region	Drivers		Front Passenger		Overall	
	%	N	%	N	%	N
Pelvis/Hip	25.2	26	40.0	8	27.6	34
Femur	28.2	29	25.0	5	27.6	34
Knee	11.7	12	0.0	0	9.8	12
Tibia/Fibula	12.6	13	25.0	5	14.6	18
Foot/Ankle	22.3	23	10.0	2	20.3	25
TOTAL	100.0	103	100.0	20	99.9	123

TABLE 6–3

DISTRIBUTION OF INJURIES IN RESTRAINED OCCUPANTS
(Gloyns et al. 1979)

Region	%	N
Ankle/Foot	30.8	12
Femur	28.2	11
Pelvis/Hip	17.9	7
Tibia/Fibula	15.4	6
Knee	7.7	3
TOTAL	100.0	39

The authors attempted to emphasize the role of floor board and instrument panel intrusion in the causation of femoral, tibial, and ankle injuries. Although the extent of intrusion could only be estimated, there was evidence to show that 67% of the tibial/fibular fractures and 75% of the fracture-dislocations of the foot and ankle were accompanied by footwell intrusion. (Knee contact points in the vehicle were absent.) As a result of this observation and the fact that cadaver studies produced a different pattern of injuries, the authors felt that the tolerance data obtained from pendulum or sled impacts using cadaveric subjects may not be realistic, since intrusion is not simulated in these tests. Finally, Gloyns et al. (1979) provided a list of specific injuries and their incidence to each region of the lower extremity as shown in Table 6-4.

Recently, Huelke et al. (1982) provided a definitive study of frequency and severity of lower extremity injuries sustained by automotive occupants. The data bank of the National Crash Severity Study (NCSS) was examined to reveal detailed information on this topic. The NCSS file contains data on 14,491 occupants who were involved in 6,628 accidents. Detailed injury information was available from 10,151 occupants who form the basis of this survey. In particular, the authors were interested in relatively severe injuries to the lower extremities, and a large portion of the paper was devoted to AIS 3 and 4 injuries, at which level the frequency of injury was 23%. In terms of occupants, 1,353 occupants sustained injuries at the AIS 3 and 4 level, and 27% of these, or 351 occupants, sustained such injuries in their lower extremities. The areas of contact and the frequency of contact are shown in Table 6-5. The instrument panel was involved in 44% of all the known contact cases (162 out of 370 cases). However, as a percentage of all cases, the frequency drops to 38.8% (162 out of 419 cases). It is also the most frequently involved contact area at the AIS 2 level, as shown in Table 6-5. The data were presented in great detail in the paper. Table 6-6 is an attempt to summarize the results. It shows the contribution of vehicle interior surfaces to five areas of injury for the lower extremities. Because of nonuniformity in the reporting procedure, Table 6-6 contains a small proportion of unknown contact surfaces or unknown areas of injury. It should also be noted that the pelvis was included as part of the lower extremity. From the point of view of injury mechanisms and treatment, it is difficult to separate the pelvis from the hip joint and the proximal femur.

The information in Table 6-6 includes all unrestrained occupants, regardless of their seating position. It is seen that the pelvis is most frequently injured by the side of the vehicle, presumably in side impacts, followed by the steering column, which affects the driver in frontal impacts. Thigh, knee, and shank injuries are most frequently attributed to the instrument panel, while those of the ankle and foot are mainly due to the floor. The medical consequences of lower extremity injuries were studied in terms of length of hospital stay and work days lost. For AIS 3 and 4 injuries, the lower extremity required approximately twice as many hospital days in comparison with a comparable injury to other body areas. The number of work days lost is about 20% higher. There is clinical evidence that arthritis can develop in the joints of the lower extremity as a result of trauma, but the frequency and severity of this problem could not be ascertained from the NCSS data base.

TABLE 6-4

THE PATTERN OF LOWER-LIMB INJURIES
(Gloyns et al. 1979)

Type of Injury	N	%
HIP AND PELVIS		
Fractures of the pelvis, not including the acetabulum	24	13.3
Dislocations or fracture-dislocations of the hip	15	8.3
Fractures of the acetabulum	4	2.2
FEMUR		
Trochanteric fractures	1	0.5
Fractures within the shaft	25	13.8
Femoral fracture, precise nature not know	15	8.3
Condylar or supracondylar fractures	3	1.6
Fractures involving the knee joint	4	2.2
KNEE		
Patella fractures	13	7.2
Dislocations of the patella	1	0.5
Fracture–dislocations of the knee	1	0.5
LOWER LEG		
Fracture extending into knee joint	3	1.6
Simple fracture of tibia and/or fibula	17	9.4
Compound fracture of tibia and/or fibula	3	1.6
Comminuted fracture of tibia and/or fibula	4	2.2
Simple fracture of tibia at lower end	2	1.1
Comminuted fracture of tibia and fibula at lower end	2	1.1
Fracture of lower leg, precise details not known	1	0.5
FOOT AND ANKLE		
Malleolar fractures	14	7.7
Displaced Potts fracture	1	0.5
Ligament avulsion	1	0.5
Fractures and/or dislocations of tarsals	19	10.5
Fracture or dislocation of metatarsal	3	1.6
Fractures of phalanges	1	0.5
Fractures or dislocated bone in foot, precise details not known	5	2.8
TOTAL	181	100.0

TABLE 6-5

PERCENT DISTRIBUTION CONTACT WITH IMPACT SURFACES
(Huelke et al. 1982)

Surface	AIS 3 and 4	AIS 2
Instrument Panel	38.8	27.0
Floor	15.1	22.1
Side	12.4	12.5
Steering Assembly	10.5	6.2
Miscellaneous	4.5	1.8
Front Seat Back	4.3	2.6
Exterior	2.2	1.3
Unknown	12.2	26.5
TOTAL	100.0	100.0

TABLE 6-6

CONTACT AREAS FOR AIS 3 AND 4 LOWER-EXTREMITY INJURIES,
PERCENT OF ALL INJURIES (ALL UNRESTRAINED OCCUPANTS)
(Huelke et al. 1982)

Surface	Pelvis	Thigh	Knee	Leg	Ankle/ Foot	Unk. Area	TOTAL
Instrument Panel	5.5	10.8	8.4	12.0	0.2	1.9	38.8
Floor	0.2	0.7	0.0	1.4	12.2	0.5	15.1
Side	6.9	2.4	0.5	1.7	0.7	0.2	12.4
Steering Asmbly	5.7	3.3	1.0	0.2	0.0	0.2	10.5
Miscellaneous	1.2	0.7	0.2	1.4	0.7	0.2	4.5
Front Seat Back	0.7	1.4	0.0	1.7	0.5	0.0	4.3
Exterior	0.0	0.5	0.0	1.0	0.5	0.2	2.2
Unknown	3.8	2.6	1.2	2.2	1.4	1.0	12.2
TOTAL	20.2	22.5	11.2	21.5	16.3	4.3	100.0

Disability and Long-Term Impairment. Huelke et al. (1982) have already indicated that lower extremity injuries tend to result in a longer hospital stay and 20% higher loss in work days. Nagel and States (1977) carried out a follow-up study on patients who have sustained a knee injury in an automotive accident in an attempt to determine the long-term effects of knee trauma. At Stanford, California, 33 patients with 35 knee injuries were called back for a checkup 1.5 to 5 years after the accident. Two of the four with severe knee injuries had developed arthritis. None of the five moderately injured patients showed signs of arthritis, and only one of 26 mildly injured patients had degenerative arthritis. In Rochester, New York, a similar follow-up was performed on

12 randomly selected knee patients, seven to nine years after the injury. One of the two severely injured patients and two out of six moderately injured patients had developed degenerative arthritis. The four mildly injured patients showed no sign of arthritis. It was concluded that arthritis will develop in severely injured patients, particularly if there was ligament damage. However, it was difficult to predict which knee would develop arthritis.

In another study on disability, Routson and States (1981) studied 89 patients who had sustained an AIS 3 injury of the lower extremity. Sixty-six were car occupants and 23 were cyclists. Four of the occupants were lost to follow-up, and one was excluded because the injury was found to be less than an AIS of 3 after careful scrutiny. In frontal impacts, the frequent injuries were fracture of the femur, tibia, and patella. In side impacts, the common injuries were fracture of the pelvis and femur. The Injury Severity Score (ISS) was computed for each patient. Hospital stay and permanent disability generally increased with ISS. The assessment of permanent disability was made subjectively by the treating physician. In terms of the various injuries sustained, permanent disability was rated over 50% for acetabular fractures and fracture-dislocation of the hip. For pelvic and femoral fractures, it was about 40%. It was also found that ISS did not correlate well with model year of the vehicle or with vehicular weight.

INJURY MECHANISMS OF THE LOWER EXTREMITIES FROM LABORATORY TESTING

The first reported dynamic testing of human femurs was performed by Mather (1968) who applied dynamic loads by dropping a weight on the shaft of the bone, but fracture patterns were not discussed. Patrick et al. (1966) performed whole-body cadaveric impact tests to study human tolerance to frontal impact. Ten unrestrained, seated embalmed cadavers were impacted into instrumented chest, head, and knee targets that simulated a vehicle interior. The knee targets were covered with 37 mm (1.5 in) of padding in most cases. Most of the fractures occurred in the distal (lower) third of the femur, including supracondylar fractures, patellar fractures, and a comminuted fracture of the distal shaft. There was one mid-shaft fracture.

Powell et al. (1974, 1975) used a pendulum to impact embalmed cadaver femurs in the longitudinal direction. Fifteen knees from nine cadavers were impacted with a rigid impactor. Most of the fractures were in the distal third of the femur, including patellar fractures. There was one fracture of the proximal (upper) shaft and one case of injury to the pelvis. Strain-gage data from the distal third of the femur indicated that bending strains were primarily responsible for the observed femoral fractures.

Melvin et al. (1975) and Melvin and Stalnaker (1976) were the first to report the use of unembalmed cadavers for knee impact research. Twenty-six cadavers (15 males and 11 females) between the ages of 45 and 90 years were impacted by an instrumented striker. The striker surface was either rigid or padded with 1 to 2 in (25 to 50 mm) of padding. Again, the fractures were principally in the distal third of the femur.

Fractures of the proximal and distal femur were observed in whole-body sled tests performed by Melvin and Nusholtz (1980). Six cadavers (four males and two females), ranging in age from 49 to 79 years were used in this study. The force-time waveform was trapezoidal in shape whenever there was femoral neck fracture. The authors hypothesized that the first abrupt change in slope or break in the trapezoidal waveform occurred as a result of neck fracture, decreasing the rate of rise of the load in the femur. The second break in the waveform was attributed to condylar or distal shaft fractures which caused an abrupt drop-off of the load. A femoral neck fracture can give rise to an instantaneous change in load-carrying ability but would be followed closely by a resumption in loading at a lower rate or a decrease in load. The ligamentous structures around the hip joint and the proximal end of the femur are thought to carry load around such fractures and thereby continue the loading through the upper leg. Fractures in other regions of the femur can subsequently occur. In contrast, when a fracture of the shaft of the femur or an extensive fracture of the condyles occurs, there would be an abrupt loss in load-carrying capability with no immediate alternative load path. This would result in a severe drop-off of load.

Viano and Stalnaker (1980) analyzed the data from a series of axial knee impact tests on six seated cadavers. A 10.1-kg (22.2-lb) impactor was used in conjunction with varying degrees of padding. The flesh was removed from the shaft of the femur to observe initiation of fracture in the bone by means of high-speed photography. When a rigid impactor was used, multiple fractures of the femur occurred, including mid-shaft and patellar fractures. The two tests conducted with light padding both produced bilateral condylar fractures. Only two of the five tests with thick padding produced fractures, one condylar and one mid-shaft. However, both of the cadavers used were considered by the authors to have bones in "abnormal" condition. The other three specimens were normal and were not fractured. In four of the rigid impacts, neck fractures were produced as well as shaft fractures. The femoral neck was not observable during the test. Thus, correlation of neck fracture with load level was not possible. However, in all four tests, the trapezoidal characteristics of the force-time waveform observed by Melvin and Nusholtz (1980) were present. Many of the specimens had multiple fractures, and the authors concluded that shaft and condylar fractures occurred after the peak load had been reached.

The cancellous bone center of the patella makes it vulnerable to concentrated loads. This phenomenon was studied by Melvin et al. (1969), employing three different impactor sizes, all rigid. Two of the impactors were flat circular surfaces with diameters of 0.612 and 0.432 in (15.5 and 10.9 mm). The third impactor was ring-shaped with outer and inner diameters of 0.5 and 0.25 in (12.7 and 6.4 mm), respectively. Patellar damage patterns varied dramatically with impact speed. Under static loading, the impactors caused a clean punch-through of the patella, but multiple fractures or near total destruction of the patella occurred during dynamic tests made at 15 and 30 ft/s (4.5 and 9 m/s).

In all of the preceding knee impact studies, the loading of the femur was intentionally through the patella and femoral condyles. It resulted primarily in fractures of the patella, femur, and/or pelvis. If the knee was not flexed greater than 90° or the loading was applied below or across the knee joint, damage to the knee ligaments and/or fractures of the tibia and fibula might result. Viano et al. (1978) impacted seated cadavers on the anterior portion of the tibia, just below the knee joint. Knee ligament tearing and/or tibia-fibula fractures were produced in 5 of the 7 specimens tested. For eight impacts that spanned the knee joint, the predominant injury mode was avulsion of the posterior cruciate ligament from the tibial plateau. The impactor had a surface that simulated a knee bolster used in cars equipped with an automatic belt system with no lap belts. Sled tests were also conducted by Viano and Culver (1979) in which shoulder-belted cadavers (without lap belts) impacted knee bolsters. The two below-the-knee impacts produced significant ligament tears.

The only extensive dynamic loading study of the lower leg was conducted by Kramer et al. (1973) for the purpose of investigating pedestrian impact trauma. In this type of impact, transverse loading of the bones is predominant. The authors conducted 209 transverse impacts against the lower legs of cadavers, using cylindrical impactors. The axes of the cylinders were horizontal to simulate vehicular bumpers striking a standing pedestrian's leg. Out of the 209 tests, 43 of the legs were fractured, 14 from both legs of the same cadaver, 14 from the right leg, and 15 from the left. There were 19 transverse fractures, 11 comminuted fractures, 3 split fractures, and 2 multiple fractures. In 8 of the cases, the type of fracture was not recorded. The frequency of impact was dependent on the location of impact. Nearly one-third of the impacts to the tibial head resulted in fractures. The probability of fracture for mid-shaft impact was about 12%.

There are two injury mechanisms for the long bones of the lower extremities. Fractures of the shaft are caused by bending or torsional loads. Fractures of the patella and those near the joints are due to direct or transmitted loads that cause localized injuries. Fractures in and around the knee joint can be attributed to direct loading, but it is not known what kinds of loads are needed to cause ankle injuries. The femur is the main transmitter of loads to the hip joint and pelvis. Various acetabular injuries can be easily explained by this mechanism.

The preponderance of fractures in the distal third of the femur does not compare well with accident statistics provided by Gloyns et al (1979). In real accidents, the bending moments can be considerably higher because of the sitting posture of occupants. Thus, shaft fractures can occur without significant injuries to the patella or the condyles. In laboratory tests, particularly in tests using a pendulum or striker, the load was applied "axially," and a large force was needed to generate moments high enough to cause bending failure. Further research is needed to determine whether there is indeed a disparity in the injury patterns between those observed in the field and those seen in the laboratory. If the disparity is real, the mode of testing cadavers needs to be investigated to see how injuries similar to those seen in the field can be reproduced with regularity in the laboratory.

Ligamentous injuries due to the knee bolster can be caused in part by the tibial tuberosity, which can be prominent enough to cause a rearward shift of the tibia relative to the femur, resulting in the avulsion of the posterior cruciate ligament. It should be noted that the knee bolster used by Viano et al. (1978) had a flat surface. The frequency of ligamentous injury may decrease with a different bolster design.

INJURY TOLERANCE OF THE LOWER EXTREMITIES

Tolerance of the following portions of the lower extremity anatomy are discussed: femur, patella, tibia, knee joint, and ankle joint. The hip joint and pelvis are covered in a previous chapter. The fracture characteristics of the fibula are excluded from the discussion because it is not a significant load carrier and, when fractured, is of relatively little concern to the medical practitioner when there is an accompanying fracture of the tibia.

Femur Tolerance. Early studies of the static strength of the femur were conducted by Weber in 1859 and Messerer in 1880 and have been summarized by Melvin and Evans (1985).

Weber performed three-point-bending tests with the force applied in 245-N (55-lb) increments midway between the supports and transverse to the longitudinal axis of the bone. The distance between the supports was 183 mm (7.2 in) in all cases. Data were gathered for four males and five females. The average maximum bending moments at fracture were 233 N$\cdot$m (172 ft$\cdot$lb) for males and 182 N$\cdot$m (134 ft$\cdot$lb) for females.

Messerer's bending experiments were performed with a hydraulic testing machine having a load measurement resolution on the order of 10 to 50 N (2.25 to 11.2 lb).

Three-point bending was conducted, with the support span of two-thirds the length of the bone (an average of 317 mm or 12.5 in for the femur). Loads were applied at midspan. Bones from six males (ages 24 to 78 years) and six females (ages 20 to 82 years) were evaluated. For lateral (left-right) loading, the average maximum bending moments at fracture were 310 N·m (229 ft·lb) for males and 180 N·m (133 ft·lb) for females.

Messerer also conducted static torsion tests on the femur. Bones from four males (ages 27 to 56 years) and seven females (ages 19 to 81 years) were evaluated. The average torsional loads at fracture were 175 N·m (129 ft·lb) for males and 136 N·m (100 ft·lb) for females. He noted that the upper and lower thirds of the femur were of lower torsional strength than the middle third. All of the bones fractured with the characteristic spiral pattern at an angle of about 45°.

Static axial compression tests of the femur were conducted by Messerer with the ends of the bone padded with felt to prevent local failure at the point of force application. The average axial compressive failure force for shaft-fractures was 7.72 kN (1735 lb) for males and 7.11 kN (1598 lb) for females. Femoral neck fractures occurred at an average force of 7.99 kN (1796 lb) for males and 4.96 kN (1115 lb) for females.

A more recent study of the static bending strength of the femur was conducted by Motoshima in 1960 and summarized by Yamada (1970). Three-point-bending tests were performed on the femurs of 35 subjects. The ends of the specimens were supported by plaster or concrete, and the force was applied at midspan in the anterior-posterior direction using a 20-mm (0.8-in) diameter cylindrical loading head. Yamada provides breaking force data as a function of age group. Bending moment at fracture would be a more meaningful measure of strength. This can be computed if the distance, *L*, between supports is known. Fortunately, this distance can be computed by working backward from the ultimate deflection, *u.d.*, and ultimate specific deflection, *u.s.d.*, data that are provided:

$$L = \frac{\text{u.d.}}{\text{u.s.d.}}$$

This provides a span between supports of 345 mm (13.6 in) The peak bending moment, *M*, at fracture may be computed using the equation

$$M = \frac{PL}{4}$$

where *P* is the applied force at midspan when fracture occurs. Applying this analysis to Yamada's breaking force data gives the results presented in Table 6-7 herein. Yamada indicates that the female femur has five-sixths of the bending strength of the male femur, and furthermore that the bending-breaking load is not significantly different between anteroposterior and lateromedial directions of loading (for any of the long bones). This is in contrast to Messerer's finding that the failure load does depend on direction of loading, since most bones have triangular or elliptical cross-sectional shapes.

During the last two decades, there have been a number of studies of the dynamic fracture tolerance of the femur, primarily as a result of research performed in connection with vehicle occupant safety. While truly acceptable criteria for predicting fracture have remained elusive, there does appear to be essentially universal agreement that the dynamic load carrying ability of the femur exceeds that under static conditions.

The enhanced load carrying capability of the femur under dynamic conditions was dramatically demonstrated by Mather (1968) using thirty-two pairs of human femurs.

TABLE 6-7

PEAK BENDING MOMENT AT FRACTURE
FOR STATICALLY LOADED WET FEMURS*
(Based on data of Yamada 1970)

Age Groups (Yr.)	Bending Moment (N• m)
20–39	234
40–49	213
50–59	203
60–69	201
70–89	184
Average	211

*Yamada does not state if these results are for males, females, or both.

For each pair, one was loaded statically, and the other was loaded dynamically with a drop weight at 32 ft/s (9.8 m/s). While the data did not enable a comparison of static and dynamic fracture forces, an energy comparison was possible. The mean value of the ratio of dynamic energy to static energy was 1.7, with a standard deviation of 0.8.

Dynamic torsional loading of the femur has been studied by Martens et al. (1980) in connection with skiing injuries. Femurs were obtained from sixty-five autopsy subjects ranging in age from 27 to 92 years. The ends of the bones were embedded in gripping blocks and torsionally loaded to failure in less than 100 ms. The mean value of peak torsional load for males was 204 N• m (150 ft• lb) and for females was 131 N• m (97 ft• lb). Comparing these data with the results of Messerer's static torsional tests shows that for males the mean dynamic peak torsional load is 17% greater than its static counterpart. For the female, however, the mean dynamic peak load is actually lower than its static counterpart by 4%. Melvin and Evans (1985) suggest that this disparity is most likely due to the smaller sample size of Messerer (7 versus 13) and the fact that two of his subjects were large-boned. Martens et al. report average energies to failure in the dynamic torsional fracture tests of 37.5 J (27.7 ft• lb) for males and 29.8 J (22.0 ft• lb) for females.

Roberts and Pathak (1977) have also studied the torsional fracture tolerance of the human femur. Specimens were obtained at autopsy within eight hours of death and stored at 20°C until tested. They were from 16 males and 19 females with an average age of 58 years, average height of 1.60 m (5.25 ft), and average body mass of 65.2 kg (143 lb). No bone abnormalities were demonstrable at X-ray. The 36 test specimens were all 370 mm (14.6 in) in length, extending from the lesser trochanter to the flare of the distal epiphysis. End restraints of polymethyl methacralate enabled the application of a torsional load. Loading was accomplished by dropping a 12-kg (26.4-lb) mass 2.9 m (9.5 ft) along a guide rod to impact a lever arm extending from one of the end restraints. For males the average peak torsional failure load was 155 N• m (114 ft• lb) with a rotation angle of 12.6°, failure energy of 18.8 J (13.9 ft• lb), and time to failure of 6.0 ms. Respective data for the females were 118 N• m (87 ft• lb), 14.0°, 16.0 J (11.8 ft• lb), and 6.5 ms.

The first study of femoral impact tolerance to be conducted as part of the automotive occupant crash safety movement was that of Patrick et al. (1966). Ten unrestrained, seated, embalmed male cadavers were tested on a deceleration-type impact sled facility. As the sled decelerated, the test subject slid forward and impacted instrumented head, chest, and knee targets that were positioned to simulate a vehicle interior. The knee targets were covered with 1.5 in (37 mm) of padding in most cases. While supracondylar fractures were the most common, intertrochanteric and shaft fractures were also observed. For the padded knee target impacts, the axial compressive force versus time profiles approximated a haversine shape and were of approximately 30 to 40 ms duration. The authors concluded that, for knee impacts against a moderately padded surface, an axial compressive force of 1400 lb (6.2 kN) is a reasonably conservative value for the overall injury threshold level of the patella-femur-pelvis complex. It is noted that volunteer subjects tolerated forces of 800 to 1000 lb (3.6 to 4.4 kN) with only minor knee pain. Furthermore, cadaver subjects in some cases sustained loads as high as 3850 lb (17.1 kN) without femoral fracture. In a subsequent publication (Patrick et al. 1967), the authors reported on tests of another two cadavers. Loads of 1470, 1710, 1950, and 1970 lb (6.5, 7.6, 8.7, and 8.8 kN) were sustained without fracture. It was suggested that loads of 1950 lb (8.7 kN) without fracture are not unreasonable.

Brun-Cassan et al. (1982) tested nine male and one female unembalmed cadavers in a vehicle body mounted on a deceleration-type sled. The deceleration pulse is said to have simulated frontal, rigid barrier impact conditions. Speeds ranged from 49.5 to 67.1 km/h (30.7 to 41.7 mph). Force transducers covered with 25 mm (1 in) of polyurethane foam were mounted at the instrument panel location for knee impact. The male cadavers were an average of 59 years of age (range 42 to 68 years), and the one female was 42 years of age. The males had an average height of 1.68 m (5.5 ft), with a range of 1.62 to 1.80 m (5.3 to 5.9 ft), and the female's height was 1.55 m (5.1 ft). The males' body mass averaged 63 kg (139 lb), with a range of 49 to 82 kg (108 to 180 lb), and the female's mass was 53 kg (117 lb). No femur fractures were sustained in any of the ten tests. While only two force-time profiles were presented with the results, the authors did provide a table of normalized peak forces and their durations. Normalization was performed using the relationship presented by Eppinger (1976):

$$\text{Normalized Force} = \text{Measured Force} \left[\frac{75}{\text{Subject Mass}}\right]^{2/3}$$

where the subject mass is expressed in kg. Furthermore, the pulse durations presented are for the initial "primary loads" (i.e., the initial load spikes) and were determined using the so-called "triangular approximation method" defined by Kroell et al. (1976) as the time interval between the zero baseline intercepts of two straight line segments providing a triangular approximation of the waveform. The normalized peak forces ranged from 3.67 to 11.4 kN (825 to 2563 lb) and the durations (triangular approximation of the initial load spike) ranged from 8 to 18 ms, with the exception of one duration of 27 ms. Impulses associated with these knee impacts ranged from 18.6 to 166 N•s (4.18 to 37.3 lb•s).

Some femur fracture tolerance evaluations involving impact to the knee have been performed with stationary, seated cadavers that were struck by a moving mass. Powell et al. (1974, 1975) applied axial compressive loads to the femurs of embalmed and fresh male and female cadavers positioned with the femur horizontal and the tibia vertical. The impactor was a 15.6-kg (34.3 lb) mass at the end of a pendulum arm. A rigid, flat striking surface was attached to the mass through force transducers, and an accelerometer was mounted on the striker (presumably for inertial compensation of the load cell outputs).

Impacts were applied directly to the patellar region, with no padding at the interface. Consequently, the primary pulse durations were short (10 to 20 ms using the triangular approximation method). A total of fifteen tests were performed on nine cadavers. The six males ranged in age from 48 to 79 years and had heights ranging from 1.73 to 1.83 m (5.7 to 6.0 ft). The three females had age and height ranges of 28 to 76 years and 1.55 to 1.70 m (5.1 to 5.6 ft). Body masses are not reported. Femur fractures resulted in seven of the fifteen tests. There was one femoral shaft fracture at a peak force of 11.6 kN (2608 lb) and one femoral neck fracture at a peak force of 10.8 kN (2428 lb). The remaining five femoral fractures were in the condylar region and were associated with impacts having peak forces ranging from 7.1 to 10.4 kN (1600 to 2340 lb). Patella fractures occurred in all eight of the tests where the femur was undamaged. In these eight tests the peak force ranged from 5.2 to 9.3 kN (1170 to 2090 lb). The authors suggest that bending effects in the femoral shaft play a significant role in femur response to longitudinal impacts.

Melvin et al. (1975) and Melvin and Stalnaker (1976) impacted the knees of twenty-six fresh cadavers with a striker mass of either 24.1 or 9.5 lb (11.0 or 4.3 kg). There were fifteen male cadavers and eleven females. While some data are missing, the available information indicates that the males ranged in age from 46 to 90 years, had body mass ranging from 106 to 237 lb (39.6 to 88.5 kg), and height ranging from 5.3 to 5.9 ft (1.63 to 1.80 m). Likewise, the available data on the females provide ranges of 45 to 89 years, 48 to 177 lb (21.9 to 65.9 kg), and 4.9 to 5.4 ft (1.50 to 1.66 m). The test subjects were in a seated posture with the thigh horizontal and the lower leg vertical or drawn backward slightly. The lower torso was free to translate rearward as a result of the impact. Impact velocities varied from 12.4 to 76.0 ft/s (3.8 to 23.2 m/s). Various levels of impactor-face padding (from no padding up to a maximum of 1 in or 25 mm Ensolite® plus 2 in or 50 mm aluminum honeycomb) were utilized in conjunction with variations in applied force pulse amplitudes and durations.

For the seven "rigid surface" impacts (to two male and one female cadavers), femoral condyle fractures occurred in two tests. The peak forces associated with these impacts were 4080 lb (18.0 kN) for a female and 4400 lb (19.6 kN) for a male. There was no femoral fracture in the other five tests, where the peak force ranged from 3640 to 5100 lb (16.2 to 22.7 kN) on four legs of male cadavers. For the twenty-eight "lightly padded" impacts (to nine male and six female cadavers), femoral condylar and/or supracondylar fractures occurred in five tests, and one undefined femoral fracture occurred in a sixth test. Three of these were associated with males and had peak forces ranging from 3050 to 6400 lb (13.6 to 28.5 kN). The remaining three were associated with females and had peaks ranging from 3000 to 4400 lb (13.3 to 19.6 kN). For the five "thick padding" impacts (to one male and two female cadavers), femoral condylar and/or supracondylar fractures occurred in two tests (on a 69-year-old female) and a fracture of the distal third of the shaft occurred on the other female cadaver (age 55 years). Forces are not available for the former, but the peak force associated with the shaft fracture was 4420 lb (19.7 kN). The male cadaver (age 72 years) sustained peak forces of 3520 and 3080 lb (15.7 and 13.7 kN) without fractures.

A series of nine impact tests was conducted using two male and two female cadavers with the thigh abducted (rotated laterally outward from the sagittal plane) through an angle of either 11° or 25°. In the first six of these tests, the direction of impact was in a sagittal plane. However, this tended to drive the thigh out of the way rather than to cause large axial force in the femur. Fracture occurred only for one osteoporotic subject. Accordingly, for the final three tests the impact direction was aligned with the longitudinal axis of the thigh (25° abduction). Under this latter test configuration, a 67-year-old female cadaver sustained a supracondylar fracture as a result of a "lightly padded" impact having a peak force of 4540 lb (20.2 kN). The opposite femur survived a peak force of 4800 lb (21.4 kN) without fracture under the same test conditions. A 46-year-old male sustained 1350 lb (6.0 kN) without fracture in a similar test using "thick padding."

In the above test program, the "primary force duration" was listed for each impact. This is the duration of a triangular approximation of the initial load spike. The durations ranged from a minimum of 2.6 ms for one of the "rigid" tests to a maximum of 22 ms for one of the "light padding" tests. The longest duration noted for a "thick padding" test was 10.7 ms. As a result of this series of cadaver tests, the researchers concluded that, in addition to a threshold force level for failure, an associated energy level of 400 ft• lb (542 J) was necessary to produce distal failures at the femur.

The pulse durations in the above study were short compared to typical durations observed in vehicle crashes. Melvin and Nusholtz (1980) performed a series of six unembalmed cadaver tests on the UMTRI sled facility in an effort to achieve longer durations and to study the effect of loading both femurs simultaneously. The seated subject slid forward during sled deceleration and struck its knees against a single impact surface mounted on two force transducers located near the expected points of impact. Although it may not be possible to separate the load produced by one knee from the other if the knees do not hit on target, the impacts were in fact well aimed, and individual right and left knee loads are listed in the test data summary. The first test utilized "light" padding (2.5 mm Ensolite®). The male cadaver was 75 years of age, had a body mass of 77.1 kg (170 lb), and had a height of 1.80 m (5.9 ft). The right leg sustained a peak force of 15.3 kN (3440 lb) that tailed-off to 10.2 kN (2290 lb) prior to dropping down to zero. The duration of the significant loading was 9 ms. The femur sustained a neck fracture and a condylar fracture. The left leg sustained an initial peak force of 18.9 kN (4250 lb), and subsequently a peak of 23.0 kN (5170 lb), after which there was a rapid drop-off. The duration of the significant loading was 11 ms. There was a femoral neck fracture and supracondylar shaft fracture as a result of this loading.

The second test subject was a 49-year-old male cadaver of 87 kg (191 lb) body mass and 1.88 m (6.2 ft) height. A padding of 50 mm (2 in) Ensolite® was used. The right leg experienced an initial peak force of 19.4 kN (4360 lb) which tailed-off to 18.4 kN (4140 lb) before dropping to zero rapidly. The duration of significant loading was 19 ms. Femoral neck, shaft, and condylar fractures resulted. The left leg sustained an initial peak load of 21.3 kN (4790 lb) that rose to 25.6 kN (5760 lb) before dropping-off. The significant duration was 21 ms. Fractures were similar to those of the right femur. The third subject was a 79-year-old male of 83-kg mass (183-lb), height unknown. Padding consisted of 25 mm (1 in) Ensolite® backed with 25 mm polystyrene foam. The right leg reached an initial peak of 21.0 kN (4720 lb), a secondary peak of 20.0 kN (4500 lb), and then tailed-off to 9 kN (2020 lb) before diminishing to zero. The significant loading duration was 17 ms. Femoral condyle and shaft fractures resulted. The left leg peaked at 19.8 kN (4450 lb) and 17.4 kN (3910 lb) and then dropped to about 8.0 kN (1800 lb), after which it gradually fell to zero. The duration was 16 ms. A femoral condylar fracture resulted.

The fourth test involved a 58-year-old female cadaver having 47.3-kg (104-lb) mass and 1.59-m (5.2-in) height. Padding consisted of 25-mm Ensolite® backed by 50-mm polystyrene foam. The load-time histories were unimodal. The peaks were 6.2 kN (1390 lb) on the right and 8.1 kN (1820 lb) on the left. The pulse durations were about 32 ms. No fractures were sustained. The final two tests involved osteoporotic subjects and will not be discussed herein. The researchers concluded that the whole-body knee impact test conditions used in this study were capable of producing femoral neck and shaft fractures which are commonly seen in field collisions. The final report (Melvin and

Nusholtz 1980) provides an extensive discussion of the correlation of pulse shape to the temporal progression of the femur fracture phenomena.

Viano and Stalnaker (1980) have reported on a study by Stalnaker et al. (1977) in which a series of thirteen knee impact tests were conducted on six cadavers using the same basic protocol as described earlier for the research program of Melvin et al. (1975) and Melvin and Stalnaker (1976). The flesh was removed from the shaft of the in-situ femur to enable high-speed cinematographic coverage of the femoral behavior during impact. The objective included determination of the time of fracture initiation relative to the time base of the applied force. All six of the rigid impactor tests produced femoral shaft fractures and also produced either a condylar or neck fracture. The peak forces ranged from 13.4 to 28.5 kN (3010 to 6410 lb). The two tests conducted with a lightly-padded impactor both produced bilateral condylar fractures and had peak forces of 16.0 and 15.4 kN (3600 and 3460 lb). Two of the five tests with a thickly-padded impactor produced femoral fractures (one condylar and one shaft), but both of these latter tests involved cadavers that were judged to have had bones of abnormal condition. The three "normal" specimens sustained impacts producing peak forces of 5.3, 13.8, and 14.0 kN (1190, 3100, and 3150 lb) without fracture. The authors concluded that femoral shaft and condylar fractures occurred after the peak force.

Cook and Nagel (1969a, 1969b) have performed drop-weight impact tests on excised cadaver legs. An inertial mass was attached at the ball of the femur. Frontal impacts were applied at the patella with the lower leg flexed 90°, or fully extended, relative to the upper leg. Lateral impacts at the knee joint in the fully extended configuration are also reported. Forces were measured with a transducer mounted between the drop weight and a 6-mm-thick (0.24 in) steel plate load distributing surface. Inertia compensation of the force transducer output does not appear to have been done to account for the effect of this rather robust plate; thus the reported force, impulse, and momentum magnitudes are less than those actually sustained by the test subject. The reported energies, however, should be correct. While the frontal impacts to the flexed legs produced patella, tibia, and femur fractures without knee ligament damage, the frontal and lateral impacts at the knee in the fully extended configuration produced extensive ligamentous injuries. There were accompanying fractures for the frontal impacts, but none for the lateral impacts.

The overall trend of the studies of femoral load-carrying capacity is that female femurs are moderately weaker than males (probably directly proportional to their reduced size, given that the inherent bone strengths are comparable). Secondly, bone conditions such as osteoporosis (decalcification of the bone) can dramatically reduce the load-carrying capacity. This is likely the primary reason for the large spread in fracture tolerance data exhibited in the literature, considering the advanced ages (and therefore significant incidence of various bone pathologies) of most of the test subjects. Finally, in spite of the above variability in the data base, it is clear that the femoral fracture tolerance depends on the temporal characteristics of the applied loads, at least for compressive loading in the longitudinal direction. Significantly higher forces can be sustained for short pulse durations than can be tolerated under quasi-static loading. These conclusions have been generally known and accepted for many years.

Analyses of the dependence of femoral fracture tolerance on the temporal characteristics of the loading received considerable attention during the mid to late 1970s. An analytical approach was taken by Viano and Khalil (1976). They developed a plane-strain finite element model. For sine-squared loading pulses with a uniformly distributed contact pressure over the lateral and medial condyles it was found that peak stresses could significantly overshoot or undershoot static stress levels at the same input force magnitude, depending on the pulse duration. Overshoots (+30% at 30 ms) occurred for pulse durations in the 15 to 60 ms range, and undershoots (−30% at 7.5 ms) occurred for pulse durations in the 3 to 15 ms range. The trend of these results are consistent with laboratory data.

There have been several attempts to devise injury criteria, using the available experimental data, that would enable the outcome (femoral fracture or no fracture) of a blow to the knee to be predicted, based on a knowledge of the applied force-time profile. Such a criterion would be useful in analyzing crash test data generated using anthropomorphic dummies with femur force transducers. (The problem has been compounded by the fact that dummies have not had humanlike biomechanical response characteristics in the knee-thigh-hip region.) Viano (1977) has developed a so-called Femur Injury Criterion (FIC) that establishes the axial compressive force, F, to produce fracture as a function of the primary load pulse duration, T, as follows:

$$F(\text{kN}) = 23.14 - 0.71T\,(\text{ms}),\quad T < 20\text{ ms}$$
$$F(\text{kN}) = 8.90,\quad T \geq 20\text{ ms}$$

A method is discussed for implementing this criterion for analyzing complicated wave shapes. It involves the use of a low-pass filter. Lowne (1982) has analyzed the data and concludes that the following criterion is appropriate for avoiding unacceptably high femur compressive loads:

- 12 kN (2700 lb) may not be exceeded, and
- 10 kN (2250 lb) may not be exceeded except for durations of less than 3 ms, and
- 7 kN (1575 lb) may not be exceeded except for durations of less than 10 ms.

Finally, Nyquist (1982) has proposed a criterion called KTHIC (Knee-Thigh-Hip Injury Criterion) where a "Femur Number" is computed by integrating an exponentially-weighted femur force over the duration of the pulse and comparing the result to a critical value (analogous to the use of the Gadd Severity Index for head injury). Each of these various techniques have some merits, but none are based on truly adequate, comprehensive analyses of all of the available experimental data. Tolerance criteria for combined loading (e.g. simultaneous torsion and axial compression) do not appear to have been addressed to date.

Patella Tolerance. Fracture tolerance data for the patella (knee cap) are available from essentially the same sources of data as those utilized above in connection with the femur.

Melvin and Evans (1985) have reported on static patella tests conducted by Messerer (1880). The posterior surface of the bone was supported on felt, and loads were applied at the anterior surface. Six tests on patellae from male subjects resulted in an average compressive fracture force of 5.87 kN (1320 lb) with a range of 5.14 to 7.58 kN (1155 to 1704 lb). Seven tests on patellae from females provided an average of 4.11 kN (924 lb) with a range of 2.20 to 5.87 kN (range 495 to 1320 lb). Each of the patellae incurred a longitudinal fracture that divided into halves.

Patrick et al. (1966, 1967) in testing twelve embalmed male cadavers observed no patellar fractures at forces below a level of about 9.0 kN (2020 lb). Linear and comminuted fractures began to appear above this magnitude, both with padded and unpadded impact surfaces. However, loads as high as 11.8 kN (2650 lb) with a padded surface were sustained without fracture for some subjects. The researchers concluded that it is not possible to predict whether failure of the patella or femur will occur first, although femoral fractures occurred most frequently.

In the nine male and one female unembalmed cadavers tested by Brun-Cassan et al. (1982) with 25 mm (1 in) polyurethane foam padding, the applied forces ranged from 3.92 to 9.80 kN (881 to 2203 lb) with primary load pulse duration (triangular approximation) ranging from 8 to 18 ms. Only one patellar fracture was noted. The subject was a 56-year-old male cadaver with body mass and height of 63 kg (139 lb) and 1.73 m (5.7 ft). The peak force and its duration were 9.41 kN (2115 lb) and 18 ms.

In the stationary cadaver impact test of Powell et al. (1974, 1975) using embalmed and unembalmed male and female cadavers, there were many patellar fractures as a consequence of using an unpadded impactor. There were a total of fifteen tests, twelve of which resulted in patellar fracture. The peak forces in these twelve tests ranged from 7.10 to 13.2 kN (1600 to 2970 lb). The three patellae that survived without fracture sustained peak loads of 6.68, 8.47, and 8.81 kN (1500, 1900, and 1980 lb).

The stationary cadaver impact tests of Melvin et al. (1975) and Melvin and Stalnaker (1976) resulted in three patellar fractures in the series of seven "rigid impact" exposures. One of the fractures involved a 4050-lb (18.0-kN) peak force (with primary force duration of 2.6 ms) sustained by a 74-year-old female cadaver. The remaining two fractures were to the left and right patella of a 57-year-old male. The peak forces were 3840 lb (17.1 kN) with 6.6 ms duration and 5330 lb (23.7 kN) with 6.3 ms duration. One other cadaver sustained rigid impact exposures. The peak forces ranged from 3640 to 5100 lb (16.2 to 22.7 kN) with durations of 5.2 to 7.0 ms without patellar fracture. With "light padding" there were six patellar fractures in the series of twenty-eight tests. Peak loads and durations are available for four of the six tests. They ranged from 3000 to 6400 lb (13.3 to 28.5 kN) and 4.7 to 8.0 ms. These fractures were associated with two male and one female cadavers having ages ranging from 62 to 78 years. The five tests with thick padding did not produce patellar fractures. The available three peak forces ranged from 3080 to 4420 lb (13.7 to 19.7 kN). No patellar fractures were observed in the nine abducted knee tests where peak forces ranged from 706 to 4800 lb (3.14 to 21.4 kN).

In the sled tests of Melvin and Nusholtz (1980), there were three patellar fractures. In one case the subject was a 75-year-old male having a 77.1 kg (170 lb) body mass. The left patella fractured during a loading pulse having an initial peak force at 18.9 kN (4250 lb) that subsequently increased to a peak of 23.0 kN (5170 lb) before dropping to zero. There was light padding (25 mm Ensolite®). The right patella experienced a peak force of 15.3 kN (3440 lb) without fracture. The remaining two fractures occurred to the left and right patellae of a 79-year-old, 83.0-kg (183-lb) male cadaver. Padding consisted of 25 mm (1 in) Ensolite® backed by 25 mm polystyrene foam. The peak forces were 21.0 and 19.8 kN (4720 and 4450 lb). In the other loading exposures of this program the patellae were subjected to peak loads ranging from 8.1 to 25.6 kN (1820 to 5760 lb) under various padding conditions and did not experience fracture. This included two osteoporotic subjects that experienced loads of 8.9, 14.2 and 15.0 kN (2000, 3190, and 3370 lb).

In the thirteen stationary-cadaver impact exposures of Stalnaker et al. (1977) there were six patella fractures. In each case involving fracture, a rigid impactor was utilized. Peak forces ranged from 300 to 640 lb (13.4 to 28.5 kN) for these fracture-producing impacts. The seven tests involving various levels of padding produced no patellar fractures, with peak forces ranging from 1190 to 3600 lb (5.3 to 16.0 kN).

Cook and Nagel (1969a, 1969b) observed some patellar fractures in their frontal impact drop tests, both with the leg flexed to 90° and with the leg straight. The associated peak forces, which are thought to be erroneously low, are 6600 and 3100 lb (29.4 and 13.8 kN), where tabulated. One test is reported where the tabulated peak force is 6500 lb (28.9 kN) and no patellar fracture is noted. The results of this study are confused by the authors' unorthodox anatomical terminology. They refer to osteophyte fractures, the meaning of which is not apparent.

Melvin et al. (1969) have studied the fracture tolerance of the patella for concentrated loadings. It is vulnerable to such loadings because of its cancellous (spongy) bone center. Three different impactor sizes were utilized. Two featured flat-surfaced circular contact surfaces and had diameters of 0.612 and 0.432 in (15.5 and 10.9 mm). The third was ring-shaped with an outer diameter of 0.5 in (12.7 mm) and an inner diameter of 0.25 in (6.4 mm). Minimum failure loads ranged from 560 to 700 lb (2.49 to 3.11 kN) and average failure loads ranged from 1030 to 1320 lb (4.58 to 5.87 kN). The patella damage pattern varied dramatically with impact speed. Clean punch-through fractures occurred at 10 and 20 mph (16 and 32 km/h) impact velocities.

The general trend of the above summary of patella tolerance to applied loads is that padding between the patella and contact surface of the impactor, to better distribute an otherwise very concentrated force, has a dramatic effect on increasing the load that can be tolerated without fracture. Patellar fracture was readily produced in rigid-surface impacts, but such conditions almost never occur when vehicle occupants impact interiors during crashes. For realistic loading environments, it appears that the patella is generally capable of carrying larger loads than the femur.

Tibia Tolerance. Early studies of the static strength of the tibia were conducted by Weber (1859) and Messerer (1880) following procedures analogous to their evaluations of femur strength, discussed earlier. Melvin and Evans (1985) have also summarized this research. For three-point-bending tests of the tibia, the distance between supports was 216 mm (8.5 in). The average peak bending moments at fracture were 165 N•m (121 ft•lb) for males and 125 N•m (92 ft•lb) for females.

Messerer's lateral three-point-bending tests on tibias utilized an average length between supports of 247 mm (9.7 in) and led to average maximum bending moments at fracture of 207 N•m (153 ft•lb) for males and 124 N•m (91 ft•lb) for females. The static torsion tests on the tibia led to average torsional loads at fracture of 89 N•m (66 ft•lb) for males and 56 N•m (41 ft•lb) for females. Messerer's static axil compression tests of the tibia resulted in average shaft failure forces of 10.36 kN (2329 lb) for males and 7.49 kN (1684 lb) for females.

Yamada (1970) has summarized tibia bending strength tests conducted by Motoshima in 1960. The testing protocol paralleled that described earlier for his tests of femurs. In the same manner as described for the femur, the ultimate deflection and ultimate specific deflection data tabulated by Yamada may be used to calculate the distance between supports in the tibia three-point-bending tests, thereby enabling bending moments to be computed from the tabulated applied forces at fracture. The span was 287 mm (11.3 in). This leads to the results presented in Table 6-8 herein. As previously stated for the femur, Yamada states that the female tibia has five-sixths of the bending strength of the male tibia, and the bending breaking load is not significantly different between the anteroposterior and lateromedial direction.

TABLE 6-8

PEAK BENDING MOMENT AT FRACTURE FOR STATICALLY LOADED WET TIBIAS*
(Based on data of Yamada 1970)

Age Group (yrs)	Bending Moment (N·m)
20–39	208
40–49	180
50–59	174
60–69	171
70–89	164
Average	184

*Yamada does not state if these results are for males, females, or both.

Analogous with the evaluation of femurs as described earlier, Martens et al. (1980) has reported on the torsional strength of the tibia. The specimens were loaded to failure in less than 100 ms. The mean value of peak torsional load for males was 111 N·m (82 ft·lb), and for females it was 71.4 N·m (52.7 ft·lb). Comparing these results to those of the static tests by Messerer indicates that, under this dynamic loading condition, the torsional strength is increased by a factor of 1.25 for males and 1.28 for females. Martens et al. report average energies to failure in the dynamic torsional fracture tests of 27.3 J (17.5 ft·lb) for the male and 18.4 J (13.6 ft·lb) for the female tibia.

Extensive human cadaver testing has been conducted in connection with pedestrian impact protection during the last decade. Much of this work has involved actual or simulated automobile bumper impacts to the tibia. The research performed by Battelle Columbus Laboratories (Pritz et al. 1975, 1978) is one of the most extensive programs. Instrumented standing cadavers were struck, and attempts were made to correlate measured loads to the injuries documented at autopsy. While one of these programs (Pritz et al. 1978) measured simulated bumper impact forces applied to the tibia, and such data can perhaps in come cases be used in judging the likelihood of a given blow to the lower legs producing fracture, the data are inherently incomplete for formulating tibial fracture tolerance criteria. While the mode of loading leading to tibial fracture in these tests was primarily one of beam bending, the loading pattern was complex as a result of the presence of foot-to-ground reaction loads and knee joint loads on the tibia as well as simulated bumper contact loads. There is no way of computing tibial bending moment distributions with any acceptable confidence for this complicated dynamic environment.

Kramer et al. (1973), in connection with pedestrian impact concerns, also applied impact loads to in-situ cadaver lower legs. Two hundred and nine tests were carried out using a so-called twin pendulum catapult. Loads were applied through circular cylindrical impactors having their longitudinal axis perpendicular to that of the tibia. The applied force was computed from an acceleration measured on the impacting mass, using Newton's law. Impact locations ranged from the center of the patella down to the distal shaft of the tibia. Impact speeds ranged from 4 to 8 m/s (13 to 26 ft/s). A wide spread in cadaver tolerance is said to have been shown by the fact that some fractures occurred at 4 m/s and a force of 1.0 kN (225 lb), and yet some legs survived a force of 5.8 kN at 7.1 m/s (1304 lb at 23 ft/s) without fracture. With a 145-mm (5.7-in) diameter impact cylinder, a 50% frequency of fracture occurred at an impact speed of 7.1 m/s with force of 4.3 kN (967 lb). On the other hand, with a 216-mm (8.5-in) diameter impact cylinder, the 50% level was 6.3 m/s and 3.3 kN (20.7 ft/s and 742 lb). Again, as with the Battelle data, it does not appear possible to formulate tibia injury criteria from the results of this program.

Knee Joint Tolerance. Viano et al. (1978) performed a series of human cadaver experiments where the proximal end of the tibia of the seated subject (90° femur-to-tibia orientation) was impacted by a foam-padded 60-kg (132-lb) mass. The impactor face was square and flat, 150 mm (6 in) by 150 mm. The impactor was positioned relative to the subject such that the center of the square face was 150 mm inferior to the approximate center of rotation of the knee joint. Under this condition the tibia was driven rearward (posterior tibial subluxation, or drawer) relative to the femur, loading the knee ligaments. Impacts at nominally 6.0 m/s (20 ft/s) resulted in some ligament avulsion fractures and tears as well as tibia and fibula fractures. The average peak applied force at the tibia was 5.15 kN (1160 lb). Isolated knee joint static response and tolerance tests for posterior subluxation of the tibia relative to the femur were conducted on five cadavers, which had previously been subjected to dynamic loads at the knee but were uninjured. Force and displacement were monitored, and the tests were run to failure. The results are summarized in Table 6-9.

TABLE 6-9

RESULTS OF PROXIMAL TIBIAL IMPACT TESTS
(Viano et al. 1978)

Subject	Sex	Age (yr)	Mass (kg)	Peak Applied Force (kN)	Injury
20817/R	M	45	55	4.27	Lateral ligament avulsion at head of fibula
20823/L	F	67	65	6.24	Multiple fractures of tibia and fibula
20824/R	F	85	59	3.28	Multiple fractures of tibia and fibula
20827/R	M	78	89	6.89	Posterior cruciate ligament avulsion, lateral ligament tear, fracture of tibia
20869/L	F	79	60	4.76	Multiple fractures of tibia and fibula
20881/R	M	69	75	5.74	None
20896/R	M	58	73	4.87	None

Following the above study of knee joint tolerance, Viano and Culver (1979) tested a cadaver subject on an impact sled with "knee restraints" placed sufficiently low to engage the proximal tibia rather than the knee. The cadaver was an 81-year-old, 54-kg (119-lb) male of 1.61-m (5.3-ft) stature. The peak resultant force on each of the two restraints was approximately 4.0 kN (900 lb). Both knees sustained stretching and contralateral central tears of the posterior cruciate ligament. The left knee also sustained a tear of the medial collateral ligament.

Ankle Joint Tolerance. Culver (1984) loaded the left and right ankles of a human cadaver subject in increasing increments in an Instron materials test machine with a cross-head speed of 4.2 mm/s (0.17 in/s). In each case the lower leg was excised from the cadaver at the mid-shaft of the tibia. The upper ends of the remaining distal tibia and fibula were potted into a steel cup for attachment to the testing machine. Properly sized shoes were placed on the feet. Axial force was applied through the cup and downward through the ankle to the shoe, which rested on the lower platen of the machine. The force was applied incrementally, with X-ray films exposed at each increment. In the right leg, audible "popping" was noted at a force of approximately 5.5 kN (1240 lb) with a 38 mm (1.5 in) cross-head travel. The foot had rotated medially 35° relative to the tibia at this point, and radiographs and physical examination by an orthopedic surgeon revealed a fracture in the anterior portion of the calcaneus. A similar phenomenon occurred in the test of the left leg. The "popping" was noted at a force level of 3.3 kN (742 lb) with a 25-mm (1-in) cross-head travel. The foot had rotated medially 37° relative to the tibia. Examination again revealed fracture of the calcaneus.

MECHANICAL RESPONSE OF THE LOWER EXTREMITIES

Mechanical response data, both static and dynamic, are minimal compared to the wealth of information summarized above regarding injury tolerance. In the broadest sense of the definition of mechanical response, one can suggest that most all of the studies of tolerance provide response data as well, since applied loads are typically well documented, and there is generally some form of information available as to how the body subsystem or component responded (e.g. moved, bent, elongated, etc.) as a result of the stimulus. These forms of response data, however, are typically inappropriate or incomplete measures for use in defining objective, quantitative definitions that can be utilized by a dummy developer. Potentially useful measures of response for dummy development are summarized below.

Femur and Tibia Response. Yamada (1970) provides load-deflection curves for the bending of long bones. Unfortunately, the loading conditions are not provided explicitly. While it is not stated, the load-deflection results appear to be based on the same tests from which the earlier discussed tolerance data were obtained. On this basis, the loading environment is three-point bending (quasi-static) with the force applied at midspan. The distances between supports were earlier calculated to be 345 mm (13.6 in) for the femur tests and 287 mm (11.3 in) for the tibia tests. Yamada's curves become meaningful if these loading conditions are accepted. His figures are reproduced as Figures 6-11 and 6-12 herein.

Torsional dynamic response data are available from the research of Roberts and Pathak (1977). These tests were described earlier in connection with femur tolerance, and peak torsional loads and angles of twist were reported. The researchers concluded that "most femurs exhibit linear torque-rotation curves up to the point of fracture." Thus, the earlier noted torque and angle values may be used to compute dynamic torsional stiffness

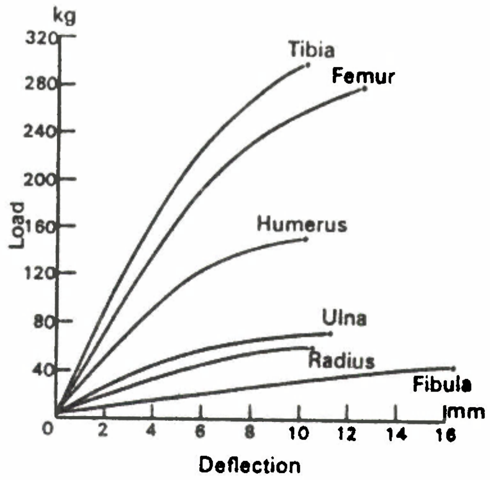

FIGURE 6-11. Femur and tibia load–deflection curves in anteroposterior bending for wet bones of cadavers age 20–39 years (Yamada 1970).

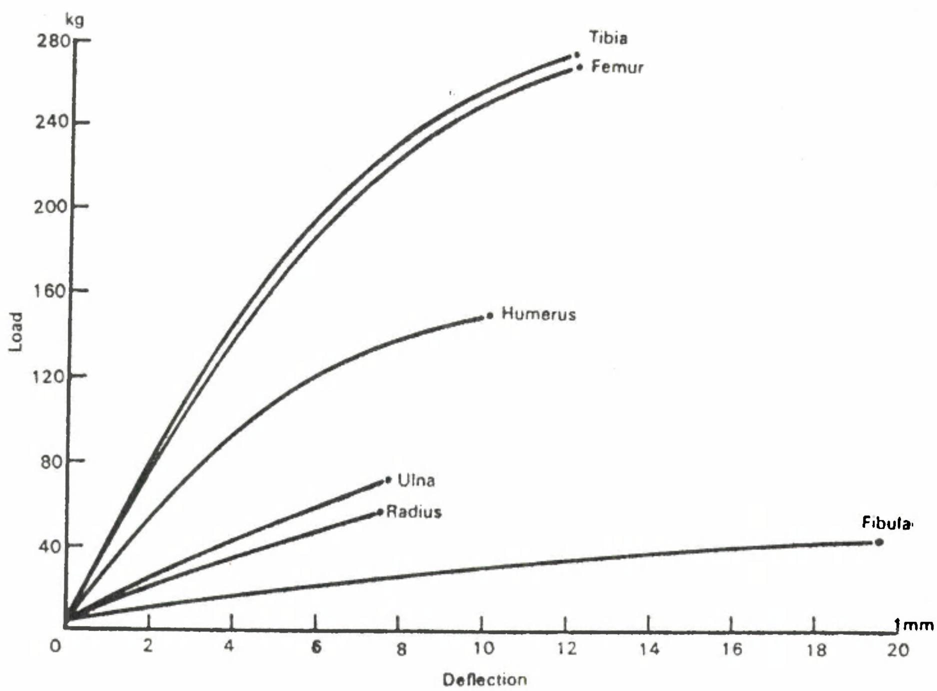

FIGURE 6-12. Femur and tibia load–deflection curves in lateromedial bending for wet bones (Yamada 1970).

values for the 370-mm (14.6-in) test sections of the femoral shaft. The average results are as follows:

Males:	12.30 N·m/deg	(9.1 ft·lb/deg)
Females:	8.24 N·m/deg	(6.1 ft·lb/deg)

Knee-Thigh Hip Response. Horsch and Patrick (1976) provide force-time and acceleration-time profiles of various mass impactors striking the knee at several velocities. Six unembalmed male cadavers were tested, whose average age was 66 years with a range of 52 to 94 years and body mass averaged 67.5 kg (148.5 lb) with a range of 49.0 to 86.4 kg (107.8 to 190.1 lb). Knee impacts directed along the femoral axis were applied using unpadded ballistic pendulums of various masses. These impacts were applied in both a whole-body test and with the leg excised. The applied force and femur acceleration data from these tests provide measures of human mechanical response (Figures 6-13 and 6-14). Calculations performed for both test modes using these data indicate that the "effective mass" of the cadaver was low compared to that of the Part 572 dummy. It was concluded that this was due to the preponderance of mass in the skeletal elements of the dummy as opposed to the considerable mass in the loosely coupled flesh of the cadaver.

A third mode of testing involved attaching the femur of the excised cadaver leg to a rigid structure (infinite mass) and monitoring the applied-force magnitudes during impact. The results (Figure 6-15) are thought to provide a measure of the behavior of the knee, particularly the flesh covering the patella, under dynamic loading. The data of Figure 6-15 were used in specifying the simulated flesh-covering at the knee of the Hybrid III dummy.

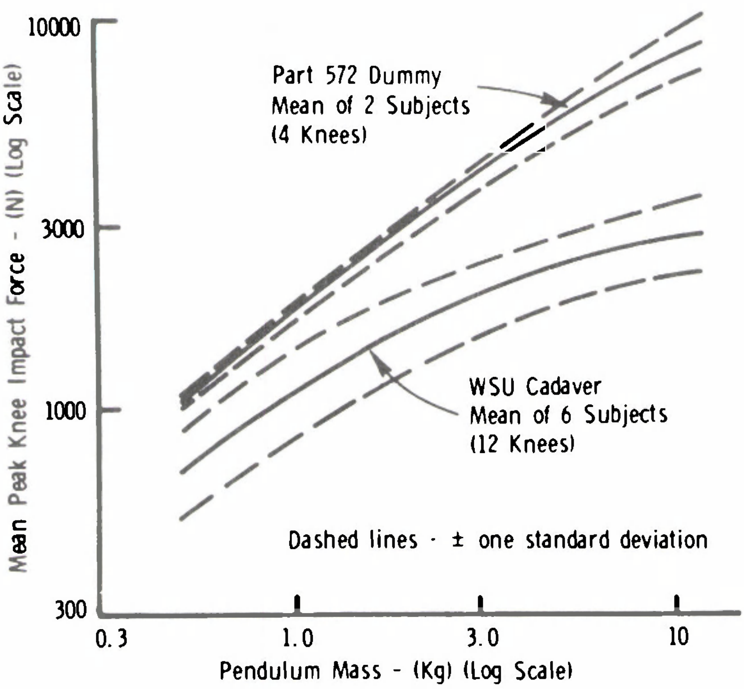

FIGURE 6-13. Mean peak knee impact force response: Comparison of Part 572 dummy and WSU cadaver subjects, whole-body test mode, 0.225 m drop height.

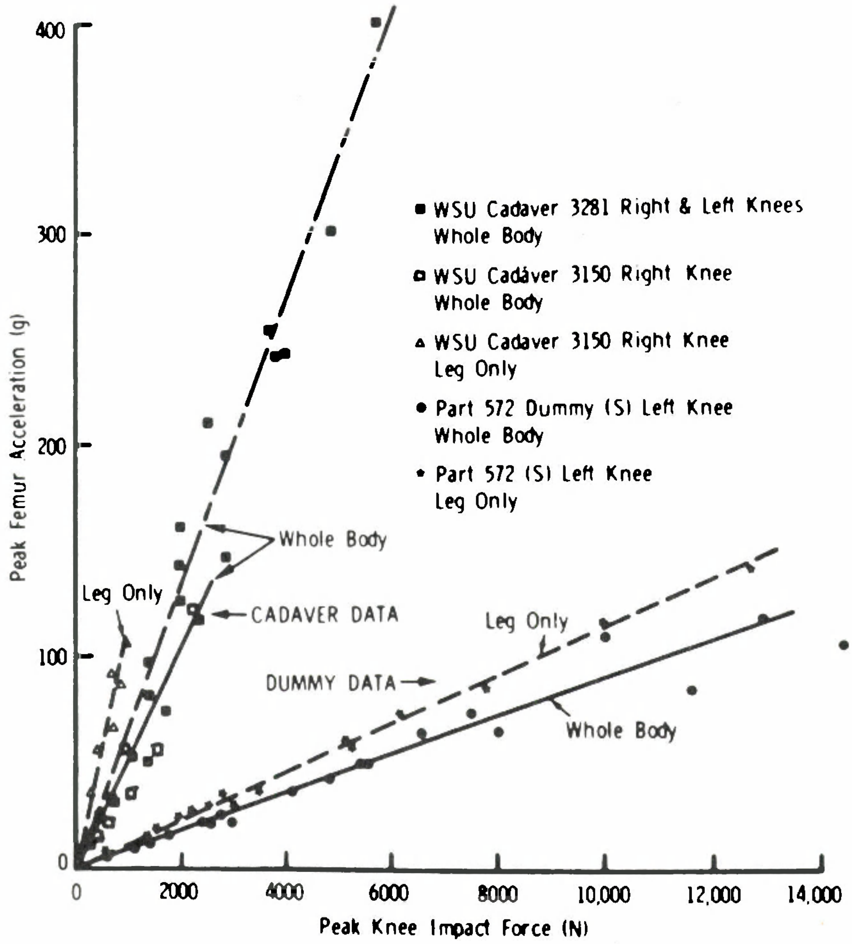

FIGURE 6-14. Peak femur acceleration vs. peak knee impact force: 0.1 m to 0.8 m drop height, 0.5 kg to 5.0 kg pendulum mass.

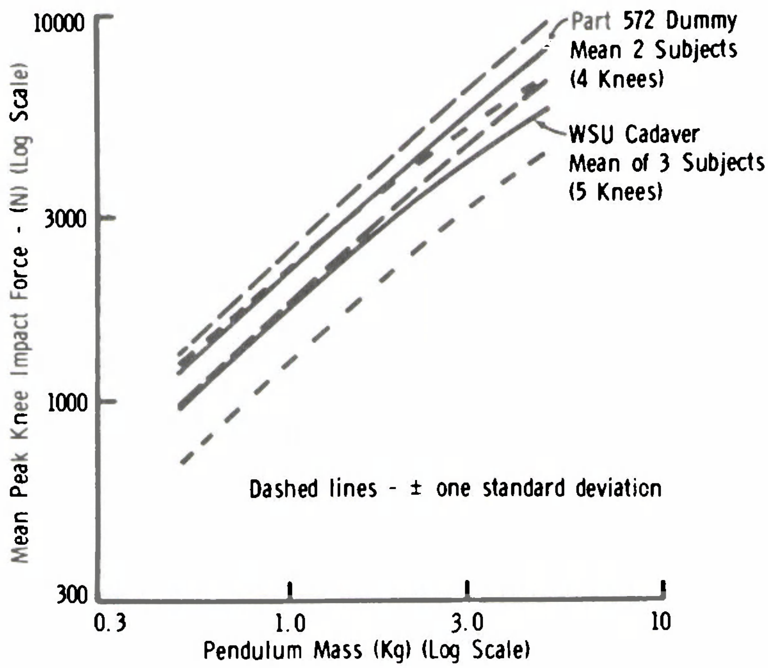

FIGURE 6-15. Mean peak knee impact force response: Leg rigidly mounted test mode, comparison of Part 572 dummy and WSU cadaver subjects, 0.225 m drop height.

Melvin and Stalnaker (1976) have conducted driving point impedance tests on two fresh cadavers and two volunteers. The electrodynamic shaker was coupled to the patella of the cadaver leg, and the patella was preloaded against the femoral condyles by a mechanical apparatus. For the volunteers, the patella-to-femur preload was established by the subject pressing his knee against a plate on the shaker. The shaker axis was along the femoral shaft axis in all cases. An A-P directed accelerometer was mounted at the sacrum. The tests were conducted at a constant 12 G acceleration input. with frequency ranging from 50-500 Hz. Pronounced resonance in the femur is said to have occurred between 150 and 400 Hz for the cadavers and 100 to 200 Hz for the volunteers. Transfer impedance tests of the cadavers revealed that, at a constant 12 G input, the ratio of transfer point (i.e., sacrum) acceleration to driving point acceleration dropped to the 50% level by the 100 to 200 Hz range and to 10% above 500 Hz. Impedance plots are included in the report (Melvin and Stalnaker 1976).

Knee Response. Studies have been conducted to quantify the force-deflection characteristics associated with the human knee being forced against (into) energy absorbing (crushable) materials. Nyquist (1974) tested a cross section of volunteers utilizing Styrofoam® of known crush characteristics. The force-deflection characteristics resulting from the knee penetrating the foam were documented, as well as anthropometric information on the subjects. Percentile scaling of both the knee anthropometry and load-deflection results are provided, along with explicit instructions for performing foam crushability qualification tests. The results of this study are suitable for use in the advanced dummy program directly, without need for interpretation or further analyses.

Hering and Patrick (1977) completed what might be termed a dynamic version of Nyquist's study. A ballistic pendulum was used to impact the knees of thirteen cadavers. Two types of crushable material were attached to the pendulum face, for penetration by the knee: Styrofoam® and aluminum honeycomb. These materials are well described in order that they can be duplicated at a later date. Dynamic force-penetration data are provided, as well as anthropometric information depicting the shapes of the knees. The flesh thickness over the patellae and over the anterior surfaces of the knees were documented. This research provides an excellent basis for developing advanced dummy knee penetration response for crushable materials. The results are usable directly, without need for further analyses.

The study of knee joint tolerance by Viano et al. (1978) included determination of joint stiffness for static posterior tibia subluxation relative to the femur. The tests were summarized earlier in Table 6-10. The linear range stiffness values for the five cadaver knee preparations evaluated has an average value of 149 N/mm (850 lb/in). While there were two female and three male subjects, the females had both the highest and the lowest individual stiffness values, and thus there is no compelling reason to compute separate values for the two sexes. Although these are static data on cadaver subjects, which had earlier sustained knee impacts, this study does provide a basis for designing stiffness into a dummy knee.

TABLE 6-10

ISOLATED KNEE JOINT POSTERIOR SUBLUXATION TEST RESULTS
(Viano et al. 1978)

	Linear Range			Ultimate		
Subject*	Force (kN)	Displ (mm)	Stiffness (N/mm)	Force (kN)	Displ (mm)	Injury
20817/L	1.43	10	149	2.22	17	Posterior cruciate ligament central tear
20823/R	1.43	14	113	2.61	32	Tibial fracture at potted attachment
20824/L	1.67	11	175	1.67	11	Avulsion fracture of tibial plateau
20827/L	2.56	18	156	2.89	35	Posterior cruciate ligament avulsion and tibial fracture at potted attachment
20881/R	1.96	30	13	3.00	20	Posterior cruciate ligament central tear

*Sex, age, mass, and height data are listed in Viano et al. 1978.

SUMMARY AND CONCLUSIONS

The lower extremities constitute approximately one-third of the body weight, and, during normal locomotion, are required to withstand large dynamic loads. Injuries to the lower extremities of automobile occupants are rarely fatal but require significantly longer periods of hospitalization and lost working days than injuries to other body regions at the same AIS level. Even so, injuries to this region constitute only a little more than 5% of the total IPR.

The frontal impact response of the upper leg during seated knee impacts has been studied extensively. This research includes information on the acceleration-time histories, force-time histories, impedance, and effective mass. Other studies have defined the geometry of engagement of the knee into crushable padding. Load-deflection data are also available for subluxation of the tibia with respect to the knee joint.

Injury tolerance data for the upper leg consists primarily of axial loads in the femur. Femur tolerance to lateral impact can be defined in terms of maximum bending moment as can the loading tolerance of the tibia in the transverse direction. There is also information on the strengths of the knee-joint ligamentous structures.

REFERENCES

Agarwal, G.C.; and Gottlieb, C.L. (1977) *Compliance of the human ankle joint.* ASME Paper No. 77-WA/Bio-2. The American Society of Mechanical Engineers, New York.

Brun-Cassan, F.; and Leung, Y.C. (1982) Determination of knee-femur-pelvis tolerance from the simulation of car frontal impacts. *Proc. 7th International Conference on the Biomechanics of Impacts*, pp. 101-115. IRCOBI, Bron, France.

Cook, F.W.; and Nagel, D.A. (1969a) Biomechanical analysis of knee impact. *Proc. 13th Stapp Car Crash Conference*, pp. 117-133. Society of Automotive Engineers, New York.

Cook, F.W.; and Nagel, D.A. (1969b) *Combined medical-engineering study of injury and damage to the knee joint in impact.* The Franklin Institute Research Laboratories, Philadelphia.

Culver, C.C. (1984) *Lower leg axial force studies: Exploratory tests using excised cadaver legs.* Biomedical Science Department, General Motors Research Laboratories, Warren, Mich. (unpublished).

Eppinger, R.H. (1976) Prediction of thoracic injuries using measurable experimental cadavers. *Proc. 6th International Technical Conference on Experimental Safety Vehicles*, pp. 770-780. U.S. Government Printing Office, Washington, D.C.

German Motor Insurers. (1975) *Interior safety of automobiles. Road traffic accidents and their consequences. A study by German Motor Traffic Insurers on 28,936 car crashes with passenger injury.* HUK-Verband, Hamburg.

Gloyns, P.F.; Hayes, H.R.M.; Rattenbury, S.J.; Thomas, P.D.; Mills, H.C.; and Griffiths, D.K. (1979) Lower limb injuries to car occupants in frontal impacts. *Proc. 4th International Conference on the Biomechanics of Trauma*, pp. 105–121. IRCOBI, Bron, France.

Goegler, E. (1962) Road accidents. *Series Chirugia Geigy*, 5 (translation, 1965).

Grattan, E.; and Hobbs, J.A. (1968) *Mechanisms of serious lower limb injuries to motor vehicle occupants.* Report No. LR-201. Transport and Road Research Laboratory, Crowthorne, England.

Hering, W.E.; and Patrick, L.M. (1977) Response comparison of the human cadaver knee and a Part 572 dummy knee to impacts by crushable materials. *Proc. 21st Stapp Car Crash Conference*, pp. 1015–1053. Society of Automotive Engineers, Warrendale, Pa.

Horsch, J.D.; and Patrick, L.M. (1976) *Cadaver and dummy knee impact response.* SAE Paper No. 760799. Society of Automotive Engineers, Warrendale, Pa.

Huelke, D.F.; O'Day, J.; and States, J.D. (1982) Lower extremity injuries in automobile crashes. *Accident Analysis and Prevention*, 14:95–106.

Kroell, C.K.; Schneider, D.C.; and Nahum, A.M. (1976) Comparative knee impact response of Part 572 dummy and cadaver subjects. *Proc. 20th Stapp Car Crash Conference*, pp. 583–606. Society of Automotive Engineers, Warrendale, Pa.

Kramer, M.; Burow, K.; and Heger, A. (1973) Fracture mechanism of lower legs under impact load. *Proc. 17th Stapp Car Crash Conference*, pp. 81–100. Society of Automotive Engineers, Warrendale, Pa.

Kihlberg, J.K. (1970) Multiplicity of injury in automobile accidents. *Impact Injury and Crash Protection*, pp. 5–26. Charles C. Thomas, Springfield, Ill.

Lowne, R.W. (1982) *A revised upper leg injury criterion.* Working Paper No. 42. Transport and Road Research Laboratory, Crowthorne, England. (Also ISO/TC22/SC12/WG6 No. 109, April 1982).

Mather, B.S. (1968) Observations on the effects of static and impact loading on the human femur. *Journal of Biomechanics*, 1:331–335.

Martens, M.; Van AuDekercke, R.; de Meester, P.; and Mulier, J.C. (1980) The mechanical characteristics of the long bones of the lower extremity in torsional loading. *Journal of Biomechanics*, 13:667–676.

Melvin, J.W.; and Evans, F.G. (1985) Extremities: Experimental aspects. *Biomechanics of Trauma*, pp. 447–459. Appleton-Century-Crofts, E. Norwalk, Ct.

Melvin, J.W.; and Nusholtz, G.S. (1980) *Tolerance and response of the knee–femur–pelvis complex to axial impacts: Impact sled tests.* Report No. UM-HSRI-80-27. The University of Michigan, Highway Safety Research Institute, Ann Arbor.

Melvin, J.W.; and Stalnaker, R.L. (1976) *Tolerance and response of the knee–femur–pelvis complex to axial impact.* Report No. UM-HSRI-76-33. The University of Michigan, Highway Safety Research Institute, Ann Arbor.

Melvin, J.W.; Fuller, P.M.; Daniel, R.P.; and Pavliscak, G.M. (1969) *Human head and knee tolerance to localized impacts.* SAE Paper No. 690477. Society of Automotive Engineers, New York.

Melvin, J.W.; Stalnaker, R.L.; Alem, N.M.; Benson, J.B.; and Mohan, D. (1975) Impact response and tolerance of the lower extremities. *Proc. 19th Stapp Car Crash Conference*, pp. 543–599. Society of Automotive Engineers, Warrendale, Pa.

Messerer, O. (1880) *Uber Elasticitat and Festigkeit der Menschlichen Knochen.* J.G. Cotta, Stuttgart.

Moffett, C.C.; Harris, E.H.; and Haslam, E.T. (1969) *Experimental and analytical study of dynamic properties of the human leg.* ASME Paper No. 69-BHF-4. The American Society of Mechanical Engineers, New York.

Nagel, D.A.; and States, J.D. (1977) Dashboard and bumper knee: Will arthritis develop? *Proc. 21st American Association for Automotive Medicine Conference*, pp. 272–279. AAAM, Morton Grove, Ill.

Nahum, A.M.; Siegel, A.W.; and Hight, P.V. (1967) Injuries to rear seat occupants in automobile collisions. *Proc. 11th Stapp Car Crash Conference*, pp. 242–266. Society of Automotive Engineers, New York.

Nahum, A.M.; Siegel, A.W.; Hight, P.V.; and Brooks, S.H. (1968) *Lower extremity injuries of front seat occupants.* SAE Paper No. 680483. Society of Automotive Engineers, New York.

Nash, T. (1969) Mechanisms and distributions of injuries in road accidents. *The Medical and Surgical Management of Road Injuries*, pp. 5–14. E.J. Dwyer, Sydney.

Nyquist, G.W. (1982) *A pulse-shape dependent knee–thigh–hip injury criterion for use with the Part 572 dummy.* Draft Report. ISO/TC22/SC12/WG6 No. 117. International Organization for Standardization, Geneva.

Nyquist, G.W. (1974) Static force–penetration response of the human knee. *Proc. 18th Stapp Car Crash Conference*, pp. 495–538. Society of Automotive Engineers, Warrendale, Pa.

Patrick, L.M.; Kroell, C.K.; and Mertz, H.J., Jr. (1965) Forces on the human body in simulated crashes. *Proc. 9th Stapp Car Crash Conference*, pp. 237–259. University of Minnesota, Nolte Center for Continuing Education, Minneapolis.

Patrick, L.M.; Mertz, H.J.; and Kroell, C.K. (1967) Cadaver, knee, chest and head impact loads. *Proc. 11th Stapp Car Crash Conference*, pp. 106–117. Society of Automotive Engineers, New York.

Powell, W.R.; Advani, S.H.; Clark, R.N.; Ojala, S.J.; and Holt, D.J. (1974) Investigation of femur response to longitudinal impact. *Proc. 18th Stapp Car Crash Conference*, pp. 539–556. Society of Automotive Engineers, Warrendale, Pa.

Powell, W.R.; Ojala, S.J.; Advani, S.H.; and Martin, R.B. (1975) Cadaver femur responses to longitudinal impacts. *Proc. 19th Stapp Car Crash Conference*, pp. 561-579. Society of Automotive Engineers, Warrendale, Pa.

Pritz, H.B.; Hassler, C.R.; and Weis, E.B. (1978) *Pedestrian impact: Baseline and preliminary concepts evaluation, Volume II: Technical discussion.* Battelle Columbus Laboratories, Columbus, Ohio.

Pritz, H.B.; Weis, E.B.; and Herridge, J.T. (1975) *Body vehicle interaction: Experimental study, Volume II.* Battelle Columbus Laboratories, Columbus, Ohio.

Roberts, S.B.; and Pathak, S.K. (1977) Torsional behavior of the human femur. *Proc. 3rd International Conference on Impact Trauma*, pp. 379-388. IRCOBI, Bron, France.

Routson, G.W.; and States, J.D. (1981) Causes and consequences of lower extremity injuries. *Proc. 25th American Association for Automotive Medicine Conference*, pp. 1-14. AAAM, Morton Grove, Ill.

Ryan, G.A. (1969) Injuries in traffic accidents. *New England Journal of Medicine*, 276:1066–1076.

Stalnaker, R.L.; Nusholtz, G.S.; and Melvin, J.W. (1977) *Femur impact study.* Report No. UM-HSRI-77-25. The University of Michigan, Highway Safety Research Institute, Ann Arbor.

States, J.D. (1969) The abbreviated and the comprehensive research injury scales. *Proc. 13th Stapp Car Crash Conference*, pp. 282–294. Society of Automotive Engineers, New York.

States, J.D.; Fenner, H.A., Jr.; Falmboe, E.E.; Nelson, W.D.; and Hames, L.N. (1971) Field application and research development of the abbreviated injury scale. *Proc. 15th Stapp Car Crash Conference*, pp. 710–738. Society of Automotive Engineers, New York.

Viano, D.C. (1977) Considerations for a femur injury criterion. *Proc. 21st Stapp Car Crash Conference*, pp. 443–473. Society of Automotive Engineers, Warrendale, Pa.

Viano, D.C.; and Culver, C.C. (1979) Performance of a shoulder belt and knee restraint in barrier crash simulations. *Proc. 23rd Stapp Car Crash Conference*, pp. 105–131. Society of Automotive Engineers, Warrendale, Pa.

Viano, D.C.; and Khalil, T.B. (1976) Plane strain analysis of a femur midsection. *Proc. 4th New England Bioengineering Conference.* Pergamon, Elmsford, New York.

Viano, D.C.; and Stalnaker, R.L. (1980) Mechanisms of femoral fractures. *Journal of Biomechanics*, 13:701–715.

Viano, D.C.; Culver, C.C.; Haut, R.C.; Melvin, J.W.; Bender, M.; Culver, R.H.; and Levine, R.S. (1978) Bolster impacts to the knee and tibia of human cadavers and an anthropomorphic dummy. *Proc. 22nd Stapp Car Crash Conference*, pp. 403–428. Society of Automotive Engineers, Warrendale, Pa.

Weber, C.O. (1859) *Chirurgische Erfahrungen and Untersuchungen.* Berlin (as cited by Messerer 1880).

Yamada, H. (1970) *Strength of Biological Materials.* Edited by F.G. Evans. Williams and Wilkins, Baltimore.